UNIVERSITA' DEGLI STUDI DI MILANO

Facoltà di Medicina e Chirurgia

Dipartimento di Medicina Traslazionale

CORSO DI DOTTORATO DI RICERCA IN

PATOLOGIA E NEUROPATOLOGIA SPERIMENTALI, CICLO XXVII

MED/04

TESI DI DOTTORATO DI RICERCA

Regulation and function of the tetraspanin-like molecule MS4A4A in alternatively activated and tumor-associated macrophages

Federica TOMAY

Matr. R09505

Tutor: Prof. Massimo LOCATI

Coordinatore del dottorato: Prof. Massimo LOCATI

INDEX

SUMMARY

Macrophages are a heterogeneous population of the innate immune system operating at the boundary between health and disease. They represent the most plastic elements of the hematopoietic system, they are found in all tissues, and their main sake is the response to pathogens by processing and presenting the antigens to the adaptive immune mediators. Among their functions macrophages mediate generation and resolution of inflammation, tissue repair and homeostasis maintenance [1]. These cells undergo specific differentiation based on the local microenvironment [2] and the presence of cytokines [3]. In accordance with the Th1/Th2 polarization, two extreme states of macrophages polarization can be defined: the classically activated, pro-inflammatory M1 macrophage phenotype induced by IFNγ and LPS and the alternatively activated anti-inflammatory M2 macrophage phenotype [4, 5]. Among all the intermediate subpopulations of activating and suppressive macrophages [6], tumor associated macrophages (TAM) embody a peculiar M2-like subset favoring tumor progression and survival, angiogenesis and metastatization, making of these cells a negative prognostic index in many malignances.

Membrane spanning 4-domains subfamily A (MS4A) is a newly described tetraspanin-like protein family, including 26 proteins in human and mice, whose members have been poorly characterized, with few exceptions [7, 8]. Most of them have been demonstrated playing a role in the immune system, either functioning as adaptor molecules for pivotal receptors (e.g. CD20/MS4A1-BCR; MS4A4B -TCR), or clustering complexes on the plasma membrane, or regulating the cell cycle.

In the present study we identified and characterized a novel MS4A protein associated with alternative macrophage polarization, in two different contexts: TAMs association and fungal infections.

MS4A4A is indeed a transmembrane molecule expressed by a special subset of M2 macrophages induced by glucocorticoids.

The topology of the protein resembles the one of the other MS4A members, since it is re-localizes within lipid raft microdomains only upon macrophage activation and its surface expression is abolished upon cholesterol depletion. Also the murine homologue we identified as Ms4a4a shares the same features of the human one.

The target has been found in human samples of Hodgkin's lymphoma (HL) with a characteristic distribution, and its abundance varies among different types of HL. However, no or very faint

staining resulted from healthy tissues, such as lymph nodes and spleen, suggesting the molecule might be implicated in both tumorgenesis and fibrosis.

Evidences of MS4A4A association with TAM also derive from the murine models *in vivo*.

Its distribution and topology makes MS4A4A an ideal target for antibody, potentially with a therapeutic significance.

In the attempt of generating a human anti-human antibody directed against MS4A4A, we identified a clone able to recognize the human and cross-reacting with the murine protein, mediating cytotoxicity of the target bearing cells. Unfortunately, the tool turned out not being able to recognize the native protein in primary cells, given that the screening was originally performed against transfectants expressing the recombinant MS4A4A.

Trying to uncover potential partners for the molecule, split-ubiquitin genetic screening was performed using MS4A4A as bait on a GC treated macrophages library.

The screening showed interactions between MS4A4A and other two MS4A members, MS4A6A, MS4A7, and two tetraspanins, CD63 and CD9, suggesting the existence of platforms resembling the tetraspanin enriched microdomains, where these proteins might gather to facilitate the formation of signaling complexes. Furthermore, the molecule turned out interacting with the b-glucan receptor Dectin1, indicating a possible role in orchestrating the responses to fungal and yeast infections [9].

The relationship with Dectin1 was assessed making use of the Dectin1 ligand Zymosan, and revealed an inverse correlation between the two molecules. An increase in MS4A4A at the surface of the Zymosan treated macrophages corresponds in fact to an internalization of the b-glucan receptor, and occur only in the presence of the particulate polymer, not the soluble one, underlying the specificity of the interaction. The evidence that in resting conditions neither MS4A4A nor Dectin1 are localized within lipid raft, MS4A4A becomes co-localized upon GC, opposite to Dectin1, which instead becomes upon Zymosan engagement when the gathering of a receptor complex is required, suggest a modulatory role for the tetraspanin.

This putative role became even more solid in vivo, where the response to the β-glucan in the KO macrophages was severely impaired both in terms of cytokines production and induction of the respiratory burst, and was observed along with a reduced internalization of Dectin1 upon stimulation.

Although further investigations need to be done, our results strongly suggest MS4A4A may act as a regulatory adaptor for Dectin1 during the recognition of pathogens.

1. INTRODUCTION

1.1. The mononuclear phagocyte system

Since first described by Elie Metchnikoff in the 19th century, it was widely accepted the monocyte-macrophage system originates from the bone marrow's hematopoietic stem cells that once committed, enter the circulation as monocytes and spread throughout the body to eventually differentiate into dendritic cells (DCs) or macrophages by entering the endothelium [10]. These bone marrow derived cells are considered mainly as professional phagocytic cells responsible for antigen presentation and cytokines production [11] and express a great number of receptors on their surface, particularly scavenger receptors and pattern recognition receptors (PRRs) (such as toll like receptors (TLRs) and C-type lectin receptors) [12]. Recently, some evidences diverted from the effective macrophages affiliation with the van Furth 's "mononuclear phagocyte system", showing how actually those cells already exist within the yolk sac much before the appearance of definitive hematopoietic stem cells and the evidences that monocytopenic mice do not present impairment in the tissue-resident macrophages content contributes corroborating this hypothesis [13] [14]. Indeed, fate mapping studies acknowledged that microglia may derive from the yolk sac, while Langerhans cells originate from the fetal liver [15-17], although both can develop also from blood monocytes, under specific conditions [18-21]. Also alveolar, F4/80^{hi} peritoneal and splenic macrophages from the red pulp were shown having a prenatal origin [17].

Hence, resident macrophages can arise from both circulating adult monocytes and embryonic–derived macrophages [22].

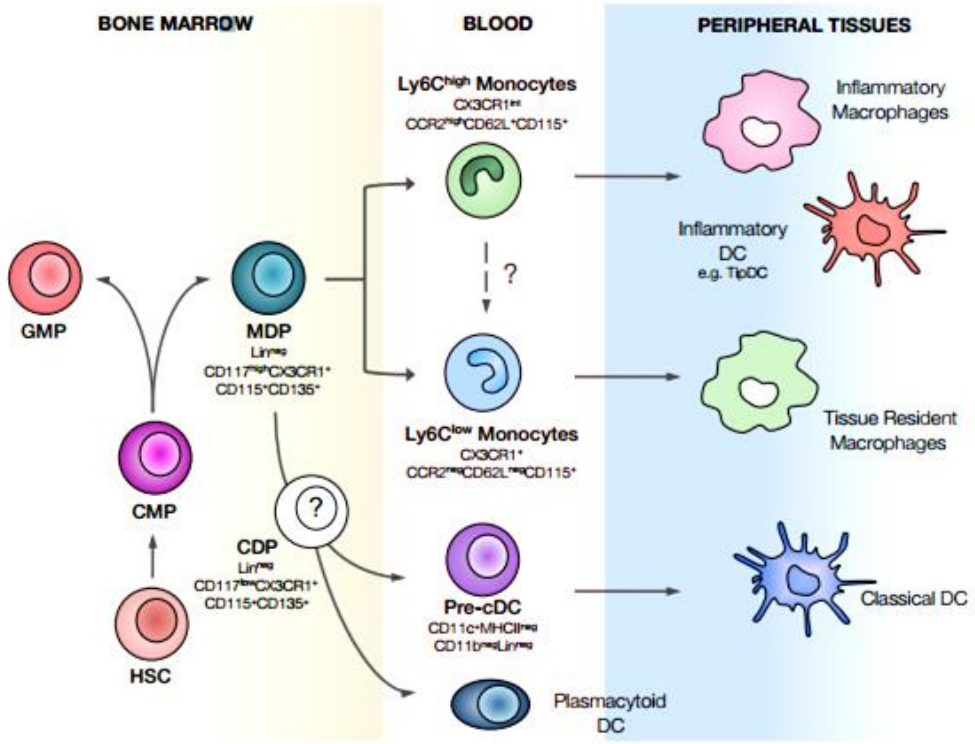

Fig.1. The Mononuclear Phagocyte System: Haematopoietic stem cells (HSC) in the bone marrow (BM) generate common myeloid progenitors (CMP), which in turn originate the macrophage and dendritic cell precursor (MDP). This latter gives rise to the monocytic and dendritic subsets. The MDP originates monocytes, which comprise at least two acknowledged subsets: Ly6ChighCX3CR1intCCR2+, or 'inflammatory' monocytes, producing high amounts of TNFα and iNOS; and Ly6ClowCX3CR1+CCR2- monocytes, or 'resident', which are involved in the homeostasis maintainance. MDP also originates all DC subsets. Classical DC are from DC-committed precursors (pre-cDC), following the MDP. Plasmacytoid DC (pDC) are from the MDP/CDP.

1.1.1. Monocytes development and functions

Monocytes are a heterogeneous population of nucleated cells (4% and 10% in mice and humans, respectively) that can be subdivided in more than a few functional subsets on the basis of their surface markers pattern and emerged as a dynamic and plastic system able to replenish the tissue

resident phagocytic compartment when required. They can even exert several cell specific activities as effector cells, including supporting arteriogenesis and angiogenesis [23].

These cells arise from myeloid precursor cells (MPC) in BM and fetal liver during hematopoiesis and their development totally depends on colony stimulating factor 1 (M-CSF) [24-26].

Fogg identified a clonotypic precursor , the macrophage/DC precursor (MDP) within the murine BM expressing a characteristic signature: LIN-/KIT+/CD135+/CSF1R+ able to give rise to both monocytes and DCs, while more recently another precursor in the BM was acknowledged that does not express FLT3 (the common monocyte progenitor, cMoP) which is not able to generate DCs [27].

Currently, two main human Mo subpopulations have been distinguished: CD14+ (which includes CD14+CD16+ and CD14+CD16-) and CD14lowCD16+ [28]

The classical monocytes represent 80-90% of the whole circulating ones and express high levels of CCR2 and release IL-10 upon LPS [29, 30]. On the other hand, non-classical and intermediate Mo exhibit a $CX_3CR1hiCCR2lo$ phenotype [31, 32].

In mice, the main subsets, both deriving from MDP and cMoPs, are $Ly6C^{hi}CX3CR1^{mid}CCR2^{+}CD62L^{+}CD43^{lo}$ and $LY6C^{lo}CX3CR1^{hi}CCR2^{-}CD62L\text{-}CD43^{hi}$ [33-36].

Both human $CD14^{+}$ and murine $LY6C^{hi}$ resemble the “classical monocytes” that once recruited upon inflammation, are rapidly trans located from the BM to the injured site (through a process highly dependent on the chemokine CCR2) [37, 38],where they can differentiate into human $CD14^{lo}CD16^{+}$ or murine $LY6C^{lo}$ phagocytes respectively, which are instead likely to represent the future blood-derived resident macrophages [38]. Development of these mature monocytes requires a step of differentiation into monoblasts and pro-monocytes, which occurs constitutively within the BM [13]. Opposite to their pro-monocytic precursors, these newly differentiated monocytes exit cell cycle and therefore lose their proliferative potential [34].

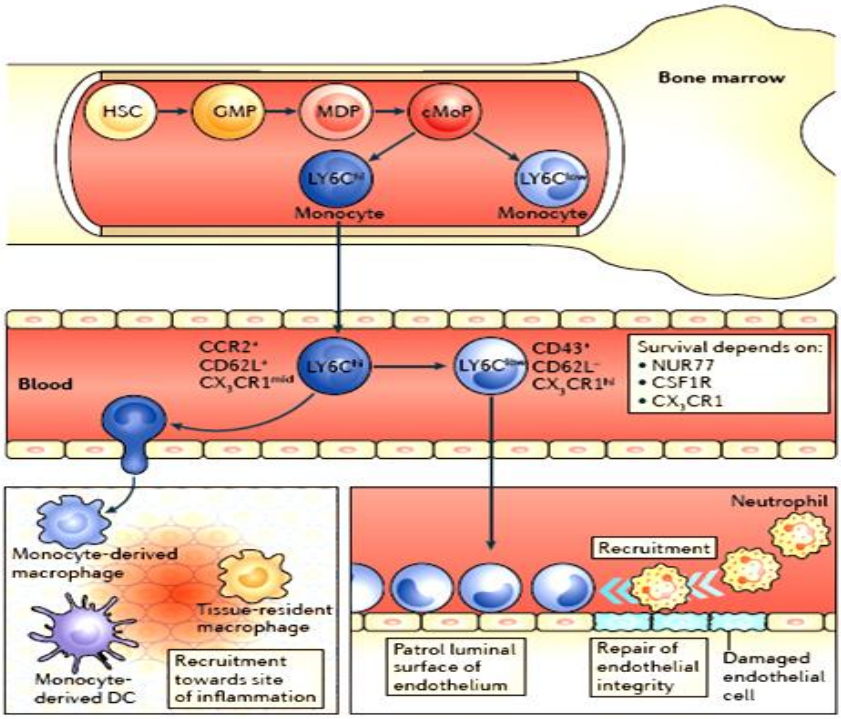

Fig.2. The murine monocyte compartment. Monocytes arose from hematopoietic stem cells (HSCs) in the bone marrow through macrophage and dendritic cell precursor (MDP) and common monocyte progenitor (cMoP) intermediates. Once entered the blood, LY6C^{low} cells patrol the endothelial surface while LY6C^{hi} cells migrate to sites of inflammation or remodeling, where they can differentiate in DCs and macrophages. Taken from Ghinoux, Nat. Rev. 2014.

The constitutive affluence of LY6C^{hi} monocytes derived macrophages seems somehow to be restricted to areas permanently exposed to a low-grade state of chronic inflammation such as gut, skin and spleen marginal zone, where these cells acquire a robust anti-inflammatory phenotype, most likely consistent with their role in maintaining the homeostasis of tissues rich in commensal microorganisms [39].

Recent intravital microscopy experiments have demonstrated how both CD14^{lo}CD16^{+} and LY6C^{lo} can move within the intraluminal endothelium orchestrating the stress responses [40, 41].

Even though commonly associated with macrophages development, monocytes can also give rise to classical dendritic cells. This differentiation is thought to take place following trans endothelial migration, while monocytes stack in the sub endothelial matrix differentiate into macrophages [42]. What is known by far is that there are some monocytes-independent DC-committed precursors. The

MDP can originate plasmacytoid DC (pDC) directly, and pre-cDC, that can differentiate into cDC, but neither pDC nor macrophages [27]. The existence of a common DCs precursor (CDP) intermediate has been proposed [43, 44], although it seems that the MDP and the CDP are phenotypically and developmentally linked [45].

1.1.2. Macrophages development

Based on their phenotype and anatomical localization, macrophages can be divided into numerous subpopulations (e.g. alveolar macrophages, Kupffer cells, osteoclasts, spleen marginal zone macrophages, sub capsular sinus macrophages.) [5]. The functions they may cover ranges from remodeling and homeostasis maintenance to scavenging activities, antigen presentation, immune response triggering.

As already mentioned, most adult tissue macrophages are not of monocytic origin but arise from embryonic progenitors and can be maintained through *in situ* self-renewal.

The so termed primitive hematopoiesis constitutes the first step that takes place in the yolk sac and involves only myeloid-erythroid cells, while the definitive hematopoiesis occurs in the aorta-gonads-mesonephros and originates the hematopoietic stem cells (HSCs) [46, 47]

In the middle of the embryonic life, both these progenitors move first to the fetal liver, where all the subsequent hematopoietic lineages will arise from, then to the other hematopoietic organs through the circulation and here they will differentiate [48].

The yolk sac fetal macrophages origin independently from the MYB transcription factor, but dependently from PU.1 and seem to skip the monocytic intermediate stage, typical of BMDMs. These cells will eventually specifically give rise to some of the skin, kidneys, spleen, brain, pancreas and lung tissue macrophages [17]. After the onset of yolk derived macrophages, monocytic precursors in the liver start differentiating into adult CD11b, F4/80, CSFR1 and LY6C expressing Mo through a MYB dependent process, and are then released and migrate to the fetal tissues, proliferate, and differentiate in tissue macrophages [16, 22, 49].

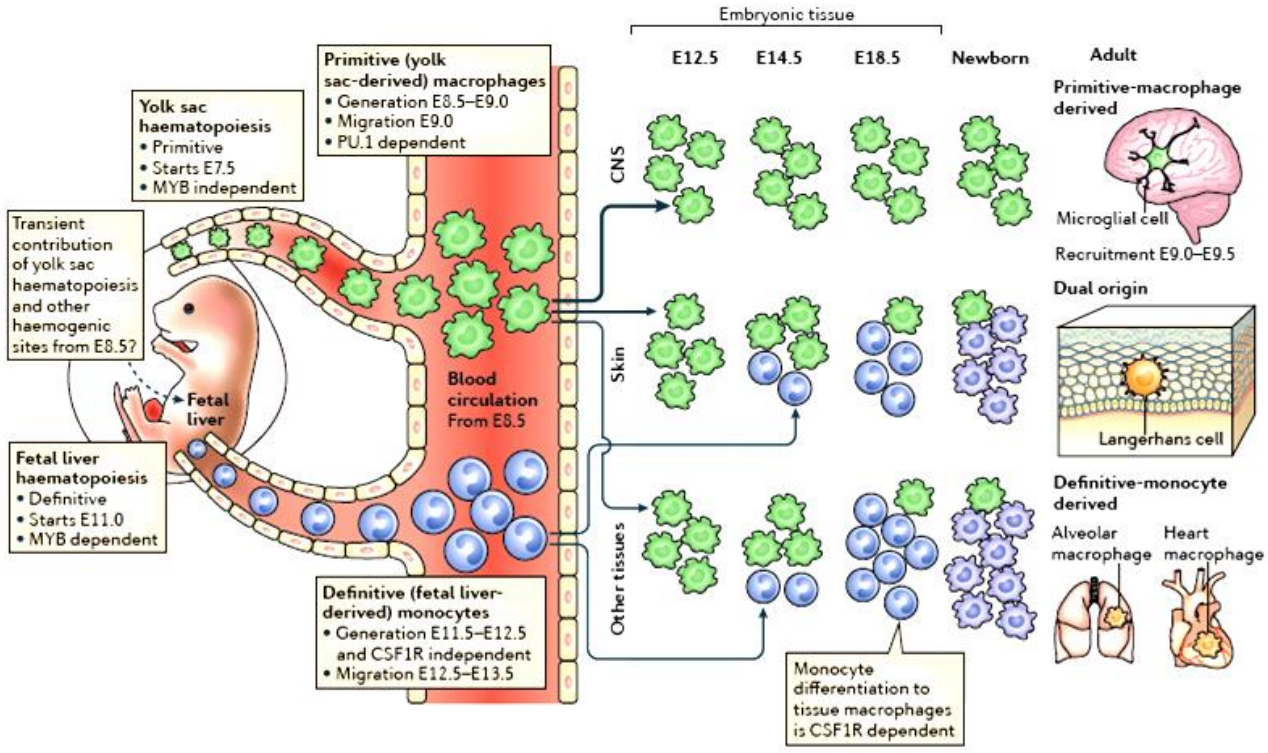

Fig. 3. Embryonic macrophage development. From embryonic day 8.5–9.0 (E8.5–E9.0) the primitive macrophages arise from hematopoietic progenitors within the yolk sac, colonizing the embryo as soon as a circulatory system is established, around E9.0–E10.0, originating the fetal primitive macrophages. Simultaneously, from E10.5 definitive hematopoiesis takes place in the aorta–gonads– mesonephros (AGM) generating hematopoietic stem cells (HSCs) with multi-lineage potential. Monocytes begin to develop in the fetal liver around E11.5–E12.5 and subsequently (E12.5–E13.5) transfer into the blood. invading embryonic tissues about E13.5–E14.5, following yolk sac macrophage colonization. It is still not clear to which extent yolk sac progenitors contribute to the development of fetal liver hematopoiesis, but that seems to occur around E8.5 (dashed arrow). The origin of resting macrophages can substantially differ among tissues. Taken from Ghinoux. Nat. Rev. 2014.

Up to date, it is still not clear which is the actual percentage of tissue macrophages derives from the embryonic hematopoiesis or is replenished from the bone marrow derived monocytes.

1.1.3. Macrophages polarization and function

Macrophages are extraordinarily plastic cells capable to adapt to several microenvironments assuming a range of different phenotypes, getting activated upon disruption of tissue homeostasis by infection, inflammation or trauma. As components of the immune system, macrophages patrol all tissues, in areas close to epithelial surfaces. Through a bunch of pattern recognition receptors (PRR) expressed on their surface, are able to recognize conserved motifs (PAMP) on the microorganism membrane, engulfing them within the phagosomal compartment and subsequently getting rid of them through lysosomal degradation [5, 10]. Recognition of the antigen leads to the secretion of cytokines, capable of recruiting mediators of the adaptive immunity, mainly neutrophils and T leukocytes, contrasting the infection [50-52].

During the recovery from derived inflammation, the tissue resident macrophages initiate a resolution phase, throughout which debris and apoptotic cells are cleared and homeostasis restored [53, 54].

However, anomalous macrophage activation can result in chronic inflammatory conditions, including atherosclerosis and rheumatoid arthritis, as well as malignant disease [55-57].

Indeed, depending on the cues they are exposed to, macrophages can polarize towards two main phenotypes: “classically activated” M1 and “alternatively activated” M2 macrophages.

M1 macrophages originates following in vitro stimulation with NK, interferon gamma (IFN-γ) alone or combined with TLR ligands (LPS) (M1a), and PAMPs (M1b) [58] via STAT1 and IRF5 transcription factors activity [59, 60]. The main feature of this group of macrophages is the production of pro-inflammatory cytokines and the improved ability in bacteria, protozoa and viruses killing and mediation of anti-tumor immunity [61]. They mainly secrete reactive oxygen and nitrogen intermediates via the inducible nitric oxide synthase (iNOS), involved in microbicide process [61], together with pro-inflammatory cytokines and chemokines, like TNFα, IL-6, IL-1β and IL-12, CCL2, CCL5 and CXCL8, [62, 63] and express genes for co-stimulatory molecules like CD80 and CD86 required for antigen presentation Two families of GTPases dominate the complex cellular response [64]. They are usually active in early phases of damage, when can promote cell cycle arrest and apoptosis of the surrounding cells, destroying intracellular microorganisms and acting as antigen presenting cells boosting the innate immune response [65]. The fate of these pro-inflammatory populations following resolution is still not clear, although it has been suggested their

exit through lymphatic [66-68] as well as their Fas-mediated cell death [69]. Also the hypothesis of an in situ conversion in tissue-resident is not to be excluded [70].

Opposite to M1, alternatively activated M2 macrophages show anti-inflammatory phenotype and are found in parasitic infection, allergy, tissue remodeling and waste elimination processes following the acute phase inflammation, and respond to exposure to IL-4 and IL-13 via IRF4, STAT6 and PPARɣ transcription factors [71, 72]. M2 macrophages display up regulation of arginase 1 (Arg1), blocking iNOS activity and therefore inhibiting NO production, secrete anti-inflammatory cytokines like IL-10, TGF-β, IL-4, IL-19, VDGF, PDGF and IL-20 crucial for inflammation resolution and are characterized by the overexpression of Yim1/2 and CD206 whereas inflammatory cytokines are down-regulated [73]. Macrophages stimulated with IL-4 and IL-13 are referred as M2a, those responding to LPS and immune complexes as M2b and those stimulated with IL-10, TGF-β or glucocorticoids as M2c [74]

In line with their involvement with TH2-mediated immune responses, M2 can also produce CCR3 and CCR4 ligands CCL22, CCL17, and CCL24 [75-77]. Based on the pivotal role they cover in homeostasis maintenance and their IL4 dependent ability of self-renewal, tissue resident macrophages are generally considered M2-like macrophages [74, 78].

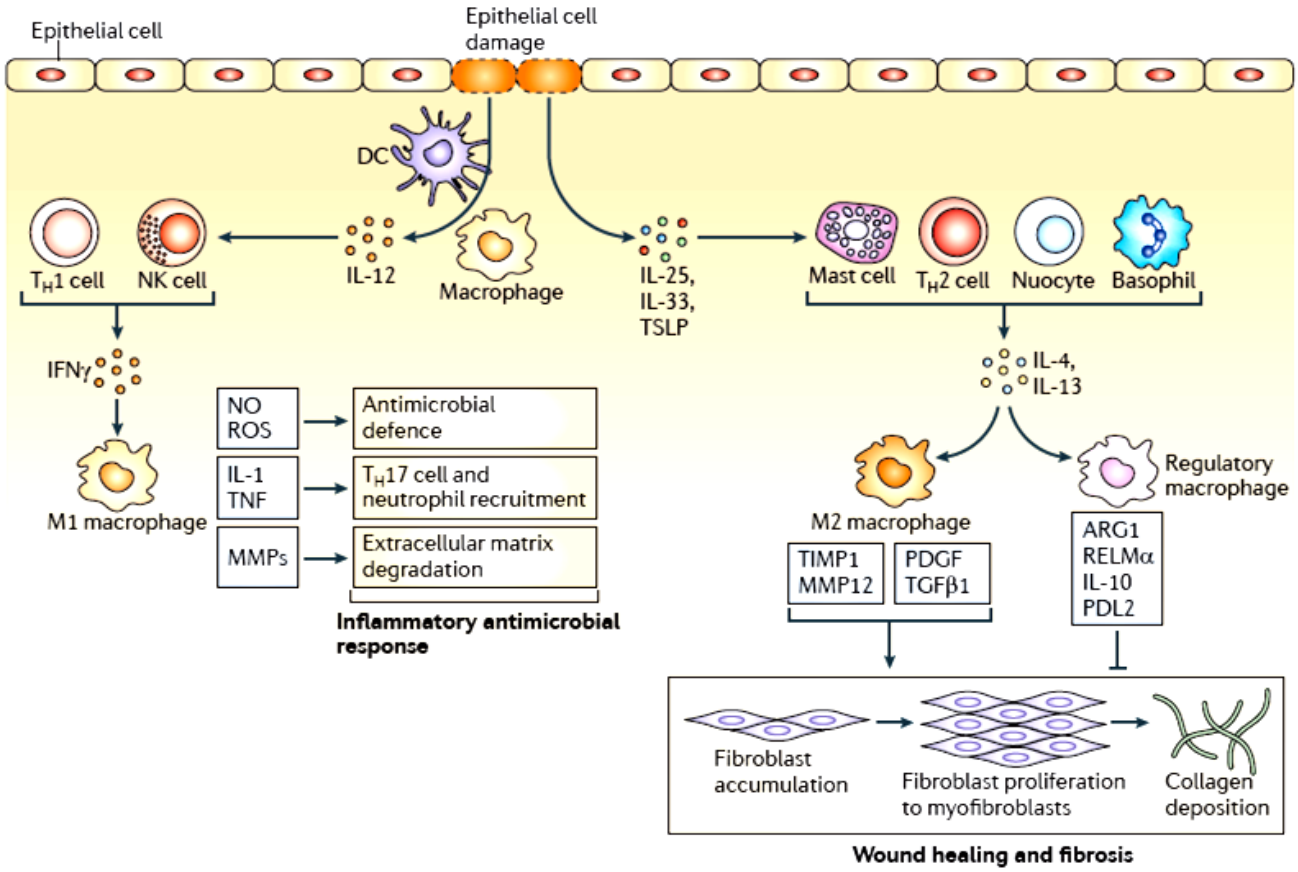

Fig.4. Regulation of inflammation and wound healing by different MQ phenotypes: Once damage occurs, the pro-inflammatory mediators which are released recruit leukocyte within the site of injury. Herein, the monocyte into M1 due to the IFNɣ produced by NK, neutrophils ecc. The main role of these M1 macrophages is the production of ROS, NO, TNFa as well as metalloproteinases to degrade the extracellular matrix, supporting the further recruitment of leukocytes and mediators of inflammation. The tissue damage that results from this activation leads to the production of IL33 and IL25 from the epithelial cells, which promotes M2 accumulation, supporting fibrosis initiation and wound healing through the secretion of growth factors and anti-inflammatory cytokines. Taken from Murray, Nat.Rev. 2011.

The preservation of this delicate M1/M2 balance seems to involve distinct mechanisms. Indeed is thought M1 are originate from circulating blood monocytes, whereas M2 macrophages are more likely being maintained by self-renewal, a process mainly dependent on IL4 [79].

1.1.4. Regulatory macrophages

The idea of a strict functional classification of macrophage phenotype is more likely representing a simplified version of a more complex scenario, which covers a much wider spectrum of different polarization stages [1].

A perfectly matching example of this variety is given by regulatory macrophages, which share common features with both pro and anti-inflammatory subsets. Indeed, this type of cells display high expression of CD206 and CD163 markers and secrete abundant IL10 and no IL12 or TNF.

However, they show high phagocytic activity and up-regulate MHC-II and others co-stimulatory molecules which may support interaction with lymphocytes [6]. Although the specific milieu required for the development of these cells has not been determined yet, it has been demonstrated that it depends at least in part on IL10, GC and TGFβ [80, 81] and, interestingly, immune complexes via FcR mediated signaling induced by TLR ligands [82]. This type of macrophages are constitutively found in uterus and placenta and represent the main subtype in tumors [83, 84].

Figure. 5. Regulatory macrophages. Typical features of M2-like regulatory MQ.

1.1.5. Tumor associated macrophages

Macrophages infiltrating solid cancers can constitute up to 50% of the entire tumor mass, being the most abundant immune population in the tumor [5] TAM are thought to arise from blood monocytes, and move within the tumor, attracted by several factors, such as CCL2, IL3 and CSF. This latter especially correlates with poor prognosis [85-88]. Herein they can enhance metastasis supporting tumor progression [89]. Indeed, TAMs exhibit a typical M2 signature due to the absence

of pro-inflammatory stimuli within the mass which instead produces IL10, preventing the differentiation of DCs from monocytes and suppressing T cells activation [90, 91]. In fact they have been shown attracting Tregs upon release of CCL22, CCL17 and CCL18 [92, 93]. Moreover these cells produce neither NO nor inflammatory cytokines because of a defect in iNOS expression and Nf-kB activation respectively, but at the same time they up-regulate a variety of M2 genes, promoting angiogenesis, remodeling and repair, confirming their role as anti-inflammatory and suppressors of adaptive immunity-macrophages [94]. Indeed, TAMs are able to secrete mediators such as PDGF, TGF and VEGF which once released through the lymphatic stream support ex novo lymph angiogenesis and metastasis [95, 96]. Additionally, vascularization can also be promoted by TAMs through the secretion of chemokines like CCL2, CCL5, CXCL1, CXCL8, CXCL12 [97, 98] and it's likely to be a consequence of the preferential localization of these macrophages in highly hypoxic areas of the tumor [99]. In turn, the production of some of these factors (particularly CCL5 and VEGF) can lead to the activation of metalloproteinases like MMP9 capable of disrupting the extracellular matrix once released, resulting in an increased invasiveness and metastatic potential [100, 101].

For several tumor types, with the exception of some stomach and colorectal tumors [102, 103], it has been proven that the higher the TAMs infiltration, the poorer the prognosis [104, 105] and this evidence was also supported by experimental approaches including macrophages depletion and overexpression.

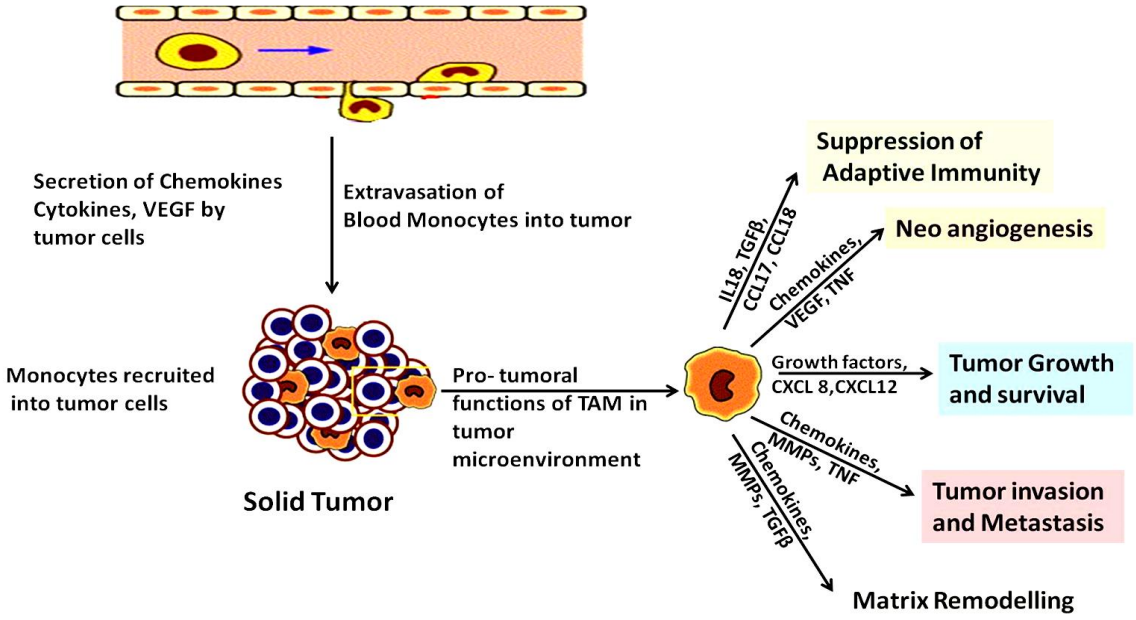

Fig.6. The role of TAMs in tumor development. The mediators produced by the tumor contribute in creating a microenvironment suitable for the differentiation of blood monocytes into tumor-associated macrophages (TAM), which promote tumor growth and metastasis, impairing matrix deposition, remodeling and vascularization.

1.2. The tetraspanin family of proteins

The tetraspanin (Tspan) family includes thirty-three highly hydrophobic small (20-50 kDa) membrane glycoproteins named by their structural characteristic of displaying four transmembrane domains, short cytoplasmic N- and C-terminals, and two extracellular (EC) loops [106]. Their expression ranges from sponges to mammals, with each organism expressing a huge number of this family members [107]. Their involvement in several biological pathways such as cell signaling, adhesion, migration, proliferation, tumor metastasis, tissue differentiation, angiogenesis, cell-cell fusion [108-111] allocates them an essential biological role.

Phylogenetic suggest the existence of sub-groups of tetraspanins based on the structural homology of their large extracellular loop (EC2) [112]. Establishing lateral interactions with several partners including integrins, C-type lectins, immunoglobulins and G-coupled receptors, tetraspanins can reorganize the plasma membrane generating characteristic tetraspanin-enriched microdomains (TEM) able to modulate a variety of processes [108, 109, 113, 114]

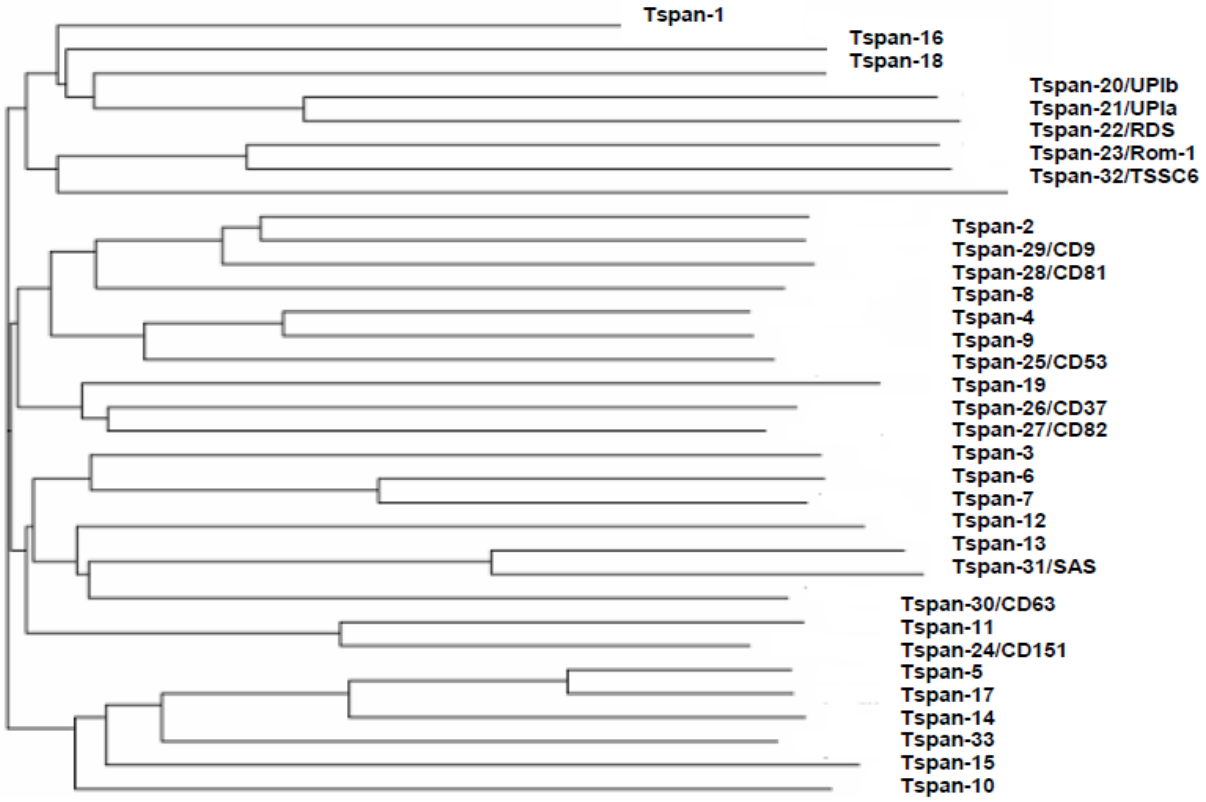

Fig.7. A phylogenetic tree of human tetraspanins Human tetraspanin amino-acid sequences were aligned and a phyologram was prepared using the ClustalW alignment program (www.ebi.ac.uk/custalw) to determine similarity between superfamily members.

1.2.1. Tetraspanins structural characteristics

The common features of tetraspanins family members are the presence of four transmembrane domains, a small extracellular loop (SEL), a large extracellular loop characterized by a conserved CCG motif and two or more Cys residues forming a disulphide bond (LEL) and cytoplasmic amino- (NH2) and carboxy-termini (COOH) [112, 115].

Min and colleagues solved the tetraspanins crystal structure, revealing the folding of the EC2 on EC1 [116].

All the transmembrane domains except the second comprise a polar amino-acid with unknown function [109] and membrane-proximal Cys residues undergoing palmitoylation, essential for interactions between Tspan and mutations within these residues for some members led to diminished lateral associations [117-119], although primary interactions are not influenced by altered palmitoylation sites [113]. This post-translational modification seems to occur thanks to the palmitate transferase, DHHC2 localized within the TEMs and its activity is crucial for Tspan interactions [120].

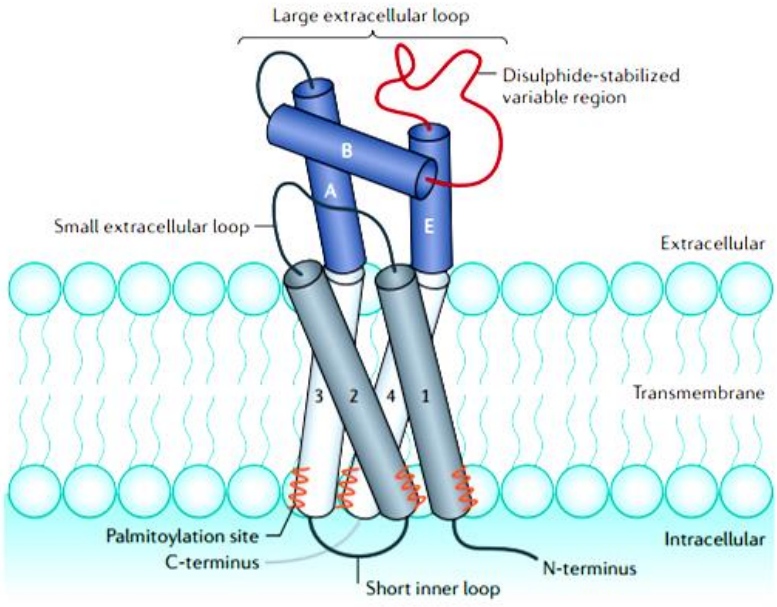

Fig.8. The tetraspanin structure. The proteins share four transmembrane (TM) helices (labelled 1–4), one large extracellular loop of about 70–130 aa connecting TM3 and TM4 with a conserved helical region and a variable region (dark red) and a small extracellular loop (13–30 aa) linking TM1 and TM2. Tetraspanins typically present short N- and C-terminal cytoplasmic tails (6–19 aa) as well as a small inner loop (about 4 aa). Palmitoylation of membrane-proximal Cys (orange lines) allows associations with other proteins within TEMs. Taken from Hemler, 2014

1.2.1.1. The extracellular loops

All is known about the small extracellular loop is that it seems to serve as a foothold for the large extracellular loop [109], which is required for all the interactions involving these proteins and as already mentioned, its folding pattern represents a signature of the different Tspan subgroups. Moreover it shows a discrete variability among different members, suggesting it may be responsible for the different roles displayed by Tspan in different cell types [121].

The LEL is characterized by a constant region with three α-helices named A, B and E and a variable region which allows interactions and can exhibit from one to three N-linked glycosylation sites, with the exception of CD81, which is not glycosylated at all [108, 109]. The levels of glycosylation within this region depend on cell type and tissue in which Tspan are expressed.

1.2.1.2. The intracellular C and N- termini

As anticipated before, both the termini in Tspan are cytoplasmic and although in the majority of the cases a role hasn't been described these regions, a function has been attributed to CD63 C-terminal. In fact, in some species, the Tyr-based lysosomal targeting motif (G-Y-E-V-M) interacts with adaptor-protein-2 (AP-2) and AP-3 supporting clathrin-mediated endocytic processes, and a similar motif can be found also in other members, such as CD82, CD151 and CD37 [113]. CD63 C-terminal can also directly interact with the PDZ domain-containing protein syntenin-1, being negatively regulate by it in terms of internalization [122].

Other proteins which demonstrated interact with Tspan at the C-terminal level are small G-proteins, phosphatidylinositol 4-kinase and protein kinase Cα [114, 123]. The role of the N-terminus has

been described only with regard to ubiquitination, a modification that seems to take place in some Tspans at the level of N-terminal Lys residues, inducing their proteosomal degradation [124].

1.2.1.3. Tetraspanin-enriched microdomains

Tetraspanins are often referred as "web", rather than single molecules, since they frequently localize within complexes where they develop self-associations and interactions with other membrane molecules [110] which may vary, depending on the biological environment [125]. These cell type specific platforms are commonly stated as tetraspanin-enriched microdomains and have been shown perform as surface membrane adaptors by modifying the availability of other receptors to signal.

1.2.1.4. Tetraspanin-enriched microdomains vs lipid rafts

The biological membrane presents several compartments made of glycerol-phospholipids, sphingolipids, cholesterol and proteins serving as signaling platforms [126, 127]. The strong interaction of sphingolipids with each another and cholesterol leads to the isolation of these lipids into disconnected but highly organized membrane structures characterized by a gel-like phase, which differs from the rest of the fluid phase phospholipidic membrane [128]. These organized microdomains have been termed lipid rafts, and cover a key role during the activation of some cell types, particularly monocytes and macrophages [129-131].

Tetraspanin-enriched microdomains differ from lipid rafts basically in the composition of the compartments and in the fact that TEMs are not affected by temperature or cholesterol depletion but can be solubilized by non-ionic detergents [127, 132]. So far only CD81 has been shown to translocate in lipid rafts upon binding of BCR and CD19/CD21/CD81 co-receptor complex[133] [134].

1.2.2.Tetraspanin interactions

The potential tetraspanins partners range from adhesion molecules, membrane receptors, to signal transduction molecules [135].

These types of interactions may occur at three different levels, based on their strength and resistance to detergent disruption [108, 109].

The primary one is direct and preserved under stringent conditions (Triton X-100) and are stable upon covalent cross-linking [108, 109, 114]. An example for this association is the partnership CD151/ integrin α3β1 [136].

Secondary ones require a first interaction with others Tspan and can only resist in mild detergents (Brij97) [137].

Tertiary associations take place within large complexes and are only stable in very weak detergents such as CHAPS and Brij58 [108, 109].

1.2.2.1. Interactions with integrins

Integrins are transmembrane receptors that regulate a number of processes, from adhesion to motility, angiogenesis and invasion [138, 139].

The main integrins associated with Tspan contain the β1 chain, generally combined with α3, α4 or α6 and only sporadically α2 and α5 [123]. The β1 chain signals through the integrin-linked kinase (ILK), permitting the connection with the extracellular matrix [140, 141].

Although the Tspan- integrins complex has a low affinity conformation, tetraspanins can affect the signaling mediated by integrins following binding of the ligand modifying actin polymerization, therefore affecting migration and cell adhesion processes.

The Tspan CD151 is expressed on epithelial and endothelial cells, Schwann cells, muscle cells, megakaryocytes and platelets [142] and by far represents the only direct interaction of a Tspan with an integrin [143] and was demonstrated affecting integrin-dependent adhesion and motility [144, 145]. Mice lacking CD151 display a decreased angiogenesis because of altered integrin signaling and missing association with TEM [146]. CD151 interacts with integrins α3β1 and α6β1 through a QRD (194-196) motif in the large extracellular loop [136] but also its cytoplasmic domain seems to play a role in the integrins internalization [147].

The importance of this interaction is reflected also in clinic, since three patients baring a mutated form of CD151 lacking the large extracellular loop displayed pretibial epidermolysis bullosa, and end-stage hereditary nephritis, confirming the pivotal role of CD151-α3β1 and CD151-α6β1 interactions in the normal arrangement of the epidermal basement [148-150].

1.2.2.2. Interactions with growth factors

The only Tspan members reported to interact with this class of receptors are CD9 and CD82.
The first one has been described networking with the heparin-binding EGF-like growth factor tyrosine-kinase receptor (HB-EGF) and hepatocyte growth factor receptor (c-Met/HGF-R) [151] implicated in epithelial-mesenchymal transition [152] and with the epithelial cell adhesion molecule (Ep-CAM) [114].
CD82 also has been shown to cooperate with c-Met activating a signaling via integrins, and this activation can be inhibited by the proximity of the ganglioside GM2 [153, 154] and can couple with EGFR, altering its activity and endocytosis depending on the Tspan expression level [109, 113]. CD82 tyrosine-based sorting motif (Y-S-K-V) in its C-terminal is responsible of its internalization of CD82 [113].

1.2.2.3. Interactions with membrane proteins

The evidences of a crosstalk between Tspan and members of the HLA family (both II and I) suggests they might also be involved in the process of antigen presentation [151] [155].
CD9 was found supporting T cell activation interacting with HLA II on DC [156], while CD53, CD37 and CD81 seem to preferentially interact with MHC class I [157].
Always CD81 together with CD82was able to interact also with the co-stimulatory molecules CD4 and CD8 on T lymphocytes [158].

1.2.3. Tetraspanins signaling and functions

It is well known that Tspan interact with a number of signaling molecules. However, considering they don't resemble receptor proteins and up to date no ligands have been described for any of the members, it sounds unlikely Tspan can activate their own signaling cascade. More likely, they seem to both directly and indirectly regulate the signaling activity of their partners in the web [135]
The use of monoclonal antibodies targeting Tspan led to several effects, such as calcium mobilization [159], direct interaction with type II phosphatidylinositol 4-kinase (PI 4K) [132, 160], protein kinase C activation and integrin α3 phosphorylation [161-163], c-jun NH2-terminal kinase

(JNK) and c-Jun dependent transcription activation [164, 165], ERK1 and ERK2 induced proliferation [164], Dectin-1 mediated IL6 production down-regulation [166].

1.2.3.1. Tetraspanins and immune system

Although the function of most Tspan has not been discovered yet , few exceptions shaded a light on their role in a number of immunological contexts.

1.2.3.1.1. CD81 and BCR signaling

The efforts to discover the role of CD81 revealed its involvement in a huge number of physiological processes, particularly regarding B and T cells signaling [167]. CD81 has been shown to interact with the BCR, enhancing its signaling activity by decreasing the amount of Ag required for B-cell activation. [110][161]. Its role depends on the association with the CD19/CD21complex at the level of the lipid rafts compartments, at the B cells surface, where the BCR is sequestered and enabled to get in touch with key signaling molecules [133, 134]. the absence of CD81 indeed results in the non-re-localization of the complex within the rafts, and an impaired trafficking of CD19 to the membrane [133, 168].

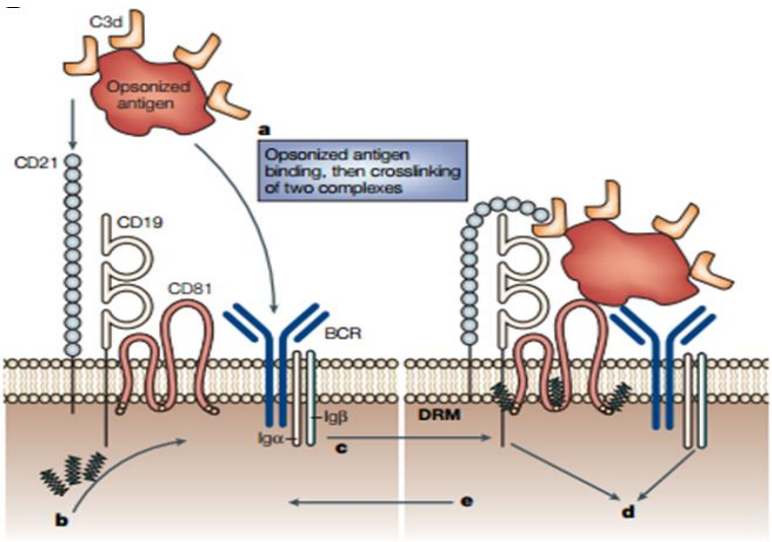

Fig.9. Crosstalk between BCR and CD81. Recognition of the antigen by BCR and CD21 results in in the palmitoylation of CD81 (b) stabilizing the complexes within the detergent-resistant micro domains (DRMs) (c), activating the signaling (d).
The process is reversible, depending on the palmitoylation state (e). From Levy and Shoham, 2005.

1.2.3.1.2. T-cells hyperproliferation in Tspan KO

Several studies performed on different Tspan KO CD151, CD81, and CD37 concurred with evidences of T lymphocytes hyperproliferation upon TCR activation by anti CD3 antibodies. [169-173].
This suggest Tspan may act as negative regulators of TCR signaling, either separating it from activator kinases or associating it with inhibitory phosphatases within the TEMs, thus preventing the phosphorylation of the TCR ITAM and the cascade through Zap-70/Syk [174, 175].

1.2.3.2. Tetraspanins and infectious disease

1.2.3.2.1. HIV-1

The human immunodeficiency virus-1 (HIV-1) infection as well as the virus release occur in macrophages, DC, epithelial and T cells through the binding of TEMs characterized by the presence of CD63, CD9, CD81and CD82 [176]. After the virus was found trafficking through the endocytic system, CD63 became matter of study, and resulted incorporated in the virions after the virus exits the host cell via late endosome-multivescicular bodies. However, the infectivity of the virus seems not to be impaired in macrophages lacking CD63 [177] although a reduction in its expression results in a diminished viral particles output [178]. The same reduction in HIV release was found in the absence of CD81 in Molt T cells [179]. It definitely seems that tetraspanins may affect the virus accessibility and infectivity in some cell types, although the process may be supported by the cooperation with other molecules, and so far, they are unlikely to act as budding cofactors.
Tetraspanins rather seem to interfere with the fusogenicity of the virions, since it has been demonstrated that the incorporation of some of them (CD9, CD82, CD81, CD63, CD231) reduce

the Env induced membrane fusion, which would explain their down-regulation in chronically infected T cells [180].

1.2.3.2.2. HCV

CD81, together with occluding and claudin1, represents a co-receptor for Hepatitis C virus (HCV) and it has been acknowledged as one of the only two Tspan capable of directly interact in trans with a molecule (HCV envelope glycoprotein E2) located on the surface of another cell [181, 182]. When missing, HCV infectivity drops, although is not totally abolished, probably because of the viral particle is not able to bind the host cell with the same efficiency [183]. Opposite to HIV, infection of HCV does not require CD81 being localized within the TEMs compartments [184].

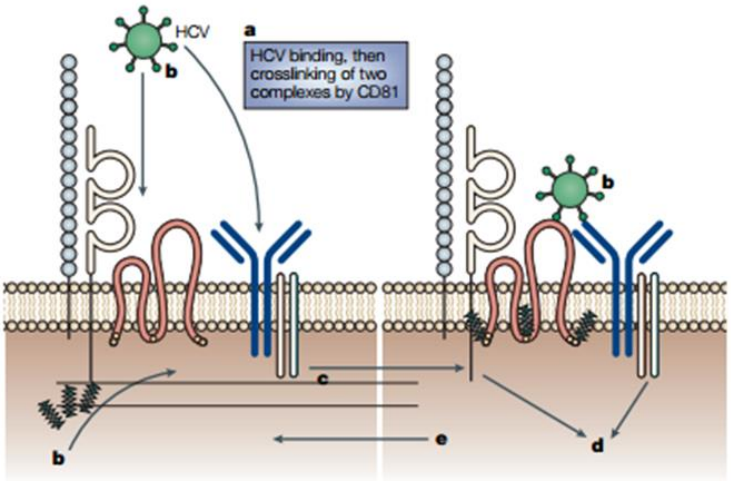

Fig.10. Function of CD81 in HCV. The dual recognition of HCV- E2 by BCR and CD81 prompts comparable effects as those described above for opsonized antigens.

1.2.3.3. CD9, CD81 and oocyte fertilization

CD9 has been shown playing a fundamental role in reproductive biology. The absence of CD9 leads to a dramatic change in the oocytes morphology and membrane proteins distribution, that prevents their fusion with sperm [185-188]. Recent data from CD81 KO mice revealed its involvement in sperm-egg fusion [189] and on the other hand, its over-expression restores fertility in CD9 KO eggs [190]. The high (45%) identity between these members may explain this compensatory effect.

1.2.3.4. Tetraspanins and cancer

Most of the information about tetraspanins expression derive from microarray data of human cancer samples and delineates recurrent patterns of Tspan expressions, allowing the identification of subgroups in diverse malignances.

The very first evidences of Tspan as tumoral stage markers comes from B cells tumors, such as lymphomas and leukemia.

Herein, the high expression of CD37 and CD53 or CD9 and CD81 correlates with lymphomas and mature-B cells leukemia or acute lymphocytic leukemia and clonal plasma cells, respectively and these differences permit the discrimination of different lymphomas in an single patient [191].

A great peripheral blood and lymph node infiltration has been shown correlating with high positivity for CD53, known to protect the memory and mature lymphocytes from apoptosis [164]. In contrast, a higher bone marrow involvement has been associated with a lowered CD9 expression [192].

These patterns of expression also recurred in other types of cancer other than B cell malignances, such as kidney cancer [193], and melanomas [194].

CD9 loss results in higher motility and metastatic capacity of melanomas [194], ovarian [195] lung [196], oral squamous cell [197], esophageal [198], cervical [199], and gastric [200] carcinomas. Its association with TGFα leads to the induction of EGFR and cellular proliferation [201].

CD63 was identified in melanomas and breast carcinomas, where its expression inversely relates with metastatic potential [202, 203].

CD82 is up regulated in thyroid benign tumors but down regulated in carcinomas and almost absent in metastasis [204].

CD151 is mainly localized at the basal level of endothelial cells, [205] and up regulated in estrogen receptor negative tumors and breast cancer, where it correlates with high grade [137]. In this latter, CD151 together with CD9 and CD81 has been demonstrated to promote adhesion interacting transiently with the substrate before the formation of lamellipodia from the cell [206].

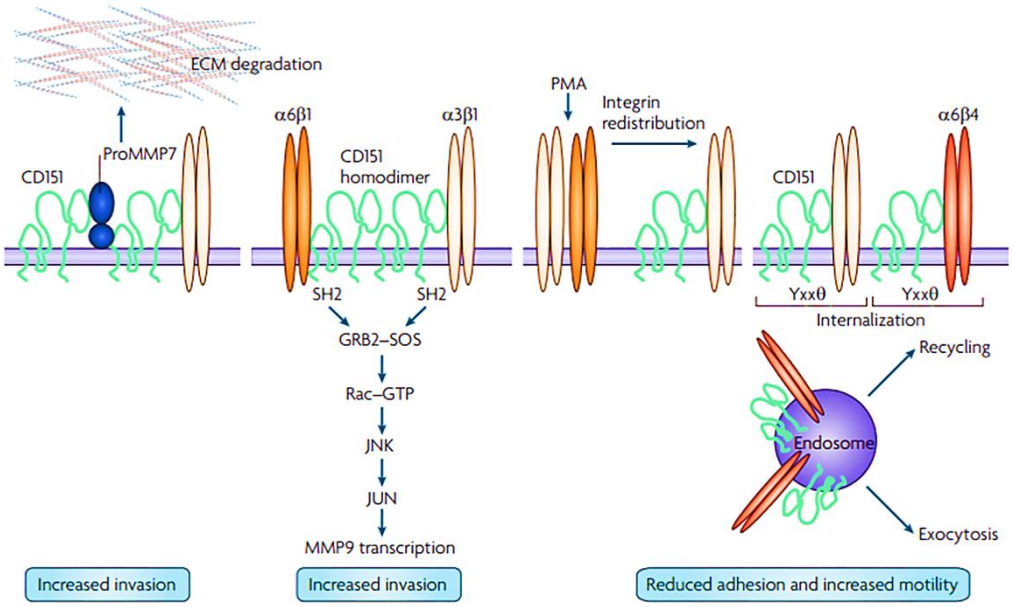

Fig.11. Role of CD151 in tumor extravasation and invasion. CD151 induces MMP9 activation promoting matrix remodeling. The recruitment and rapid turnover of laminin-binding integrins from CD151 through exosomes impairs the adhesion process. From Zoeller, Nature, 2009.

These structures are in proximity with substrates of PKC, thus regulate migration through cytoskeleton reorganization [205]. In the skin, CD151 associates with laminin 5 [151, 207] contributing to the formation of hemi desmosomes [208]. Moreover, CD151 overexpression enhances motility, and metalloproteinase MMP-9 [209] while its knock-down results in motility loss in primary melanocytes [210], clearly implicating CD151 in the regulation of cell adhesion and tumor metastatization [211]. Also different types of prostate carcinomas show diverse expressions of CD151, CD9 and CD53 [212].

1.3. MS4A protein family

The membrane-spanning 4-domain, subfamily A (MS4A) includes highly hydrophobic proteins with four putative transmembrane domains with an overall amino acidic identity of 25-40%, that comprises at least 26 members in mouse and humans [7, 213].

The overall domain organization is consistent among the members, both at the transcript and at the protein level with few exceptions, and they all include splice variants, usually generating truncated forms. All the boundaries exon/intron/exon show consensus splice-donor and –acceptor sequences, with recurrent exon/GTGAGT-intron-CAG/exon sequences [214].

These proteins share the secondary structure with tetraspanins although they present a different primary backbone [135]. Despite the noteworthy conservation of the first two transmembrane domains (VLGAIQIL sequence in the first transmembrane domain and GYPFWG in the second), the hydrophilic N- and C-termini (although in all the members they result rich in Pro residues) and the fourth transmembrane domains, probably the one involved in the interaction with other proteins, these molecules exhibit a higher degree of dissimilarity [215].

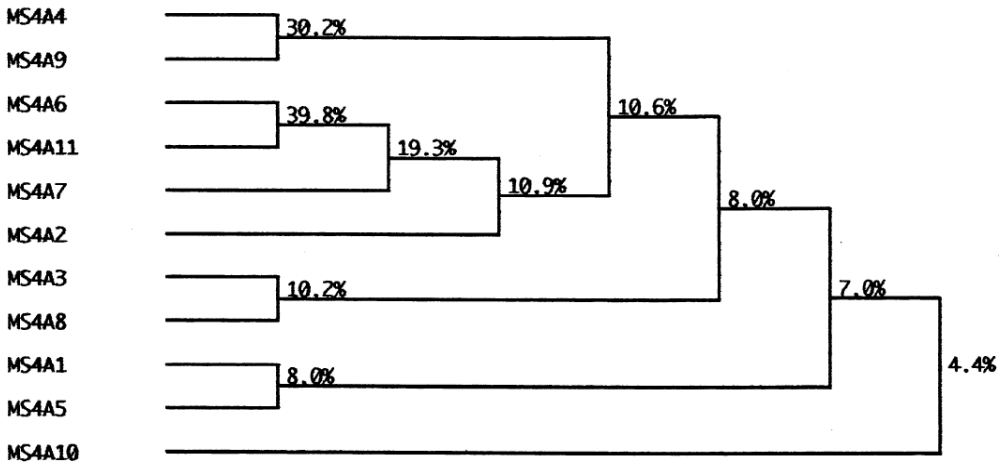

Fig. 12. **Phylogenetic analysis for MS4A family members**. Tree construction performed following Higgins' method (Higgins et al., 1992). The percentages refer to the degree of identities. Adapted from Ishibashi, Gene, 2001.

The short intracellular loops between second and third transmembrane domains are also conserved and include phosphorylation sites for protein kinase A and C, covering a hypothetical role in cell signaling.

The members of this family are typically found in lymphoid tissues such as intestines, spleen and thymus and most of them are expressed in lymphoid and hematopoietic cells, therefore likely to play a relevant role in immune system although some clones do also exist in non-lymphoid tissues.

At present, all the genes belonging to the MS4A family are linked on a 600Kb region on chromosome 11q12-13 in human and on chromosome 19 in mouse [216, 217], suggesting a cluster of related genes evolved from recent duplication events.

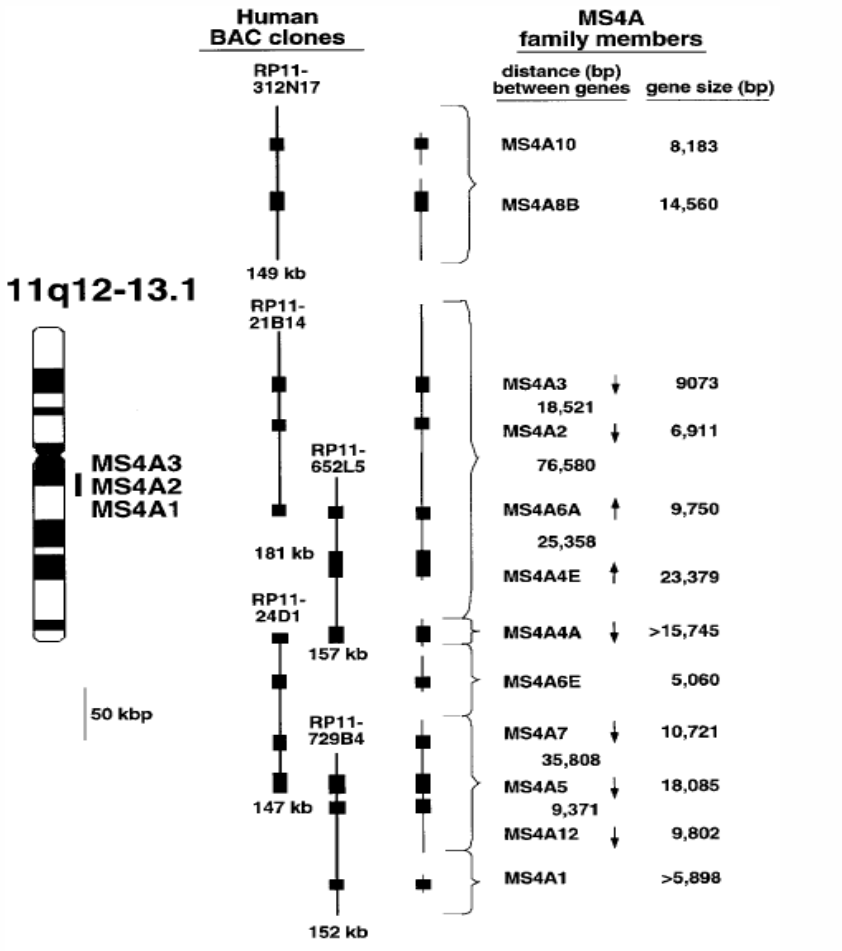

Fig. 13. Structural organization of the human MS4A gene cluster on Chromosome 11q12.
From Yinghua Liang, Immunogenetics (2001)

Most of the MS4A proteins are encoded by six exons except for MS4A2, MS4A5, and MS4A6E. The cytoplasmic N-terminal of MS4A2 is encoded by two exons, while MS4A5 and MS4A6E proteins lack in the C-terminal domain. Moreover, the latter exhibits only two transmembrane domains, making it the smallest MS4A member (5060 bp). On the other hand, MS4A4E results the longest gene with its 23,379 bp [218].

Chromosome 11q13 is a genomic region linked to atopy and allergic disease, with nucleotide sequence polymorphisms in MS4A2 and MS4A3 correlating with disease susceptibility [219-222]. Whether sequence polymorphism recognized in the MS4A2 and MS4A6A genes equally combine with allergic disease hasn't yet been established [223, 224].

The same polymorphisms within Chr 11q12 are also recurrently found in some cancers such as renal oncocytomas [225], lung cancers [226, 227], ovarian tumors [228], and atopic allergies [220]. By the way only one mutation seems not to be enough to determine the onset of the disease.

	MS4A1	MS4A4	MS4A5	MS4A6	MS4A7	MS4A8	MS4A9	MS4A10	MS4A11
Spleen	+++	−	−	−	+++	−	+	−	+
Thymus	+	−	−	−	−	−	+	−	++
Intestine	−	+	−	+	+	+++	−	+	+
Colon	−	+	−	+	+	+++	−	−	+
Lung	+	−	−	−	−	+	++	−	+
Testis	−	−	++	−	−	−	+	−	−
Ovary	−	−	−	−	−	−	+	−	−
Heart	−	−	+	+	−	−	−	−	±
Muscle	−	−	−	−	−	−	−	−	−
Kidney	−	−	−	+	−	−	−	−	−
Liver	−	−	−	−	−	−	−	−	−
Brain	−	−	±	−	−	+	++	−	−
Pancreas*	nt	−	++	−	−	nt	nt	nt	nt

Fig.14. Expression profile of MS4A clones by northern blot. +++, highly expressed;++, moderately expressed; +, weakly expressed; ±, very weakly expressed; -, not expressed; nt, not tested. From: Ishibashi, Gene, 2001

The most well-known MS4A genes are MS4A1 (CD20), MS4A2 (FcεRIβ) and MS4A3 (HTm4), although recently several new members have been described [229-231]. Despite the homology in structure and sequence, MS4A proteins present different regulation at the transcriptional level and their functional properties may change within different cell types.

1.3.1. CD20/MS4A1

CD20 is an activated-glycosylated phosphoprotein with a molecular weight of 35 kDa, long N- and C-terminal ends placed within the cytoplasm. It was first described by Tedder and Engel in 1994 as a B-cell precursors and mature B cells specific marker involved in the signaling and cell cycle progression of these lymphocytes [232].

Its overexpression in fibroblasts resulted in the formation of a homo- or probably heterotetrameric receptor complex behaving as a Ca^{++} permeable-ligand independent-cation channel. It seems to constitutively co-localize with the B cell receptor, dissociating from it once this latter is engaged by its ligand [233-235]. CD20 oligomerization occurs within specific plasma membrane domains, called lipid rafts, promoting Ca++ conductance and the progression of the cell cycle and eventually apoptosis, once the molecule is activated.

Several works speculated the CD20 membership to a wider transmembrane complex that includes BCR and CD40 [236-239]. These two proteins seem in fact to activate and down-regulate CD20 respectively, with a mechanism that involves CD20 internalization [238, 239].

Since its expression is found from late pro-B cells to memory cells, but neither on early pro-B cells nor plasma blasts and plasma cells [233], mAb against CD20, in first place Rituximab, represent one of the most effective passive immunotherapeutic drugs for the cure of B-cell lymphomas, autoimmune disease [240, 241] and non-Hodgkin's lymphoma [242-244].

In the attempt to search co-expression and potential association of CD20 with other MS4A members in order to find some alternative targets for therapy,

MS4A4A, MS4A6A, MS4A7, MS4A8B and TMEM176A and TMEM176b expression was analyzed in B cell lines. MS4A4A and MS4A8B and the two TMEM were not detected neither in normal nor in B cells lines, while MS46A and MS4A7 were only weakly expressed in terms of transcript, but undetectable in terms of proteins, pointing out that CD20 does not form oligomers with its cognates MS4A proteins [8].

1.3.2. FcεRIβ/MS4A2

FcεRIβ, together with an IgE-binding α, β and two γ-chains constitute a tetrameric receptor complex [245] generally expressed on cells responsible of allergic responses, like basophils and mast cells where mediates interactions with IgE opsonized antigens mediating acute allergic

reactions [219, 246]. Although generally present ad a tetramer in humans, the complex may occasionally lack in the β-subunit [247, 248].
The signaling cascade activated by FcεRI upon ligand biding, leads to the issue of cytoplasmic mediators and the secretion of lipid mediators and cytokines.
The major FcεRI β isoform mediates a strong enhancement of effector cells capability to mount an allergic response, while the truncated variant (βT) inhibits the expression of the receptor on the surface, dampening this effect and regulating the immune reaction.
The genomic region baring the β-chain sequence has been described as linked to atopy and polymorphisms within this gene are associated with atopic syndromes, making it a putative marker for allergic diseases, although a specific phenotype for this locus hasn't been described yet.

1.3.3. HTm4/MS4A3

HTm4 is a protein of 214 amino acids, principally localized in the nuclear membrane, which .expression has been reported both in lymphoid and myeloid hematopoietic lineages, although it seems to be prevalent in basophils, and almost absent in monocytes, granulocytes, CD19+ B cells and naïve T cells [249]. The use of polyclonal antibodies revealed its presence in a variety of tissues such as hematopoietic cells of human fetal liver, adult lymph nodes, the lymphoblast in the cortical thymus, ovary, mammary epithelium, testis, pancreas, prostate, stomach and in the fetal brain ventricular zone.
Kutok and colleagues, in 2005, considered that, given the high expression of the protein in fetal hematopoietic cells and in the thymus cortex, which contains the earliest lymphoid precursors, HTm4 might play an important role in hemato-lymphoid development.
Also in some malignancies a weak staining revealed the presence of HTm4, specifically in endometrial, ovary, breast and prostate adenocarcinoma, but the meaning of its presence within the tumor microenvironment is not clear.
Interestingly, as well as reported for FCERIβ, the TaqI polymorphisms (RFLP) within its introns also seem to correlate with atopic asthma.
The evidence HTm4 expression levels drop upon late stage differentiation may suggest it may contribute to regulation of the cell proliferation [213] and recent studies indeed found HTm4 able of binding the cyclin-dependent kinase-associated (CDK-associated) phosphatase-CDK2 (KAP-CDK2) complexes on its C-terminal region, promoting KAP phosphatase activity and determining

the cell cycle arrest at the G0/G1 phase. Recently it has been demonstrated how actually regulation by HTm4 occurs by interfering with cell cycle progression [250].
For what concerns murine models, a sturdy expression has been found in developing brain, with the strongest staining within the glial cells and fetal neurons, so called Cajal-Retzius and subplate-like cell, reinforcing a preexisting idea of HTm4 involvement in cortical organization [251]

1.3.4. Other MS4A members

1.3.4.1. MS4A4A

This member presents an open reading frame containing 205 amino acids that include a consensus protein kinase C (PKC) phosphorylation site at the level of the intracellular loop.
Liang and Tedder found MS4A4A being expressed in colon and small intestine in two bands of different sizes in mouse but couldn't detect any positivity in the same human samples.
However, a strong positivity was found within all the human hematopoietic cell lines, which do all express the full length transcript, although a second smaller transcript seems also to be expressed from the B-cell line BJAB, in which almost half of the cDNA encodes the truncated protein.
These splice variants generally excise the third transmembrane-encoding exon, joining the first two transmembrane domains with the fourth one, and since this latter is followed by a hydrophobic region barely long enough to pass the membrane [7], alternative splicing within this region may generate a protein with four transmembrane domains missing the second extracellular domain.
Recently, in a gene expression profile study of classically and alternatively activated macrophages, MS4A4A was identified as an IL-4 regulated gene, suggesting a potential role in orchestrating lipid metabolism, defense against ROS and basal expression of inflammation associated genes [252].

1.3.4.2. MS4A5

The full length MS4A5 is a 200 amino acids protein characterized by a protein kinase A phosphorylation site (KRKTT) in its intracellular loop.
The main splice variant is generated from the excision of the third transmembrane domain and the second extracellular loop encoding exons causing the fusion of the first/second transmembrane

domains with the fourth one and resulting in a three transmembrane domains isoform with an extracellular C-terminal.
This member is mildly expressed in pancreas, heart, brain and testis in humans [213].

1.3.4.3. MS4A6A

MS4A6A is 178 amino acid long and displays as well a protein kinase A and three protein kinase C phosphorylation site (KRLT) within the intracellular loop.
A 70 amino acid shorter variant lacking the fourth transmembrane and cytoplasmic domains originates from the alternative splicing of the third transmembrane domain, generating the only known MS4A member without a C-terminal.
Its expression has been found in heart , kidney, and small intestine and its expression may be linked to development since no transcript is visible in human fetus samples [213].

1.3.4.4. MS4A7

MS4A7 is characterized by 240 amino acids sequence with a n acknowledged protein kinase A and four protein kinase C phosphorylation sites (KKSS) at the C-terminal. Currently, three splice variants are known, among which one shares high identity with MS4A6E.
The expression of this member is restricted to the spleen in human, small intestine and colon in mouse [7].

1.3.4.5. MS4A9

Its ORF has 226 amino acids and includes a consensus tyrosine phosphorylation site (KNVPENVY) at the C-terminal, while the long hydrophilic N-terminal displays three protein kinase C phosphorylation sites. Expression was found in thymus, testis, lung, brain, and ovary [213].

1.3.4.6. MS4A10

Characterized by 726bp, its gene includes 6 exons with transcripts that result primarily expressed during oncogenesis or embryogenesis but are infrequent within normal tissues [213].

1.3.4.7. MS4A11

Its ORF has 247 amino acids with a protein kinase A phosphorylation site (KKMT) and four protein kinase C phosphorylation sites at the intracellular loop.
It IS expressed in colon, thymus, intestine, spleen, lung, heart and testis [213].

1.3.5. MS4A in Alzheimer disease

As cell membrane proteins, MS4A members were shown to take part in the regulation of calcium signaling, a process strictly connected with neurodegeneration [253].
Alzheimer's disease (AD) is the most common human complex neurodegenerative pathology. Because of the constant increase in life expectancy, the incidence of AD is keeping on growing [254]. AD causes a progressive brain neuronal loss, which normally ends up with the death of the patient and although its etiology is still not clear, genetic factors seem to play a pivotal role.
Recently, several variants within the MS4A gene cluster, in particular the MS4A4/MS4A6E/MS4A6A locus, have been associated with the disease within recent serial genome-wide association studies (GWAS) [255].
Common variants located within highly expressed MS4A6A transcripts were significantly associated with Alzheimer. Further copies of the protective (minor) allele were associated with lower MS4A6A expression of each transcript and in heterozygous subjects, expression of the protective allele transcripts was lower. Regardless the genotype, MS4A6A transcripts were increased in blood from AD people and they were also widely expressed in tissues and cells. These evidences suggest that high levels of MS4A6A in Alzheimer's disease are detrimental. Inhibiting the molecule may therefore promote a more neuroprotective activity, although further work is needed to establish whether this is actually the case [256].

1.3.6. MS4A and cancer

The fact most of MS4A members seem to be involved in cell cycle regulation, implicates they play a significant role in tumor development, either promoting cell proliferation and supporting carcinogenesis, or acting like a marker of differentiation.
Their presence has been described on both normal and neoplastic tissues, therefore the understanding of their role among different cell types and malignances, may represent a valid tool for the therapeutic exploitation of these molecules, as happened for the Rituximab target CD20.

1.3.6.1. MS4A8

MS4A8 ORF's comprises 268 amino acids but no phosphorylation sites has been found for this member.
Its putative function was first described in a murine model of malignant melanoma within a subset of tumor associated macrophages (TAMs) profiled as stabilin1-lyve1 f480 positive cells, induced by IL4, GC and tumor conditioned medium and regulated by an integration of the p38 MAPK and the glucocorticoid receptor (GR) pathways, therefore acknowledged as a marker of macrophage alternative polarization. Indeed, when transfected with the murine sequence for MS4A8B (Ms4a8a), RAW264.7 cells showed both up-regulation of the M2 marker arginase I (argI) and a specific gene signature characterized by Tcfec, spink5, sla and sorl1, active in immune regulation. In the same study Ms4a8a+ RAW264.7 cells turned out supporting the tumor growth when transplanted in vivo, opposite to what happened with the transplantation of the same cells transfected with the control plasmid [229].
One year later, Michel et al. defined its expression as not restricted to hematopoietic cells, but extended in differentiated intestinal epithelium. Interestingly, MS4A8 expression was not detected in colon carcinoma and when overexpressed in carcinoma cell lines it led to a reduction in proliferation and migration rate and an overexpression of the intestinal differentiation marker cytokeratin 20, making MS4A8 a differentiation marker for colonic epithelial cells [257]

Very recently, MS4A8B mRNA was detected by RT-PCR in 13 types of human normal and cancer tissues, resulting over-expressed specially in prostate cancer. Furthermore, the immunohistochemistry performed for MS4A8B and PCNA proteins as diagnosis index of

proliferative activity, revealed a positive association of both markers with the tumor severity in 140 prostate cancer samples [258]

In vitro, MS4A8B knockdown and overexpression resulted in G_1-S cell cycle arrest or accelerated S phase entry, respectively and it was able to modulate the expressions of Cyclin D_1, Cyclin E_1 and PCNA.

Lentiviral infection of pancreatic tumor cell lines with sh-MS4A8B caused a reduced growth rate of the tumor mass when injected subcutaneously in mice [258].

1.3.6.2. MS4A4B

MS4A4B was first described by Venkatamaran in 2000, as selectively expressed in Th1 cells and both transcript and protein are down-regulated during T-cell differentiation under Th2 conditions [215, 259].

It as well shows a differential expression during immature thymic development, existing in naive CD4+ and CD8+, NK cells, thymocytes at pre-commitment and at mature stages. It was also reported in myelo-monocitic lines, but disappeared upon stimulation with MCSF.

MS4A4B is negatively regulated by IL4 via STAT6 signaling but not affected by either IL-12- or IFN-gamma since its expression was found in STAT4, STAT1 and INFɣ KO.

It localizes at the cell surface within detergent-resistant membranes and migrates into lipid rafts upon activation of naive primary T cells [215].

Using it as baits in a yeast split-ubiquitin library screen for T regulatory cells, MS4A4B has been demonstrated to interact with MS4A6B and with GITR, Orai1, and other surface receptors and in, more in detail, interaction of MS4A4B with GITR (a negative regulator for Tregs and activator for effector T cells) augments GITR signaling and T cell IL-2 production in response to GITR stimulation.

By making use of this innovative version of the more common yeast two hybrid assay, Howie provided for the first time a process whereby MS4A proteins, may boost Ag signals through the lateral association with co-stimulatory receptors.

In other words, Ms4a4b enhances the sensitivity of GITR for its ligand, lowering the threshold for the amount of antigen needed to trigger the response [230].

By far, MS4A4B expression was never reported in malignant cells. This is consistent with the evidence that it actually works as survival modulator to preclude the overgrowth of the activated cells.

Its inhibitory activity towards proliferation occurs by affecting the cell cycle progression enhancing the expression of the cell cycle inhibitor subunits $p16^{Ink4a}$, $p21^{Cip1}$ and $p27^{Kip1}$, and diminishing cyclin A and B and Cdk2 activity and promoting de phosphorylation of Rb with blockade of transcription and cell cycle arrest.

Also the impact of MS4a4B on the intracellular Ca^{++} production that activates the Ca^{2+}/CaM signaling pathway leading to the up-regulation of Camk2a, promoting the transcription of Cdk inhibitors has to be taken into account.

At the same time, the evidence ms4a4b is not expressed in apoptotic cells, points out the potential protective role of the molecule towards T cells, most likely prolonging their survival [215].

The selective expression of Ms4a4b on inflammatory T cells allowed the production of an antibody able to target these cells, that was successfully tested in a model of experimental autoimmune encephalomyelitis (EEA) ameliorating the EEA severity, through the suppression of ms4a4b bearing T cells [260].

More recently, ms4a4b has been shown to localize within ciliated airway epithelial cells and its loss correlates with epithelium loss during severe asthma. Its expression augmented during primary bronchial epithelial cells differentiation, decreased during rhinovirus infection, and BEAS cell line transfected with it shown inhibition of pro-inflammatory cytokines suggesting an important role in the maintenance of airway epithelial cells homeostasis [261].

1.3.6.3. MS4A12

In contrast to the majority of members of the MS4A family, MS4A12 has never been described in cells of the hematopoietic or lymphatic lineage.

MS4A12 stains specifically the apical membrane of epithelial cells within the colonic crypts and has been described as a novel colon-specific gene typically expressed in normal mucosa which is thought to support malignant transformation, being part of the store-operated Ca2+ (SOC) channel and thus able to promote proliferation and chemotaxis of colon cancer cells by modifying signaling through epidermal growth factor receptor (EGFR) [262].

The rational for this very specific expression was given by Koslowsky, who discovered that MS4A12 activity is ruled by a homeobox transcription factor binding element on its promoter that recognizes the intestine-specific endogenous transcription factors CDX2 [263].

These findings make MS4A12 suitable for becoming a novel candidate for therapeutic antibodies targeting.

1.4. C-type lectin receptors

C-type lectin receptors were initially regarded as proteins that recognize carbohydrates via a different fold in a calcium-dependent manner, through a carbohydrate recognition domain (CRD) [264]. The C-type lectin receptors family includes over 75 different transcripts of both classical and non-classical members, with 17 sub-groups based on the domain structure [264, 265]. 'Classical' C-type lectins like DC-SIGN and langerin associate with the ligand in a calcium-dependent manner, while they are considered 'non classical' when the binding does not occur in the presence of Ca++ and in this case the domain is mentioned as a C-type lectin-like domain (CTLD) [264]. Some receptors belonging to this subgroup are dectin-1, CLEC-2 and CLEC9A.

1.4.1. The C-type lectin-like receptors group V

The non-classical C-type lectin-like receptors group V consist in a separate subfamily of proteins, (which includes the so called Dectin1 cluster members Dectin-1, CLEC-2, CLEC9A, AICL, CLEC-1, LOX-1, and MICL) that are expressed in monocyte, dendritic and endothelial cells, in which they share the same domain structure, and are encoded within the same region on human chromosome 12 and murine chromosome 6 named natural killer (NK) gene complex [266]. These all are type II, single-pass transmembrane molecules with a single CTLD activated in a calcium-independent manner, a stalk region, a transmembrane region and a cytoplasmic end that usually consists in a signaling or internalization sequence consisting in a ITAM-like, ITIM and/or tri-acidic sequences [267-269].

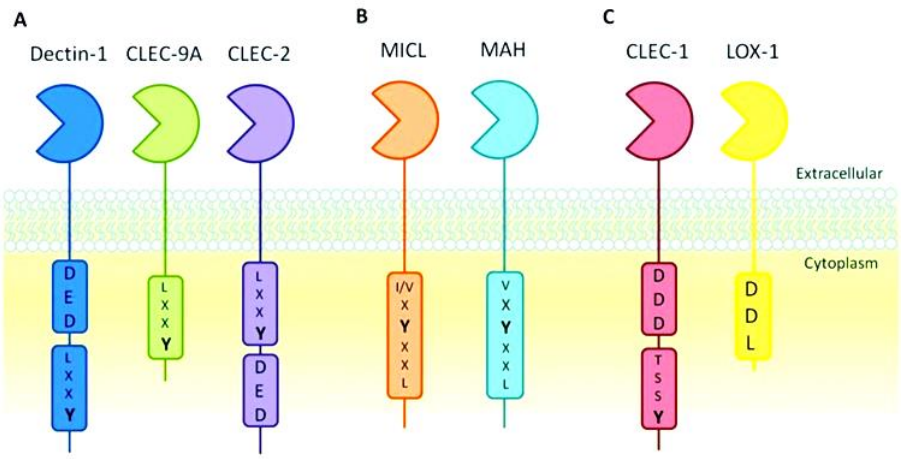

Fig.15. The Dectin-1 cluster. A: The activatory receptors Dectin-1, CLEC-2 and CLEC-9A with ITAM-like and DED tri-acidic motifs, (except CLEC-9A). B: The inhibitory receptors MICL and MAH with canonical ITIM motifs. C: CLEC-1 with its uncharacterized DED- Y-based motif and the C-type lectin-like scavenger receptor LOX-1, with a DDL motif. From Plato et al.2013

1.4.1.1. Dectin-1

Microorganisms display peculiar and highly conserved components on their surface called pathogen-associated molecular patterns (PAMP) that can be recognized by specific pattern-recognition receptors (PRRs), like TLRs and the C-type lectins, expressed on antigen presenting cells [270, 271].

Both human and murine hortologs are primarily expressed on myeloid cells including monocytes, DCs, neutrophils and macrophages as well as on some T cells subpopulations [272], human B cells, mast cells and eosinophils and, as recently reported, mice microglia [273-275]. Dectin1's expression levels on these cell populations change among different tissues with the sites of pathogen entry (e.g. lungs, spleen and gut) showing the greatest levels and playing therefore an essential role in the immune responses against pathogens [272, 276]. The main two human isoforms are distinctly expressed in different cell types and so occurs in different mouse strains [277]. Cytokines, chemokines or microbial factors can modulate Dectin1 expression [278, 279]. For instance, IL10, LPS and dexamethasone cause down-regulation of Dectin1 [278] while IL4, IL13 and GM-CSF cause Dectin1 expression to be highly up-regulated. Furthermore, the systemic provision of both purified β-glucans and *Candida albicans* increases Dectin1 expression in leukocytes, opposite to what happens during polymicrobial sepsis [279, 280]. It has also been proven that glycosylation promotes murine Dectin1 surface expression [281].

The importance of Dectin1 in host defense has recently been established by making use of knock out mice, which shown an impaired immune response to *Pneumocystis carinii* [282] and *Candida albicans* [283] fungal infections, although the latter work found Dectin-1 not being essential for the defense against *Candida albicans*, most likely because of the different paths of infection, fungal strains used and mice genetic background [284].

1.4.1.1. Expression and structure

Dectin1 belongs to the so called dectin1 cluster, within the natural killer gene complex on human chromosome 12 and mouse chromosome 6 [266, 285]. At least two isoforms of murine Dectin1 exist that encode either the full length or the stalk-less version of the receptor through alternative splicing, (fig), therefore presenting differences in the capability to bind β-glucans and promote cellular responses [277]. Both these forms are N-glycosylated at two sites at the extracellular level [286].

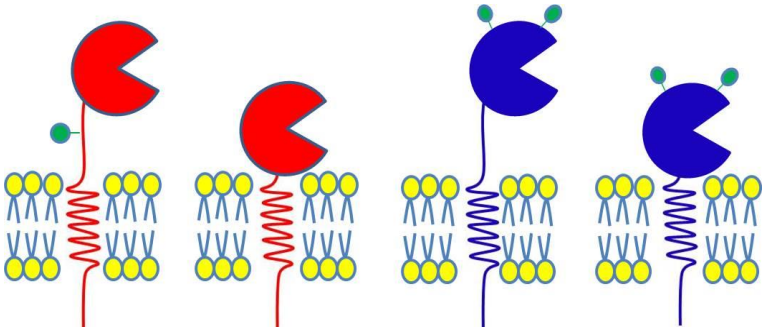

Fig. 16. Human and Dectin1 isoforms. Human (red) and murine (blue) Dectin1 isoforms. All the isoforms contain an extracellular CTL domain, a transmembrane domain and a cytoplasmic one. Both the murine forms are N-glycosylated at two sites at the extracellular level (green), while only the human full length one presents one glycosylation site.

In humans, eight isoforms derive from alternative splicing, of which only the main two are functional for the binding of β-glucan [273] and the major of which lacks the stalk region and has no glycosylation sites. The other one contains an N-glycosylation site in its stalk region instead [273, 287]. Not much is known about the other minor isoforms, except that one is kept in the cytoplasm and shows association with a Ran-binding protein, (RanBP) [288]. The functional importance of this interaction is still to be determined.

As already mentioned, Dectin-1 C-type lectin-like domain has a binding site for β-glucan (which W221A/ H223A mutation impairs its binding activity), connected by a stalk to a transmembrane domain followed by a short cytoplasmic terminal [286]. Unlike many other lectins, the absence of Cys residues in Dectin1 stalk region, suggests it may operate as a monomer, rather than dimerizing. The signaling motif within its cytoplasmic tail consists in a YXXL motif that undergoes

phosphorylation of the Tyr residue by Src family kinases, thus promoting signaling cascade through the phospholipase C (PLC) γ2 pathway [289, 290].

1.4.1.1.2. The dectin-1 ligand, β-glucan

Although several ligands have been described, Dectin1 is better known for its ability to recognize β-glucans, polymers of D-glucose, the major component of fungal cell walls. It is indeed estimated that more than 50% of the cell wall of *Saccharmoyces cerevisiae* is made up of β-glucan polymers [291]. Some of the Dectin-1 ligands, like Curdlan and Zymosan, are commonly used to explore the role of this receptor in *in vitro* and *in vivo*. Curdlan is purified from *Alcaligenes faecalis* and is made of polymers of linear glucan, while Zymosan is purified from *Saccharmoyces cerevisiae*, and since it contains mannan, chitin and other proteins, it can activate other receptors besides Dectin-1 [292]. Dectin1 was initially described as a DC specific receptor that modifies T cell function recognizing an unidentified ligand on their surface [293, 294]. It was first acknowledged as a β-glucans receptor after a screen of a murine macrophage cDNA expression library with Zymosan [295]. Dectin1 specificity for β-glucans was then further tested using oligosaccharides microarray technology, confirming that actually the receptor binds β (1-3)-linked oligomers of glucose in a metal ion dependent manner [294] and that at least a branch of heptasaccharides is required for the binding to occur [296]. The Ca^{++} dependent mechanism behind this process is not fully understood yet, however at least two residues flanking a superficial groove on the protein surface, Trp221 and His 223, have been associated with the binding [286]. and the glucan polymers helical structure may itself support this interaction[296]. Thanks to its β-glucan specificity D ectin1 resulted recognizing various fungal species including *Candida*, *Pneumocystis*, *Saccharomyces, Aspergillus, Coccidoides and Penicillum* [9, 282, 283, 297-302] and, more recently, some members of Mycobacterium family [303], although the specific ligand on these microorganisms remains unknown [303-305]. Studies on cell lines showed that Dectin1 can also interact with an endogenous ligand on apoptotic cells [306].

1.4.1.1.3. Signaling pathways

The interaction between β-glucan and Dectin-1 induces the secretion of several cytokines and chemokine, such as IL -6, IL -12,IL-10, IL-23, IL-2, TNFα and CXCL2, regulates ligand uptake via phagocytosis and endocytosis and activates the respiratory burst and the synthesis of arachidonic acid metabolites [270, 271], covering a fundamental role in managing fungal infections.
Dectin1 signaling occurs through an short N-terminal immune-receptor tyrosine-based activation (ITAM)-like (also called hemi-ITAM) and tri-acidic [DED] motifs in its cytoplasmic tail and can activate either a Syk dependent , leading to both canonical and non-canonical NF-kB activation, or a Syk independent signaling pathway (Fig.17). The typical ITAM motif exhibited by all the B cells, T cells and Fc receptors, includes a consensus sequence with two tyrosine residues, 10-12 AA apart: YxxI/Lx YxxI/L [51, 267, 307-309]. Once the receptor is bound with its ligand, the Tyr are phosphorylated by Src kinases, allowing Syk kinases recruiting through their SH2 domains [310, 311]. However, opposite to the more common ITAM receptors where the phosphorylation of both Tyr is required for Syk engagement, one phosphorylated Tyr is enough for Syk to associate with Dectin1, although both SH2 domains are needed [289, 312].

Canonical NF-kB activation

As demonstrated in DCs challenged with *Candida albicans* or Zymosan, the association of Dectin1 with the spleen tyrosine kinase Syk kinase leads to the activation of the phospholipase Cγ2 (PLCγ2) which in turn results in the recruitment of the caspase-recruitment domain containing protein (CARD9), the adaptor protein B-cell lymphoma leukemia 10 (Bcl-10) and the mucosa associated lymphoid tissue lymphoma translocation protein 1 (MALT1) complex, that activates the canonical p65/c-Rel/NF-κB pathway [313, 314]. CARD9 seems to play an intermediary role in connecting Dectin-1 signaling to NF-κB activation and it takes part to the secretion of IL-12 [313, 315].
Moreover, mice KO for CARD9 display lower survival rate following *Candida albicans* infection compared to the WT mice [313]. The mechanism by which CARD9 is recruited by PLCγ2 and initiates the downstream cascade seems to involve the PKCδ isoform [316].

Also Dectin1- mediated IFN-β production upon *C. albicans* infection resulted from Syk/ Card9-driven signaling but relies on the transcription factor IRF5 recruitment [317].
Despite its important role, not all the cellular responses regulated by Dectin1/Syk pathway depend on CARD9 (e.g. the MAP kinase ERK) [318].

Non canonical NF-kB activation

Other than the canonical one described above, Dectin-1 can mediate a non-canonical NF-kB activation pathway exploiting NF-κB-inducing kinase (NIK) through Syk dependent activation, leading to the assembly of p52 dimers and RelB [319].

Syk independent pathway

Furthermore, a Syk-independent pathway involving Ras and the serine-threonine kinase Raf-1 activation can be triggered by Dectin-1, integrating with the Syk cascade at the level of NF-kB activation. In fact, the Raf-1- phosphorylated p65 generates a p65-RelB dimer, thus isolating RelB, preventing its association with DNA, in favor of Raf-1-dependent IL-12p70 as well as many others pro-inflammatory cytokines production required for the differentiation of T_H1 cells.

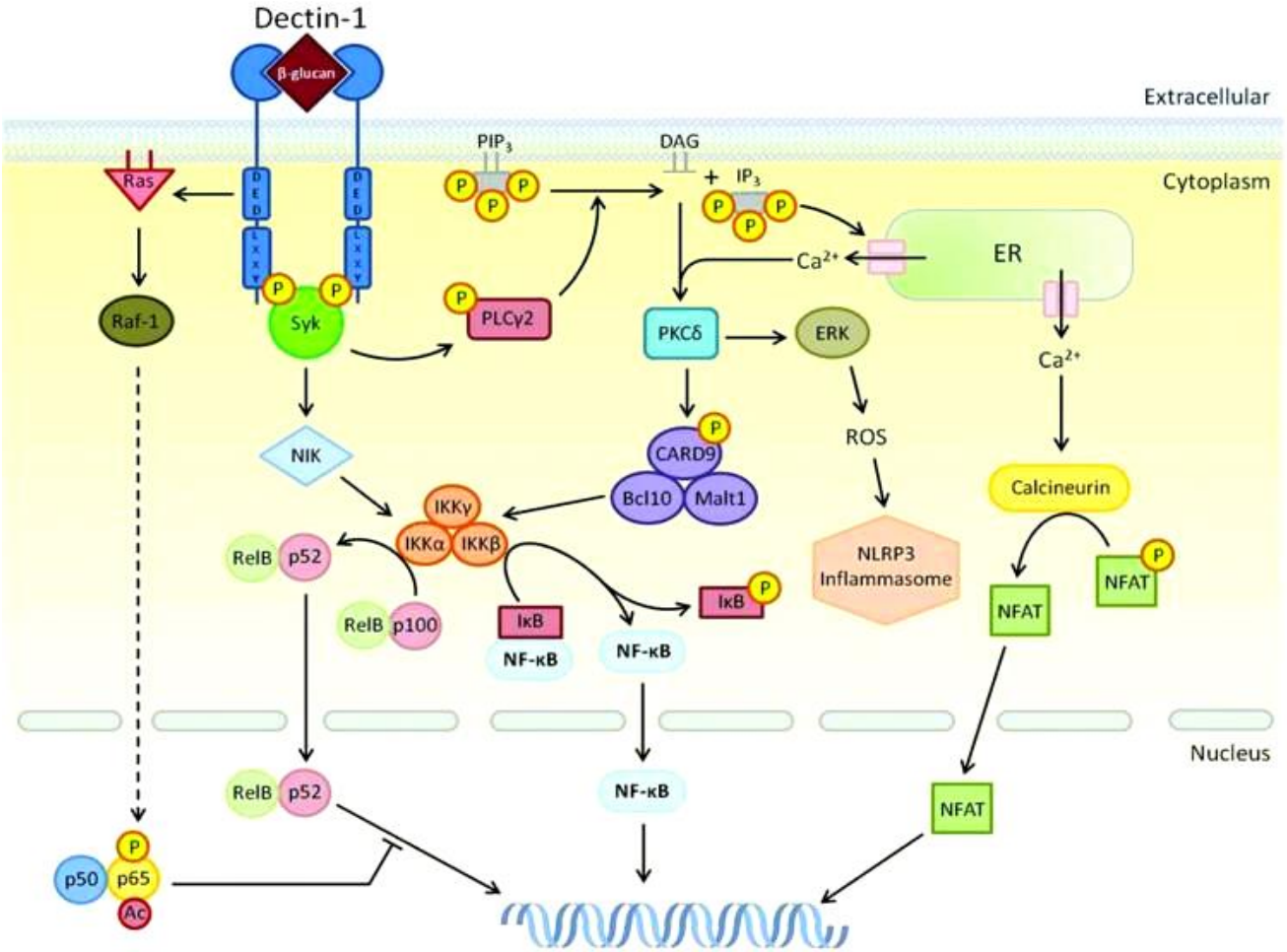

Fig. 17. Dectin-1 signaling network. Recruitment of Syk upon interaction with the ligand activates PLCγ 2/Ca2+ mediated signaling triggering PKCδ that phosphorylates CARD9-Bcl10-Malt1 and controls calcineurin/NFAT and ROS/NLRP3 inflammasome. CARD9 complex activates NF-κB and c-Rel, promoting transcription. Syk can also initiate a non-canonical NIK pathway, mediating the activation of RelB and p52, which can be however inhibited by the Raf-1-mediated pathway that phosphorylates p65. This can in turn sequestrate RelB, preventing its interaction with the NF-κB complex.

Dectin1 can also signal via calcineurin/ NFAT through the PLCγ activated by Syk, inducing as ultimate effect the expression of IL-2 and IL-10 and the fate regulation of Tregs and other lymphocytes populations [320].
The complexity of the Dectin1 signaling pathway clearly reflects the importance of this receptor in tuning and finely regulating the immune response.

Dectin1 is also uniquely able to elicit mediators of adaptive immunity without coupling with TLR, resulting for instance in the induction of Th1 and Th17 CD4+T cells following *C. albicans* and *M. tuberculosis* infection of DCs [314, 321]. Moreover it can also switch specific Tregs populations into IL17 producing non Th17/non regulatory T cells with intermediate phenotype through DCs activation (Osorio 2008). Dectin1 has also been implicated , along with TLRs, in the enhanced functionality of CD4(+)CD25(+) T regs in Zymosan treated Type 1 Diabetes murine models [322].
Finally, other than CD4+ cells, Dectin1 antibody mediated targeting can determine CD8+ T cells differentiation into cytotoxic T-lymphocyte [323, 324].
Noteworthy, all the responses mediated by dectin1 turned out being cell-type specific [325, 326].

1.4.1.1.4. Dectin1 and other receptors

Always more evidences have been given, proving that multiple PRRs need to be primed by microbes in order to be able to induce an efficient immune response. Association of Dectin1 with MyD88 coupled TLRs is for instance required for a proper induction of the cytokine repertoire (especially for TNFα in macrophages), [327], phagocytosis and for boosting the respiratory burst [328, 329] . On the contrary, TNF and IL10 do not require Dectin1-TLRs interaction for being

produced in DCs [314, 328] and in the same cells, the administration of Dectin1's ligands and/or TLR2 ligands results in the down-regulation of IL12 in favor of a higher expression of IL23, orchestrating in this way the Th17 responses [330].
Dectin1 can also interact with other pattern recognition receptors, like DC-SIGN , initiating the arachidonic acid metabolites pathway in human DCs [331] and promoting the fungal recognition by murine macrophages through the mouse hortolog SIGNR1 [332].

1.4.1.1.5. Dectin1 and tetraspanins

Other than PRRs, Dectin1 generates several interactions with tetraspanins within the TEMs located within the plasma membrane [159]. Mantegazza and colleagues beautifully described its association with CD63 showing the internalization of both molecules upon challenging with yeast particles by DCs, that was inhibited when soluble β-glucan laminarin was added to the cell culture. On the other hand, no internalization occur when DCs were given with the mannose receptor (MMR) ligand Dextran, indicating the specificity of the interaction during the phagocytic process, although its functional significance hasn't been elucidated yet [333].
Also the leukocyte-specific tetraspanin CD37 seems to interact dectin-1, since CD37 KO macrophages show higher Dectin1 induced IL-6 production despite the reduced dectin-1 surface expression and along with these findings, RAW264.7 cells show up-regulation of Dectin1 when transfected with CD37 cDNA. Also the co-immunoprecipitation of dectin-1 and CD37 performed by the same group in transfected HEK293T confirmed the former results [166]. It has been speculated that CD37 stabilizes Dectin1 at the membrane level, somehow down-regulating Dectin-1 signaling. Consecutive to these findings, van Spriel and colleagues confirmed in vivo that CD37 KO mice are better protected from *Candida albicans* infections, as they secrete more IL-6 and immunoglobulin (Ig) A compared to WT, [334].

1.4.1.1.6. Dectin1 and cancer

Being expressed on the surface of several APCs, Dectin1 recently became of significant interest in the context of anti-tumor innate immunity.
Human breast cancer development is sustained by the production of IL13 from anti-inflammatory Th2 cells due to the tumor driven induction of CD134L expression from DCs. In the attempt of

reprogramming Th2 into T cells with a pro-inflammatory phenotype (Th1), Wu and colleagues demonstrated how targeting the tumor associated DCs with the Dectin1 ligand β-glucan in vivo inhibits STAT6 phosphorylation leading to a down-regulation of CD134L. At the same time, the activation of Dectin1 by β-glucan in the presence of breast cancer supernatant, promotes IL12/p70 secretion expanding Th1 and CD8+CTL populations at the expense of Th2, inducing tumor necrosis [335].

NK-mediated killing of tumor cells is partially orchestrated by Dectin-1 expressed on DCs and macrophages [336, 337]. As previously described, in fact, Dectin1 is able to activate the transcription factor IRF5 leading to IFNβ production and thus modulating NK cells responses and the receptor is mandatory for the NK tumoricidal activity in vitro, as observed in Dectin1 deficient mice.

Moreover, Dectin1 is capable of directly binding N-glycan structures expressed on the surface of malignant melanoma, lung carcinoma, lymphoma and fibrosarcoma cell lines and these cells are more vulnerable to Dectin1 dependent-NK cell-mediated killing [338].

1.4.1.2. CLEC-2

1.4.1.2.1. CLEC-2 expression pattern

CLEC-2 has been initially discovered in a screening for NK receptors, and resulted later on expressed on DCs, monocytes, granulocytes, and especially on platelets [339, 340]. In two out of tree splice variants of the murine homolog the transmembrane region is missing, thus confining them within the cytoplasm [288, 341] the hemi-ITAM (YxxL) is also present on this member and seems to cover a main role in platelets signaling in response to rhodocytin (Suzuki-Inoue et al., 2006), a component of the venom of the snake *Calloselasma rhodostoma*, that determines platelet activation and blood coagulation [339].

It has been described that rhodocytin can interact with the collagen binding integrin α2β1/GPIb/IX/V complex [342], although mice lacking both the integrin and the GPIb subunit can still mount a response to rhodocytin [343], suggesting the presence and activation of another receptor on platelets subsequent to rhodocytin stimulation.

More recently ,CLEC-2 has been found a peripheral blood neutrophils activation receptor promoting the secretion of pro-inflammatory cytokines, particularly TNFα, and phagocytosis of Ab-coated beads but without triggering the respiratory burst [344].

1.4.1.2.2. CLEC-2 structure and signaling

As well as the other members of the CTLR, also CLEC2 requires Syk activation to induce cellular responses [312, 339, 345, 346] through its highly conserved tri acidic DED motif upstream the YXXL motif enabling an HemITAM-independent tyrosine-based signaling that, opposite to the ITAM-based receptors, is preceded by a Src mediated SH2-Syk binding of the ITAM-like sequence, phosphorylating it and leading to its activation [347]. CLEC2 phosphorylation seems to depend basically on its association with lipid rafts and, indirectly, on actin polymerization, and induce a signaling cascade activated by Rac1 and, subsequently PLCγ 2 [348].

The receptor seems to exist as a dimer as a dimer in resting platelets and switches to larger complexes following activation [349, 350] sometimes coupling with TLRs activity upon exposure to LPS, also increasing IL10 production in myeloid cells [351].

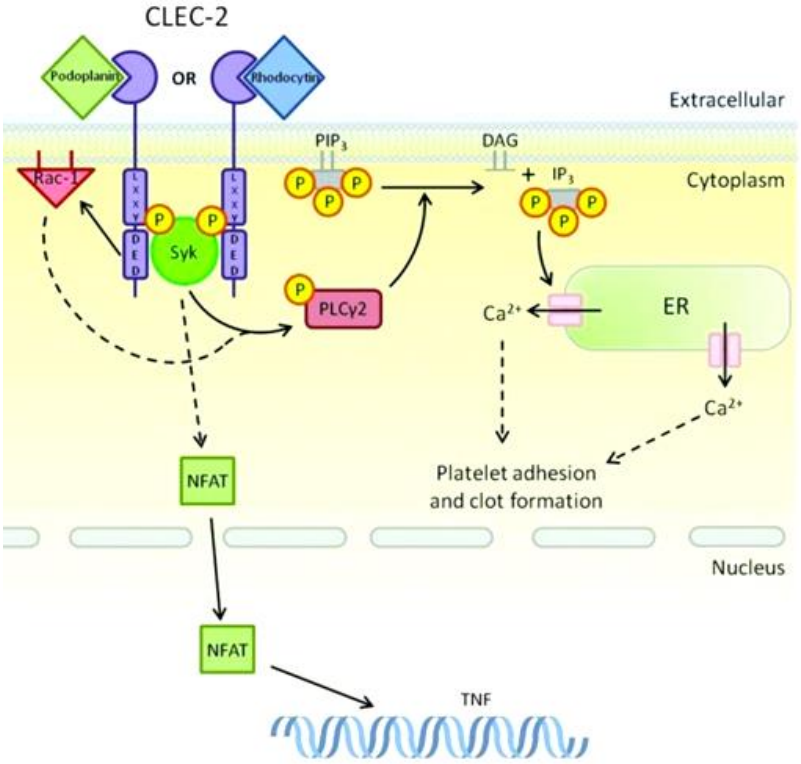

Fig. 18. ITAM-like-bearing CTLRs within the Dectin-1 cluster. As well as Dectin-1, there are two additional receptors that contain ITAM-like motifs. These receptors share Syk as a primary downstream signaling kinase; however, the lack of a tri-acidic in CLEC-9A and the presence of an isoleucine prevent the endocytic and activation functions of this receptor. CLEC-2 utilizes its tri-acidic motif to complement activation through Syk resulting in adhesion and clot formation in platelets. Dashed arrows represent a pathway that has yet to be fully defined.

1.4.1.2.3. CLEC-2 in hemostasis and thrombosis

In 2009 May and colleagues demonstrated a fundamental role for CLEC2 in platelets aggregation, making use of an antibody mediated depletion of the receptor in vivo, showing how although the CLEC-2-deficient platelets exhibited normal adhesion under flow, their ability to coagulate was impaired, as resulted from the increased bleeding times and diminished occlusive thrombus formation [352]

1.4.1.2.4. The CLEC-2 ligand, podoplanin

Another ligand proposed for CLEC2 is the endogenous transmembrane sialoglycoprotein podoplanin expressed on type I lung alveolar cells, tumor cells, kidney podocytes and lymphatic endothelial cells [353-356]. Podoplanin-induced platelet aggregation depends on Src family kinases and PLCγ2, as confirmed by podoplanin expressing-HEK293T cells, which are able to activate platelets [312, 339] and to bind CLEC2 expressing cells through a podoplanin mediated recognition [355] suggesting a mechanism by which tumor cells may approach and bind platelets to promote tumor growth, given the huge number of growth factors produced by these cells.

1.4.1.2.5. CLEC-2 and HIV-1

As well as its cognate molecule DC-SIGN, CLEC-2 seems to promote the binding of HIV-1 both by platelets and CLEC-2-transfected cells through its ectodomain [357]. Since the binding seems to take place during the viral budding process, it has been postulated the host protein involved in the recognition by CLEC2 is actually podoplanin [340].

1.4.1.3. CLEC9A

The first report about CLEC9A dates back to 2008, when Huysamen first identified it as C-type lectin-like activation receptor [267]. It shares similar features with the other members of the Dectin1 cluster, including multiple splice variants, of which the main one is expressed on plasmacytoid dendritic cells where it recognizes its F-actin ligand express indistinctively on the surface of all necrotic cells [307, 358-360] priming the activation of CTL [361, 362] via an internal cross-presentation pathway, therefore just cross-presenting without inducing cytokine production [363].

Similarly to Dectin-1 and CLEC-2, CLEC9A signals via Syk through a YXXL motif within its cytoplasmic tail [267, 307]. A crucial difference is that human CLEC9A has been shown to be expressed as a disulphide-linked glycosylated dimers [267].

2. AIM OF THE STUDY

This thesis is focused on the characterization of the regulation and function of the tetraspanin like molecule MS4A4A in alternatively activated macrophages.

In the first part we describe the regulation of the molecule by M2 stimuli, particularly GC.

In the second one we explore its association with tumor associated macrophages in human lymphoma samples and we describe the development of a MS4A4A targeting human anti human monoclonal antibody.

Finally in the third part we investigated the relationship between MS4A4A with the β–glucan receptor Dectn1 *in vitro* and *in vivo.*

3. MATERIALS AND METHODS

Chemicals and antibodies

Poly-L-lysine and Cycloheximide were from Sigma-Aldrich (St. Louis, Missouri, US). Sodium azide (NaN_3), paraformaldehyde (PFA), Triton X-100, glycine, Tween 20, phenylmethylsulfonyl fluoride (PMSF), EDTA and chemicals for lysis buffer, Phosphate Buffered Saline (PBS) and reducing sample buffer were from Merck Chemicals (Darmstadt, Germany). Lipofectamine 2000 was from Invitrogen (Life Technologies Ltd, Paisley, UK). Normal goat serum (NGS) was provided by Dako (Glostrup, Germany). Vibrant Lipid Raft Cholera Toxin B 594 was purchased from Molecular Probes (Life Technologies Ltd).

Recombinant murine chemokines were from R&D Systems (Minneapolis, Minnesota, US); recombinant human ones from Miltenyi Biotec (Bergisch Gladbach, Germany)

For Western blot and co-immunoprecipitation, antibodies for goat anti-human Dectin1 and rabbit anti human CD9 were from R&D, rabbit anti human CD63 was from SIGMA Aldrich, goat anti beta actin was from Santa Cruz. Mouse anti MS4A4A was from Abcam (Cambridge, England).

Anti-rabbit and anti-mouse IgG-horseradish peroxidase conjugated secondary antibodies were provided by Ge Healthcare GmbH (Freiburg, Germany). Anti-goat IgG-horseradish peroxidase conjugated secondary antibody was from Santa Cruz.

For confocal microscopy analysis and flow cytometry, anti-human MS4A4A monoclonal antibody and mouse IgG2a isotype control were from R&D Systems. Antibodies for human Dectin1-PerCP, CD206-FITC, CD163 AF700 and mouse IgG2a isotype control were from BD Biosciences (San Jose, California, US). Alexa Fluor-conjugated secondary antibodies, CellRox Deep Red Reagent, fluorescein conjugate Zymosan BioParticles, Hoechst-33342 and 4',6-diamidino-2-phenylindole (DAPI) were purchased from Molecular Probes.

Non conjugated-endotoxin free Zymosan was from Invivogen (San Diego, California).

Plasmids

Human MS4A4A, MS4A6A, MS4A7, Dectin1, CD63 were expressed with pcDNA3.1 vector (Invitrogen), pEGFP-N1 or pmCherry-N1 vectors (Clontech, Mountain View, California, US), amplifying the codifying sequences with primers with the restriction sites for BamHI and XhoI or KpnI in order to have the CDS sequences without stop codon and in frame with the reporter genes, where present.

Cells

Authentication of cell lines was assured by regular morphology checks and growth curve analyses. Cells were regularly tested for mycoplasma infection by PCR.

Cell culture and transfection

Chinese hamster ovary (CHO-K1) cell line wild type or stably expressing the human MS4A members, Dectin1, CD9 and CD63 (untagged or Pegfp/mCherry-tagged) and human embryonic kidney (HEK293 and HEK293T) cell lines wild type or stably expressing human MS4A4A were grown in DMEM (Lonza, Basel, Switzerland) completed by adding 10% fetal bovine serum (FBS) (Euroclone, Milan, Italy), 100 U/ml of penicillin/streptomycin (P/S) (Lonza), 25 mM HEPES (Gibco, Life Technologies Ltd). Transfectants were obtained by lipofection with the indicated plasmids, according to Lipofectamine 2000 manufacturer's instructions and selected with 650 µg/ml G418 (Invitrogen, Life Technologies Ltd).

Human macrophage preparation and culture

Macrophages were generated differentiating blood monocytes obtained from buffy coats from healthy donors by Ficoll-Hypaque (Ficoll, Biochrom) gradient centrifugation. In order to induce their differentiation into macrophages, monocytes (1x106/ml) were cultured for seven days in

Petriperm culture dishes in Iscove's Modified Dulbecco's Medium (Lonza) supplemented with 10% heat-inactivated fetal bovine serum (FBS) and 100 ng/ml M-CSF (MACS, Miltenyi Biotec) (M0).
For M1 polarization, macrophages were resuspended in medium containing 0.1 µg/mL LPS (E. coli strain 055:B5, Sigma) and 20ng/mL IFNγ (R&D) for 24 h. For M2 polarization, macrophages were incubated for 18 h with 20 ng/ml IL-4 and/or Dexamethasone (10-6M) (Sigma), 10 ng/ml TGF-β (Peprotech) or 20 ng/ml IL-10. In all experiments comparing M0, M1 and M2 macrophages, the cells were generated in parallel from the same donor's monocytes.

In vitro stimulation with opsonized particles

LPS and Mannan-coated latex beads were prepared by passive adsorption. Approximately 2 × 10^9 polystyrene latex beads (Sigma-Aldrich), 3 µm in diameter, were washed twice (10,000 g for 10 min) in 0.1 M of carbonate-bicarbonate buffer, pH 9.6, and incubated with 500 µg of Mannan from *Saccharomyces cerevisiae* or LPS from *E.coli* (Sigma-Aldrich) in 500 ml of the carbonate-bicarbonate buffer for 1 h at 37°C. The beads were then washed twice with HBSS (Invitrogen), incubated in 5% BSA for 2 h at 37°C to block nonspecific binding sites, washed again, re-suspended in HBSS, and stored at 4°C before use. Macrophages were then treated for 2h in complete medium at 37°C, 5% CO_2. Excess of beads was then washed and cells were prepared for mRNA extraction, FACS or immunofluorescence.

Co-Immunoprecipitation and Western blotting.

Macrophages were cultured as previously described. Before stimulation, the cells were washed with PBS and cultured in fresh DMEM with 10% FBS and then challenged with 100µg/mL of Zymosan. PBS alone was also used as a control. After incubation for 2h at 37°C, cells were rinsed once in ice-cold PBS and lysed with lysis buffer (50 mM Tris HCl pH 8 + 150 mM NaCl + 5 mM EDTA + 5mM EGTA + 1% NP-40 + 10% glycerol) freshly prepared and supplemented with protease inhibitors EDTA-free (Roche, Basel, Switzerland) and 100 µg/ml PMSF and lysed for 30 minutes at 4°C in agitation.
After 20 min centrifugation at 13000 rpm at 4°C, cell supernatants were quantified by DC Protein Assay (Bio-Rad, Hercules, CA).

For co-immunoprecipitation, 200μg of protein were pre-cleared from cell lysates with 30 μl of protein G–agarose–Sepharose beads (GE Healthcare) for 1h at 4°C. The pre-cleared lysates were then incubated without (control) or with 5 μg of goat anti Dectin1 (R&D), rabbit anti CD63 or rabbit anti CD9 (Sigma) over night at 4°C, followed by incubation with 30 μl of the protein G beads for 3h at 4°C. The beads were washed four times in lysis buffer, resuspended in 30μl Laemmli Sample Buffer (Bio-Rad), containing 0.71 M β-mercaptoethanol, heated at 95°C for 5 minutes and applied to 12% SDS-PAGE and blotted to nitrocellulose membranes (Bio-Rad). Membranes were blocked in 3% non-fat dry milk (Nestlé, Vevey, Switzerland) 1% BSA (Sigma Aldrich) in PBS over night at 4°C, rinsed three times with PBS-T for 5 min and then incubated overnight at 4°C with 1:500 dilution in PBS + 5% BSA of the indicated primary antibody. MS4A4A was detected by immunoblotting using mouse anti-MS4A4A antibody (Abcam). Membranes were washed 5 times for 5 min with PBS 0.1% Tween (PBS-T) and incubated for 1 hour at RT with 1:5000 dilution in PBS-T + 5% BSA of anti-mouse/goat IgG-horseradish peroxidase conjugated secondary antibody. Membranes were washed 5 times for 5 min with PBS-T and incubated with chemiluminescent HRP substrate Immobilon Western (Millipore, Billerica, Massachusetts, US). Blots were acquired by ChemiDoc XRS Imaging System (Bio-Rad).
Bands were detected as approximately 50 kDa (b-actin), 25kDa (Dectin1, MS4A4A, CD9), 70kDa (CD63).

Mice

All knockout mice are backcrossed to C57BL/6J background and housed under specific pathogen-free
conditions. Mice in each group were littermate controlled and used at 6 to 12 weeks of age. All procedures with the animals were in accordance with institutional guidelines and with national (DL 116, Gazzetta Ufficiale della Repubblica Italiana, supplement 40, 18-2-1992) and international law and policies (European Economic Community Council, 1987, Directive 86/609, Official Journal of European Communites L 358,1; and Institute of Laboratory Animal Resources, Committee on Life Sciences, National Research Council, 1996, Guide for the Care and Use of Laboratory Animals). Animal procedures were also reviewed and approved by the Institutional Ethical Committee at Humanitas Clinical and Research Center.

Generation of Ms4a4a loxP/loxP and conditional Ms4a4a KO mice.

Mice heterozygous for Ms4a4a-loxP were generated by Ozgene (Bentley, WA). The Ms4a4a loxP allele was created by inserting loxP sites within the exon 3 of the Ms4a4a gene, flanking exon 3. Overview of this construct is shown (Fig). Ms4a4a-loxP mice were interbred with LysM-cre mice to generate the desired conditional knockout genotype (Ms4a4a-loxP/loxP; Cre +/+). Mice homozygous for Cre recombinase linked to the Lysozyme M (LysM) promoter are commercially available from Jackson Laboratories.

Transgenic mice used for experiments were confirmed to be desired genotype via standard genotyping techniques, using the primers identified using MacVector and the Primer3 algorithm (see below). Control mice used in this study were Ms4a4a-loxP/loxP; Cre -/- mice (WT).

.

primer_01F WT	CCCCTTCTTCAGTGTACATAGGAT
primer_02R conKO	GGATAGCTAGAGCAGAGAAATACC

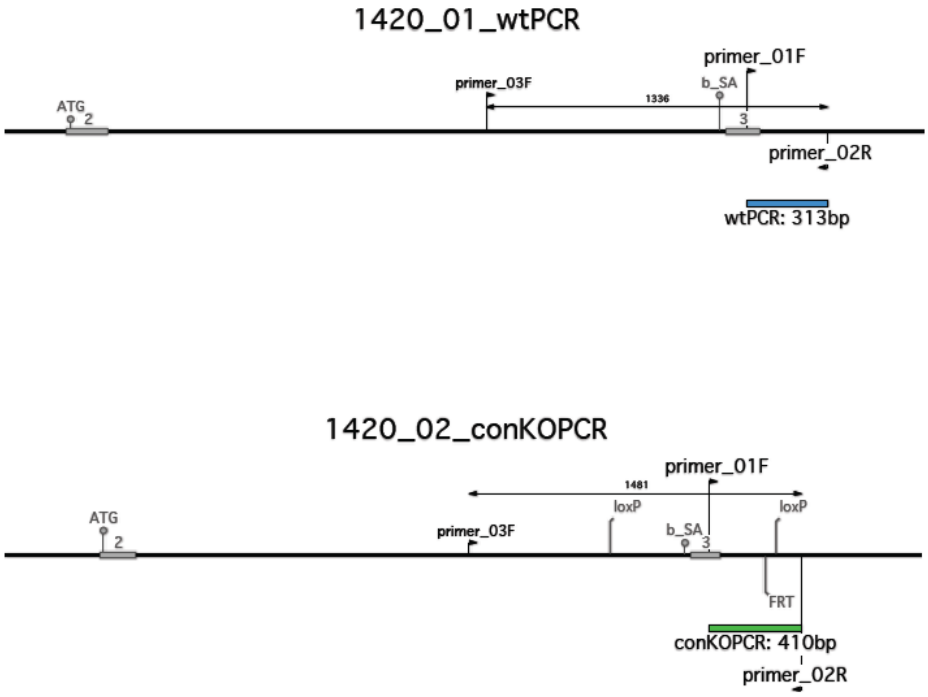

Fig1. Knock-out construct and primers used for the *flox* genotyping.

BMDM, PEC, splenic and blood macrophages isolation

Peritoneal elicited macrophages (PEC) derived from mice intraperitoneally (i.p.) injected with 1 ml of the exudate-inducing compound thioglycollate (3% thioglycollate medium w/o dextrose, BD; Franklin Lakes, NJ) and collected after 4 days by peritoneal lavage with sterile phosphate-buffered saline and plated in 10% fetal calf serum (FCS)-RPMI 1640 medium for 24 h before treatment.

Mouse resident peritoneal macrophages were obtained by washing the peritoneal cavity with 5 ml of ice-cold sterile RPMI 1640 medium, and cultured in a humidified incubator containing 5% CO2 at 37°C in 10% fetal calf serum (FCS)-RPMI 1640 medium for 24 h before treatment.

BM cells were obtained from femurs of B6 WT and Ms4a4a−/− mice and incubated overnight at 37°C with complete medium. Non adherent cells were then cultured in DMEM containing 10% FCS and 30 ng/mL mM-CSF (Miltenyi Biotec) for 7 days in ultra-low attachment plates (Corning Life Sciences).

After incubation, the non-adherent cells were removed by washing with serum-free medium and the adherent cells were incubated in 10% FCS-RPMI 1640 medium. For M1 polarization, macrophages were incubated with 100ng/mL LPS (E. coli strain 055:B5, Sigma) and 20ng/mL m-IFNγ (R&D). For M2 polarization, macrophages were incubated with 20 ng/ml m-IL-4 (Miltenyi Biotec) and/or Dexamethasone (10-6M) (Sigma).

Splenic macrophages were obtained by removing the spleen by lifting it at one end and cutting away from the body and placing it on a sterile mesh. Through a sterile syringe plunger the organ was mashed and the cells were collected in a petri dish containing 5 ml of cold RPMI 1640. The cell suspension was 5 times with RPMI 1640 by pelleting cells at 300 g for 15 minutes at 4°C and the the cell pellets was resuspended in 5 ml HBSS for separation by Percoll (280-320 mOsm/kg H2O and 1.070 g/ml density) density gradient centrifugation. Cells were layered on top of the gradient and span at 400 g for 30 minutes at 4°C without brake. The isolated cells were extensively washed in HBSS and plated.

For blood derived macrophages, blood from cardiac puncture was isolated and layered on a Ficoll gradient to obtain PBMC. Cells were extensively washed in PBS and plated in complete RPMI in the presence of mM-CSF for 6 days for differentiation.

TAM isolation from RCC xenograft

TAM were obtained from a xenograft model of human renal cell carcinoma (RCC) in SCID mice. Solid fresh cancer was disaggregated with collagenase cocktail and red blood cells were lysed with ACK buffer. Tumor cells were isolated using a cocktail of anti-CD15 and anti-CD33 antibody-conjugated magnetic beads and MACS columns (Miltenyi Biotec) positive selection. TAM in the negative fraction were eventually purified by positive selection using anti-CD11b antibody-conjugated magnetic beads and MACS columns (Miltenyi Biotec).

Enzyme-Linked Immunosorbant Assay (ELISA)

PEC and BMDM were seeded into 12-well plates (7 x 10^5 cells/well) and grown under normal conditions for 24 h. The medium was replaced by complete DMEM alone or with 25ug/mL Zymosan particles. Supernatants were collected after 24 h and mIL6, mIL10 andmTNFa were measured using sandwich ELISA (R&D Systems). The optical density (O.D.) of each well were analyzed at 450 nm by SoftMaxPro 5.3 software.

Reverse-transcriptase and Real Time polymerase chain reaction

Total RNA was obtained using Trizol (Invitrogen, Carlsbad, CA). Reverse transcription was performed on 1µg RNA template using High Capacity cDNA Reverse Trascription Kit (Applied Biosystems). Quantitative PCR was performed with Sybergreen Master Mix (Applied Biosystem) and 500 nM primers in 50 µl total volume in a ViiA™ 7 Real-Time PCR System (Applied Biosystems).

All Primers used are listed in Table...

Each sample was amplified with 1 cycle at 95°C for 10 min and 39 cycles at 95°C for 15 sec and 60°C for 1 min.

Results are expressed as the fold of increase in mRNA expression with respect to the control cells (M0), and normalized on the housekeeping gene GAPDH.

target gene	primer F (5'-3')	primer F (5'-3')
hMS4A4A	CTGGGAAACATGGCTGTCATA	CTCATCAGGGCAGTCAGAATC
mMs4a4a	CTGCATAGGAGTATCCCTCTCT	GTCTCTGCCTTGGTAGGATTTG
hMS4A6A	CTGGTGGGTTTCATTATCCT	CAGACTGGCTTTGGCTGTAT
mMs4a4B	GTCTCCGGATCCCTGTCC	TTCAGAGTTAGACTGGCAACGA
mMs4a4c	CTGTTGTAACTCCAGCGAGGT	ATGGTTGAAGCGTCACAGG
mMs4a4D	CCCACAAATAGAGTCCCACATC	GGGCAGCAGAAACAGTATCC
hCD163	GGGATGTCCAACTGCTATCAA	GACTCATTCCCACGACAAGAA
mcd163	CAGACTGGTTGGAGGAGAAATC	CAGCTTCCAGAGACAAGTCAA
hCD206	GGAGTGATGGTTCTCCTGTTTC	CCTTTCAGCTCACCACAGTATT
hCD9	CTGTTCTTCGGCTTCCTCTT	CTCCTGGACTTCCTTAATCACC
hCD63	TACTGTGGGCTGTGGGATTA	CAGCTACCACCAGCACATTT
hDectin1	CCTGGGTACCATGGCTATTT	GGGTTGACTGTGGTTCTCTT
mDectin1	CTCAGCCTTGCCTTCCTAAT	AGCAGTGTCTCTTACTTCCATACAC
GAPDH	TCCACTGGCGTCTTCACC	GGCAGAGATGATGACCCTTTT
mGAPDH	AACAGCAACTCCCACTCTTC	CCTGTTGCTGTAGCCGTATT
mIL6	GGATACCACTCCCAACAGACCT	GCCATTGCACAACTCTTTTCTC
mIL10	GGTTGCCAAGCCTTATCGGA	ACCTGCTCCACTGCCTTGCT
mTNF	GAAAAGCAAGCAGCCAACCA	CGGATCATGCTTTCTGTGCTC
mIL12	GGAAGCACGGCAGCAGAATA	AACTTGAGGGAGAAGTAGGAATGG

Table.1. Primers used for qPCR.

Flow cytometry

Flow cytometry was performed using a BD LSRFortessa™ flow cytometer and analysis run with FACSDiva 6.1.1 software (BD Biosciences) or Flowjo (Treestar).

Cells were stained with anti-human: MS4A4A-PE (R&D), CD3-APCH7, CD20-APC, CD14-FITC, CD14-PE, CD206-FITC, Dectin1-PerCP (BD Biosciences) and CD163- Alexa700 (BioLegend). Intracellular staining was performed using Cytofix/Cytoperm KIT (BD Biosciences). Dead cells were excluded by LIVE/DEAD Fixable Cell Stain Kit (Invitrogen).

Immunohistochemistry

Patient selection

12 female and 24 males with a median age of 50 years (range 29-86 years) were enrolled in this study. Lymph nodes surgically isolated from 26 patients with lymph proliferative diseases (19 nodular sclerosis HL, 3 mixed cellularity HL, 4 non-classic HL) and from 8 patients with non-proliferative disease (1 dermatopathic lymphadenopathy, 2 non-necrotizing granulomatous lymphadenopathy, 5 chronic lymphadenopathy) from January 1997 and June 2014. This study was conducted in accordance with the Declaration of Helsinki.

From each patient enrolled in the study, 2-mm thick tissue slides from formalin-processed and paraffin- embedded tumor sections were processed for immunohistochemistry. After deparaffinization and rehydration sections were immersed in Diva Decloaker antigen retrieval (Biocare Medical) bath for 15 minutes, then incubated with 3% H2O2 for 20 minutes to block endogenous peroxidases. Slides were stained with primary antibodies raised against MS4A4A (HPA029323, Sigma Aldrich) and CD68 (clone KP1, Dako) for one hour at room temperature. 30 minutes incubation with the MACH 4 Universal HRP-Polymer kit (Biocare) followed. Diaminobenzidine tetrahydrochloride (Dako) was used as chromogen. Nuclei were lightly counterstained with a freshly made hematoxylin solution (Medite). The sections were further washed in water, mounted, and analyzed under an optical microscopy.

Slides were digitized using the Olympus dotSlide computer-aided image analysis system (Olympus Hamburg, Germany). Acquired digital images representing whole-tissue sections were evaluated for image quality and subsequently segmented based on RGB scale. Immunoreactive surface was expressed as percentage.

Confocal microscopy

Macrophages were seeded on poly-L-lysine coated 14 mm diameter glass glasses (Menzel-Gläser, Thermo Fisher Scientific, Waltham, Massachusetts, US) in 24 wells plate, treated as described above and fixed with 4% paraformaldehyde (Euromedex). Cells were washed with Ca2+/Mg2+ PBS and maintained in Ca2+/Mg2+ PBS or permeabilized with 0.05% Triton X-100 in Ca2+/Mg2+ PBS for 5 minutes. Nonspecific ligands were blocked with 5% goat serum (Dako) in Ca2+/Mg2+

PBS containing 2% bovine serum albumin and 0.1% glycine for 1 hour at room temperature. Cells were then incubated with the following primary antibodies: mouse anti–human MS4A4A mAb (R&D Systems), rabbit anti-human Dectin1, rabbit anti-human CD63 and rabbit anti-human CD9 (SIGMA Aldrich). Irrelevant immunoglobulins G (IgGs) were used as the isotypic control. After incubation over night at 4°C, cells were washed and incubated with 1 μg/mL of Alexa Fluor 488–conjugated goat anti–mouse IgG and Alexa Fluor 647–conjugated goat anti–rabbit IgG (Invitrogen) for 1 hour at room temperature. 4′,6-diamidino-2-phenylindole (DAPI; Invitrogen) or Hoechst 33342, Trihydrochloride, Trihydrate (Molecular Probes) were used to stain DNA. After each step, cells were extensively washed with Ca2+/Mg2+ PBS + or Ca2+/Mg2+ PBS + 0.05% Tween 20 (Merck). Specimens were finally mounted on glass slide (Menzel-Gläser) with 20 μl FluoSave reagent (Calbiochem, Merck4Biosciences, Darmstadt, Germany) and kept in dark at RT for 24 hours. High-resolution images (1024 x 1024 pixels) were acquired sequentially with a 60X 1.4 N.A. Plan-Apochromat oil immersion objective by using a FV1000 laser scanning confocal microscope (Olympus; Hamburg, Germany). Differential Interference Contrast (DIC- Nomarski technique) was also used. Images were assembled, cropped by ImageJ software (NIH). Quantitative colocalization and statistical analysis were performed by Imaris Coloc 4.2 (Bitplane AG, Zurich, Switzerland) software and FV1000 1.6 colocalization software (Olympus). Quantification of Pearson's Coefficient of Correlation (PCC) was performed inside a selected region of interest per image, representative of the analyzed cell. For statistic, colocalization analysis was performed on at least 50 cells representative of each experimental condition/donor.

ROS production detection

In order to measure the generation of reactive oxygen species (ROS), CellROX Deep Red reagent (Life Technologies C10422) was used according to the manufacturer's instructions. Briefly, 2.5 × 10^5/ well PECs or BMDMs cells were seeded in a 24 well plate in complete medium and incubated for 30' with CellROX Deep Red reagent along with Hoechst 3334 dye (1 μg/mL) to discriminate the nuclei. Cells were left untreated or treated with 20ug/mL Zymosan for 2 hours at 37°C. Fluorescence was monitored at 350ex/461em (Hoechst) and 640ex/665em (CellROX) and analysis was performed for each ROI using Xcellence-rt software (Olympus) Live-cell confocal microscopy was performed with an Olympus Cell-R epi-fluorescence microscope.

Split-ubiquitin screening with GC treated macrophages library

Split-ubiquitin NubG-X library from glucocorticoids polarized macrophages was constructed by Hybrigenics Services.

MS4A4A cDNA was cut from pcDNA3 plasmid and directionally cloned into the bait construct pBT3-N in which LexA-VP16-Cub cassette (supplied by Dualsystems Biotech), is fused to the N-terminus of the bait protein. The bait construct was transformed into the *S. cerevisiae* strain NMY51 (MATa his3Δ200 trp1–901 leu2–3,112 ade2 LYS2::(lexAop)4-HIS3 ura3::(lexAop)8-LacZ ade2::(lexAop)8-ADE2 GAL4) using standard procedures [364]. For two-hybrid screens, transformants were grown on selective medium lacking leucine, tryptophan, histidine, and adenine, with addition of 20 mM 3-amino-1,2,4-triazole (3-AT). Positive clones were sequenced by colony PCR using the primer set pPR3N-FOR: 5'-GTCGAAAATTCAAGACAAGG-3' and pPR3N-REV 5'-AAGCGT GACATAACTAATTAC-3'. Library plasmids were isolated from positive clones and retransformed into NMY51 to test bait dependency. Only preys activating the histidine and adenine reporters in the presence of MS4A4A and not pCCW-Alg5 or pBT3STE were considered true interactors.

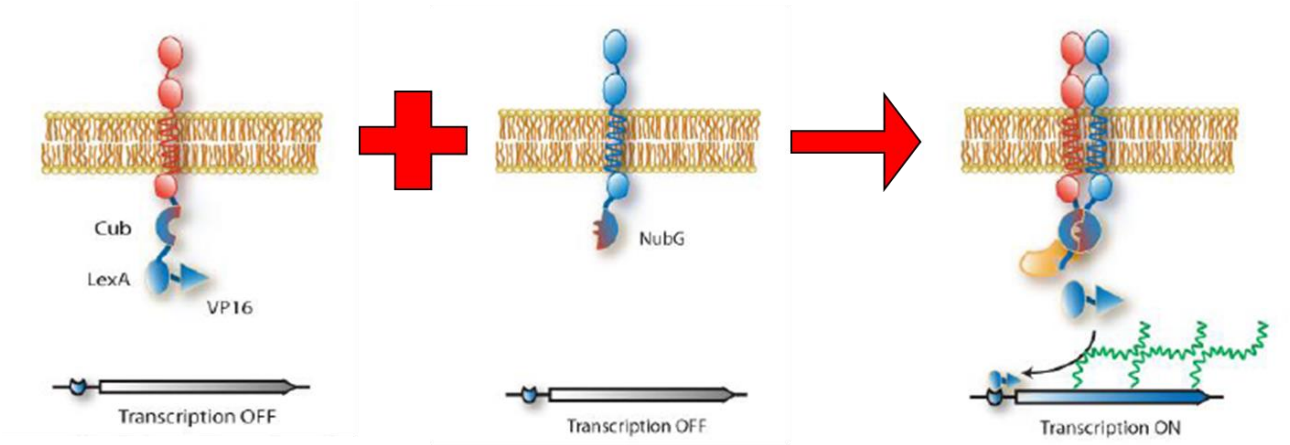

Fig.2. The Split-ubiquitin yeast two hybrid principle. The bait is in frame with the C-terminal of ubiquitin (Cub) and a transcription factor (LexA-VP16) and a TF. When the prey fused with the N-terminal half of ubiquitin (NubG) interacts with the bait, split-ubiquitin is reconstituted and cleaved by proteases, releasing the TF, which enters the nucleus activating the reporter genes and allowing the growth of the yeast carrying the interaction.

The system is based on the reconstitution of ubiquitin, a highly conserved protein which labels other proteins for degradation [365]. Once the target is ubiquitinated, it moves to the 26S proteasome, where it is degraded. The poly-ubiquitin chain can then be cleaved off the target and recycled. This process is dependent on ubiquitin specific proteases (UBPs) which recognize folded ubiquitin and detach the polypeptide chain next to the last residues (a Gly-Gly motif).

Nils Johnsson and Alexander Varshavsky, discovered that yeast ubiquitin can be split into two parts, the N-terminal ubiquitin and C-terminal ubiquitin becoming not recognizable by the UBPs [366]. Whenever they are co-expressed from the same cell, they reassemble and become ready to be cleaved.

The strong affinity is mediated by the isoleucine at position 3. When this is mutated with a glycine (NubG), it loses affinity for Cub when co-expressed. Johnsson and Varshavsky exploited these findings to create a protein complementation assay by fusing a protein X to Cub and a second protein Y to NubG. An interaction between X and Y brings the two halves in close proximity, reconstituting the ubiquitin, that can be now recognized and cleaved by UBPs. As outcome, whenever an artificial TF is cloned in frame with Cub it will be cleaved off from the membrane and able to translocate into the nucleus where it will bind the promoter located upstream of a reporter gene via its DNA binding domain. The reporter genes used in the DUALmembrane system are two auxotrophic growth markers (HIS3 and ADE2), whose activation allows the yeast to grow on selective minimal medium lacking histidine or adenine, and lacZ, encoding the enzyme β-galactosidase. The interaction between two proteins at the membrane level will result into a transcriptional activation, growth of yeast and color development in a β-galactosidase assay.

FLIM-FRET

The Physical Phenomenon of Fluorescence

Interaction between light and matter is described by the Einstein theory (Einstein A., Zur Quantentheorie der Strahlung, 1917. Physikalische Zeitschrift 18: 121–128). Three types of interaction are possible:

- **Absorbtion**, when a photon interacts with a molecule and is absorbed; the photon's energy is transferred to the electron and stored as potential energy, allowing a jump from a state E_m to a state E_n. This is a very quick process, happening in femtoseconds
- **Spontaneous emission**, when an electron in an excited state En can return to a fundamental state. In this process a photon of energy $E_n - E_0 = hv$ is emitted
- **Stimulated emission** is a process that occurs in presence of an external electromagnetic radiation. An electron in excited state E_n can interact with a photon of energy hv and release another photon with same frequency and phase.

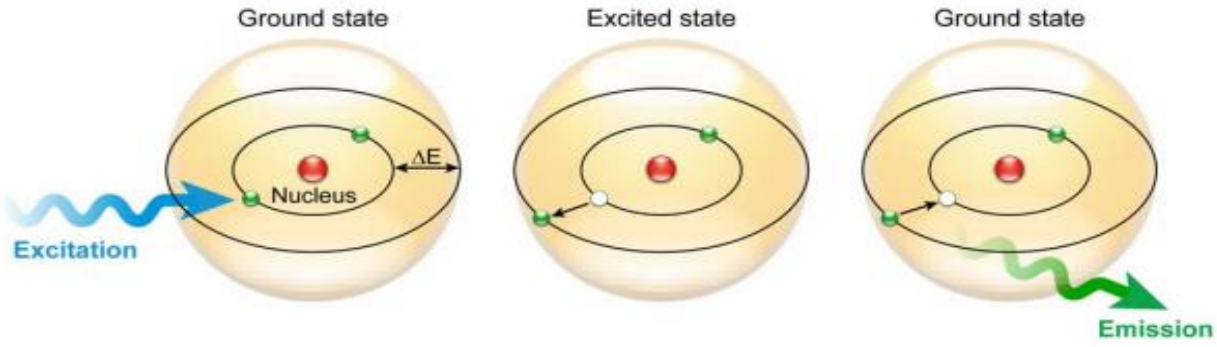

Figure . **Fluorescence principle**. Schematic representation of fluorescence according to the classical Bohr model. Absorption of a light quantum (blue) set off an electron to move to a higher energy orbit. After existing in this excited state for a certain time (the fluorescence lifetime), the electron drops back to its former orbit and the fluorochrome disperses the excess energy by emitting a photon (green). From Ishikawa-Ankerhold, 2012

Here we focus on luminescence, which is a spontaneous emission from an excited state (Lakowicz J. 2006).

Luminescence is commonly divided in fluorescence and phosphorescence, according to the type of excited state. Fluorescence is the transition from a singlet state S^1 to the ground state; this is a quite quick process – happening in nanoseconds – with an opposite spin electron in the ground state. It's a permitted transition so it possesses very high emission intensity. Transition from a triplet state T^1 to the ground state occurs between two electrons with same spin; this transition is not permitted by selection rules and the emission intensity is much lower.

Almost all fluorophores follows three general rules:

- Fluorescence is emitted at a lower energy than excitation, i.e. at longer wavelength (Stokes Shift)
- Emission spectra are usually irrespective of excitation wavelength (Kasha's rule), because energy is first dissipated through vibrational relaxation
- Absorption and emission spectra are generally symmetric. This is called Mirror rule and is due to fluorophores having similar vibrational states in the electronic ground and excited states.

Lifetime of a fluorophore τ is the average time of the decay process from an excited state to the ground state. Fluorescence lifetimes are usually short (order of magnitude 1-10ns), while phosphorescence lifetimes are much longer (order of magnitude $1\text{-}10^3$ ms, but in some cases can be even longer).

Absorption and radiative emission can be described with a Jablonski diagram. Transitions from each state are shown as vertical lines between states, because transition times fall in the order of magnitude of 10^{-15} s.

After absorption, fluorophores relax to the ground vibrational state. This is still an electronically excited state. At this point, one of these types of decay can occur:

- **Fluorescence,** if the electron falls from a singlet state to the ground state.
- **Quenching,** when the fluorophore relaxes in a non-radiative way (mainly heat), due to the interaction between the fluorophore and molecules from the solvent . Most frequent case is the presence of O_2
- **Intersystem crossing,** the fluorophore shifts from a singlet state to a triplet state. According to selection rules, transitions from this state to ground state are avoided so the fluorophore undergoes phosphorescence. The fluorophore can even return to a singlet state (in milliseconds) and then relax with radiative emission of fluorescence.

- **Resonance energy transfer.** Energy can be transferred non-radiatively between two fluorophores via dipole-dipole interactions, if the distance between two fluorophores is in the range of tens of nanometers.

Resonance energy transfer (RET)

Resonance energy transfer is a process in which a fluorochrome in excited state (donor), transfers energy to another non-excited fluorophore (acceptor) and occurs when the emission spectrum of the former overlaps with the excitation spectrum of the latter. The efficiency of energy transfer is proportional to spectral overlap and is described in terms of Forster distance (R_0).
The rate of energy transfer $k_T(r)$ is given by

$$k_T(R) = \frac{1}{\tau_D}\left(\frac{R_0}{r}\right)^6$$

where r is the distance between the donor (D) and acceptor (A) and τ_D is the lifetime of the donor in the absence of energy transfer. The efficiency of energy transfer (E) is the fraction of photons absorbed by the donor which are transferred to the acceptor

$$E = \frac{k_T(r)}{\tau_D^{-1} + k_T(r)}$$

By substituting the previous equation, last one can be rewritten as

$$E = \frac{R_0^6}{R_0^6 + r^6}$$

Efficiency is normally calculated as the relative variation of fluorescence intensity of the donor in presence F_{DA} and absence F_D of the acceptor, as in

$$E = 1 - \frac{F_{DA}}{F_D}$$

Fluorescence Lifetime Imaging Microscopy (FLIM) FRET

The interpretation of intensity-based FRET measurements is often limited by experimental conditions and may originate artefacts, such as concentration and efficiency of the fluorochromes, signal cross-contamination, variations in excitation intensity and exposure duration, and photobleaching. The fluorescence lifetime τ is affected by energy transfer, but basically unaffected by the above-mentioned limitations. Therefore, measuring the lifetime via FLIM provides essential information on FRET and improves many limitations related to intensity-based FRET.

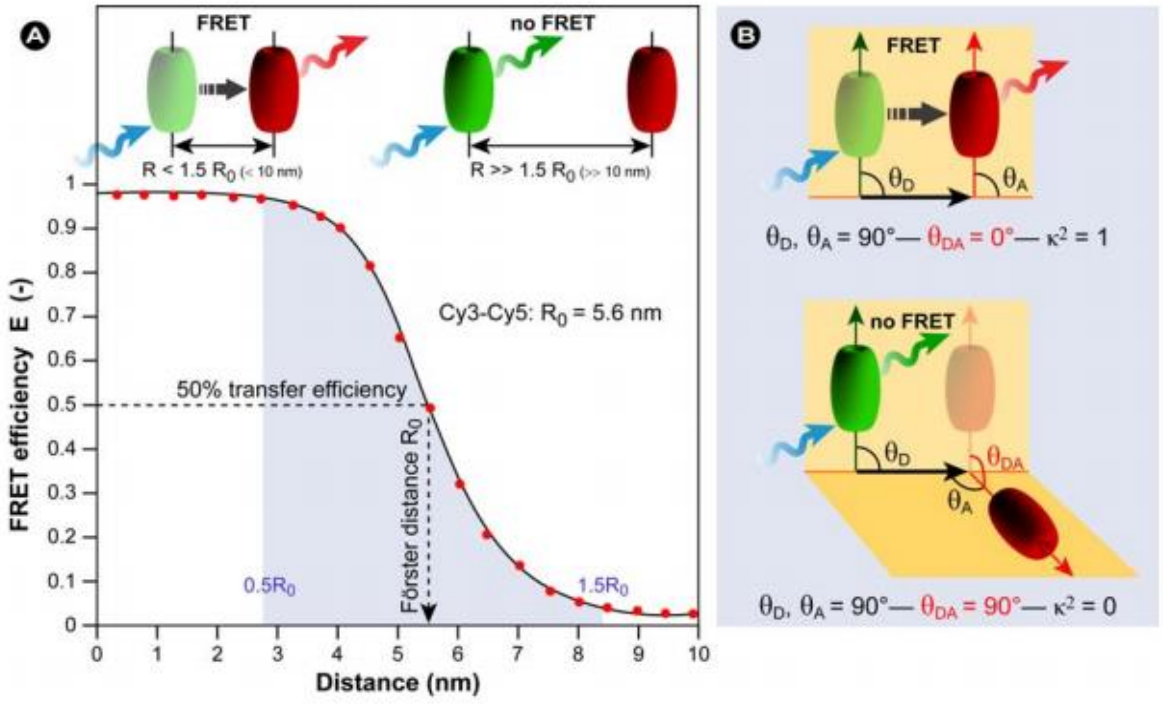

Figure. **The FRET photo physical process**. FRET depends on the proximity of donors and acceptors fluorescent molecules and their spectral overlapping. Whenever the donor is excited but the acceptor is too far away from it, only the donor fluorescence can be detected. However, when the acceptor is closer, FRET phenomenon occur. The more the donor intensity emission decreases, the better the acceptor emission will be detected. From Ishikawa-Ankerhold, 2012

FLIM is a technique that maps the spatial distribution of the lifetimes which does not change upon intensity variations as long as sufficient signal is available to be detected. Additionally, lifetime values are not dependent on the fluorochromes concentration, the excitation light intensity, or on the fluorescence detection efficiency (Lakowicz 1992) and are normally indifferent to moderate levels of photobleaching (Van Munster 2004).

In FLIM-FRET, the acceptor presence causes energy transfer and loss of donor's excited state faster than in its absence. Consequently, the donor fluorescence lifetime drops.

In case of FLIM-FRET, efficiency (EFRET) may be calculated according to:

$$E_{FRET} = 1 - \frac{\tau_{DA}}{\tau_D}$$

where τDA and τD are the excited-state lifetimes of the donor in the presence and absence of the acceptor, respectively.

CHO-K1 cells (1x106 cells in a 6 well plate, in DMEM without P/S) were transiently co-transfected using Lipofectamine2000 with the plasmids described above and tested for interaction by FLIM-FRET using a two photon microscope (Trimscope II, LaVision Biotec, Bielefeld, Germany), based on Olympus BXW51 upright microscope with 60x objective (LUMFL60x Olympus, Japan).

Light was separated using a IR700 long pass filter and detected with a FLIM X16 module (LaVision Biotec, Bielefeld, Germany).

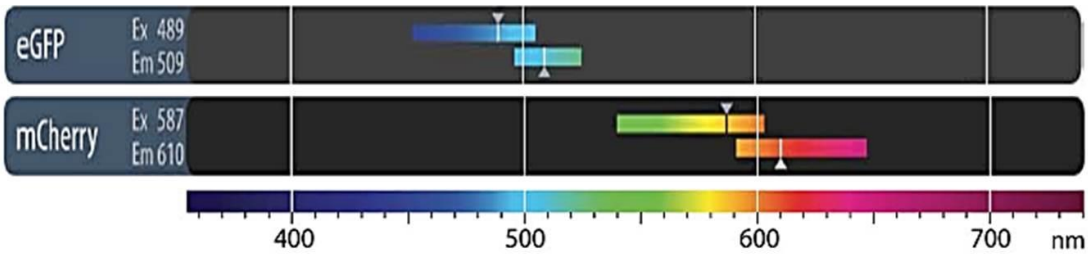

Donor	Acceptor	Donor Excitation λ_{max} (nm)	Acceptor Emission λ_{max} (nm)	Donor QY (–)	Acceptor ε ($M^{-1}cm^{-1}$)	Förster Distance (nm)
EGFP	mCherry	507	510	0.60	72,000	5.1

Figure. EGFP-mCherry couple photophysical properties. Spectra of the reporters chosen to detect interaction between molecules.

Humanized anti-MS4A4A antibody generation by Phage Display Library

Anti-MS4A4A antibodies were isolated from HX02 human Fab phage display library (Humanyx Pte Ltd, Singapore) via in vitro selection.

The library was derived from 22 anonymous donors' blood and tissues after informed consent and consists of $3 \times 10^{\wedge 10}$ M13 phagemids, each one encoding and presenting one different antibody in a Fab format. DNA fragments encoding Heavy Chains (HC), Light Chains (LC), and the linker were amplified from reverse-transcribed mRNA by PCR and ligated into pComb3X phagemid vector. Amplified products were purified from agarose gel with QIAquick Gel Extraction Kit (Quiagen) and transformed into competent TG1 bacteria, subsequently infected with the M13KO7 helper phage so that the phage-displayed antibodies can be selected on immobilized antigen.

The library was panned against transiently transfected HEK 293T expressing MS4A4A.

The amount of protein expressed at the surface level by the transfectants was tested by Flow cytometry and epifluorescence microscopy on HEK 293T cells expressing MS4A4A in frame with a GFP reporter.

In the first round of panning $10^{\wedge 13}$ CFU/mL phages were mixed with $5x10^{\wedge 6}$ non transfected HEK 293T cells for depletion in DMEM+1%FBS media for 1h at 4°C on a rotor. After centrifugation, the supernatant was mixed with HEK293T expressing MS4A4A-eGFP FOR 1h at 4°C in agitation. Cells were washed 6 times with complete media (DMEM+ 1%FBS) and once with PBS. Phage elution was performed using a Glycine buffer pH 2.2 for 10 min followed by neutralization with Tris buffer pH 8 and centrifugation of the cells. Supernatant was incubated with E. coli TG1 bacteria (Stratagene) for amplification. The output of this round was determined to be $3,2x10^{\wedge 5}$ phages.

The second round of panning was done similarly using $2x10^{\wedge 12}$ phages as an input and $10^{\wedge 6}$ phages as output.

For the third round CHO cell line was used together with HEK 293T. $2x10^{\wedge 12}$ phages were used as input as above. After acidic elution, the eluted phage were mixed with non-transfected CHO followed MS4A4A-EGFP transfected CHO as a back-to-back panning with HEK 293T. After elution for MS4A4A-EGFP transfected CHO, the output was determine to be 3000 clones.

192 colonies were picked for screening. Phage was rescued for each colony and supernatants were incubated on non-transfected and MS4A4A transfected HEK 293T cells in 96 well-plates for phage

ELISA screening. Binding was detected by HRP-conjugated anti-m13 phage antibodies (Amersham Bioscience).

Binding phages were eluted by washing the cells with cold glycine buffer (50 mM glycine, 150 mM NaCl, 200 mM urea, 2 mg/ml polyvinylpyrrolydone, pH 2.8) at 4°.

The positive Fabs were then converted into full-length IgG1 molecules. VH and VL chain genes were amplified by PCR using primers for the human framework with the addition of restriction sites and cloned into eukaryotic expression vectors with constant antibody domains. IgG1 was expressed by transient transfection of mammalian cells in serum-free medium and purified on protein A affinity columns. The concentration of purified antibodies was measured by optical absorbance at 280 nm.

Affinities of 4 IgG clones for human MS4A4A and mouse Ms4a4a.

HEK-293T cells were transiently transfected with a hMS4A4A-coding pcDNA3 or mMs4a4a-coding pcDNA3plasmid by lipofection and stained with increasing concentrations of each IgG for 1 h on ice. Anti-human IgG A488-coupled secondary antibody was used at 1:4000 dilution followed by PBS washes. Fluorescence was read in a EnVision Multilabel plate reader (PerkinElmer).

Peptide competition assay for D1 antibody.

D1 antibody was coupled with a PECy7 fluorochrome with PE/Cy7Lightning-Link, (Innova Biosciences), following the manufacturer instructions. A peptide corresponding to MS4A4A's second extracellular loop was incubated at indicated concentrations together with 1ug/ml concentration of D1-PECy7 coupled antibody () at room temperature for 30 min. HEK cells transfected with MS4A4A were then added to the mix and incubated for another 30 min. Antibody staining was quantified by flow cytometry.

Epitope mapping

Based on sequence D1 antibody is able to bind, 6 residues were mutated in the second extracellular loop. Mutations were generated from the hMS4A4A-GFP construct using QuickChange kit

(Agilent), according to manufactures instructions. Each mutant was transfected HEK 293T cells and after 48h hours cells were harvested for FACS staining using either D1 or H10 biotinylated antibodies at 1mg/ml concentration followed by Streptavidin PE-coupled secondary staining.

Antibody-dependent cytotoxicity assay.

48 h after transfection, HEK-293T cells were loaded with 10 mM of the calcein-AM dye (Life Technologies) for 1 h at 37°C followed by 3 washes with complete medium. Human NK cells were isolated on the same day using a human NK cell isolation kit (Macs Miltenyi). $10^{\wedge 4}$ HEK-293T cells were first incubated with increasing concentrations of antibodies in a round bottom 96-well plate for 1h at RT. $10^{\wedge 5}$ NK cells were then added to each well (1:10 ratio), spun down, and incubated for 4 h at 37°C. Plates were then centrifuged and 70 µL of supernatant was transferred in a black plate for fluorescence reading. Samples were measured using a Spectramax Gemini dual-scanning microplate spectrofluorimeter (Molecular Devices, Sunnyvale, Calif.) . Percent lysis was calculated as:

(Test release - spontaneous release/maximum release - spontaneous release) x 100

H1L1 clone was used as control antibody as well as non-transfected cells were.

Statistical analysis

GraphPad 6 Prism software was used to perform Student's t-test or ANOVA using Bonferroni algorithm. A p-value ≤ 0.05 was regarded as statistically significant. Level of significance was indicated by asterisks (***$p < 0.001$; **$p < 0.01$; and *$p < 0.05$). Error bars show SEM, if not other indicated, of each experiment. Experiments were performed at least in triplicate.

4. RESULTS

4.1. MS4A4A expression, regulation and structure

4.1.1. Selective MS4A4A mRNA Expression in hematopoietic cells and alternative macrophages

In a previous study performed in our lab, the analysis of the transcriptional profile associated with human macrophage M1 and M2 polarization led to the identification of a subset of tetraspanin-like genes, MS4A (membrane-spanning 4-domain family, subfamily A), selectively expressed in polarized macrophages. The evaluation of these molecules expression in several cell lines and primary culture, revealed the specific association of one of these candidates, MS4A4A, with a number of tissues, all somehow related to immune functions.

The microarray analysis and the following validation by q-PCR confirmed MS4A4A being almost mutually expressed in alternatively activated macrophages (M2) (Fig.1 A and B).

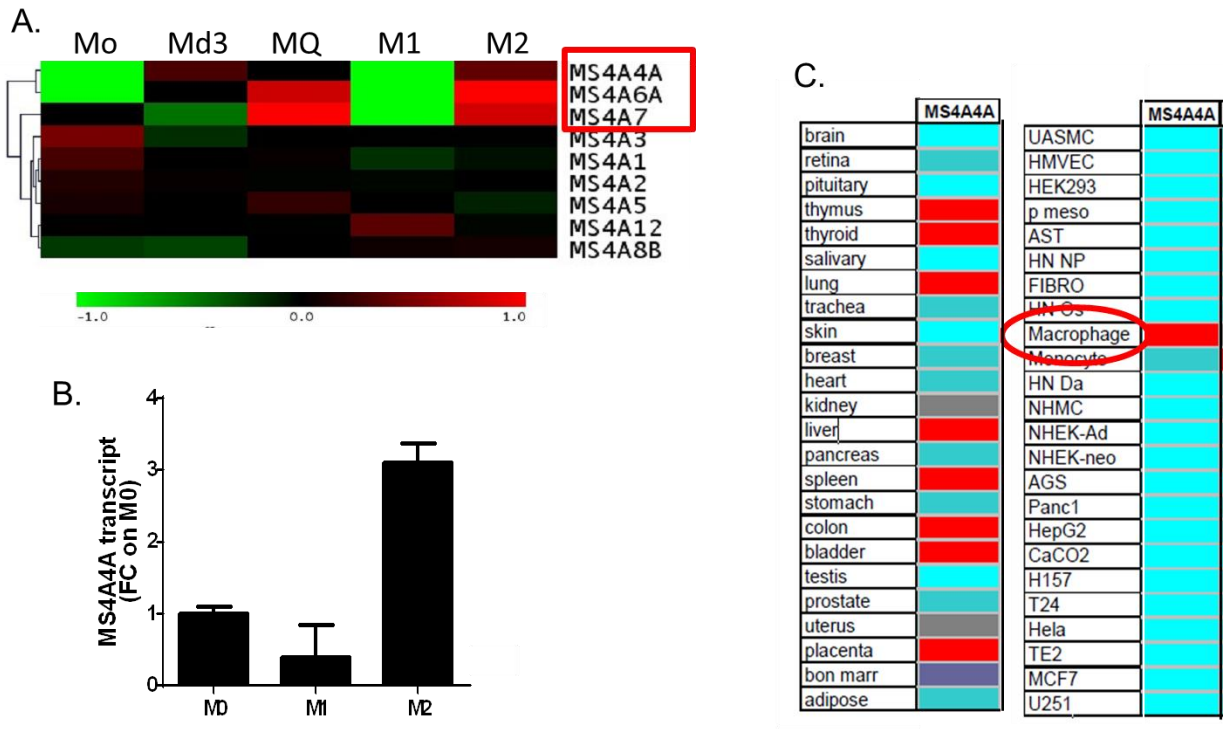

Fig.1. Expression of MS4A4A in tissues, cells and polarized macrophages. A. . Microarray analysis highlighting the expression of MS4A4A in M2 polarized human macrophages (reported in Martinez et al. J Immunol., 2006). Mo: Monocytes; Mo-d3: monocytes after 3 days of culture with M-CSF; MQ: monocyte-derived macrophages; M1: classical macrophages; M2: alternative macrophages. B. Validation of microarray data by qPCR. C. .MS4A4A expression profiling in tissues and primary cells.

4.1.2. MS4A4A is a four-transmembrane domain protein expressed on the cell surface

The open reading frame of MS4A4A encodes a protein of 239 aminoacid residues. The computational analysis performed with the TMHMM program for prediction of transmembrane helices based on hidden Markov model showed four hydro phobic, putative transmembrane regions, (65-85aa, 99-119aa, 138-158aa, 180-200aa) (Fig.2B) forming a smaller and a larger extracellular loops, with a long intracellular amino- and a short intracellular carboxy-terminals (Fig.2B and C), resembling the tetraspanins structure. According to the sequence, the molecule is lacking an N-terminal signal peptide.

In order to determine whether MS4A4A was indeed a cell-surface molecule, we generated a mammalian expression vector encoding MS4A4A in frame with a C-terminal GFP tag. HEK 293 cells were transiently transfected by lipofection with the MS4A4A and the mock GFP plasmids for 24h. Total internal reflection fluorescence (TIRF) imaging demonstrated the cell-surface expression of MS4A4A characterized by a punctate distribution, in contrast with the HEK293 cells transfected with the GFP control vector which show the spread staining pattern with green fluorescence in the cytoplasm(Fig.2D). These results indicated that MS4A4A is indeed a transmembrane protein.

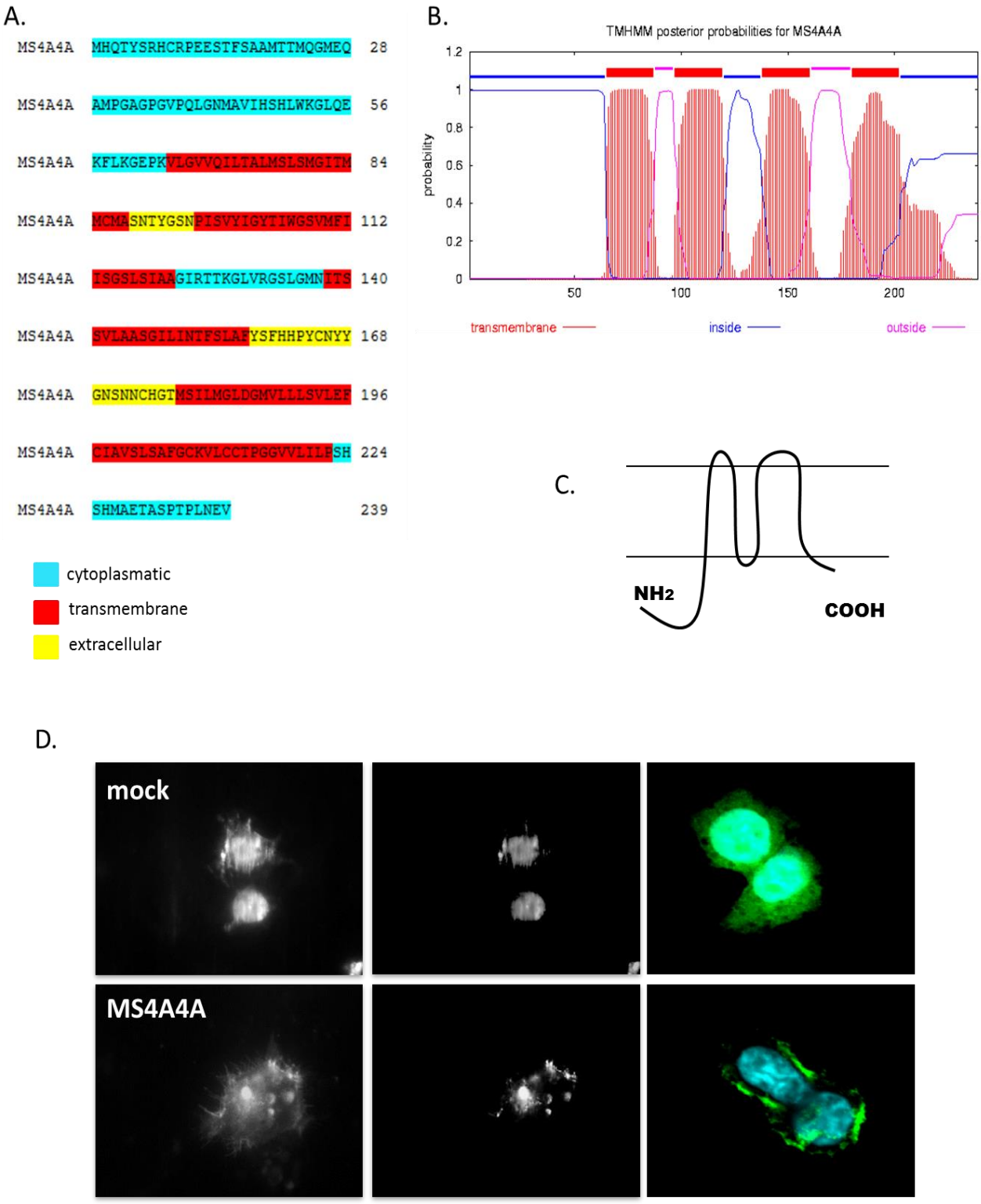

Fig.2. Molecular characterization of MS4A4A. (A). Aminoacid sequence of MS4A4A with the predicted cytoplasmic (cyan), transmembrane (red) and extracellular regions (yellow). The

sequence is available on the NCBI website, Reference Sequence: NP_683876.1. (B) Computational analysis of the amino acid sequences of MS4A4A, using the TMHMM program (http://genome.cbs.dtu.dk/services/ TMHMM/), predicting four-transmembrane hydrophobic domains. (C) Schematic illustration of the tetraspanin-like structure of MS4A4A. Amino (NH2) and carboxyl (COOH) termini are indicated. (C). Membrane localization was further analyzed by TIRF microscopy. 293T cells were transfected with the mock and MS4A4A-GFP plasmid and analyzed with a 60x oil immersion objective.

4.1.3. MS4A4A is induced in macrophages by anti-inflammatory mediators

Given that the alternative phenotype can be induced in macrophages by different stimuli, MS4A4A expression was validated upon several anti-inflammatory treatments.

As reported in *Materials and Methods*, monocytes were isolated from healthy donors' buffy coat and cultured for 7 days with 100 ng/ml M-CSF and eventually polarized for 18 h with different alternative stimuli: 20 ng/ml IL-4, 20 ng/ml IL-10, 10 ng/ml TGF-β, or dexamethasone (Dex) 10-6M. Since Schmieder and colleagues described the synergistic induction of the CD20 homolog Ms4a8a expression in BMDMs by the combination of LPS and M2 mediators (Schmieder 2011), cells were also treated with combinations of IL4 and Dex or IL4/Dex and LPS in order to figure out whether MS4A4A is also responding to the same arrangement of stimuli.

After the treatment, MS4A4A expression was assessed both at the transcriptional level by q-PCR and at the protein level by flow cytometry.

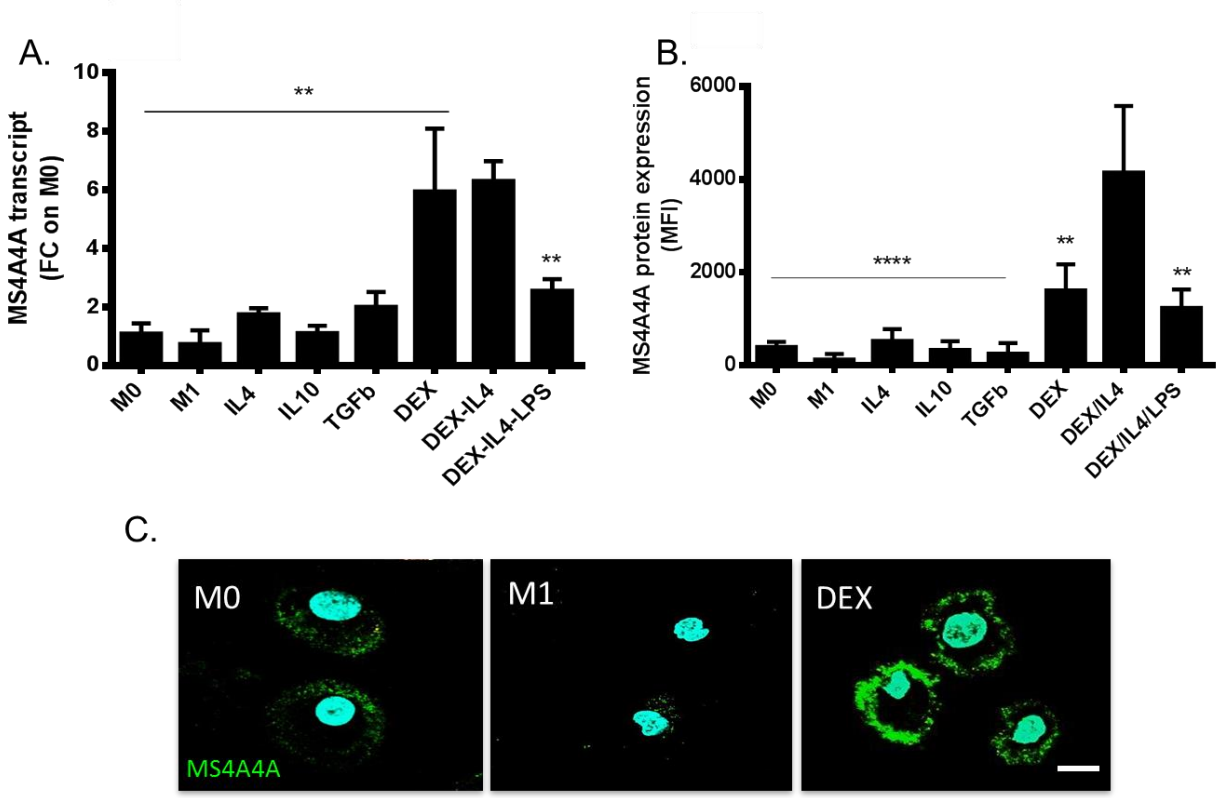

Fig.3. MS4A4A is up-regulated by Dex and IL4 and down-regulated by LPS. A. q-PCR from macrophages treated with different M2 and M1 stimuli and their combinations. Expression is indicated as fold increase respect to mature macrophages (M0). B. Mean fluorescence intensity (MFI) of the expression of MS4A4A at the membrane level, normalized on the isotype control . Results are expressed as mean ± SD of 8 different experiments. (*p < 0.05). C. Immunofluorescence of resting human macrophages (M0), stimulated 18h with 20ng/mL IFNγ+100ng/mL LPS (M1) or 10-6M Dex (M2).

As shown in Fig.3, MS4A4A is mainly induced by dexamethasone both at the transcript and at the protein level. A little induction in the mRNA can be achieved also upon IL4, TGfb and the combination of IL4/Dex/LPS, although the levels are not comparable with the glucocorticoid (GC) alone.

The FACS analysis confirmed the MS4A4A dependence on IL4 and Dex, underlying the down-regulatory effect of LPS in the expression of the molecule, classifying MS4A4A as a marker of macrophage anti-inflammatory phenotype.

Human macrophages (M0) were also polarized into M1 (LPS/IFNɣ) and M2 (Dex), fixed in 4%PFA and permeabilized in 0.05% Triton-X before assembling the coverslips with the mounting medium for the confocal analysis of the protein localization.
The confocal analysis corroborated once again the membrane topology of the molecule, which is consistent in primary cells (Fig.3C).
Despite the absence of MS4A4A induction by the combination of Dex/IL4/LPS, a synergistic effect on MS4A4A expression was given by the combination of Dex/IL4 compared to the single treatments.

4.1.4. MS4A4A is co-expressed with M2 polarization markers

To test whether MS4A4A+ macrophages can be considered *bona fide* M2 macrophages, a staining with two widely acknowledged M2 markers such as the macrophage mannose receptor (CD206) and the scavenger receptor A (CD36) was performed and MS4A4A expression analyzed by flow cytometry (Fig.4). The cells were differentiated from healthy donors buffy coats and polarized either with IFNɣ (20gn/mL)/LPS (100ng/mL) to acquire the M1, or with Dex (10-6M) /IL4 (20ng/mL) for the M2 phenotype, or left untreated (M0). After 24h the cells were stained with CD206, CD36 and MS4A4A. In the M2 condition, almost half of the cells acquired a triple positivity, and an average of 60% of the cells expressing either CD206 or CD36 or both was also MS4A4A+, while the cells negative for both the M2 markers were also negative for MS4A4A. Also in resting conditions, 16% of the cells positives for at least one of the two M2 markers, is also MS4A4A positive, indicating that MS4A4A+ cells can be acknowledged as M2 macrophages.

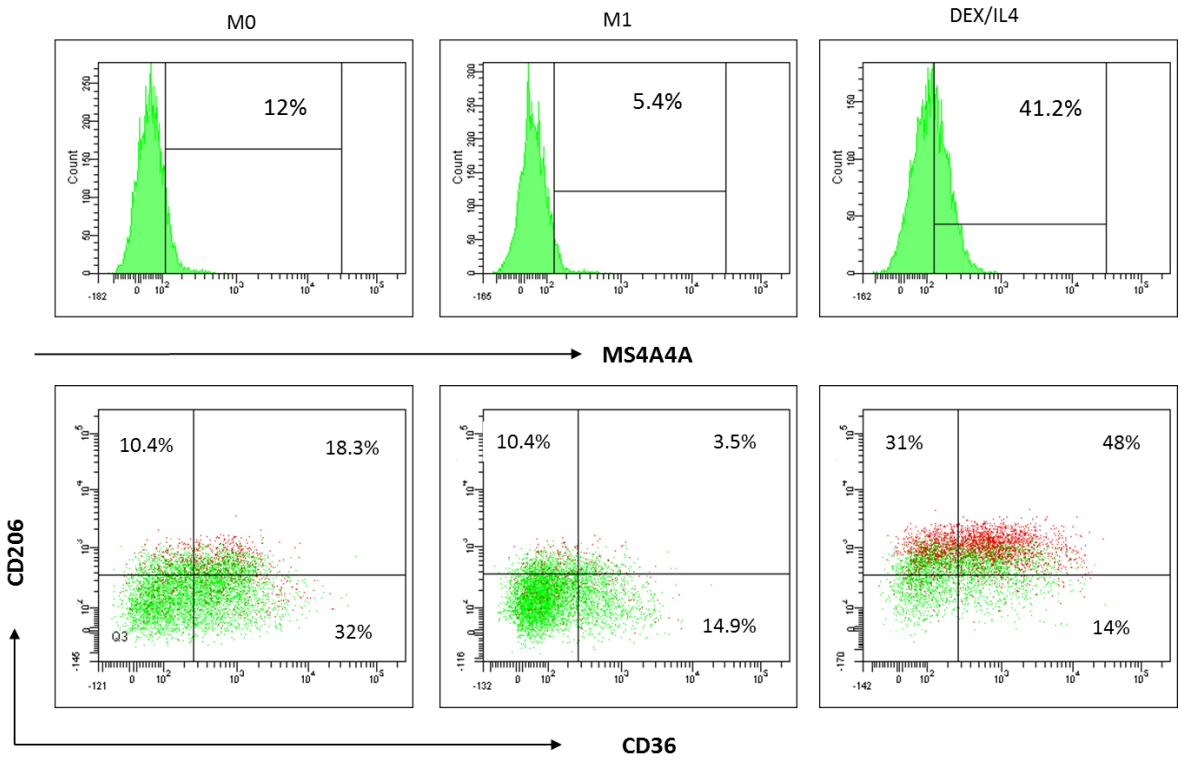

Fig.4. MS4A4A+ population is co-expressed with others M2 markers. FACS analysis of MS4A4A+ macrophages (red population) and their profile with regard to CD206 and CD36 in M1 and M2 polarizations.

4.1.5. Induction of MS4A4A expression in macrophages by M2 mediators is mainly regulated by GR signaling

Glucocorticoids are powerful anti-inflammatory compounds capable of inhibiting all stages of inflammation as well as playing a pivotal role in cell metabolism.

All the cellular responses to GC is attributed to their binding to the intracellular GR (Glucocorticoid Receptor) [367]. The GC hormone crosses the plasma membrane and moves into the cytoplasm where it binds to the high-affinity GR, releasing it from the interaction with the inhibitory complex it is associated with,, thus unmasking the GR nuclear localization signal. Upon activation, GR traslocates into the nucleus, dimerizes, and binds to DNA through its central domain characterized by a DNA binding motif by targeting specific nucleotide palindromic sequences called GRE (Glucocorticoid Response Elements) or nGRE (Negative GRE) [368].

The dependency of MS4A4A expression on glucocorticoid receptor activation was confirmed challenging the cells with two different concentrations (1ug/mL and 100ng/mL) of the GR competitor antagonist Mifepristone (Mf). Cells were treated with the IL4, Dex or Dex/IL4 alone, or together with the antagonist for 18h and a significant inhibition of both Dex and Dex/IL4 treated macrophages expression occurred in a dose dependent manner, at both the transcript and the protein level (Fig.5A). The same behavior was exhibited by another M2 marker, the scavenger receptor for the hemoglobin-haptoglobin complex, CD163, which expression is well known being regulated by GC (Sulahian 2000, Tang 2013).

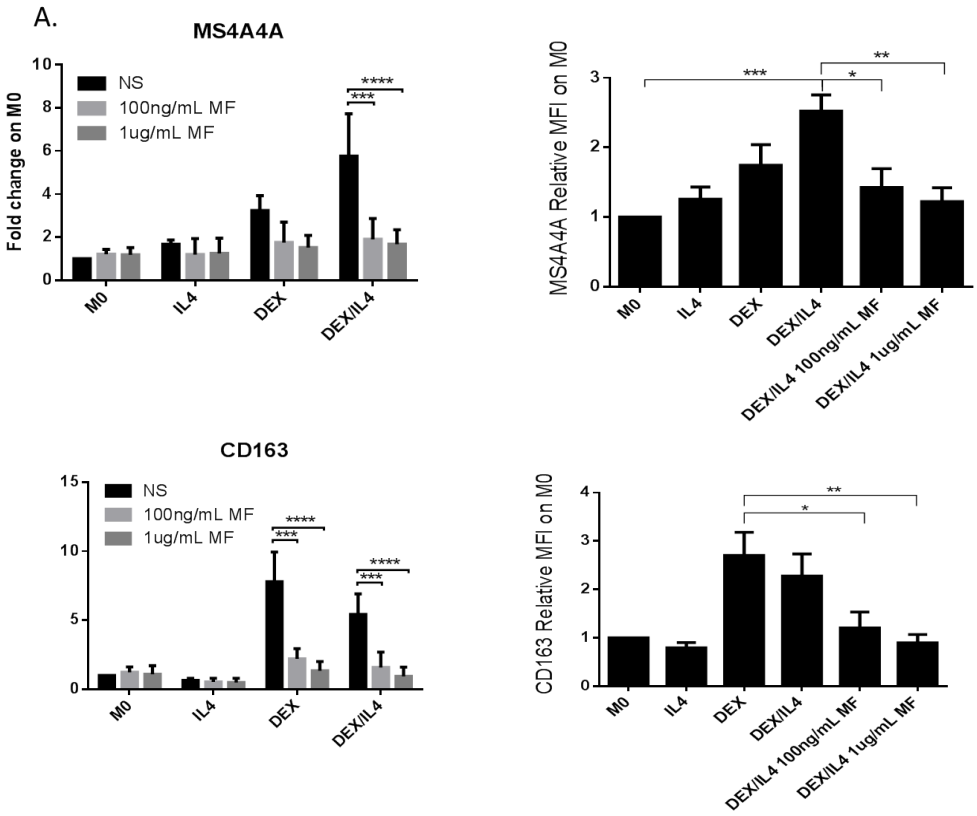

Fig.5. MS4A4A overexpression is found upon GC treatment and is blocked by Mifepristone.
(A) MS4A4A and CD163 expressions in human macrophages was analyzed in the presence of increasing concentrations of the glucocorticoid receptor antagonist Mifepristone. MS4A4A (left) and CD163 (right) expressions were determined by qRT-PCR and FACS analysis.

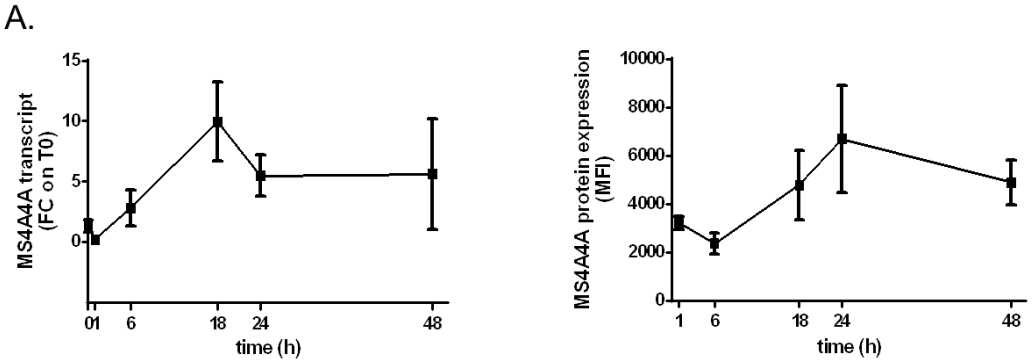

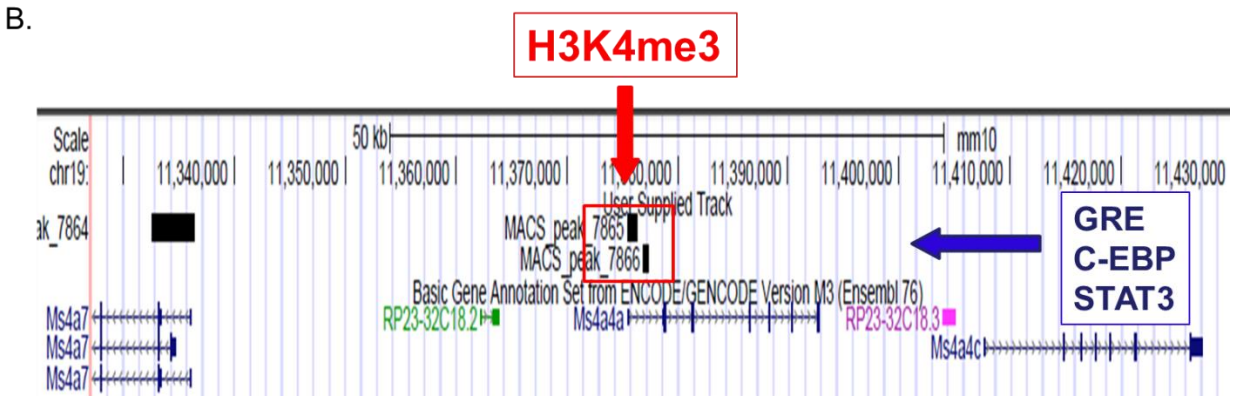

Fig.7. Dexamethasone kinetic and schematic representation of the putative promoter elements regulating MS4A4A. A. Time course of MS4A4A expression in Dex treated macrophages for the indicated time points at the transcript (left) and protein (right) level. Results are shown as mean and SEM of n = 6 and are representative of two independent experiments. The p-value was (*$p < 0.05$) according to ANOVA with Bonferroni algorithm. Values represent the relative induction of MS4A4A normalized to the housekeeping gene GAPDH for qPCR and isotype for FACS and are given as the fold-induction over M0 or T0 set at 1. In the time point graph the relative MFIs are normalized only on the isotype control. B. The black rectangles at the 5' of MS4A4A represent the highly conserved H3K4me3 regions, containing several GRE each, that are likely to regulate MS4A4A expression. Also the C-EBP and STAT-3 binding sites found in this region can be bound by the GR.

The analysis performed with the T.Tsunoda, and T.Takagi software TRANSFAC R.3.4. revealed that both these regions were characterized by a huge number of C/EBP, STAT1, STAT3 but no STAT6 transcription factors binding sites. Particularly, more than 30 palindromic glucocorticoid responsive element (GRE) sequences were identified within this region. Interactions and also co-stimulatory effects has been demonstrated for the GR with both C/EBP and STAT3.

Indeed, IL6 activated -STAT3 has been described acting as a co-activator of the Glucocorticoid Receptor Signaling, arranging a trans-activating/signaling complex that can be both dependent or independent on IL6 responsive element [369].

On the other hand, GC have also been acknowledged playing a role as ligand in the nuclear receptor PPARɣ expression regulation through C/EBP interaction [370].

Grave's syndrome is a very common form of autoimmune hyperthyroidism to which glucocorticoids represent the most effective treatment. In order to understand the *in vivo* effect of glucocorticoids on MS4A4A expression, monocyte were isolated from three Graves's patients before and after glucocorticoids administration (1mg/patient) and RNA was extracted to perform q-PCR analysis (Fig.8). MS4A4A expression was up-regulated in all samples upon GC treatment. Particularly, patient1 and 3 were at their first GC injection, while patient2 was at his 5th injection, justifying the apparently lower induction with a higher basal level of MS4A4A due to the chronic GC treatment .

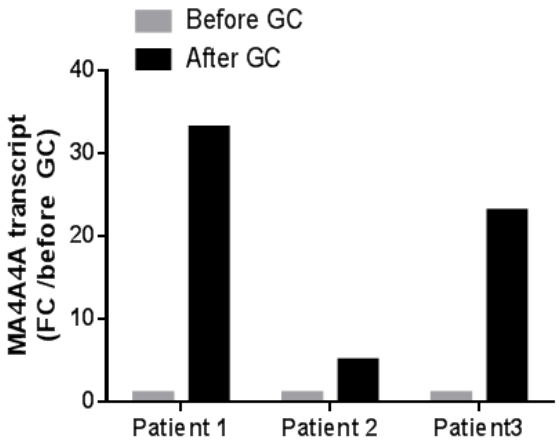

Fig.8. MS4A4A expression after Dex treatment in vivo. MS4A4A mRNA expression from Grave's syndrome patients monocytes before and after treatment with 1mg Dexamethasone. Expression is indicated as fold increase respect pre-treatment.

4.2. MS4A4A and tumor associated macrophages

4.2.1. MS4A4A is overexpressed in TAM in vivo but not in vitro

TAM mainly consist of M2-like macrophages displaying almost no cytotoxicity for the tumor cells because of their very low production of pro-inflammatory cytokines and their poor antigen presentation activity [371].

Schmieder's group acknowledged that for Ms4a8a overexpression induction, the simultaneous treatment of bone marrow derived macrophages (BMDMs) *in vitro* with both the M2 mediators Dex/IL-4 and tumor-conditioned media (TCM) was required. MS4A8A TAMs were also identified *in vivo*, in subcutaneously transplanted tumors of murine malignant melanoma (B16F1) and murine mammary adenocarcinoma (TS/A) [229].

Renal cell carcinoma (RCC), the most common human kidney cancer, and it is commonly infiltrated with tumor-associated macrophages (TAM) able to promote malignant progression [372]. We consequently isolated RCC tumors from a RCC xenograft model, purified the populations through magnetic selection, and compared the expression of MS4A4A in TAM, tumor tissue and peritoneal cells from the same mice by qPCR. As reported in Fig.9, TAM population displayed the highest expression of the protein, with only a little expression within the tumor tissue, which might be due to the presence of residual macrophages in the sample after collagenase treatment.

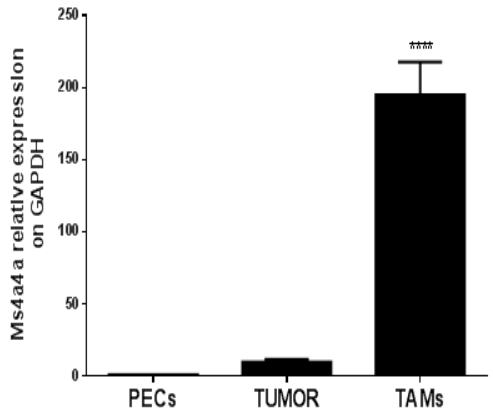

Fig.9. Ms4a4a is expressed in TAM *in vivo*. Ms4a4a transcriptional analysis of RCC xenograft derived TAMs and PECs. The values were normalized in GAPDH housekeeping gene and expressed as fold change on peritoneal macrophages set as 1. (n=3). *p<0.05.

In the attempt to characterize the behavior of the protein in humans and trying to reproduce the *in vivo* experiment in an *in vitro* setting, we co-cultured human mature macrophages with combinations of Dex/IL4 and the TCM of breast cancer (MDA-MB-231), renal carcinoma (RCC), hepatocellular carcinoma (HepG2) and Burkitt's lymphoma (Daudi) for 48h and check at the MS4A4A expression by qPCR *in vitro* (Fig.10).

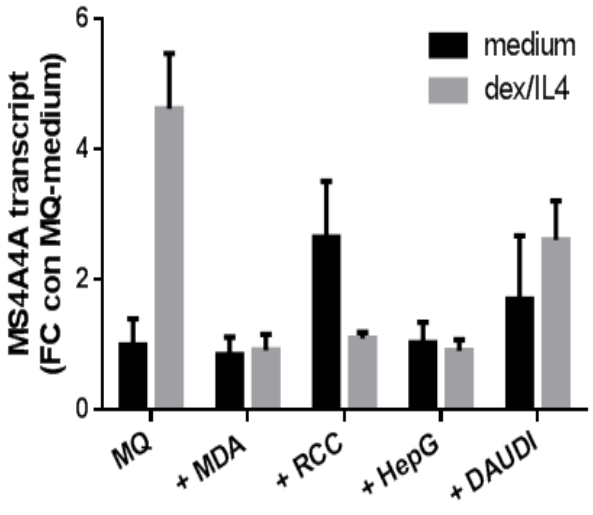

Fig.10. MS4A4A is not affected by TCM in vitro. Expression analysis of MS4A4A mRNA (n=3) from human macrophages co-cultured for 48h with TCM of the indicated cell lines alone or in combination with Dex/IL4. Results are shown as mean and SEM. The p-value was (*p < 0.05) according to ANOVA with Bonferroni algorithm. Values represent the relative induction of MS4A4A normalized to the housekeeping gene GAPDH and given as the fold-induction over M0 or set at 1.

As shown in Fig.10, MS4A4A didn't respond to the same combination required for Ms4a8a up-regulation *in vitro*, given that most of the TCM were not enhancing the molecule's transcript.
The stromal microenvironment certainly represents a more realistic context in which analyze a TAM associated protein.

The findings of an MS4A4A expression in vivo prompted us to evaluate its presence in human samples.

4.2.2. Identification of MS4A4A in human lymphoma

Immunohistochemical stainings were first performed in normal tissues (spleen and lymph node) and showed a very weak expression of MS4A4A. In the spleen, no staining was observed within germinal centers or in lymphocytes, and the only positivity was derived from cells surrounding the vessels (Fig.11A). Regarding the normal lymph-node the only immune-positive cells were found within the peri-lymphatic adipose tissue (Fig. 11B).

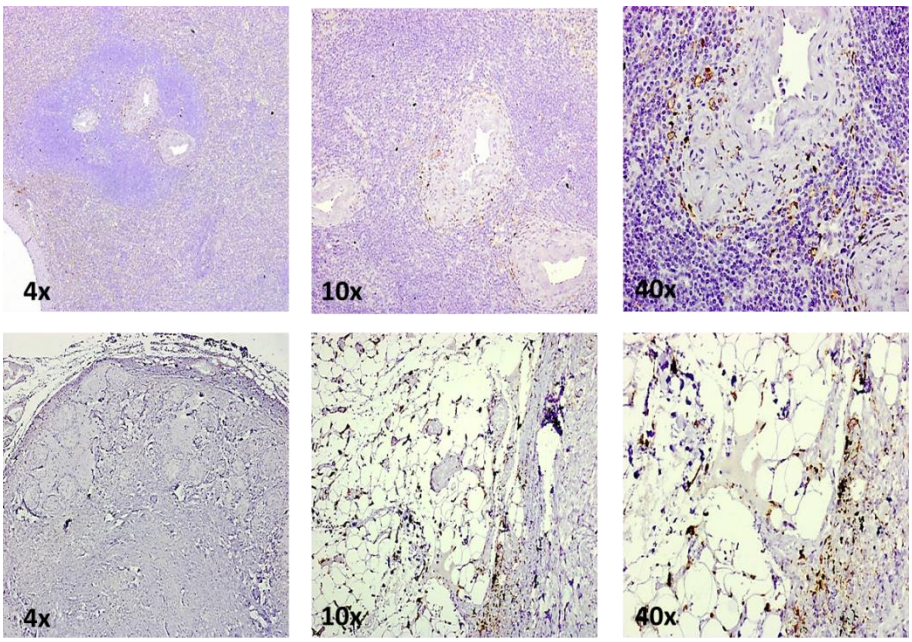

Fig.11. Representative immunohistochemistry for MS4A4A in normal tissues. Immunohistochemical stainings of formalin fixed paraffin- embedded sections of human normal spleen (upper panel) and normal lymph node (lower panel) with anti-MS4A4A antibody, counterstained with hematoxylin.

Hodgkin lymphomas (HL) bad prognosis has been long correlated with a high infiltration of TAM [104, 373]. We therefore analyzed the expression of MS4A4A in histological samples of nodular sclerosis, mixed cellularity and non-classic HL, subdividing them in chemo resistant (n=13) and

chemo sensitive (n=11). The reactive lymph nodes isolated from the same patients that do not exhibit neoplastic features were also examined

The computer aided analysis of the immune reactive areas expressed as percentage of the total section of each sample revealed no significant differences either between tumor and non-tumor samples (7.00 ± 0.91 vs 3.75 ± 1.30) or between chemo resistant and chemo sensitive samples (7.50 ± 1.37 vs 5.00 ± 1.03), yet the trend of the differences is in the right direction, particularly for the first comparison. (Fig.12)

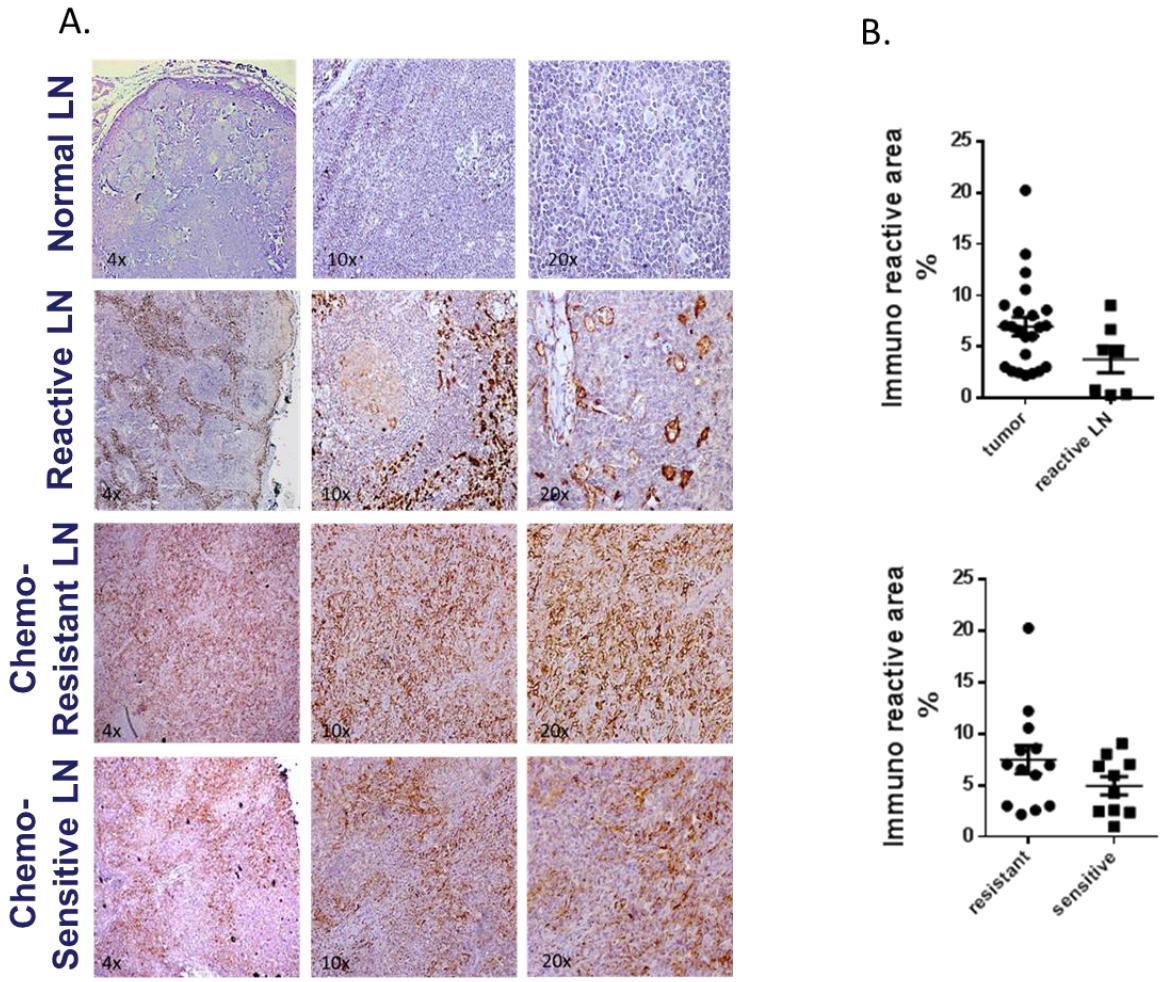

Fig.12. Identification of MS4A4A positive cells in human lymphoma. A. Immunohistochemical stainings of formalin fixed paraffin- embedded sections of normal lymph node, reactive LN, chemo-resistant Hodgkin Lymphoma and chemo-sensitive Hodgkin Lymphoma, with anti-MS4A4A, counterstained with hematoxylin. B. Comparison of immune reactive areas among

tumor and non tumoral samples. (upper) Comparison between lymphomas (7.00 ± 0.91) and non-neoplastic, reactive LN (3.75 ± 1.30). (lower) Comparison between chemo-resistant (7.50 ± 1.37) versus chemo-sensitive lymphoma samples (5.00 ± 1.03).

Because of the distribution of the positive staining mainly within areas free of lymphocytes but potentially associated with macrophage activity (vascularization and fibrosis), we performed a double staining for the macrophage marker CD68 together with MS4A4A.

As expected, the results showed that almost the totality (98%) of the cells positive for MS4A4A were also positive for CD68 within the lymphatic tissue (Fig.13, left), while about 5% of cells staining positive for MS4A4A were observed in the fibrous subcapsular septa and in the adipose tissue, that were not positive for CD68 (Fig.13 right). Based on their smaller, round morphology, these cells are likely to embody recruited monocytes on their way to differentiation. On the other way around, not all the CD68 positive cells were also MS4A4A+, clearly indicating the existence of a subpopulation of macrophages that within the tumor, supports functions typically exerted by M2-like macrophages.

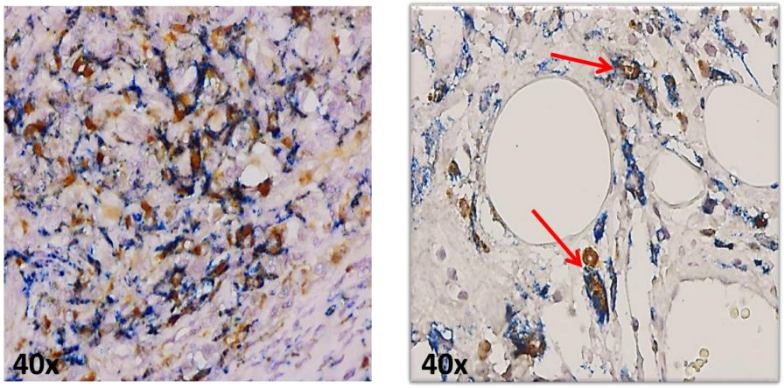

Fig.13. CD68-positive macrophages co-express MS4A4A. Double immunohystochemical staining for MS4A4A (blue) and macrophage marker CD68 (brown) of formalin fixed paraffin-embedded sections of Hodgkin lymphoma, showing the presence of a subpopulation of MS4A4A+ macrophages.

In the set of stained lymphoma samples, tumors with uniform and strong expression, as well as specimens with weaker and more heterogeneous expression were observed (Fig. 12). However, reactivity was detected in all the sections analyzed, with a consistent progressive peripheral enhancement from the perinodular capsule to the more centripetal fill. The germinal centers were always negative, confirming MS4A4A is not expressed by lymphocytes. Interestingly, positivity was accentuated in all the perivascular regions and in the fibrotic areas surrounding the tumor (Fig. 14), suggesting these positive cells might be associated with both neovascularization and tissue remodeling, in line with a TAM profile. Together, these evidence contribute in making MS4A4A a suitable target for antibody based therapy.

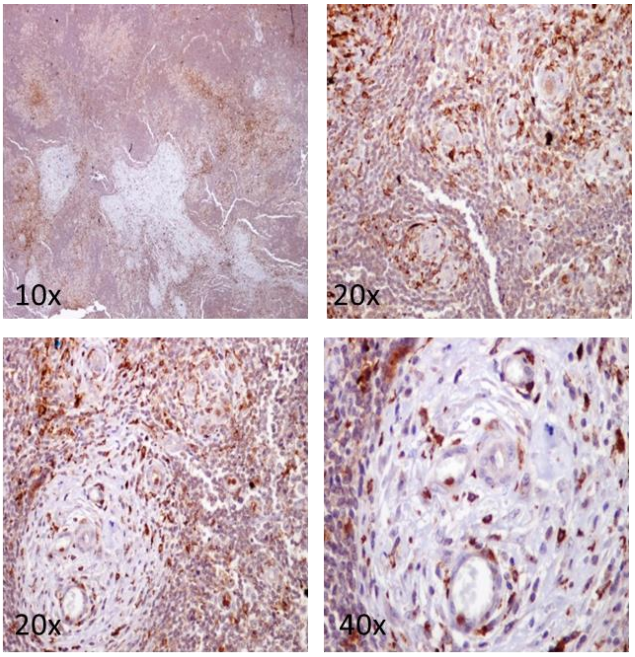

Fig.14. Predominance of MS4A4A positive cells within the perivascular area and in fibrotic tissue. Representative MS4A4A immunostaining of formalin fixed paraffin- embedded sections of Hodgkin Lymphoma indicating a consistent expression within fibrosis (upper) and around the vessels (lower).

4.3. Isolation of an MS4A4A targeting humanized antibody by phage display library

Phage particles displaying the members of the library were isolated from a phage display library derived from 22 anonymous donors' blood and tissues, and consists of 3×10^{10} M13 phagemids, each one expressing a different antibody in a Fab format. DNA fragments encoding Heavy Chains (HC), Light Chains (LC), and the linker were amplified by PCR and ligated into the phagemid vector. Amplified products were then transformed into TG1 *E.coli*, and rescued by infection with the M13KO7 helper phage. Our strategy was based on panning this library against transiently transfected HEK 293T expressing the recombinant MS4A4A protein.

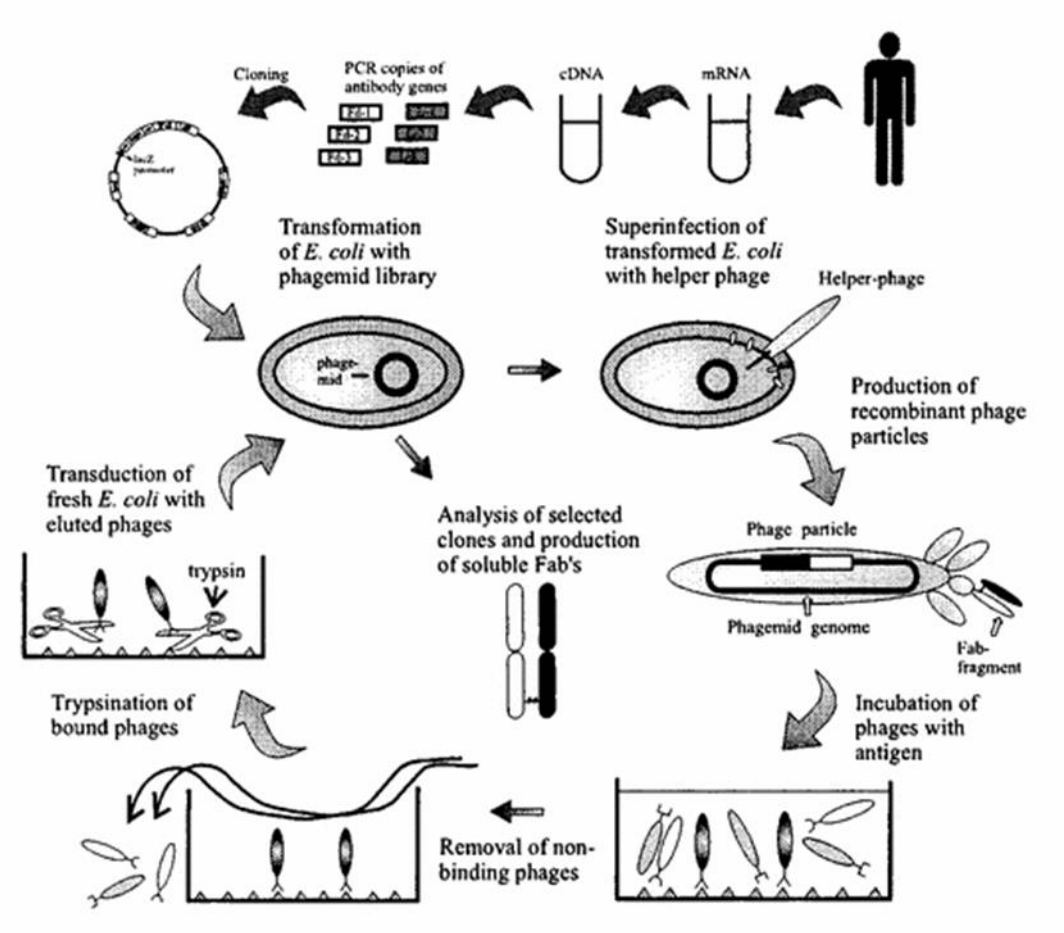

Fig. 15. Scheme of human antibody libraries generation procedure. The RNA is isolated from peripheral blood and tissue of volunteers and retro-transcribed into cDNA. Its following

amplification by PCR generates fragments which are going to be cloned in vectors and expressed in frame with the phage surface protein (pIII). The library will eventually undergo multiple steps of purification, to isolate the clones recognizing the antigen.
Each phage binding better to the MS4A4A transfected HEK plate compare to non-transfected was further confirmed by repeating the binding experiment using the corresponding Fab.
8 clones were selected as positives out of which 5 were identical hence reducing the number to 4 unique clones, later confirmed by sequencing: D1 (+4 identical), H10, H12 and B8.
These 4 selected phage clones were converted into full-length IgG1 molecules as previously described [374] and purified on affinity column.

In order to evaluate the affinity of the positive clones for the target protein, HEK-293T cells were transiently transfected with the hMS4A4A –pcDNA3 expressing plasmid and stained with increasing concentrations (in a range from 100pg/mL to 10ug/mL) of each antibody for 1 h on ice. Anti-human IgG Alexa Fluor 488 conjugated secondary antibody was used at 1:4000 dilution to detect the interactions. Fluorescence was examined for each interaction, revealing an absence of binding in non-transfected cells and a really low affinity for the clones E12 and B8 in both species (Fig.16). D1 and H10 were instead chosen for further characterization, due to their good binding capacity to the human protein transfectants, although only D1 was able to recognize the protein in both species (Fig.16B and C).

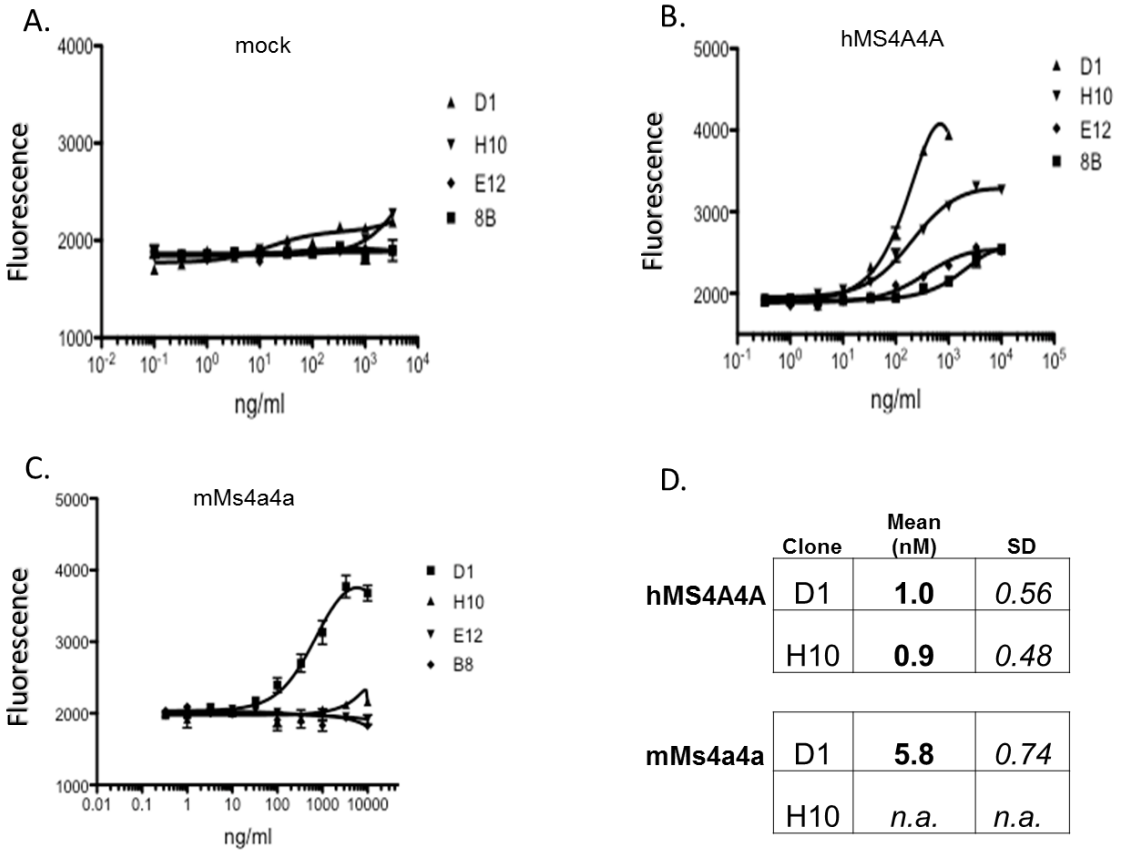

	Clone	Mean (nM)	SD
hMS4A4A	D1	**1.0**	*0.56*
	H10	**0.9**	*0.48*
mMs4a4a	D1	**5.8**	*0.74*
	H10	*n.a.*	*n.a.*

Fig.16. Relative affinities of 4 IgG clones for human MS4A4A and mouse Ms4a4a. (A) HEK cells transfected with the mock pcDNA3 plasmid showing no antibody binding to the cells. (B) Under the same experimental conditions, the D1 antibody recognized with nM affinity the human transfectant (hMS4A4A) and (C) is also able to cross-react with the murine mMS4a4a. (D) Table showing relative affinities for D1 and H10 antibodies calculated on triplicate wells.

In order to identify the epitope recognized by the two clones, an epitope mapping assay was performed. The sequence derived from the clones CDR sequencing and corresponding to the second extracellular loop, were subjected to site directed mutagenesis. Six amino acids were mutated (Fig.17A) starting from the hMS4A4A-GFP vector, and the resulting plasmids were used to transfect HEK293 cells (Fig.17C) to validate the binding capacity of the antibodies by flow cytometry (Fig.17B). Two mutations, Y145A and Y148A resulted in a complete abrogation of the antibody binding.

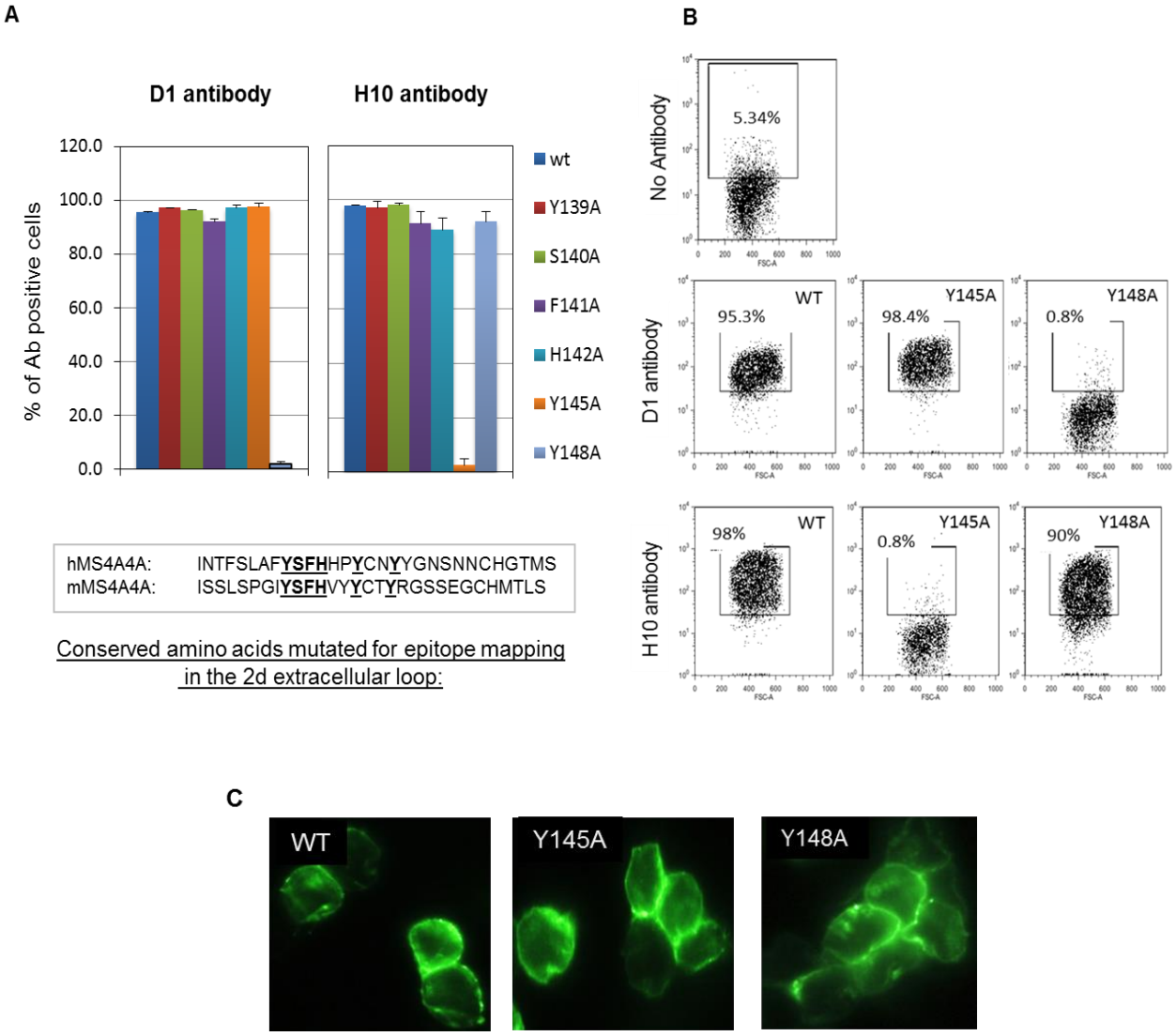

Fig.17. Epitope mapping for D1 and H10 antibodies. (A) Bar graphs showing % of cells staining positive for the respective antibodies and (B) Representative FACS plots of the same experiment. (C) Surface expression of hMS4A4A expression for WT, Y145A and Y148A mutants was verified by immunofluorescence microscopy

The binding affinity of the two clones was further confirmed in immunofluorescence in transfected cells. 24h after transfection with hMS4A4A construct HEK293 cells were coated on coverslips

pretreated by poly-L-Lysine. The day after, 1mg/ml of each clone (D1 or H10) was incubated for 1h on ice. After PBS washing, cells were fixed with 100% methanol for 5 min. Anti-human Alexa Fluor 488 IgG was used as a secondary antibody (Fig.18).

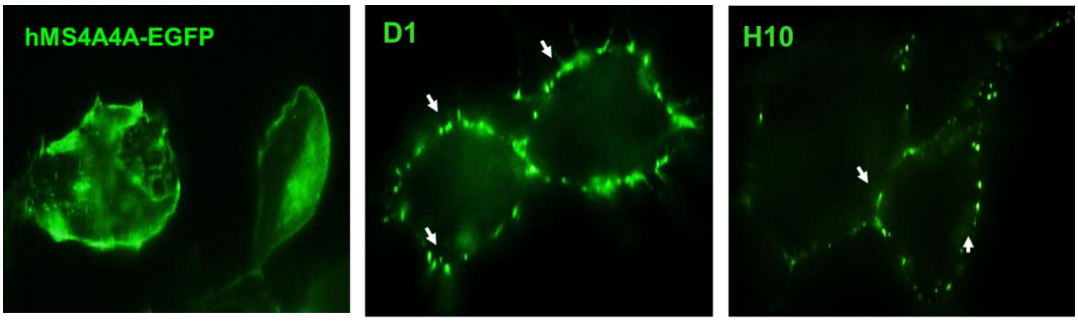

Fig.18. Immunofluorescence staining for human MS4A4A on transfected HEK cells using D1 and H10 clones. A punctate staining is observed for both antibodies (white arrows) as reported for CD20-like proteins. Immunoflourescence of HEK expressing hMS4A4A-GFP is shown for comparison. Images were taken using a Nikon TS100 inverted microscope.

Antibody-dependent cell-mediated cytotoxicity (ADCC) is the mechanism of cell-mediated killing of an antibody opsonized cell by a cytotoxic effector cell through the lysis of the target, classically mediated by natural killer (NK) cells by the release of their cytotoxic granules content. ADCC efficacy depends on several factors, including the antibody affinity and FcR-binding affinity. IgG are the most common subclass for therapeutic antibodies, and ADCC is the main mechanism of action for a number of therapeutic monoclonals, including the anti-MS4A1/CD20 rituximab.

We hence performed an antibody dependent cytotoxicity assay to evaluate the effects of our two clones. 48 h after transfection with hMS4A4A-GFP tagged or untagged constructs, HEK-293T cells were loaded with 10 mM of the calcein-AM dye for 1 h at 37^{o}C followed by 3 washes with complete media. Human NK cells were isolated on the same day from buffy coat using a human NK cell isolation kit (Macs Miltenyi). 10^^{4} HEK-293T cells were first incubated with increasing concentrations of antibodies in a round bottom 96-well plate for 1h at room temperature. 10^^{5} NK cells were then added to each well (1:10 ratio), spun down, and incubated for 4 h at 37^{o}C. Plates were then centrifuged and 70 uL of supernatant was transferred in a black plate for fluorescence

assessment. Only background HEK-293T killing was observed using a control anti dengue antibody (H1L1 clone) as well as with un-transfected cells (Fig.19 mock). On the contrary, D1 clone was able to mediate cell killing of both transfectants with a dose dependent effect (Fig.19).

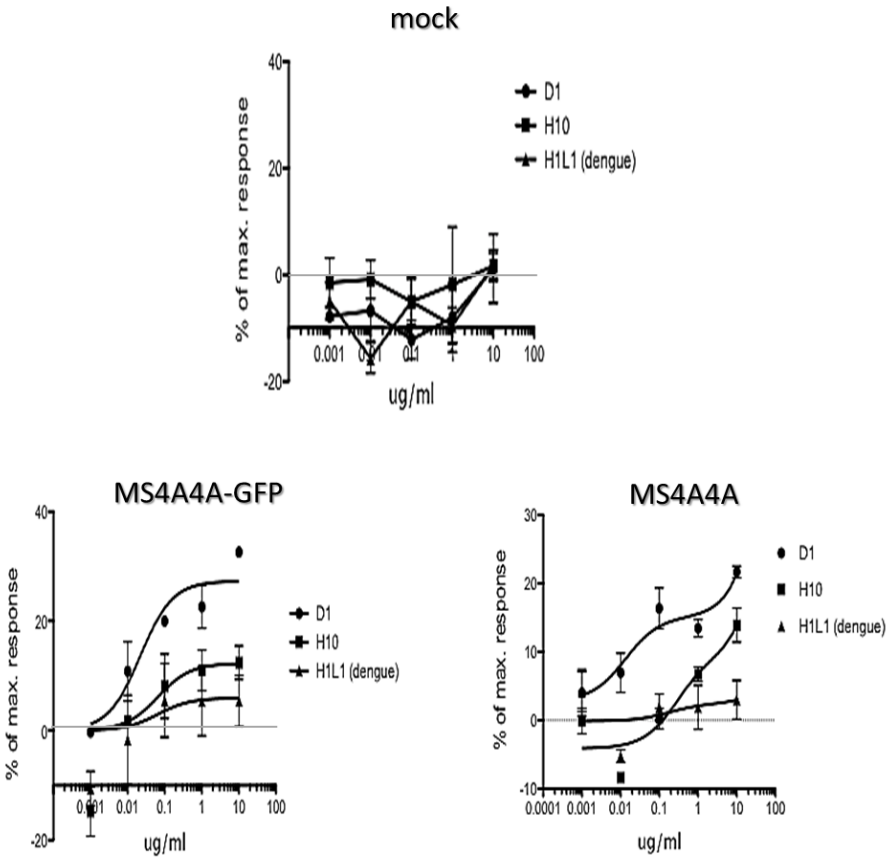

Fig.19. D1 and H10 antibody-dependent cell cytotoxicity. The assay was performed in HEK cells transfected with empty vector (mock), MS4A4A-GFP or MS4A4A untagged plasmid. In live cells calcein-AM is converted to a green-fluorescent calcein by intracellular esterases. The insoluble product can be retained by cells with integral membranes but is released by damaged ones. Analysis was performed by plotting mean percentages of calcein release ±SD from 3 independent experiments. Excitation:485 nm; Band-pass filter: 530 nm.

Because of its better performances in most of the assays executed, we chose D1 for further characterization.

To examine whether the D1 clone compete with the corresponding peptide to bind with MS4A4A, a competitive binding by flow cytometry was performed (Fig.20). A peptide corresponding to hMS4A4A second extracellular loop was incubated at the indicated concentrations together with 1ug/ml concentration of D1 PE Cy7–coupled antibody at room temperature for 30 min. HEK cells transfected with hMS4A4A were then added to the mix and incubated for another 30 min. When the peptide concentration was increased, the binding of D1 antibody to MS4A4A transfectants was diminished. These results suggest that D1 clone is specific for the protein.

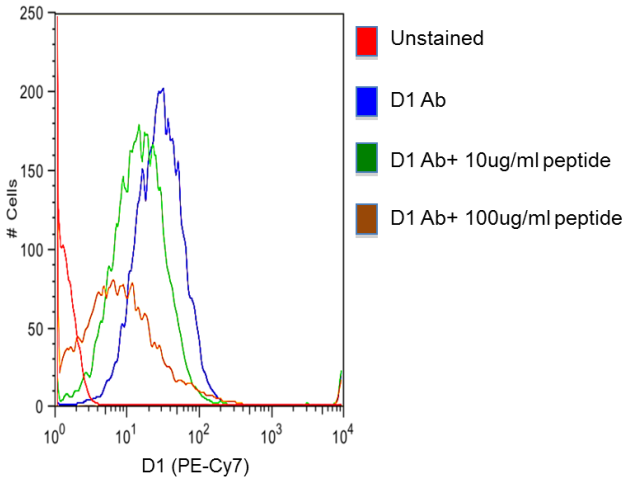

Fig.20. Peptide competition assay for D1 antibody. HEK-MS4A4A transfectants were incubated with increasing concentrations of the competing peptide and antibody staining was quantified by FACS.

We then moved to test the antibody on different types of transfectants and primary cells.

First, we compared its binding capacity on cells transfected with the empty pcDNA3 plasmid or with the pcDNA3-MS4A4A. The staining with PE mouse anti-MS4A4A (R&D) or D1-PECy7 (100ng/sample) on the transfected cells was performed on ice for 30' in PBS supplemented with 1% BSA. The cells were then washed and analyzed by flow cytometry (Fig.21).

The results indicated that both the antibodies can effectively bind the MS4A4A transfectant with a higher efficiency than the empty vector (EV). However, the commercial Ab showed lower background (10% positives cells) along with a higher binding ability (45% positives cells) compared to D1 (14% staining against the EV vs 27% on the MS4A4A transfectant).

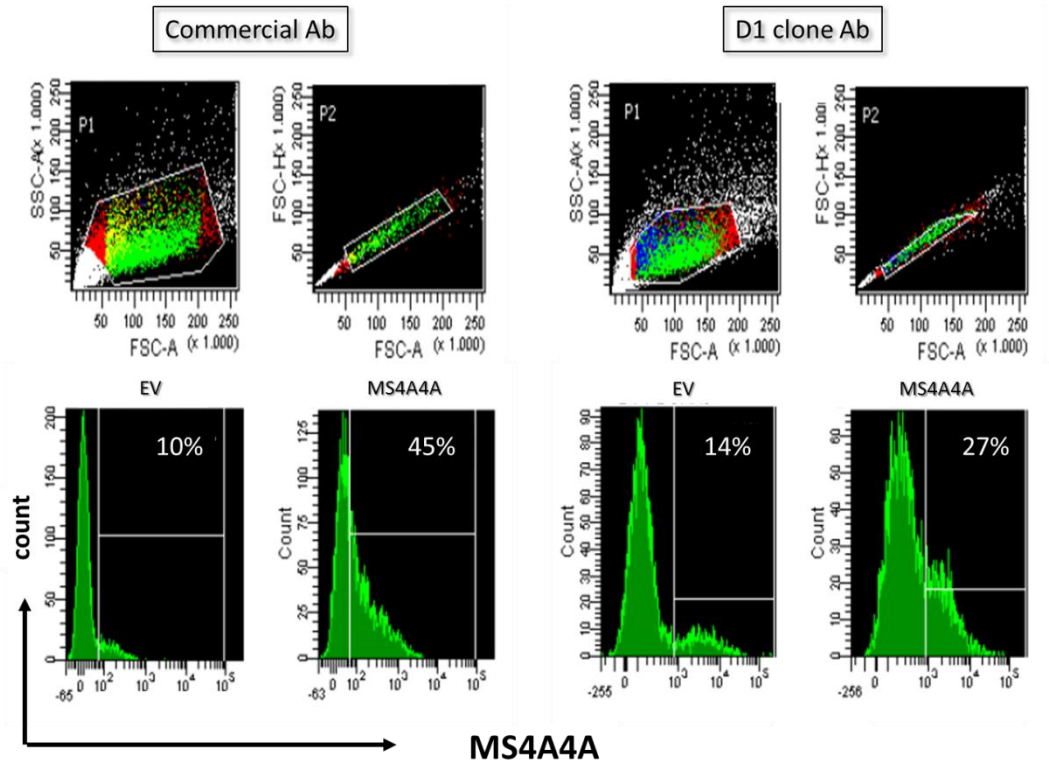

Fig.21. D1 recognizes the recombinant MS4A4A with a lower affinity when compared to the commercial monoclonal anti-MS4A4A. FACS analysis of HEK293 transfected with the control (EV) or the MS4A4A-pcDNA3 plasmid, to assess D1 ability to bind the target compared to the commercial monoclonal.

The same staining was then performed on human primary monocytes and differentiated macrophages. PBMCs were isolated from healthy donors buffy coats by Ficoll gradient. The cells were depleted in erythrocytes and stained with the two antibodies as described above.

In the case of PBMCs markers for B cells (CD19), T cells (CD3) and CD14 to gate monocytes were added to the mix. The FACS analysis confirmed once again the non-specificity of D1 compared to the commercial monoclonal. Indeed, the latter gave a positive staining within a subpopulation of CD14 intermediate, consistent with our previous findings according to which MS4A4A is not highly expressed in monocytes. On the contrary, D1 recognized subpopulations of CD14 high, CD14 intermediate and also lymphocytes subpopulations (Fig. 22A).

A.

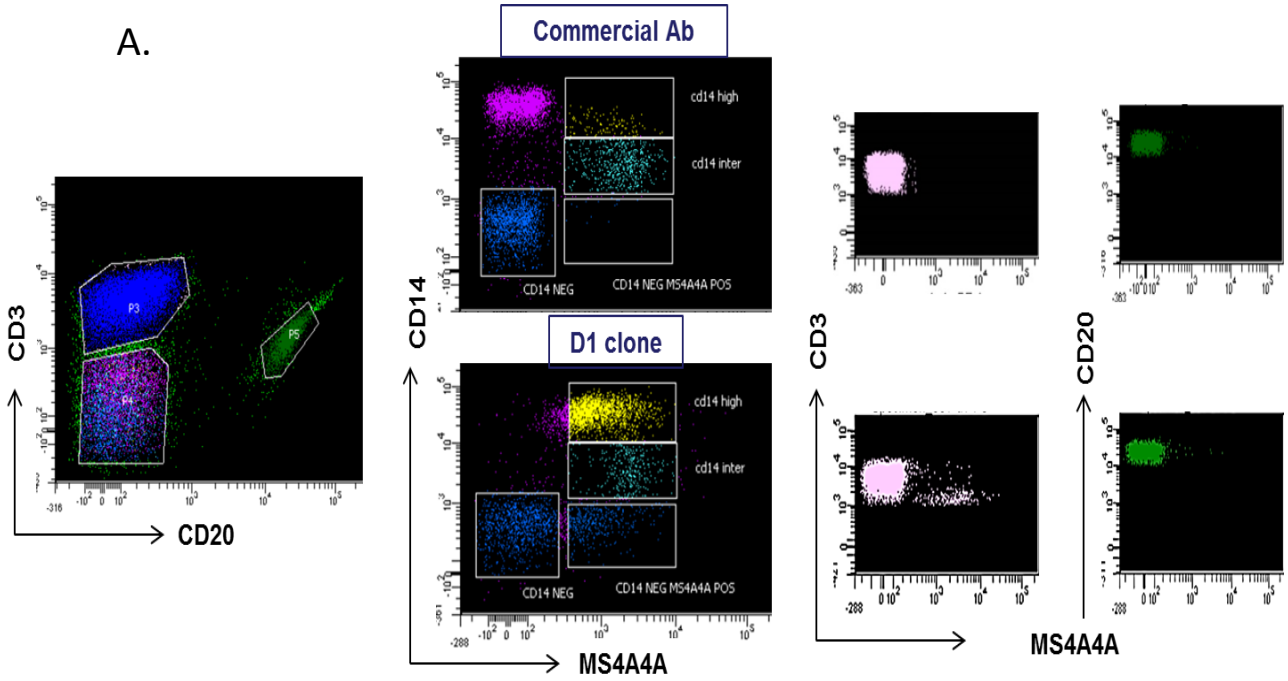
Commercial Ab
cd14 high
cd14 inter
CD14 NEG
CD14 NEG MS4A4A POS
D1 clone
cd14 high
cd14 inter
CD14 NEG
CD14 NEG MS4A4A POS
CD14
MS4A4A
CD3
CD20
P3
P5
CD3
CD20
MS4A4A

B.

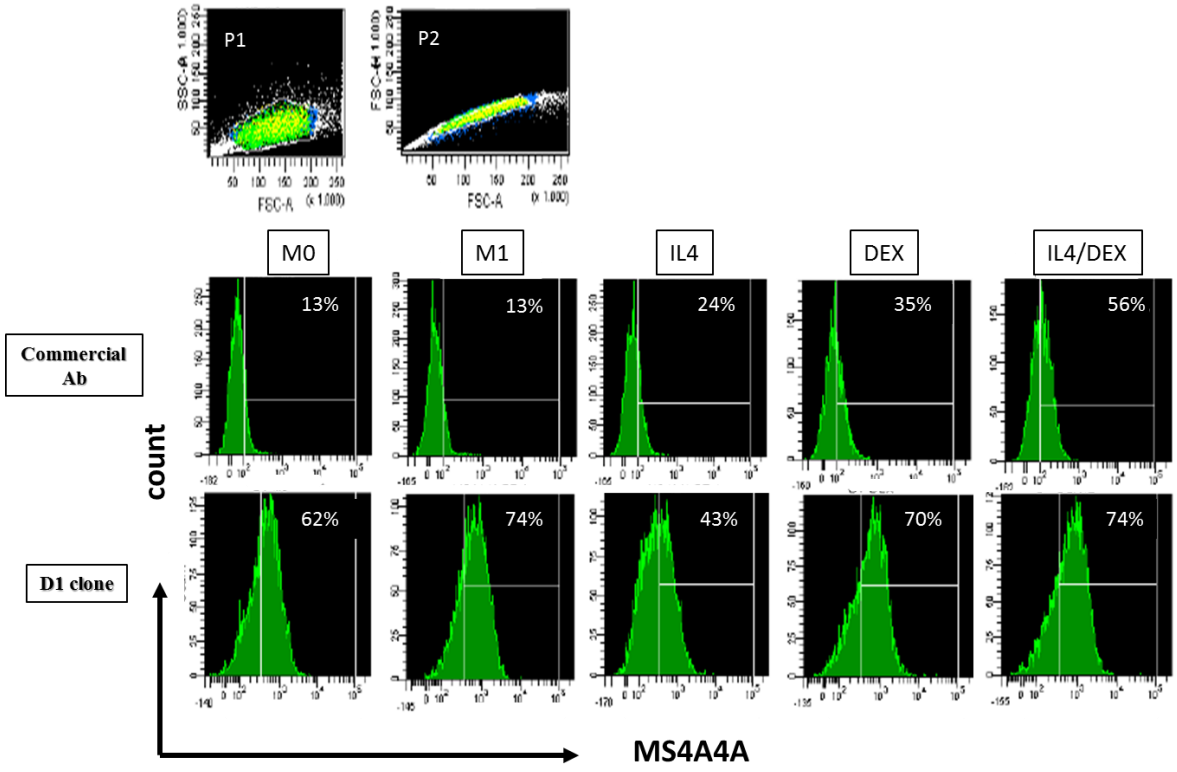
P1
P2
FSC-A
M0
M1
IL4
DEX
IL4/DEX
Commercial Ab
D1 clone
13%
13%
24%
35%
56%
62%
74%
43%
70%
74%
count
MS4A4A

Fig.22. D1 recognizes the native MS4A4A with a lower specificity when compared to the commercial monoclonal anti-MS4A4A. FACS analysis of freshly isolated PBMCs (A) and differentiated macrophages (B) stained with the R&D antibody or D1 (100ng/sample).

The monocytes isolated from the same buffy coats were differentiated and polarized with both M1 and M2 stimuli, in order to validate whether D1 was able to recognize the MS4A4A overexpression upon anti-inflammatory stimulation. Again, the home made antibody didn't allow any distinction in terms of MS4A4A induction with M2 mediators, while the commercial one did. In the M1 condition, in fact, the same percentage of positive cells as the Dex/IL4 combination (74%) was detected, meaning that the antibody is not recognizing only MS4A4A.The antibody was validated also in immunohistochemistry and immunofluorescence (Fig.23), and compared to the commercial antibody. In both cases, the pattern of the two Ig was not the same.

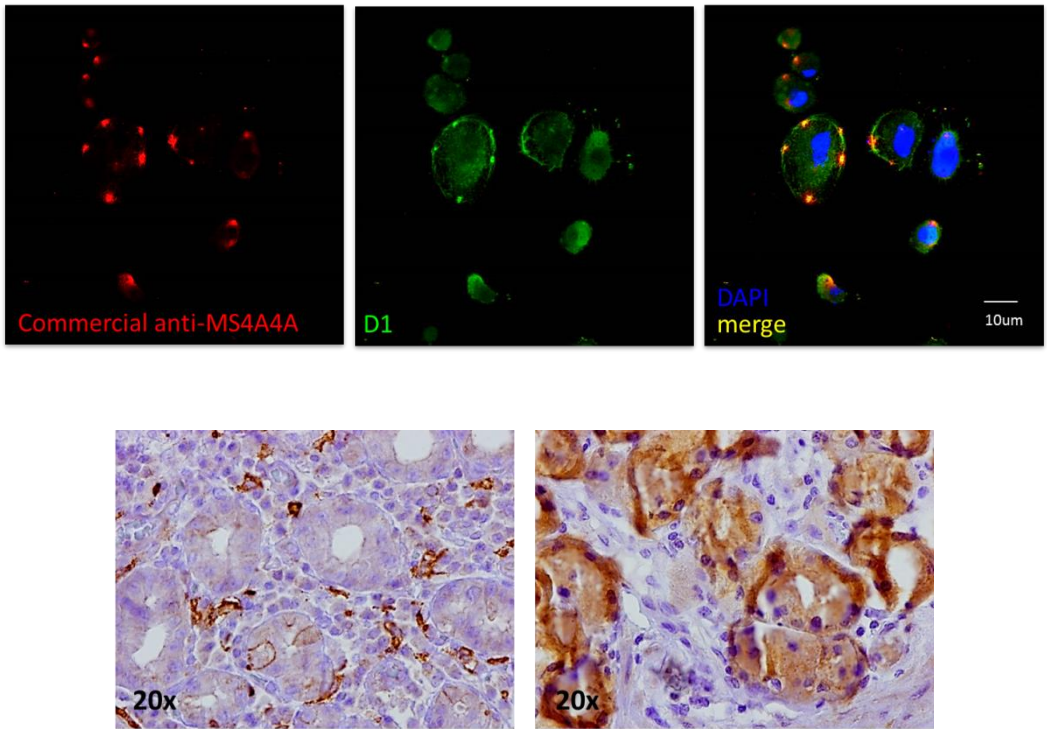

Fig.23. Comparison between D1 and commercial anti-MS4A4A antibody in immunofluorescence and immunohistochemistry. (Upper panel) Double staining with anti-MS4A4A and D1 on human macrophages. The image on the left represents the merge of the two,

demonstrating D1 non-specific recognition of MS4A4A. (Lower panel) Immunohistochemistry of paraffin embedded stomach sections, stained with anti-MS4A4A (left) and D1 (right).

4.4. MS4A4A interactions and function

4.4.1. MS4A4A is found within membrane lipid rafts upon GC stimulation

MS4A4A belongs to the MS4A family, that includes among its members some well characterized molecules, such as CD20 and Ms4a4b, which has been demonstrated co-localizing with raft detergent-resistant lipid microdomains upon recruitment [215, 375].

Lipid rafts are domains on the plasma membrane characterized by high concentrations of cholesterol and sphingolipids and are well known to be able to organize trafficking and signaling molecules on the membrane bilayer. Association of a molecule within the raft usually results in its activation or in a signal transmission [376].

As MS4A4A shares the same structure with these CD20 and Ms4a4b and it is also expressed on the cell surface we verified whether it was as well localized within lipid rafts by immunofluorescence. We therefore labeled human resting and polarized macrophages with the Cholera Toxin-B (CT-B), which binds to the glucosphingolipid GM1 ganglioside (GM1) localized within the rafts [377] and MS4A4A (Fig.24A). The cells were collected from three donors and an average of 150 ROI corresponding to single cells were evaluated in confocal microscopy in order to calculate for each of them the Pearson's correlation between the two channels corresponding to the two markers CT-B and MS4A4A. The analysis generates a value between +1 and −1 included, where 1 means total positive correlation, 0 no correlation, and −1 total negative correlation.

As shown in Fig.28B, at the basal level no co-localization occurs between MS4A4A and the rafts, while once the cells are given with Dex, the co-localization index raise up to 0.7.

This partially indicates the re-localization of the molecule upon GC treatment, although a discrete portion of the proximity might be due to the *de novo* expression of the protein upon GC.

Trying to clarify this point and understand whether Dex induces a re-localization of MS4A4A along with its neo synthesis, cells were treated for 2h with Dex and analyzed for co-localization. Such a range of time in fact is not enough for GC to activate the transcription machinery, but is enough to promote the membrane reorganization. As shown in Fig.24B and confirmed by Pearson linear regression analysis (Fig.24C), re-localization occurred already after 2h Dex treatment, indicating the GC stimulation induces MS4A4A association with the rafts.

A.

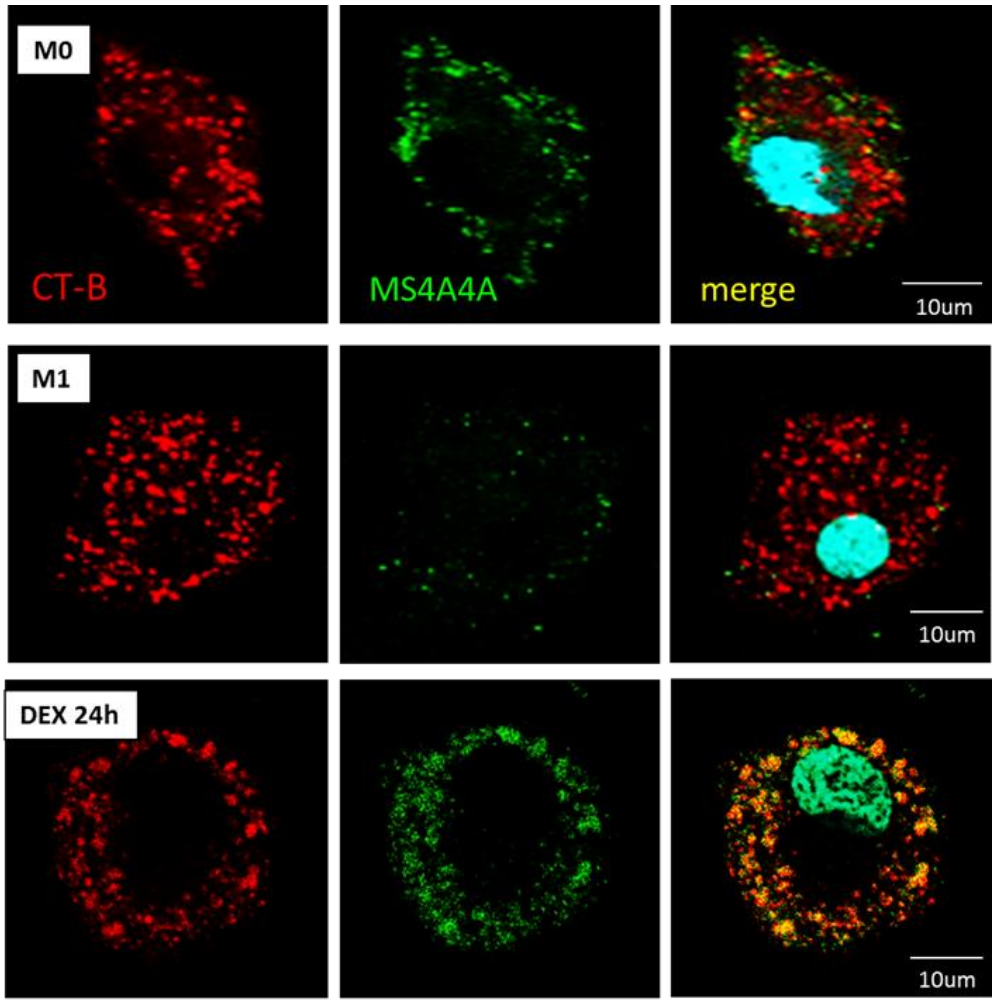

B.

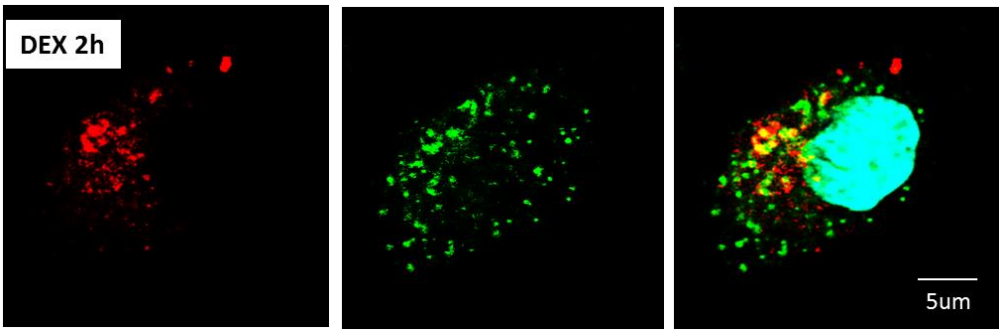

C

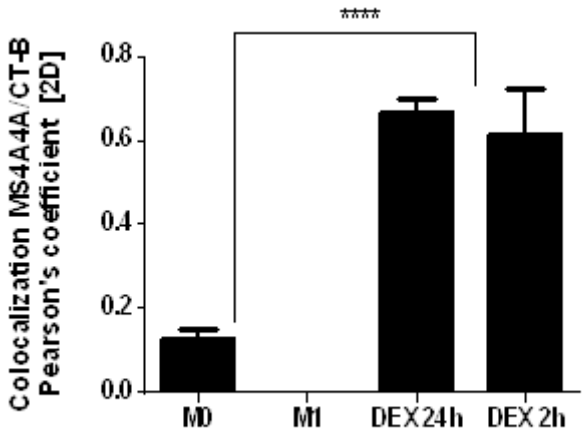

Fig.24. GC induce re-localization of MS4A4A within lipid rafts. A. Immunofluorescence of resting and polarized human macrophages labeled for MS4A4A (green) and Cholera Toxin-B (CT-B, red) showing co-localization upon Dex challenge. The co-localization the two molecules is represented by overlay of the images, illustrated by yellow merge. (M0, resting macrophages; M1, IFN/LPS treated macrophages; Dex 24h, macrophages treated for 24h with GC). B. Dex 2h, macrophages treated 2h with GC) C. Pearson's coefficient for MS4A4A and CT-B channels, calculated on 150 ROIs per condition $\pm$ SEM, analyzed from 3 donor's macrophages. * denotes $p<0.05$.

Cholesterol depletion is routinely employed to establish the lipid rafts' contribution in cellular process and it can be performed using methyl-beta-cyclodextrin (MβCD), which extracts cholesterol from the outer side of the plasma membrane by sheltering it in a hydrophobic cavity [378, 379]. Cyclodextrins are cyclic oligosaccharides of α-(1–4)-linked D-glycopyranose units which typically exist as hexamers (α cyclodextrins), heptamers(β cyclodextrins) or octamers (γ cyclodextrins). β-cyclodextrins display the highest affinity for cholesterol and are the most effective in extracting cholesterol from cellular membranes.

So, we set up a protocol of cholesterol depletion from primary macrophages, so as to observe whether alteration of rafts would affect MS4A4A expression (Fig.25).

Macrophages were polarized as usual for 18-24h and then given with 5mM final MβCD. The medium was then removed and cells were labeled for the rafts with the CT-B, then fixed in 4%PFA without permeabilization , stained with MS4A4A overnight and mounted for the confocal analysis

(Fig.25A). In parallel, part of the cells were stained with anti- MS4A4A to be analyzed by flow cytometry to look at the surface expression of MS4A4A (Fig.25B).

Results showed a significant reduction of the protein upon cholesterol disruption, corroborating the hypothesis of an association of MS4A4A with cholesterol enriched microdomains.

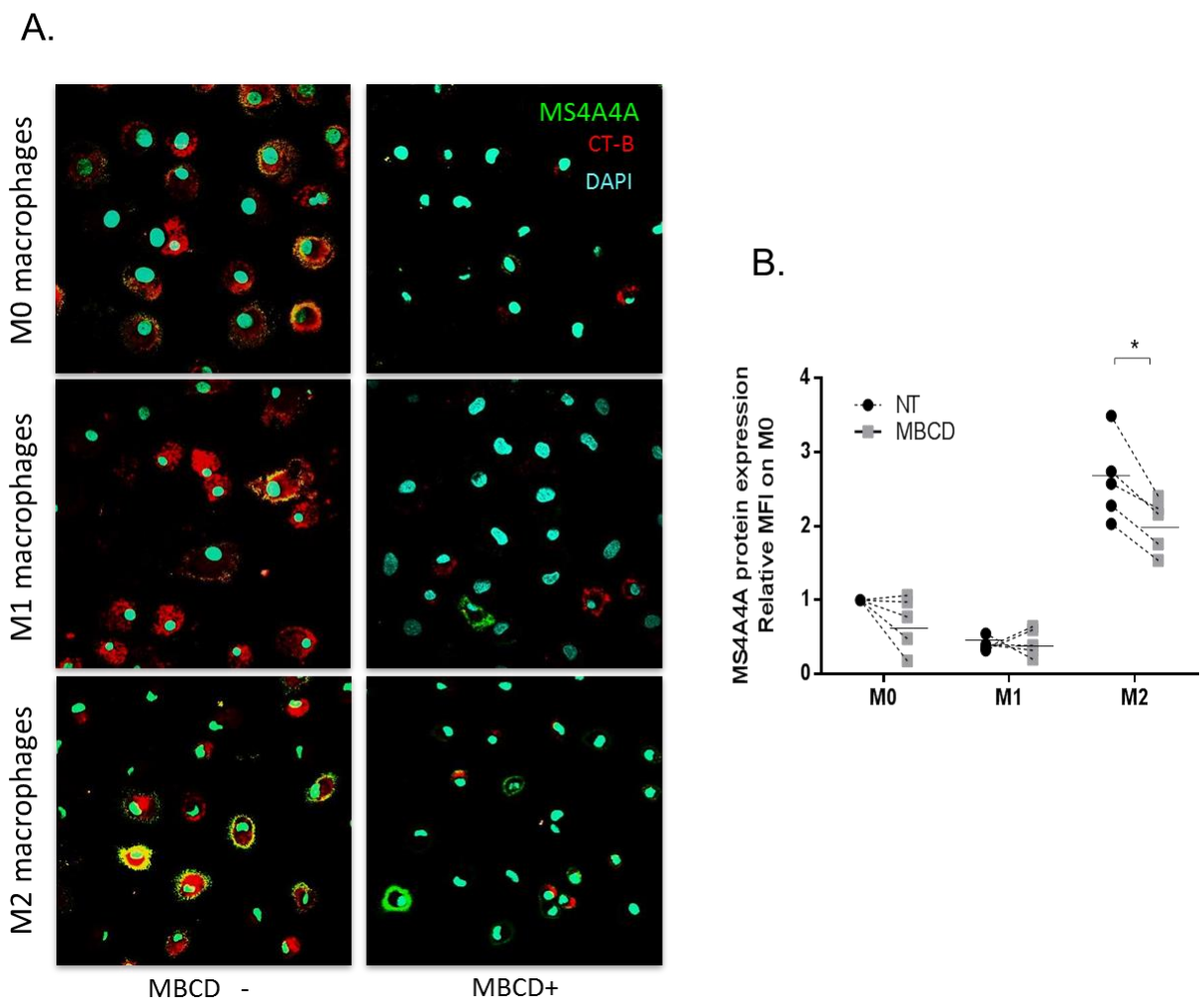

Fig.25. MS4A4A expression is impaired upon cholesterol depletion. (A) Immunofluorescence of cholesterol depletion following MβCD (red: CT-B; green: MS4A4A). Cells were polarized for 24h and afterwards given with 5mM MβCD for 1h. Co-localization of the markers is visible as yellow color. (B) FACS analysis showing the reduction of MS4A4A at the membrane level upon cholesterol enriched domains depletion by MBCD. *, $P < 0.05$

4.4.2. MS4A4A forms homo and heterodimers on the cell surface

With the attempt of discover a bit more about MS4A4A role on the plasma membrane of macrophages, we decided to explore its potential interactors adopting the yeast split-ubiquitin screen. This approach is a variation of the traditional yeast two hybrid, with the key advantage of allowing the measurement of the protein interactions at the surface level instead of in the nucleus, as described in *Materials and Methods*. [380]. The library was generated by Hybrigenic Services, France. The starting material was total RNA extracted from human monocytes derived macrophages treated for 24h with Dexamethasone. The resulting cDNA was directionally cloned into pPR3-N to generate the NubG-X library.

MS4A4a was expressed as C-terminal ubiquitin LexA-VP16 fusion (pBT3-STE vector) in the *S. cerevisiae* strain NMY51 and tested for their capacity of activating the transcription of the histidine and adenine reporters exclusively upon ubiquitin re-association. The ability of MS4A4A to activate transcription of the reporters was verified with a transmembrane positive control. Then, the library was interrogated with MS4A4A as bait out on SD-Leu/-Trp/-His/-Ade agar plates complemented with 10mM 3-AT.

A number of integral membrane proteins resulted interacting with MS4A4A in a bait-dependent fashion (Fig.26).

A total of 89.7 million interactions were analyzed an 178 clones gave a positive readout and were sequenced. Most of them resulted in false positive interactions, mostly by clones expressing ribosomal or mitochondrial proteins, heat shock proteins, cytochrome oxidase, proteasome subunits, collagen-related proteins, zinc finger-containing proteins.

9 specific integral membrane proteins were shown to interact with MS4A4A in a bait dependent fashion. Only the very high, high and good confidence-scored interactions were considered for further investigation.

Surprisingly, one third of the positive clones were represented by MS4A4A itself and other two MS4A members with unknown function, which have been however already described in a microarray study performed by Martinez and colleagues as associated with macrophages alternative polarization [381]. This suggests MS4A proteins form homo and heterodimers with the other members, within districts of the membrane that might resemble the tetraspanin enriched microdomains (TEM).

Another third of the clones is represented by a set of molecules associated with fungal pathogens clearance. Among them, the β-glucan receptor Dectin1 is the most well-known one.

The rest of the clones were the Fc epsilon receptor 1 subunit gamma (FCƐRIγ), the Ceramide synthase 2 (CerS2) and the leptin receptor overlapping transcript (LEPROT).

A.

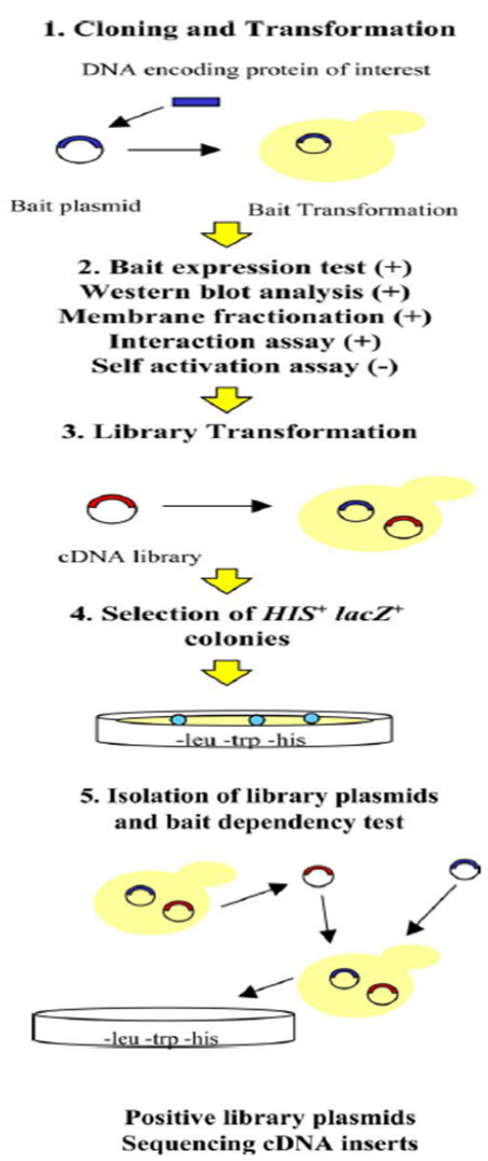

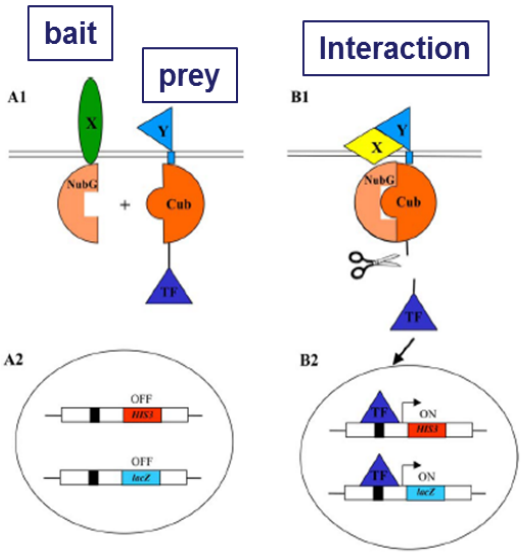

B.

GENE	N. OF CLONES
Dectin1	4
CD63	19
CD9	6
MS4A4A	18
MS4A6A	5
MS4A7	4
FCER1G	4
CerS2	2
LEPROT	4

Fig.26. Identification of potential partners interacting with MS4A4A by Split Ubiquitin Yeast two Hybrid. (A) Scheme illustrating the procedure and topology of bait and prey constructs used in the split-ubiquitin screen. The bait is expressed in frame with the C-terminal portion of Ub and includes the sequence for a transcription factor. In the case of a positive interaction, the partner,

fused with the N-terminal, reconstitutes the Ub, which becomes cleavable, and releases the TF, which migrates into the nucleus, activating the transcription of the reporter genes. (B) Identities of the top scored bait-dependent MS4A4A binding partners from the yeast split-ubiquitin screen.

Although the yeast two hybrid technique provides an important hint about possible co-expression and co-localization of two proteins, it doesn't give evidences of a direct interaction.
In order to validate the two hybrid results in a more "*in vivo*" environment, we therefore performed a FLIM-FRET experiment in CHO transfectants.
As described in Materials and Methods, the FRET phenomenon occurs when the excited fluorescent donor transfers in a non-radiative way part of its energy to an acceptor molecule at its ground-state. The efficiency of this process is inversely reliant on the sixth power of the distance between the two molecules and the phenomenon can only occur when the distance between the fluorophores is in the range of 10nm. Since intensity based FRET can be affected by several factors such as fluorophore concentration or environmental effects, therefore giving rise to a variety of optical artifacts [382], fluorescence lifetime imaging microscopy (FLIM), which is unaffected by these alterations, was chosen to validate MS4A4A interaction with the targets (Fig.27).

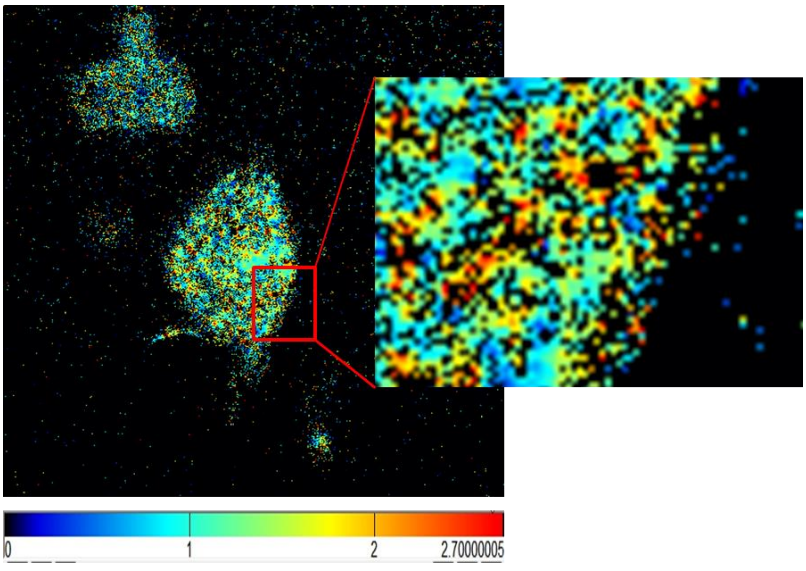

Fig.27. Pseudocolor lifetime image of Dectin1-MS4A4A axis. Reduction of lifetime corresponds to quenching caused by non-radiative energy transfer (FRET events).

MS4A4A, MS4A6A, MS4A7, Dectin1, CD9 and CD63 were expressed as fusion proteins with

mCherry or eGFP and stably overexpressed in different combinations in CHO cells maintained in medium supplemented with G418. 2*10^5 cells from each combination were seeded onto poly-L-lysine treated coverslips, fixed and imaged using two photon microscopy. FLIM images were produced to calculate the FRET activity between mCherry and eGFP and hence to evaluate the interaction between MS4A4A and its putative interactors.

The analysis confirmed the interactions between MS4A4A and itself and the other two MS4A members, and between MS4A6A and MS4A7, corroborating the hypothesis of the these proteins clustering on the plasma membrane. Also Dectin1 was confirmed interacting with both MS4A4A and MS4A6A and a decrease in the lifetime of MS4A7 with respect to Dectin1 was also detected, although not significant. No FRET took place between MS4A4A and neither CD63 nor CD9 (Fig.28).

Both CD9 and CD63 are known associate with Dectin1, taking part during the endosome and lysosome formation during the yeast/fungal particle internalization, respectively [333]. However, phagocytosis of pathogens requires specific PRRs and the activation of a cell-specific signaling cascade that might not be reproducible in a system like the one provided by CHO cells.

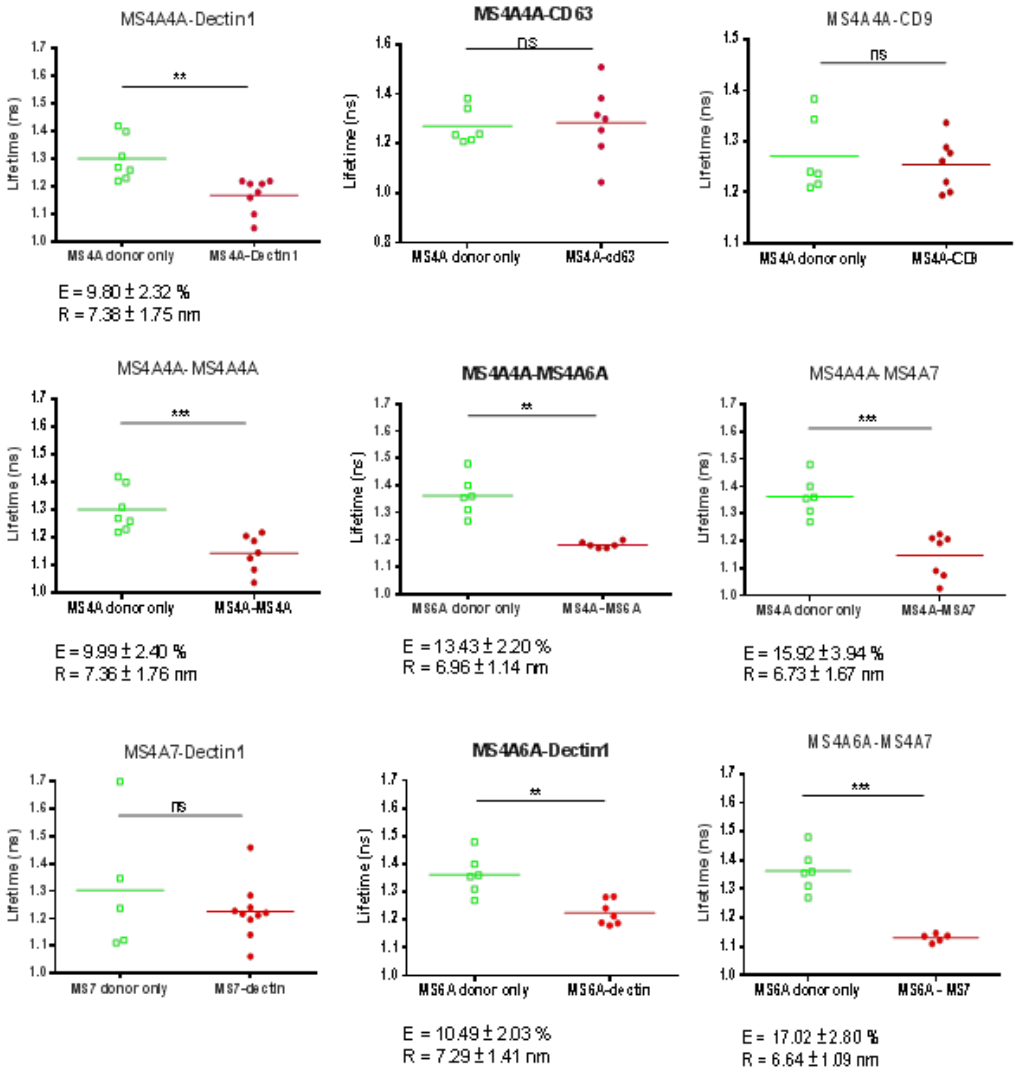

Fig. 28. Validation of the YtH by FLIM-FRET. Mean fluorescence lifetime values and their standard deviations of eGFP in CHO expressing combinations of molecules in frame with the fluorescent reporters (eGFP_X+ mCherry_Y) . The decay was evaluated in comparison to the eGFP_X alone and the decrease of eGFP fluorescence lifetime in the presence of mCherry_Y indicates the incidence of FRET between mCherry and eGFP, hence the interaction of X and Y. FRET efficiency (E) and the Förster radius (R) expressing the distance between the molecules are given for the significant interactions ($n \geq 5$) ±SD. *, $P < 0.05$

We therefore moved back to primary cells in order to evaluate whether an interaction was detectable upon engagement of Dectin1 with its ligand, β-glucan, at different time points.

Human macrophages differentiated on coverslips were challenged with Zymosan, an insoluble preparation of cell wall from *S. cerevisiae*, for 15' and 1h. Cells were then fixed in 4%PFA, permeabilized with TritonX-100, immune-stained with MS4A4A and Dectin1, CD63 or CD9 antibodies and mounted for confocal microscopy analysis.

Fig.29 shows the recruitment, at different extents, of all the molecules to phagosomes during internalization of Zymosan particles, indicating a possible cooperation in the clearance of pathogens. At the basal level, instead, MS4A4A seems to co-localize extensively only with Dectin1, which is normally expressed at the surface level and undergoes internalization upon activation.

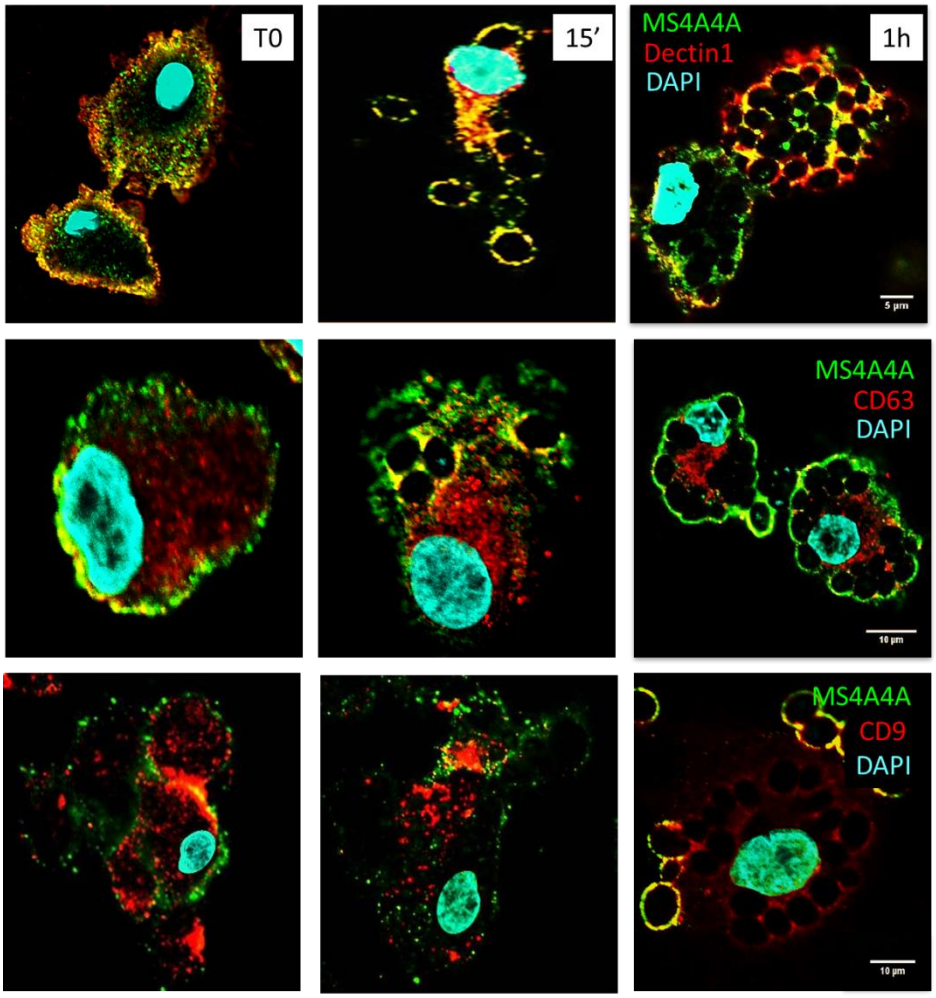

Fig.29. MS4A4A is co-expressed with Dectin1, CD63 and CD9 before and after Zymosan treatment. Immunofluorescent staining of primary cultured macrophages challenged with Zymosan for the indicated time points. Pictures are representatives of at least 6 independent experiments.

A co-immunoprecipitation (co-IP) assay was therefore employed to validate the YtH approach and to determine whether the co-expression seen by microscopy represents physical proteins interactions occurring in human primary macrophages.

Fig.30 shows the co-IP experiments on four of the interactions identified in the YTH assay, for which commercial antibodies were available.

In these experiments, human macrophages were isolated from three donors, left untreated (M0) or treated for 18h with Dexamethasone (DEX), or for 2h with the Dectin1 ligand Zymosan (ZYMO), and lysed in NP-40 Lysis Buffer. This detergent is weaker than TritonX-100 and helps better preserving proteins interactions. After pre-clearing with protein-G to reduce non-specific binding, lysates were incubated overnight with the antibodies against Dectin1, CD9, CD63 or MS4A6A. The following day cells were incubated with protein G-coated beads and eventually denatured in SDS-loading buffer. Proteins were then separated on a 12% SDS-PAGE, transferred to nitrocellulose membranes, and revealed with anti MS4A4A or, as a control, with the pull-down antibodies.

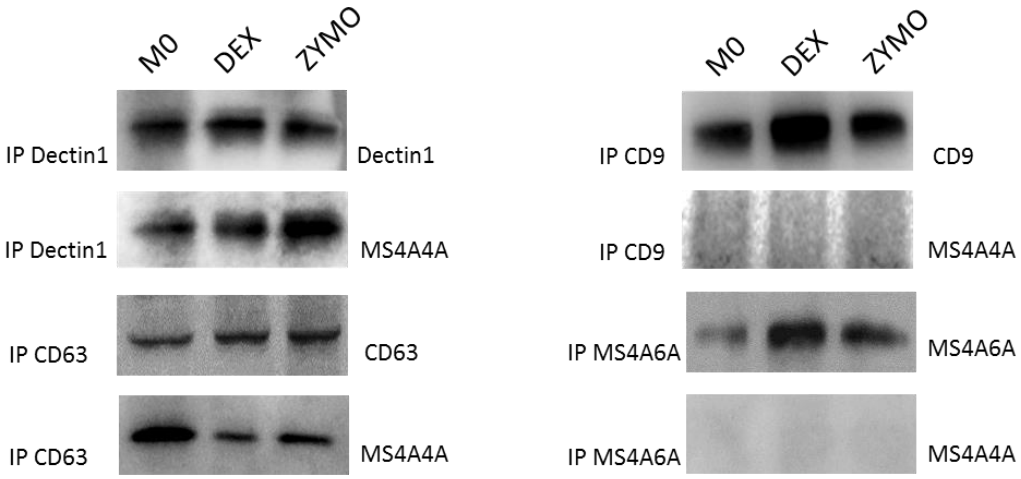

Fig.30. Co-immunoprecipitation of MS4A4A with its potential interactors. Human macrophages left untreated or treated with 10^{-6}M Dex for 18h or Zymosan (100ug/mL) for 2h were lysed with 1% NP-40. 200ug of cell lysates were immunoprecipitated with 5ug anti-Dectin1 or anti CD63 (left), anti CD9 or anti-MS4A6A (right) and analyzed by immunoblotting. Every sample was blotted with the IP antibody to confirm the immunoprecipitation, and anti-MS4A4A, to confirm the interaction.

The experiment confirmed the interaction of MS4A4A with Dectin1 in all the conditions examined, in line with the YtH and the FLIM-FRET data. CD63 interaction with MS4A4A was also confirmed in primary cells, differently from what was seen in CHO cells, probably because of the different features of these two cell types.

On the other hand, opposite to YtH and FLIM-FRET, neither CD9 nor MS4A6A were capable of immune-precipitate MS4A4A. This result may be due to several aspects that need further investigation. In both cases, the lack of interaction might depend either on the transient nature of the association, which occurs for a very limited period of time during the phagocytic process or on the detergent NP-40 used to lyse the cells, that may cause the disruption of weak protein complexes (a more gentile one should be therefore used for this purpose, e.g. Brij-35). Another explanation might be the indirect association of some of these molecules, which create complexes on the plasma membrane, but although in close proximity, are not physically connected.

4.4.3. MS4A4A response to different polysaccharides

Considering that Dectin1 was the only molecule validated for MS4A4A in all the assays performed, we decided to focus our attention in studying the nature of this interaction. Dectin 1 belongs to the pattern-recognition receptors family that includes among other members TLRs, Type 3 Complement Receptors and Scavenger Receptors. As already addressed, Zymosan is a yeast cell wall preparation, mainly composed of glucan and mannan (a mannose polymer), which is consequently able to activate PRR other than Dectin1, particularly TLR2and TLR6 and the mannose receptor (MR).

We therefore examined the MS4A4A expression in response to of various fungal polysaccharides in order to understand whether its regulation was differently affected by different components of microorganisms cell wall.

Human monocytes were differentiated into macrophages and passive adsorption mannan/LPS opsonized latex beads or Zymosan were added to the culture for different time points and mRNA and protein expression analyzed by q-PCR and FACS respectively. Expression levels of Dectin1 were also assessed as control, since its behavior towards these components has already been established.

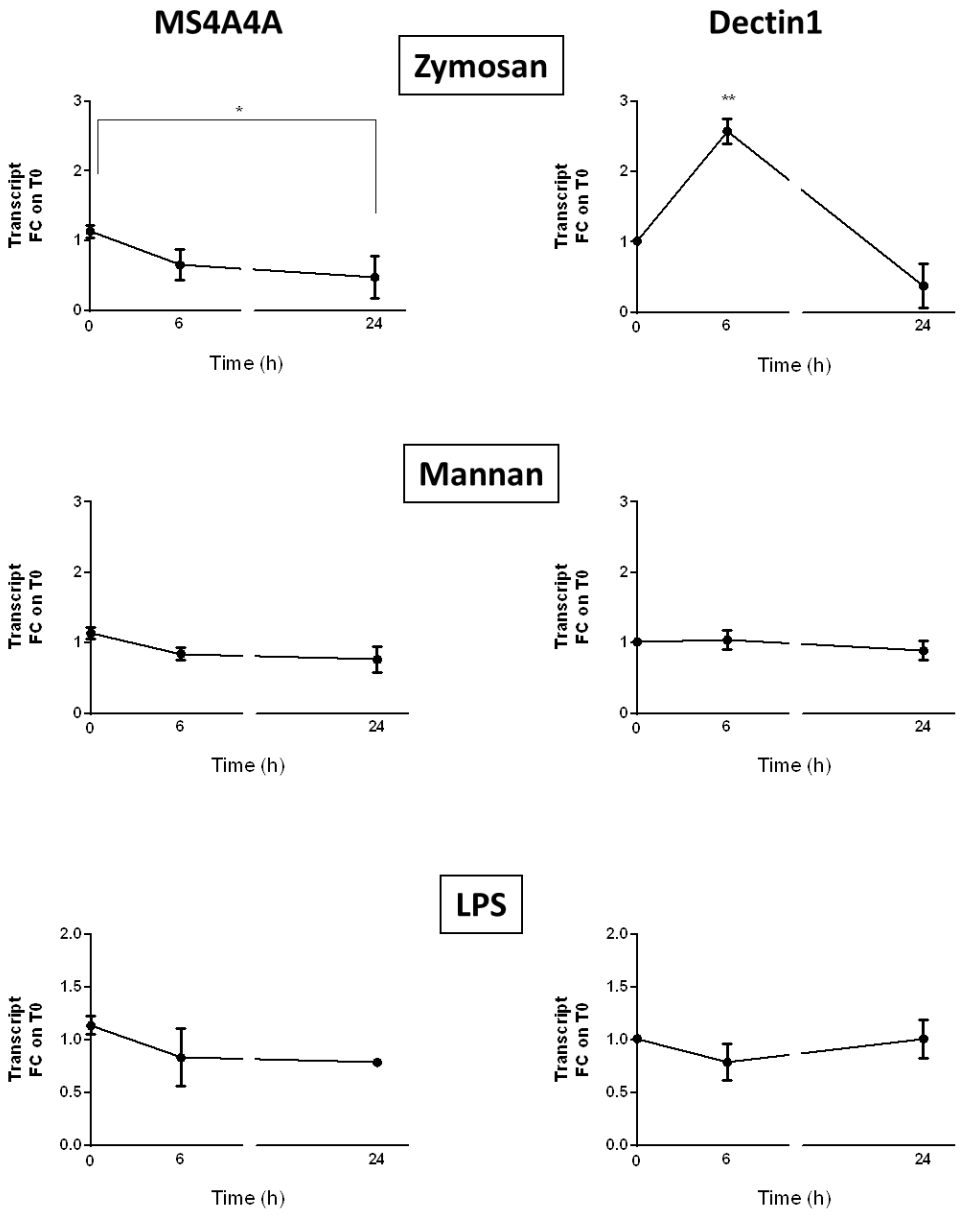

Fig.31. MS4A4A and Dectin 1 response to polysaccharides opsonized particles (transcript) Transcriptional analysis of macrophages treated with polystyrene latex beads opsonized with Mannan or LPS, or zymosan (20 particles/cell) for the indicated time points. Expression was normalized on GAPDH (ΔCT) and ΔΔCT was further calculated on macrophages at time 0, set as 1. N=3 ±SEM. *, P < 0.05

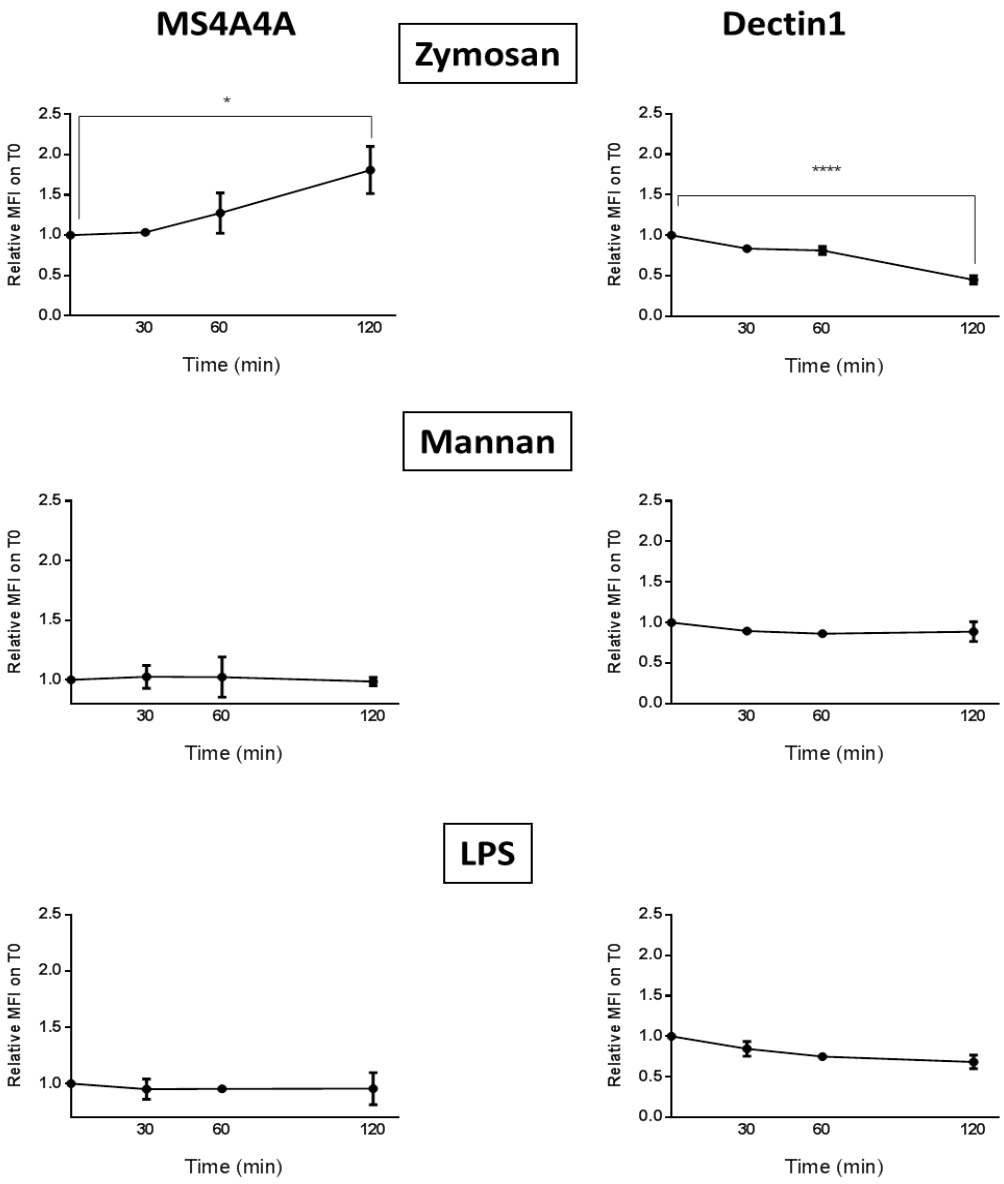

Fig.32. MS4A4A and Dectin 1 response to polysaccharides opsonized particles (protein) FACS analysis of macrophages treated with polystyrene latex beads opsonized with Mannan or LPS, or zymosan (20particles/cell) for the indicated time points. Expression was normalized on isotype and the resulting MFI was normalized on M0 at T0 set as 1. N=3 ±SEM. *, P < 0.05

As shown in Fig.31 and Fig.32, the treatment with the opsonized particles didn't effect neither Dectin1 (as expected) nor MS4A4A, indicating that the activation upon Zymosan mainly occurs because of a β-glucan mediated effect. Also the distribution of the two markers resulted remarkably different when immunofluorescence was performed by confocal microscopy, despite there were no differences in the number of internalized particles.(Fig.33)

Interestingly the expression on the surface assessed by FACS of the two proteins suggest opposite behaviors in response to Zymosan binding, with an increase in MS4A4A expression that culminates at 2h of treatment and a parallel reduction, due to its ligand-dependent internalization [383], of the β-glucan receptor Dectin1.

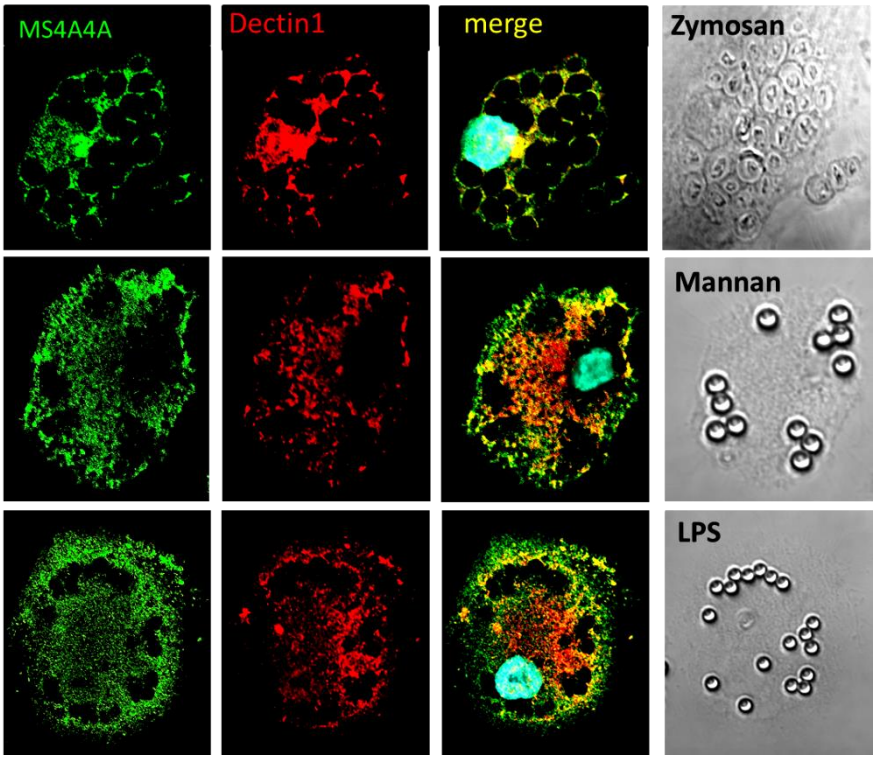

Fig.33. Distribution of MS4A4A and Dectin1 upon polysaccharides opsonized particles AND Zymosan phagocytosis. Human macrophages were given with 20/cell particles of zymosan or mannan/LPS coated polystyrene latex beads of 3 μm (approximately the same size of a zymosan particle) for 2h at 37°C, fixed and permeabilized, and labeled with anti MS4A4A (green) and anti-Dectin1 (red). Phagocytosis was visualized by confocal microscopy. Pictures are representatives of at least 3 independent experiments.

4.4.4. MS4A4A expression is negatively related to Dectin1 expression upon β-glucan stimulation

Several works report a different ability by different β-glucans to induce Dectin1 activation [384, 385]. Indeed it has been demonstrated that Dectin1 is able to bind to all the types of β-glucan, but it exerts its antimicrobial activity only in the presence of particulate polymers, most likely through a mechanical effect of these latter on the formation of the so called "phagocytic synapse" which induces the removal of the inhibitory tyrosine phosphatases [386], allowing to activate a robust immune response only when strictly required.

Whole glucan particles (WGP), is a particulate from *S. cerevisiae* β-glucan preparation made of long polymers of β-1,3 [387]. Opposite to Zymosan, WGP lacks a TLR- promoting activity [386], but similarly to it, it triggers Dectin-1-dependent responses, including phagocytosis, cytokines production and ROS by APCs.

Similarly to particulate WGP, soluble PGG binds specifically to Dectin-1, yet it is incapable of activating the receptor dependent responses as all the others soluble b-glucans, in spite of their molecular weight.

The fact MS4A4A and Dectin1 co-localizes at the membrane level but display opposite behavior upon Zymosan stimulation, prompted us to evaluate its response to other forms of β-glucan.

The macrophages were stained with anti-MS4A4A and anti Dectin1 at 4°C for 20 min to prevent receptors internalization, then Zymosan, was added, part of each sample was shifted to 37°C to allow phagocytosis and/or internalization to occur, part was kept on ice. After 1h and 2h incubations, the percentage of receptor internalized was calculated from the mean fluorescence intensity (MFI) values as 100 x [MFI (37°C sample) /MFI (4°C sample)], after normalization with the respective isotypes (Fig.34).

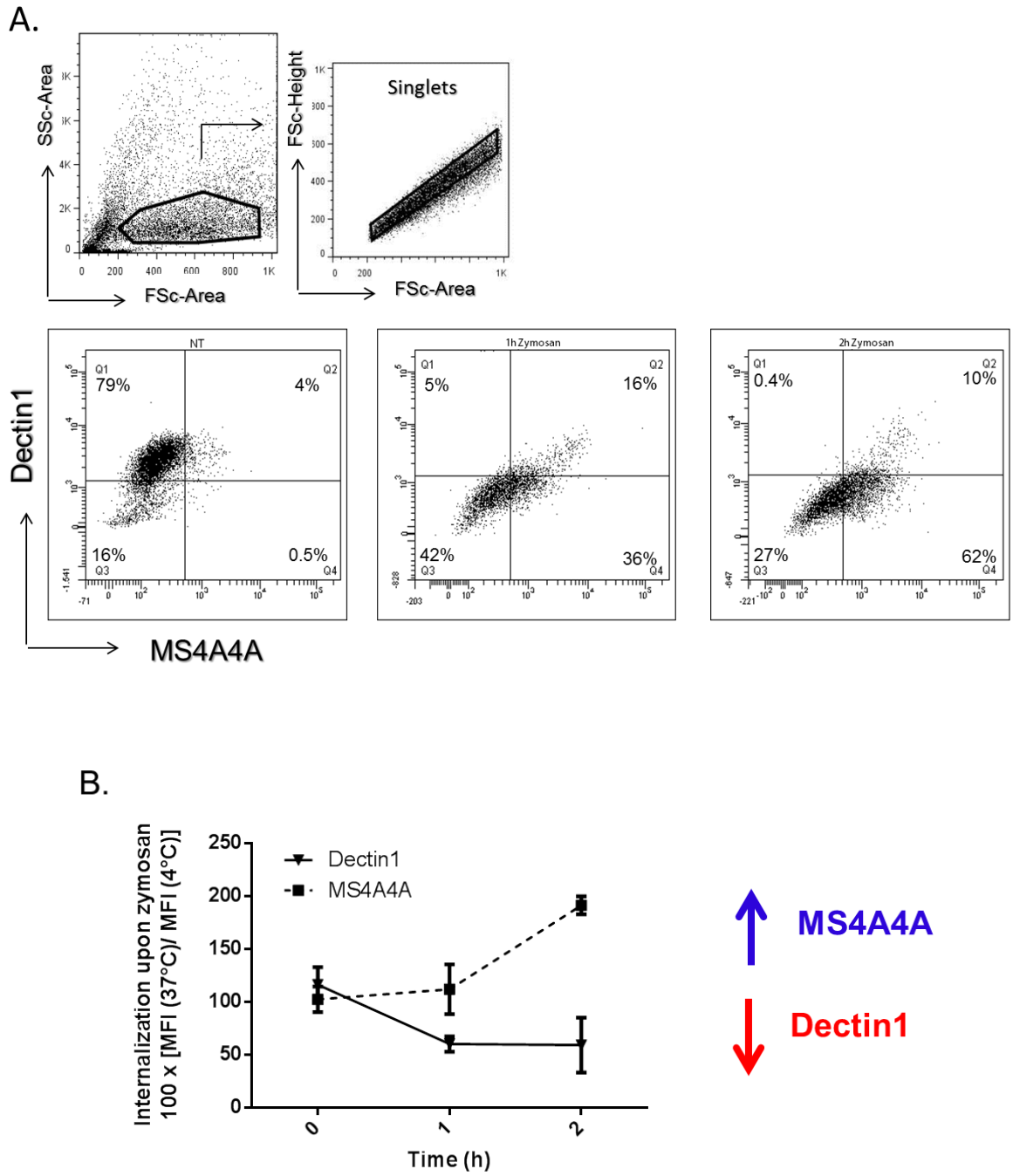

Fig.34. MS4A4A expression is negatively related to Dectin1 one. Staining for MS4A4A and Dectin1 of human macrophages untreated (0) or treated for the indicated time with zymosan (50ug/mL). (A) Representative dot plot displaying the inverse correlation between the expression of the two molecules. (B) Relative MFI±SEM of 3 independent experiments of antibody feeding. Macrophages were given with Zymosan , half of each sample was kept on ice, the rest shifted to

37°C to allow phagocytosis and/or internalization. After the indicated incubations, cells were labeled with anti-MS4A4A and anti Dectin1 at 4°C for 20', and analyzed by flow. The MFI were normalized on the respective isotype, and the percentage of receptor internalized (or not) was calculated from the mean fluorescence intensity (MFI) values as 100 x [MFI (37°C sample) /MFI (4°C sample)]. (*, $P < 0.05$)

As shown in the dot plot (Fig.34A) Dectin1 positive cells drop from 83% at the basal level to 21% after an hour stimulation, to almost 10% after 2h.

On the contrary, MS4A4A positives cells raise from ~5% in the resting cells, to 52% after 1h, to 72% after 2h. The trend looks the same in all the experiments performed, indicating that a sort of regulation may exist between the two molecules, such that one negatively affects the other ones expression at the membrane level, considering that their levels are modulated within the same population of cells.

The way the antibody feeding is carried out indicates Dectin1 is actually internalized and not only down-regulated upon β-glucans biding.

We therefore repeated the FACS experiment on macrophages, this time challenging them with the particulate WPG and the soluble PGG, for 2h (Fig.35).

What we found out, further reinforced the hypothesis of a mutual regulation between Dectin1 and MS4A4A. Indeed, besides responding with an up-regulation upon Zymosan, MS4A4A is significantly (+51%) overexpressed in the presence of the specific Dectin1 ligand WGP, which as mentioned above, is unable to trigger TLRs responses and is therefore an exclusive stimulus for the C-type lectin receptor, as confirmed by the reduction at the membrane level (-77%) due to its internalization.

Moreover, MS4A4A does not respond to the soluble β-glucan PGG, and so doesn't Dectin, meaning the two molecules respond selectively to the same stimuli. Indeed, PGG is able to bind Dectin1, but it does not induce the activation of its signaling pathway. MS4A4A may therefore function as an adaptor molecule, regulating Dectin1 availability to signaling.

β-glucans		kDa	μm
Zymosan	particulate	-	3
WGP	particulate	-	3
PGG	soluble	16	-

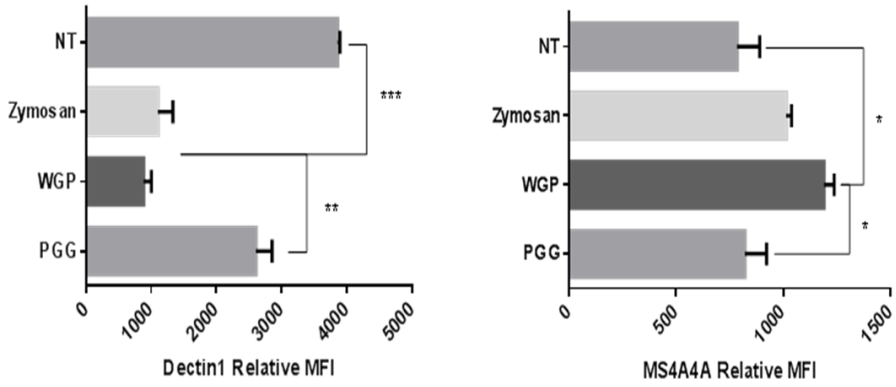

Fig.35. MS4A4A responds selectively to particulate β-glucans, but not to soluble ones, reflecting Dectin1's behavior. Flow cytometry analysis of surface expression of MS4A4A and Dectin1 upon treatment with Zymosan and WGP particulates, and the PGG soluble form of β-glucans. The cells were treated 2h with the different polysaccharides and stained for 20' with anti-MS4A4A and anti- Dectin1 and analyzed by FACS. Results are mean ±SEM of three independent experiments. (*, $P < 0.05$)

4.4.5. MS4A4A and Dectin1 localize within lipid rafts after engagement with Zymosan

It is well known that receptor signaling can occur in specific membrane lipid raft or caveolae which act as platforms for the association of adaptors/receptors signaling complexes [127, 388].

Dectin1 expression and function have been described being negatively regulated by Dexamethasone in both resident and elicited murine peritoneal macrophages. Noteworthy, the ability of the receptor to bind Zymosan was strongly impaired in the presence of GC [278].

Moreover, localization of Dectin1 within lipid rafts seems to be required for its signaling and for the activation of phagocytosis and cytokine secretion in DC [290].

Starting from these assumptions, we performed an immunofluorescence experiment on primary macrophages to evaluate the localization of Dectin1 with respect to lipid rafts. Cells were labeled with the CT-B, fixed and stained with anti-Dectin1 and examined in confocal laser scanning microscopy (Fig.36A).

As already demonstrated, MS4A4A is barely found within the rafts in normal conditions (Fig.) and as shown in Fig. 36A and B, Dectin1 is not co-localizing within lipid raft either.

A further assessment of the lack of association of Dectin1 with the cholesterol enriched micro domains was performed by giving the cells with MβCD and analyzing Dectin1 expression at the cell surface by flow cytometry. As shown in Fig.36B, Dectin1 wasn't affected by the cholesterol depletion induced by the cyclodextrins, indicating that, unlike MS4A4A which expression was at least partially impaired upon the treatment, the C-type lectin receptor does not resides within these membrane compartments before engagement.

On the other hand, once given with Zymosan, a strong co-localization is found between Dectin1 and MS4A4A in lipid rafts, particularly in proximity of the granules, suggesting a role in signaling and/or receptor clustering (Fig.37A). MS4A4A may in fact act as an adaptor molecule, transporting Dectin1 within the raft, favoring the interaction of this receptor with kinases and/or other signaling molecules contained in these membrane structures.

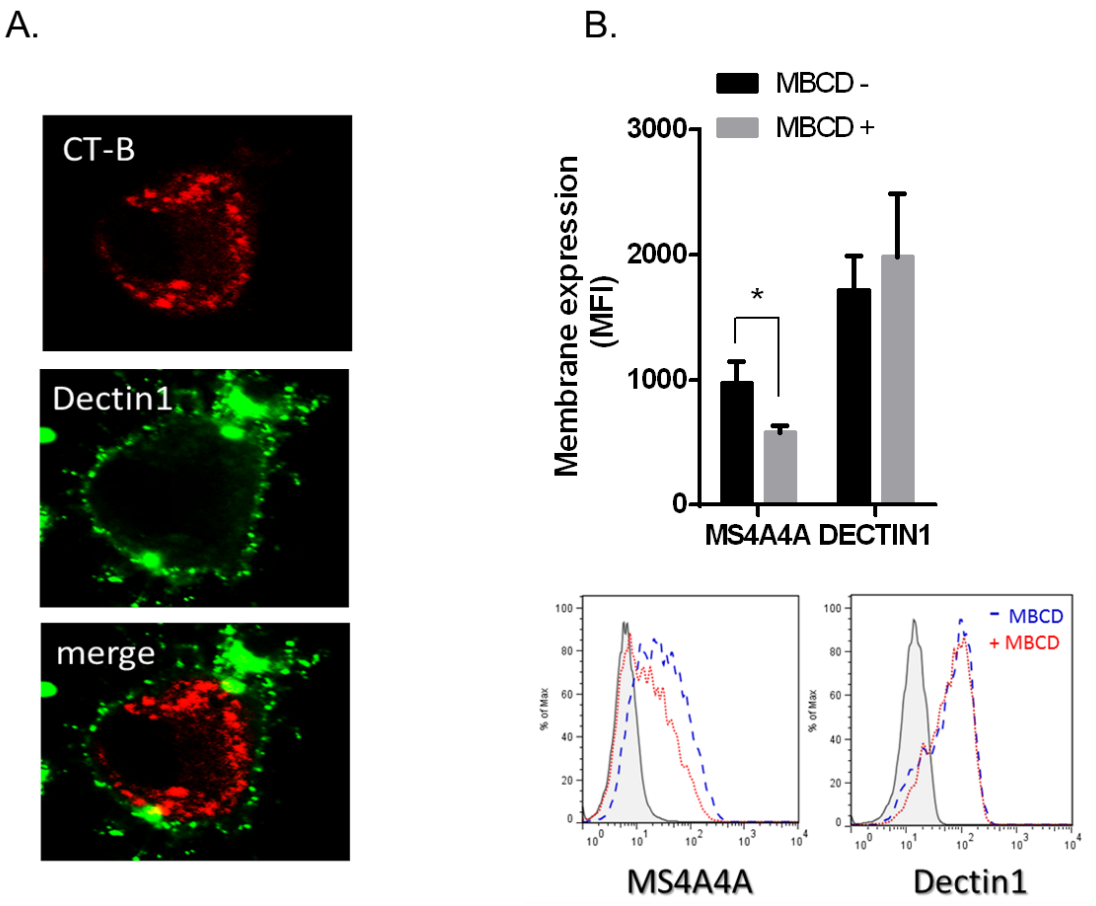

Fig. 36. Dectin1 does not localize within the lipid rafts before and it is not affected by cholesterol depletion. (A) Immunofluorescence staining for Dectin1 and Lipid Rafts (CT-B) on macrophages, representative of 2 independent experiments. Co-localization (merge) between the proteins, if present, is indicated in yellow. (B) Macrophages were treated for 1h with 5mM MβCD to deplete cholesterol, stained for MS4A4A and Dectin1, and analyzed by flow cytometry. The upper graph shows the mean ±SEM of n=4 experiments. *p<0.05.The lower panel is a representative histogram of the expression of MS4A4A and Dectin1 upon MβCD treatment.

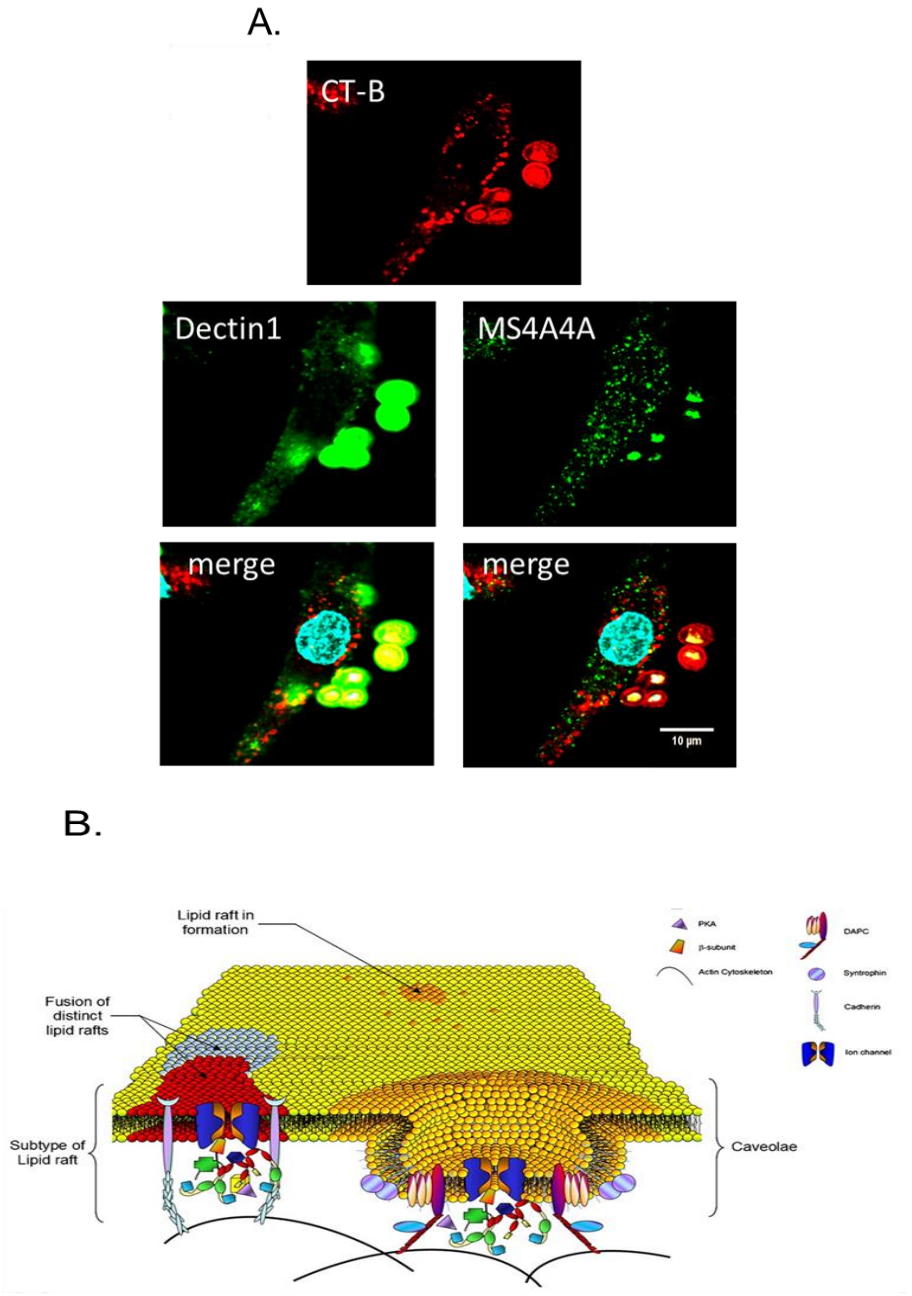

Fig37. Dectin1 and MS4A4A localize within lipid rafts after engagement with Zymosan. (A) Immunofluorescence staining for MS4A4A, Dectin1 and Lipid Rafts (CT-B) on macrophages upon zymosan treatment, representative of 2 independent experiments. Co-localization (merge) between the proteins is indicated in yellow. (B) Schematic representation of lipid raft structures in a plasma membrane. Lipid rafts float in the membrane, constituting distinct signalling platforms depending on lipid raft subtype and composition. Adapted from Maguy 2006, Cardiovascular Research.

4.5. Identification of the murine Ms4a4a

In an effort to identify the corresponding murine MS4A4A (Ms4a4a), with the perspective of generating a murine model lacking in the protein expression within the monocytes/macrophages lineage for the *in vivo* study of its function, a BLAST analysis has been performed in order to evaluate all the possible candidates. The MS4A gene family itself presents a murine correspondent [213], but on average the hortologs, with the exception of MS4A1/CD20 (80%), do not share high sequence homology. Indeed, based on the sequences available on genomes databases (Genome Brawser, NCBI), the only homologs identified for MS4A4A were the murine Ms4a4b, Ms4a4c and Ms4a4d. By the time we began studying this protein, indeed, the sequence for Ms4a4a hadn't been identified yet by the Mouse Genome Project. The only evidence confirming its existence derived from a clone (clone I420104A15) from the cDNA of osteoclast-like murine cell (http://www.ncbi.nlm.nih.gov/nucest/BY320061?report=GenBank) and a partial mRNA of 373 bp long was reconstructed from that cDNA clone, although it was incomplete at the 3' end. On the NCBI 37a, Aug 2007 genome, the pre-messenger resulted having 3 exons and covering 5.91 kb. The 5'UTR contains about 125 bp and there is an in frame stop 27 bp before the Met.

Since the homology in the DNA sequence doesn't necessary mean homology in the function, we started analyzing the protein sequence, in order to find something with a higher degree in homology with the human MS4A4A. We found out a sequence we named Ms4a4a, that, in spite of the low homology both at the genomic (42,4%) and transcript level (35,7%), displayed 74% similarity with the human protein.

The analysis were performed with the global sequence alignment programs BLASTP (http://blast.ncbi.nlm.nih.gov) and Emboss-Needle (http://www.ebi.ac.uk/Tools/psa/emboss_needle/) using the Needleman-Wunsch algorithm.

The data obtained are summarized in Fig. 38B

A.

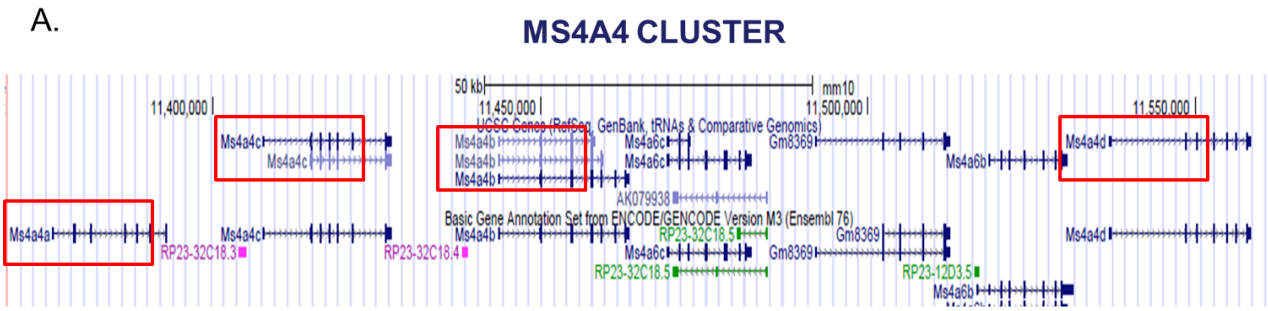

B.

	DNA		mRNA		PROTEIN	
Gene	%similarity	%identity	%similarity	%identity	%similarity	%identity
Ms4a4a	42.4	42.4	35.7	35.7	74	61
Ms4a4b	39.5	39.5	52.1	52.1	60	42
Ms4a4c	42.9	42.9	50.8	50.8	60	44
Ms4a4d	40.2	40.2	48.4	48.4	57	40

Fig. 38. Discovery of murine Ms4a4a sequence. (A) Mouse Ms4a4 cluster. Adapted from Genome Browser website. (B) Percentages of similarity and identity between human MS4A4A gene, transcript and protein and the murine putative hortologs. Alignments were performed with BLASTP and Emboss Needle programs. NCBI Reference Sequences: Ms4a4a: XM_986941.3; Ms4a4b: NM_021718.2; Ms4a4c: NM_029499.3; Ms4a4d: NM_025658.4

No phenotype for Ms4a4a has yet been reported and the gene's *in vivo* function is yet unknown.

PSORT II analysis for the prediction of protein localization sites in cells (http://psort.hgc.jp/) trained on yeast data predicts that the subcellular location of this protein is most likely 33.3 %: endoplasmic reticulum; 22.2 %: plasma membrane; 22.2 %: mitochondrial; 11.1 %: vesicles of secretory system; 11.1 %: Golgi. The protein doesn't display neither N-terminal signal peptide nor tyrosines within the tail, therefore seems unlikely it acts as a signal transduction molecule. No cleavage site motif for mitochondrial targeting were found, neither were ER Membrane and peroxisomal retention signals.

Pfam analysis (http://pfam.janelia.org), confirmed the protein belongs to CD20-like family.

At present, according to Entrez Gene database, Ms4a4a gene has been confirmed mapping on chromosome 19, its total length is 17268 bp (11450013-11467280), with an mRNA of 836 bp, and a CDS of 711 bp which encodes for a protein of 236 aa. The intron-exon organization is maintained

between the two species (Fig.39A) and the prediction of the tertiary structure by TMHMM reveals the same four transmembrane domains architecture, with cytoplasmic terminals, and two extracellular loops (Fig.39B-C), consistent with MS4A4A characteristics. To examine whether mMs4a4a is also a trans membrane protein, HEK293 cells were transfected with the Ms4a4a-GFP plasmid. The TIRF analysis of the transfectants confirmed the same localization of the murine protein at the cell surface.(Fig.39D)

A.

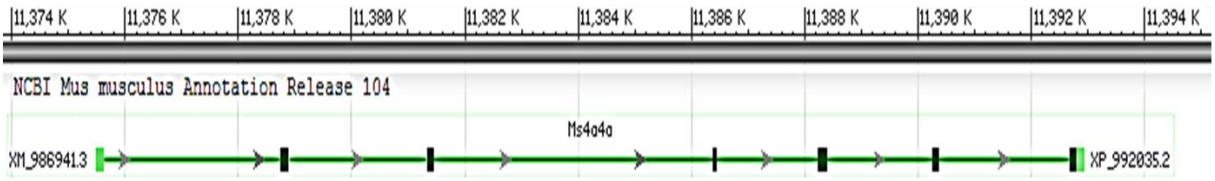

B.

	From nt	To nt	Length(bp)	Intron lenght
EXON 1	1	109	108	
EXON 2	3215	3374	159	3106
EXON 3	5802	5930	128	2428
EXON 4	10861	10917	56	4931
EXON5	12709	12867	158	1792
EXON6	14739	14840	101	1872
EXON7	17149	17268	119	2309

C.

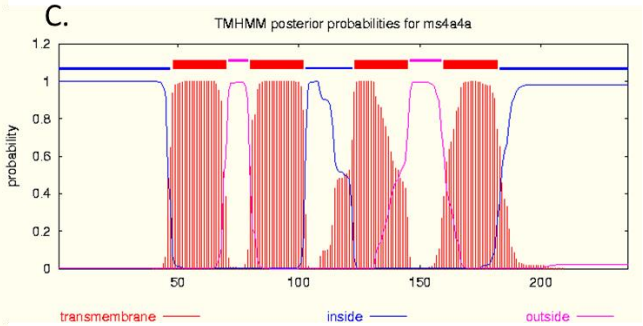

D.

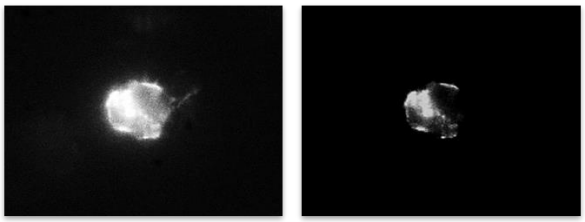

Fig.39. Molecular features of murine Ms4a4a. (A) The Ms4a4a gene record is predicted by automated computational analysis and derived from a genomic sequence (NT_039687.8) annotated using gene prediction method: Gnomon, supported by EST evidence. The gene contains 7 exons, displaying the same organization of the human gene, and codifies for a 236 aa protein.(B) Comparison of the amino acid sequences of the human and murine MS4. The predicted transmembrane domains are indicated in red. (C) Analysis of the amino acid sequences of the mMs4a4a, using TMHMM program (http://genome.cbs.dtu.dk/services/), predicting the expected four transmembrane hydrophobic domains resambling the human homolog, with cytoplasmic amino and carboxyl termini. (D) HEK293 cells were transfected with the mMs4a4a-GFP plasmid and the protein localization was assessed by TIRF microscopy, confirming the expression at the cell surface.

4.5.1. Murine Ms4a4a expression in tissues and response to polarization

Once identified the putative ortholog of MS4A4A, we evaluated its expression in primary cells and tissues, and its responses to polarization compared to the other Ms4a4 members. RNA was collected from several cells and tissues of C57/B6 mice, including dendritic cells, CD8+/CD4+ T lymphocytes, B lymphocytes, liver, lung and kidney. (Fig40A) The Ms4a4a transcript distribution revealed the selective expression of Ms4a4a in macrophages, in line with the human protein expression pattern (Fig.39).

Murine peritoneal elicited macrophages were obtained after 4 days thyoglicollate (injected intraperitoneally), by washing the cavity with 5mL cold saline and subsequently polarizing the cells with the same protocol applied for human cells: M1 (LPS 100ng/mL+IFN-γ 20ng/mL) or M2 (IL-4 20ng/mL or Dexamethasone $10^{\wedge -6}$M). After 18h RNA was extracted by Trizol and Ms4a4a, Ms4a4b, Ms4a4c, Ms4a4d expression assessed by q-PCR (Fig.40B and C).

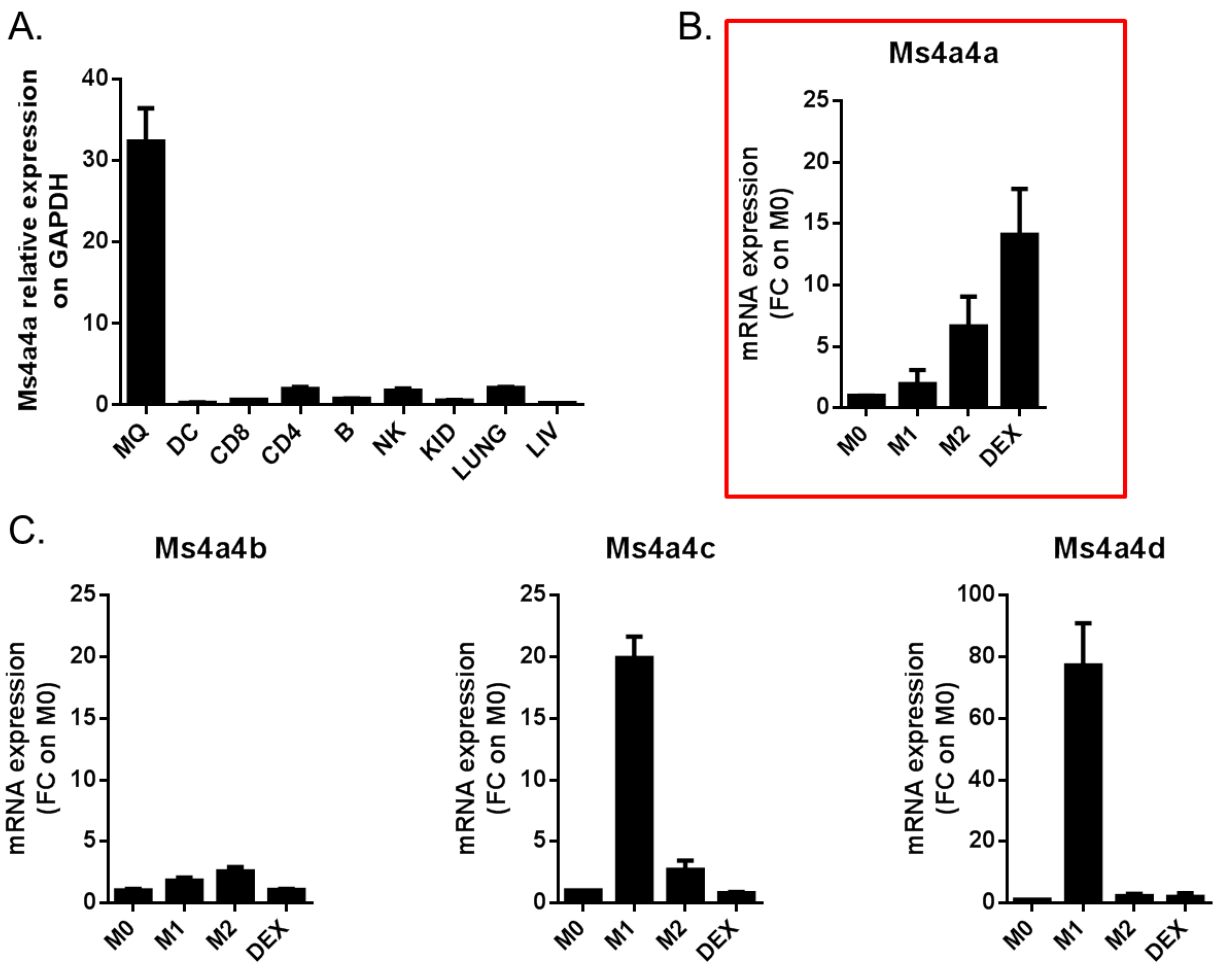

Fig.40. Ms4a4a expression and response to polarization. (A) Ms4a4a expression in murine primary cells and tissues. qPCR for Ms4a4a highlighting its association with macrophages. (B) Ms4a4a response upon polarization analyzed by q-PCR, reflecting the same induction pattern of the human hortolog. (C). Ms4a4b, Ms4a4c and Ms4a4d expression upon polarization. Expression is indicated as fold increase respect to non-treated macrophages (M0). Results are expressed as mean ±SD of 3 experiments. * $p<0.05$.

As shown in Fig.40, Ms4a4a is exclusively expressed in macrophages and is the only homolog resembling the human MS4A4A polarization pattern of expression, with an increase of the transcript in the presence of GC and, to a lesser extent, IL4. Ms4a4b is known not being expressed by macrophages. The other two members do not respond at all to alternative polarization stimuli, but result up-regulated only in the presence of pro-inflammatory mediators.

4.5.2. Con-Ms4a4a Ko mice display normal phenotype

To examine the function of Ms4a4a *in vivo* we generated mice deficient in the protein selectively in the myeloid lineage breeding homozygous Ms4a4a-flox animals obtained from Ozgene with LysM/Cre animals.

At first sight, mice were viable, had no visible abnormalities and had normal peripheral leukocyte counts. Splenocytes from Ms4a4a-conKO and WT mice had a similar antigen phenotype and no abnormalities were evident (Table.1).

Cell type	marker	WT cells (%)	KO cells (%)
Neutrophils	$CD11b^{hi}$; $Gr1^{hi}$	0.733±0.11	0.433±0.09
Dendritic cells	CD11c+; CD11b+	2.402±0.07	2.042±0.36
B lymphocytes	B220	59.413±2.97	60.200±1.01
T lymphocytes	CD3	24.830±2.01	25.816±1.19
NK cells	NK1.1	0.019±0.001	0.013±0.01
macrophages	CD11b+; $F4/80^{hi}$	0.710±0.07	0.556±0.18
eosinophils	$Gr\text{-}1^{int;}$CD11b+;F4/80+	0.346±0.10	0.386±0.09

Table.1. Differential splenocyte counts. Splenocytes were isolated from matched Ms4a4a-conditional knockout mice (KO) and wild-type mice (WT) and cell types were identified with flow cytometry. Macrophages were identified as autofluorescent, F4/80+ cells. Data represent average ±SEM of n=3 mice per type.

4.5.3. Con-Ms4a4a Ko mice derived macrophages show impaired response to Zymosan

Given its proven association with Dectin1, the expression of the receptor at the cell surface was assessed by flow cytometry, together with two other molecules associated with fungal recognition,

TLR2 and MHCII. As shown in Fig. 41, Dectin1 expression was the only one resulting impaired in the conKO compared with the WT mice, with a significant reduction at the basal level.

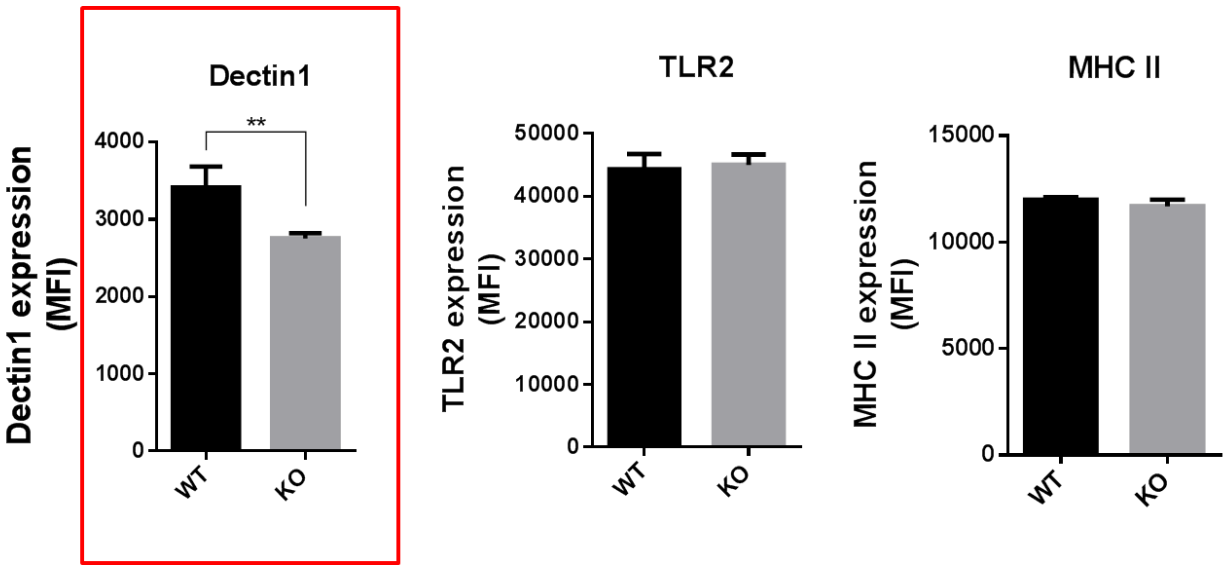

Fig.41. Ms4a4a-conKO displays a Lower basal expression of Dectin1. Peritoneal elicited macrophages were withdrown from the animals and immediately assessed in flow cytometry, after staining with anti-Dectin1, anti-TLR2 and anti MHCII antibodies.

We next assessed the Ms4a4a KO macrophages response to zymosan. Thioglycollate PEC from Ms4a4a-knockout mice displayed comparable zymosan internalization, as confirmed by the FACS analysis performed on these cells challenged with Zymosan-FITC for 5, 15 and 30 minutes (Fig.42A). Also the levels of ERK phosphorilation were pretty much equal between the two conditions Fig42B). However, Dectin1 expression resulted somehow impared, with a lower basal level in the KO cells accompained by a delayed internalization of the receptor (Fig42C).

As mentioned before, one critical cellular process mediated by Dectin1 in rensponse to β-glucans binding is the generation of ROS.

We therefore examined that response in peritoneal-elicited macrophages and BMDM. ROS levels produced by Ms4a4a-conKO animals compared to WT, PEC and BMDM were seeded in 24well plates and were labeled with HOECHST to counterstain the nuclei and stained them with the ROS-

responsive dye CellROX Deep Red reagent to detect the oxidative stress in time lapse. After 30' incubation with the reagents, cells were transferred into the CellR microscope humidified chamber (37°C, 5%CO_2) and imaged the fluorescence production for 2h. Although no respiratory burst was induced in PEC (data not shown), in line with previously described evidences [389] we observed a significant decrease of approximately 50% in ROS generation in KO cells compared to the WT ones (Fig. 42D).

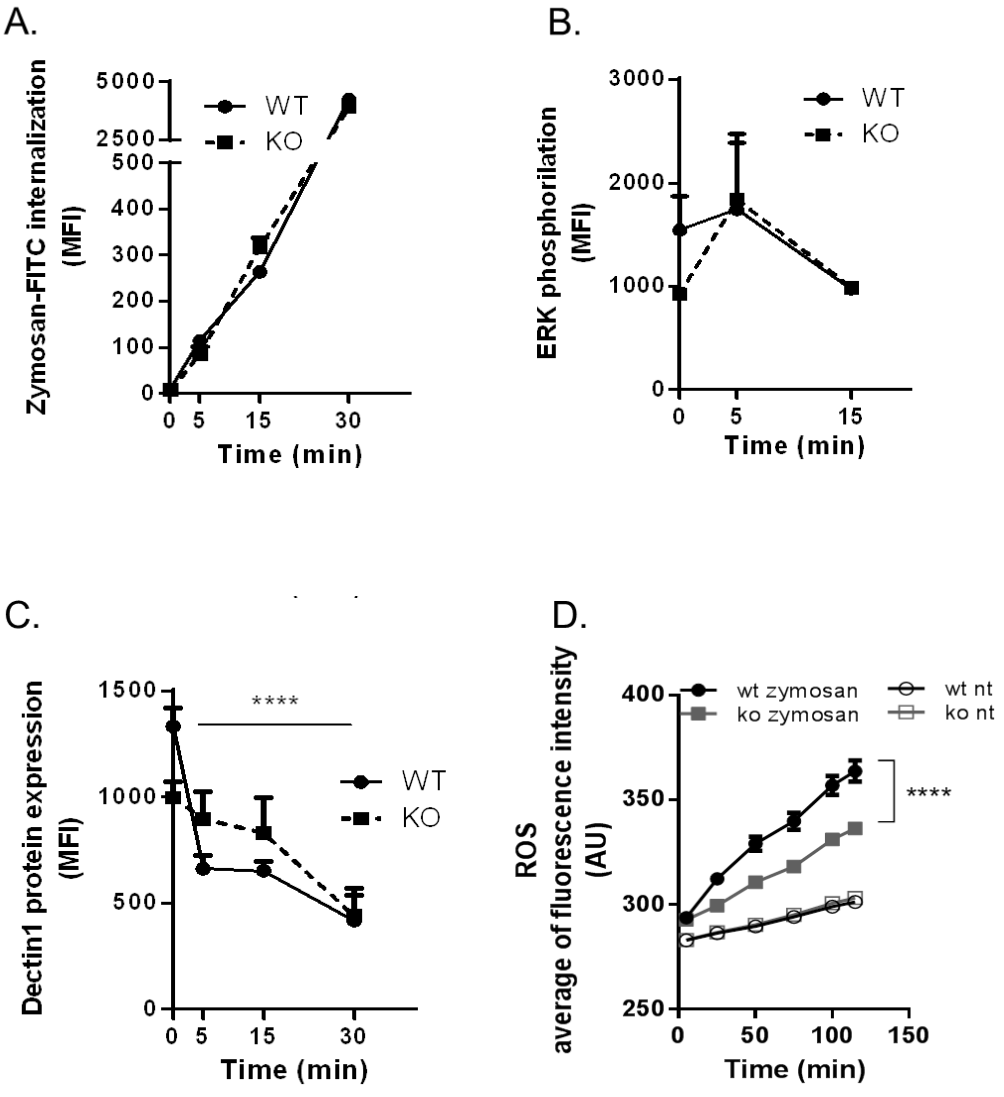

Fig.42. Impaired inflammatory response in Ms4a4a KO macrophages. (A) PEC were treated with Zymosan-FITC for the indicated periods of time and the internalized particles were evaluated

by flow cytometry. (B) ERK phosphorilation and (C) Dectin1 internalization were analyzed by flow cytometry in PEC given with non labeled Zymosan for the indicated time points. Data are represented as mean ±SEM of n≥3. **(D)** Diagram of the mean fluorescence intensity (± SEM) induced by ROS production from BMDM in the presence of zymosan (50ug/mL) in WT and KO cells. An average of 100 ROI was analyzed for each time point in each sample. Every time, n=3 mice per condition were used, and the experiment was repeated twice.

Besides the impairment in Dectin1 internalization and respiratory burst induction, the inability of the Ms4a4a-conKO to mount an inflammatory response against zymosan resulted also from the significant impairment in the cytokines secretion, evaluated by the release of IL6, IL10 and TNFα in the supernatant of peritoneal elicited macrophages (Fig.43upper). In this case, we couldnt detect any substantial flaw in the production of the cytokines in Ms4a4a KO BMDMs cultured with zymosan, (data not shown).

Finally, in order to understand whether the downregulation of the cytokines derived form a defect in the induction of the gene expression or in a failure in the secretion mechanism A q-PCR was performed on the cytokines' cDNA from PECs given with Zymosan for 6h or 24h. The experiment confirmed a significant reduction in the expression of IL10, accompained to a decrease in IL6 and TNFα in the KO cells compared to the WT (Fig.43lower).

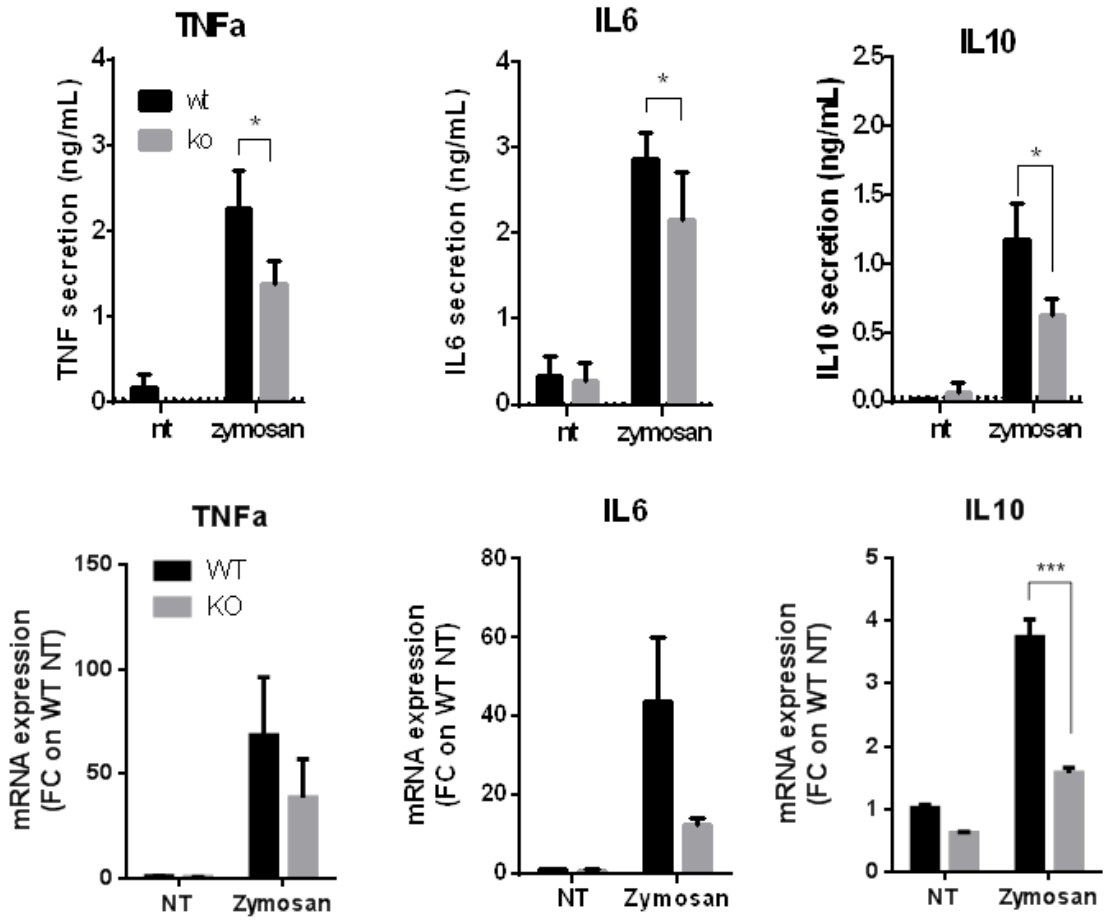

Fig.43. Down-regulation of cytokines secretion in Ms4a4a-conKO. (upper panel) Dectin1-related cytokines secretion measured by ELISA in the supernatant of WT and KO PEC treated with zymosan for 24h. For every experiment n=3 mice per condition were used. The graphs show mean (± SEM) of two independent experiments. *, $P < 0.05$ and **, $P < 0.01$. (lower panel) q-PCR of PECs for the analysis of the transcript of the examined cytokines. Cells were challenged with 100ug/mL Zymosan and mRNA was extracted after 6h (TNF) or 24h (IL6 and IL10) to evaluate transcript regulation. Data represent mean (± SEM) of triplicates of two experiment. **, $P < 0.01$; and ***, $P < 0.001$

Together with these evidences, the observation of a substantial induction in IL12 transcript (not shown) , which upon fungal/yeast stimulation is driven exclusively by a TLR2-mediated, Dectin1-independent pathway, suggests a mechanism by which the cell may compensate the impaired Dectin1 signaling cascade, mounting an alternative immune response-

5. DISCUSSION

An significant amount of evidences has established a role for the MS4A protein family, especially CD20 and FcεRIβ, in the immune system context.

MS4A4A is a novel member of the membrane-spanning 4-domain family, subfamily A, (MS4A) gene family, which members share structural features including four transmembrane domains, two extracellular loops and two cytoplasmic terminals [215]. The MS4A family counts at least 26 members in human and mouse including CD20, FcεRIβ, HTm4 [7, 213]. Chromosome mapping revealed that most of these human genes are located in chromosome 11q12-q13, which is linked with higher susceptibility to allergy and atopic asthma [390, 391], while in the mouse, they are found in chromosome 19 [217, 392]. The presence of a cluster of genes and their chromosomal localization strongly suggests an immunological significance. Until few years ago, the only characterized members of the family were CD20 (MS4A1), HTm4 (MS4A2) and FcεRIβ (MS4A3). CD20 is a non-glycosylated transmembrane protein selectively associated with B cells [392, 393], but not found in plasma cells [394, 395]. Some works suggest it may act as a Ca^{2+} channel or Ca^{2+} channel regulator [233], although increasing evidences indicate it is not only implicated in Ca^{2+} signaling but also in the activation, differentiation and apoptosis of B cells [396, 397].

Noteworthy, CD20 provided a fundamental target for the development of a therapeutic antibody against B cell lymphoma and autoimmune diseases, Rituximab, which up till now can be considered one of the most effective antibody therapeutic available [397].

HTm4 is instead primarily located on the hematopoietic cells nuclear membrane, and plays a pivotal role in their differentiation [250].

FcεRIβ is part of the IgE receptor complex, and as such contains an ITAM motif in its C-terminal domain that directly contributes to IgE mediated cell signaling [248, 398, 399]. The functions of most of the other members remain essentially indeterminate.

In the first part of this thesis, we demonstrated that the family member *MS4A4A* is selectively expressed in macrophages and differentially up-regulated in M2-like macrophages. Among the stimuli tested, glucocorticoids resulted the most effective ones in inducing MS4A4A transcript and protein. A synergistic induction by GC and IL4 was also observed, although the restored MS4A4A basal expression levels upon treatment with the GC competitor antagonist Mifepristone and the

evidence of a strong up-regulation of the protein upon CG administration *in vivo* in human macrophages, indicates a direct effect mediated by the steroids.

Indeed, the analysis of the putative promoter located upstream the MS4A4A gene revealed the presence of a considerable number of glucocorticoids responsive element (GRE) transcription factor binding sites, indicating the possibility of a direct effect mediated by the GC receptor (GCR).

Although the pathway is likely to be mediated directly via GCR, it has to be considered GC can also modify the gene expression through a GRE-independent mechanism, which is partially mediated by protein-protein interactions of the GC receptor with other DNA-binding factors or co-activators. For instance, through C/EBP interaction dexamethasone has also been acknowledged playing a role in the nuclear receptor PPARɣ expression regulation, which in turn is known regulating, for instance, the phagocytosis of apoptotic cells [400].

As it turned out from the bioinformatics sequence analysis, MS4A4A does not include any ITAM domain, like other MS4A members do (e.g. FcεRIβ) ,and it's therefore unlikely it functions as a signal transduction molecule. Alignment of the MS4A4A protein sequence with CD20 shows a 44% similarity on the amino acid level, with the highest degree of identity within the first three transmembrane domains, suggesting it may work more similarly to CD20, given that also the membrane topology is conserved between the two molecules.

MS4A4A is a 239 amino acid protein with cytoplasmic amino- and carboxy-terminals and four transmembrane domains forming two extracellular loops.

Cell membrane localization was experimentally confirmed by immunofluorescence microscopy of HEK cells transfected with eGFP-tagged MS4A4A or with the empty eGFP constructs and by staining human primary macrophages. Also at the protein level, MS4A4A displays an overexpression induced by M2 stimuli.

In the meantime, the bioinformatics investigation was applied also for the murine MS4A4A homolog, and allowed us to discover a gene encoding for the putative Ms4a4a. Subsequent analysis of the molecule features and regulation upon polarizing M1 and M2 mediators acknowledged this gene as the human homolog, sharing the same GC dependence, structure and membrane topology.

M2 macrophages play a crucial role in a variety of processes, such as tissue remodeling, homeostasis maintenance, angiogenesis, immunosuppression and tumor development. Opposite to classical pro-inflammatory M1 macrophages, M2 display a very low microbicide and tumoricide functions due to their reduced secretion of reactive oxygen and nitrogen species and pro-inflammatory cytokines. Tumor-associated macrophages (TAM) are M2-like cells characterized by a heterogeneous population highly represented among stromal leukocytes in many malignances, and

which define the link between cancer and inflammation [401]. TAM dramatically withstand tumor growth, negatively affecting the clinical outcome of cancer bearing subjects [4, 104, 402].
Particularly, overexpression of this type of macrophages in lymph-node specimens from patients with Hodgkin's lymphoma (HL) has been associated with poor prognosis [104].
Since MS4A4A was mainly found being expressed in M2 macrophages, and given that in mouse it resulted significantly overexpressed in RCC associated TAMs, we analyzed the protein expression in a small cohort of Hodgkin's lymphoma samples by immunohistochemistry, finding out a considerable number of MS4A4A+ cells in all the samples examined. Although not statistically significant, the percentage of immune reactive area within the tumor samples was higher than in those samples we identified as control lymph nodes (7.00 ± 0.91 vs 3.75 ± 1.30).
Other than the narrowness of the casuistry, the main reason for this lack of significance might be due to the fact these lymph nodes were derived from the same HL patients, and cannot therefore be referred as "normal", since they were characterized by abnormal lymphadenitis, often associated with sinus histiocytosis. The only two cases of real normal tissues examined (spleen and lymph node) showed almost no positivity for MS4A4A. Subcapsular sinus macrophages in the lymph nodes physiologically support antiviral humoral immune responses [403, 404]. However, the predominant accumulation observed in perivascular areas within the lymphomas and within the fibrotic tissue surrounding the tumor is consistent with a TAM, or at least a M2-like phenotype. TAM differentiate from circulating blood monocytes that infiltrate the tumor, where they can exert different functions. Perivascular macrophages may indeed play an important role in the vascularization process, enhancing tumor growth, invasion and metastasis. On the other hand, pro-fibrotic macrophages can produce PDGF, TGFβ1 and insulin-like growth factor 1 (IGF1), activating fibroblasts, and overexpressing metalloproteinases (MMP) to orchestrate the extracellular matrix deposition, therefore directly participating in wound healing [405].
Interestingly, some MS4A4A positivity was also found within the perinodal adipose tissue (PAT), fat depots in which lymph nodes are embedded and which supports the lymph node functions, providing lipid supply powering immune activation as well as making available fatty-acid that sustain local immunity [406]. These regions are characterized by a high number of DCs, particularly within the omental tissue. Charriere and colleagues described the ability of preadipocytes to develop into macrophages [407], and these cells display a diverse phenotype during inflammation or disease, expressing greater amounts of co-stimulatory molecules, apart from MHCII and T cells stimulation, which are lost [408]. Also these type of cells seem to reflect an M2-like behavior.

Nevertheless, the heterogeneity observed within the lymphoma subtypes, might also derive from the different content in M1 or M2 polarized macrophages, resulting in different staining patterns. In fact, the double immunohistochemistry for MS4A4A and the macrophage marker CD68 revealed the presence of a subpopulation of MS4A4A positive macrophages, indicating that only macrophages can express MS4A4A, although not all of them do it. We therefore identified a subpopulation of macrophages that expresses MS4A4A and this subpopulation is highly represented within the tumor compared to non-neoplastic tissues.

Recently, a link between tumors and GC has been found which might at least provide a hint for the correlation among MS4A4A, GC ant TAM. These lipid hormones can in fact be produced, other than the adrenal gland by the intestinal epithelium. Sidler and colleagues demonstrated that both cell lines and primary tumors can express steroidogenic enzymes and bioactive GC, inhibiting the activation of T lymphocytes, contributing to tumor immune evasion [409] Whether this occurs also in lymphomas, it has yet to be determined.

Antibody-based cancer therapies have been effectively reflected into clinic representing the most encouraging treatments in oncology. The use of monoclonal antibodies (mAb) directed against a particular lineage of hematopoietic cell have been proven as useful therapeutic targets [410]. Particularly, anti-CD20 mAbs dramatically improved the treatment of lymphoma patients.

MS4A4A+ macrophages resemble *bona fide* TAMs and its expression was found in different types of lymphomas, as well as other types of cancers (e.g. gastric carcinoma, data not shown). Large-scale analysis of tumor specimens, might validate its suitability for an even broader targeted therapy.

On top of that, MS4A4A is a surface molecule and therefore easily detectable by antibodies for specific cellular populations recognition.

All these features including sequence similarity to other MS4A family members, especially CD20, suggest that MS4A4A might possess a therapeutic potential as antibody target.

Using a phage-display system, various antibody fragments can be displayed on the surface of filamentous phages containing the antibody gene as a phagmid and in this way, humanized antibodies can be developed for clinical applications. In this study, with the idea of generating a tool comparable with Rituximab, able to detect and selectively induce cytotoxicity in the target MS4A4A bearing macrophages, we made use of this technique to generate a human anti human monoclonal antibody.

Out of 4 clones identified from the library screening, the final product, clone D1, was able to mediate antibody dependent cytotoxicity and antibody-dependent (NK) cell-mediated cytotoxicity of the MS4A4A expressing cells. More importantly, D1 was the only clone cross-reacting with the mouse hortolog Ms4a4a. The epitope mapping confirmed a specificity of the antibody for a sequence of 6 amino acids within the second extracellular loop, and the binding of the clone was significantly impaired by the presence of a correspondent competitor peptide.

Unfortunately, once evaluated in primary cells and compared with the commercially available antibodies recognizing MS4A4A, D1 showed a reduced affinity along with a decreased specificity for the target.

Moreover, the antibody was not able to properly recognize the murine molecule.

All these evidences might be caused by the wrong panning strategy. The library was in fact screened against transfectants, therefore leading to the selection of clones able to recognize the protein in its recombinant form, not necessary in its native one, in which also the loops conformation might be altered.

In the very next future the library is going to be screened again against primary cells, with the perspective of isolating a clone capable of binding the native MS4A4A.

In the second part of the thesis the interactions and the functions of MS4A4A were explored.

Lipid rafts are liquid-ordered specialized plasma microdomains acknowledged to play an important role in regulating signaling by ITAM receptors. Dexamethasone treatment has been previously shown reducing membrane fluidity, altering raft lipid fatty acyl composition [411]. Since some members of the protein family were found co-localizing with raft detergent-resistant lipid microdomains upon recruitment [215, 375], we examined MS4A4A localization with respect to these compartments under resting and polarized conditions. Under resting conditions no co-localization occurred between MS4A4A and the rafts, while in the presence of GC almost the totality of MS4A4A was co-localizing with the rafts.

Although a discrete ratio of the proximity might be due to the *de novo* expression of the protein upon GC, this mediator actually induces the re-localization of MS4A4A within the rafts, as proved by the evidence of an increase in the co-localization index after only 2h of GC treatment. As demonstrated in the first part of the results, in fact, the messenger starts being induced after 6h treatment, and the protein expression is not triggered before 18-24h, meaning that the co-localization after 2h is a direct effect of GC on the membrane organization.

GC signaling via classical GRs has been previously demonstrated occurring also within lipid raft or caveolae microdomains platforms where multimeric signaling complexes can be clustered and it can be observed both in the presence or absence of a steroid ligand.
Lipid rafts are considerably rich in sphingolipids and cholesterol [412] and CD20 association with these compartments is cholesterol-dependent [413].
The cholesterol-depleting agent MβCD was used to further confirm the association of MS4A4A with rafts. The treatment led to the disruption of cholesterol enriched microdomains and significantly diminished the MS4A4A expression at the surface level, demonstrating an important role for these structures in MS4A4A surface localization and raising the hypothesis that the molecule may function as an adaptor, clustering membrane receptor complexes in the same way tetraspanins do.
Noteworthy, lipid rafts and caveole are important scaffold for the correct functioning of endocytic receptors and are associated with the phagocytic uptake of pathogens and particles [414]. Also microglia signaling is triggered by Src-SHP-2 and CD36 recruitment to lipid rafts [415]
and is required for phagocytosis of amyloid-β42 [416].

With the attempt of determine a role for MS4A4A on the plasma membrane of macrophages, we decided to explore its potential interactors adopting the yeast split-ubiquitin screen, a variant of the traditional yeast two hybrid, with the key advantage of allowing the measurement of the protein interactions directly at the surface level. 6 integral membrane proteins were shown to interact with MS4A4A in a specific way, among which MS4A4A itself, MS4A6A and MS4A7, the tetraspanins CD63 and CD9 and, more importantly, the β-glucan receptor Dectin1. The validation of these interactions was assessed by FLIM-FRET on CHO transfectants and ultimately on human macrophages by classical co-immunoprecipitation.
The interaction of MS4A4A with Dectin1was reproduced in all the experiments. CD63 interaction with MS4A4A was confirmed only in primary cells, not in CHO cells, probably because of the different features and above all the different functions exerted by these two cell types., while interactions among MS4A4A, MS4A6A and MS4A7 were validated only by FLIM-FRET, suggesting these molecules cluster on the plasma membrane in complexes comparable to the tetraspanin enriched microdomains, where they may orchestrate the localization of receptor complexes, such as the C-type lectin receptors one.
On the other hand, we couldn't validate association for CD9. In all cases, the lack of interaction might depend either on the transient nature of the association, or on the indirect association of some

of these molecules, which create complexes on the plasma membrane, but although in close proximity, are not physically connected.

The evidence of MS4A members to associate with each other and with of other molecules was first described by Howie and colleagues, who reported MS4A4B self-association and with MS4A6B and the co-stimulatory molecules GITR and Orai1 [230], again suggesting they may work as adaptors for the protein complexes assembly in the membrane [135, 417]. This type of associations are frequent among tetraspanins ,including CD9 and CD63 [418-421] but even so, highly specific, and are usually found within a "raft" type microdomains [127, 422].

CD63 antigen is usually detected in endosomal particles but it is also presented on cell surfaces (Latysheva et al., 2006) and it is known to interact with Dectin1 during the phagocytic process, when the particle is translocated through the endosomes in the lysosomes to be degraded.

We next asked whether the interaction of MS4A4A with Dectin1, CD63 and CD9 had functional consequences, especially for Dectin1 co-stimulation.

Zymosan is an extract from the cell wall of *S. cerevisiae*, which is commonly used to mimic fungal infection, since it stimulates innate immune cells to mount a response through the involvement of Dectin-1 and TLR2 [9, 283] [289, 328, 423].

We observed the recruitment, at different degrees, of MS4A4A, CD63, CD9 and Dectin1 to phagosomes during internalization of Zymosan particles, indicating a possible cooperation in the clearance of pathogens mediated by MS4A4A which also at the basal level, co-localizes with Dectin1, which is normally expressed at the surface level and undergoes internalization upon activation [326, 386].

We confirmed the interaction of MS4A4A with the PRR Dectin1 is highly specific because the two molecules are not affected by other polysaccharides (mannan and LPS) because their regulation depends selectively on β-glucans. Moreover, we provided evidences that MS4A4A, as well as Dectin1, is able to discriminate among different types of β-glucan. Dectin1 in fact exerts its antimicrobial activity only in the presence of particulate polymers, not soluble ones, through the formation of a "phagocytic synapse" involving tyrosine phosphatases [386], inducing a robust immune response only when strictly required. The increase at the membrane level of MS4A4A was maximal in the presence of the Dectin1 specific ligand WGP, while the soluble form of polymer , PGG, was not inducing any up-regulation of the tetraspanin. Interestingly, to an increase of MS4A4A corresponds a decrease of Dectin1 at the surface level, indicating that a sort of mutual regulation may exist between the two molecules, such that MS4A4A overexpression corresponds to

the simultaneous Dectin1 internalization , considering that their levels are modulated within the same population of cells.

Opposite to MS4A4A which in primary cells is strongly induced by GC, Dectin1 expression and function have been described being negatively regulated by Dexamethasone in both resident and elicited murine peritoneal macrophages, where its efficiency in Zymosan binding was dramatically impaired in the presence of GC [278].

We demonstrated that Dectin1 and MS4A4A co-localize in resting macrophages and it is not constitutively expressed within cholesterol enriched membranes before engagement, as demonstrated by MBCD treatment, but re-localizes within these domains upon Zymosan stimulation, corroborating the assumption that the receptor association is required for its signaling and for the activation of phagocytosis and cytokine secretion in DC (Xu, 2009). Indeed, two important members of Dectin1 signaling cascade, Syk and PLCγ2, are known being recruited to lipid rafts upon the activation of the receptor, suggesting that these microdomains play a key role in Dectin-1 signaling.

How previously described by Ms4a4b, which association with GITR on T cells induces the TCR mediated signaling amplification upon ligand stimulation, the association of MS4A4A with Dectin1 may influence the receptor activity, functioning as a tuner for the anti-fungi/yeasts response.

Finally, in the attempt to better characterize the function of MS4A4A in more physiological environment, we moved to an in vivo setting, generating a conditional knockout mouse lacking Ms4a4a in the myeloid lineage, and we assessed the response to Zymosan of these macrophages compared to wild type ones.

Dectin-1 engagement by Zymosan or fungi triggers the activation of several pathways, including NFAT and NF-kB activation upon Src-Syk and MAPK-ERK phosphorylation aimed to mount a variety of immune responses. These responses include phagocytosis and killing of the pathogen, mediated by the secretion of antimicrobial reactive oxygen species and the production of cytokines and chemokines. [424-426].

Our preliminary experiments showed a severe impairment in the macrophages driven response to Zymosan. Although the phagocytosis rate and the phosphorylation of ERK was not impaired, KO macrophages displayed a lower basal expression as well as a delayed internalization of Dectin1 upon engagement, which reinforces the hypothesis of an adaptor function for Ms4a4a, which seems to act in an opposite fashion compared to the leukocyte-specific tetraspanin CD37, which instead stabilizes Dectin1 in APC membranes, affecting IL6 production [166].

Additionally, Ms4a4a absence was reflected by a significant decrease in ROS production by BMDM upon Zymosan, that during phagocytosis is triggered by the assemblage of the phagosomal membrane and is totally dependent on Src/Syk kinases.

Furthermore, the inability of the Ms4a4a-conKO to mount an inflammatory response against zymosan resulted also from the significant impairment in the cytokines secretion, evaluated by the release of IL6, IL10 and TNFα which was determined by a downregulation at the mRNA level, indicating a defect in these genes transcription activation by the conKO. Interestingly, the transcript level of IL12, which is induced only via MyD88/TLR2 signaling, is increased in conKO zymosan stimulated macrophages (not shown), suggesting a compensation mechanism by which the cell can get rid of the pathogen.

Dectin-1 triggers activation of Syk , which is not required for phagocytosis but is required for stimulation of ROS production and for some cytokines, such as IL-10 and IL-6 [427].

Therefore, it is likely that this kinase is the key to explain the majority of the effects observed in the conKO. Ms4a4a might in fact promote Syk association to Dectin1, leading to the release of cytokines and triggering the respiratory burst.

Although not totally understood yet, this work describes the first functional interaction between an MS4A member and a C-type lectin identified so far.

Definitely, further efforts are required to uncover the role of MS4A4A in the context of tumors and fungal infections. One of the most urgent future perspectives will be definitely to assess its behavior in in vivo models of these two conditions, in order to characterize a defined phenotype for this molecule.

A positive outcome from the second screening of the anti-MS4A4A antibody cross-reacting with the murine homolog would eventually provide us an irreplaceable tool to better examine MS4A4A function in vivo, given that by far, no commercial tools are available for targeting the murine molecule.

6. BIBLIOGRAPHY

1. Mosser, D.M. and X. Zhang, *Activation of murine macrophages.* Curr Protoc Immunol, 2008. **Chapter 14**: p. Unit 14 2.
2. Steinman, R.M. and J. Idoyaga, *Features of the dendritic cell lineage.* Immunol Rev, 2010. **234**(1): p. 5-17.
3. Taylor, P.R., et al., *Macrophage receptors and immune recognition.* Annu Rev Immunol, 2005. **23**: p. 901-44.
4. Mantovani, A., et al., *Macrophage polarization: tumor-associated macrophages as a paradigm for polarized M2 mononuclear phagocytes.* Trends Immunol, 2002. **23**(11): p. 549-55.
5. Gordon, S. and P.R. Taylor, *Monocyte and macrophage heterogeneity.* Nat Rev Immunol, 2005. **5**(12): p. 953-64.
6. Biswas, S.K. and A. Mantovani, *Macrophage plasticity and interaction with lymphocyte subsets: cancer as a paradigm.* Nat Immunol, 2010. **11**(10): p. 889-96.
7. Liang, Y. and T.F. Tedder, *Identification of a CD20-, FcepsilonRIbeta-, and HTm4-related gene family: sixteen new MS4A family members expressed in human and mouse.* Genomics, 2001. **72**(2): p. 119-27.
8. Zuccolo, J., et al., *Expression of MS4A and TMEM176 Genes in Human B Lymphocytes.* Front Immunol, 2013. **4**: p. 195.
9. Brown, G.D., et al., *Dectin-1 mediates the biological effects of beta-glucans.* J Exp Med, 2003. **197**(9): p. 1119-24.
10. Geissmann, F., et al., *Development of monocytes, macrophages, and dendritic cells.* Science, 2010. **327**(5966): p. 656-61.
11. Mantovani, B., M. Rabinovitch, and V. Nussenzweig, *Phagocytosis of immune complexes by macrophages. Different roles of the macrophage receptor sites for complement (C3) and for immunoglobulin (IgG).* J Exp Med, 1972. **135**(4): p. 780-92.
12. Hajishengallis, G. and J.D. Lambris, *Microbial manipulation of receptor crosstalk in innate immunity.* Nat Rev Immunol, 2011. **11**(3): p. 187-200.
13. Takahashi, K., M. Naito, and M. Takeya, *Development and heterogeneity of macrophages and their related cells through their differentiation pathways.* Pathol Int, 1996. **46**(7): p. 473-85.
14. Yamada, M., M. Naito, and K. Takahashi, *Kupffer cell proliferation and glucan-induced granuloma formation in mice depleted of blood monocytes by strontium-89.* J Leukoc Biol, 1990. **47**(3): p. 195-205.
15. Ginhoux, F., et al., *Fate mapping analysis reveals that adult microglia derive from primitive macrophages.* Science, 2010. **330**(6005): p. 841-5.
16. Hoeffel, G., et al., *Adult Langerhans cells derive predominantly from embryonic fetal liver monocytes with a minor contribution of yolk sac-derived macrophages.* J Exp Med, 2012. **209**(6): p. 1167-81.
17. Schulz, C., et al., *A lineage of myeloid cells independent of Myb and hematopoietic stem cells.* Science, 2012. **336**(6077): p. 86-90.
18. Kanitakis, J., P. Petruzzo, and J.M. Dubernard, *Turnover of epidermal Langerhans' cells.* N Engl J Med, 2004. **351**(25): p. 2661-2.
19. Merad, M., et al., *Langerhans cells renew in the skin throughout life under steady-state conditions.* Nat Immunol, 2002. **3**(12): p. 1135-41.
20. Ajami, B., et al., *Local self-renewal can sustain CNS microglia maintenance and function throughout adult life.* Nat Neurosci, 2007. **10**(12): p. 1538-43.
21. Mildner, A., et al., *Microglia in the adult brain arise from Ly-6ChiCCR2+ monocytes only under defined host conditions.* Nat Neurosci, 2007. **10**(12): p. 1544-53.
22. Guilliams, M., et al., *Alveolar macrophages develop from fetal monocytes that differentiate into long-lived cells in the first week of life via GM-CSF.* J Exp Med, 2013. **210**(10): p. 1977-92.
23. Avraham-Davidi, I., et al., *On-site education of VEGF-recruited monocytes improves their performance as angiogenic and arteriogenic accessory cells.* J Exp Med, 2013. **210**(12): p. 2611-25.
24. Cecchini, M.G., et al., *Role of colony stimulating factor-1 in the establishment and regulation of tissue macrophages during postnatal development of the mouse.* Development, 1994. **120**(6): p. 1357-72.

25. Dai, X.M., et al., *Targeted disruption of the mouse colony-stimulating factor 1 receptor gene results in osteopetrosis, mononuclear phagocyte deficiency, increased primitive progenitor cell frequencies, and reproductive defects.* Blood, 2002. **99**(1): p. 111-20.
26. Wiktor-Jedrzejczak, W. and S. Gordon, *Cytokine regulation of the macrophage (M phi) system studied using the colony stimulating factor-1-deficient op/op mouse.* Physiol Rev, 1996. **76**(4): p. 927-47.
27. Fogg, D.K., et al., *A clonogenic bone marrow progenitor specific for macrophages and dendritic cells.* Science, 2006. **311**(5757): p. 83-7.
28. Passlick, B., D. Flieger, and H.W. Ziegler-Heitbrock, *Identification and characterization of a novel monocyte subpopulation in human peripheral blood.* Blood, 1989. **74**(7): p. 2527-34.
29. Weber, C., et al., *Differential chemokine receptor expression and function in human monocyte subpopulations.* J Leukoc Biol, 2000. **67**(5): p. 699-704.
30. Ziegler-Heitbrock, H.W., et al., *Differential expression of cytokines in human blood monocyte subpopulations.* Blood, 1992. **79**(2): p. 503-11.
31. Frankenberger, M., et al., *Differential cytokine expression in human blood monocyte subpopulations: a polymerase chain reaction analysis.* Blood, 1996. **87**(1): p. 373-7.
32. Belge, K.U., et al., *The proinflammatory CD14+CD16+DR++ monocytes are a major source of TNF.* J Immunol, 2002. **168**(7): p. 3536-42.
33. Jakubzick, C., et al., *Minimal differentiation of classical monocytes as they survey steady-state tissues and transport antigen to lymph nodes.* Immunity, 2013. **39**(3): p. 599-610.
34. Geissmann, F., S. Jung, and D.R. Littman, *Blood monocytes consist of two principal subsets with distinct migratory properties.* Immunity, 2003. **19**(1): p. 71-82.
35. Palframan, R.T., et al., *Inflammatory chemokine transport and presentation in HEV: a remote control mechanism for monocyte recruitment to lymph nodes in inflamed tissues.* J Exp Med, 2001. **194**(9): p. 1361-73.
36. Hettinger, J., et al., *Origin of monocytes and macrophages in a committed progenitor.* Nat Immunol, 2013. **14**(8): p. 821-30.
37. Serbina, N.V. and E.G. Pamer, *Monocyte emigration from bone marrow during bacterial infection requires signals mediated by chemokine receptor CCR2.* Nat Immunol, 2006. **7**(3): p. 311-7.
38. Serbina, N.V., et al., *Monocyte-mediated defense against microbial pathogens.* Annu Rev Immunol, 2008. **26**: p. 421-52.
39. Zigmond, E. and S. Jung, *Intestinal macrophages: well educated exceptions from the rule.* Trends Immunol, 2013. **34**(4): p. 162-8.
40. Carlin, L.M., et al., *Nr4a1-dependent Ly6C(low) monocytes monitor endothelial cells and orchestrate their disposal.* Cell, 2013. **153**(2): p. 362-75.
41. Auffray, C., et al., *Monitoring of blood vessels and tissues by a population of monocytes with patrolling behavior.* Science, 2007. **317**(5838): p. 666-70.
42. Randolph, G.J., et al., *Role of tissue factor in adhesion of mononuclear phagocytes to and trafficking through endothelium in vitro.* Blood, 1998. **92**(11): p. 4167-77.
43. Onai, N., et al., *Identification of clonogenic common Flt3+M-CSFR+ plasmacytoid and conventional dendritic cell progenitors in mouse bone marrow.* Nat Immunol, 2007. **8**(11): p. 1207-16.
44. Naik, S.H., et al., *Development of plasmacytoid and conventional dendritic cell subtypes from single precursor cells derived in vitro and in vivo.* Nat Immunol, 2007. **8**(11): p. 1217-26.
45. Auffray, C., et al., *CX3CR1+ CD115+ CD135+ common macrophage/DC precursors and the role of CX3CR1 in their response to inflammation.* J Exp Med, 2009. **206**(3): p. 595-606.
46. Orkin, S.H. and L.I. Zon, *Hematopoiesis: an evolving paradigm for stem cell biology.* Cell, 2008. **132**(4): p. 631-44.
47. Cumano, A. and I. Godin, *Ontogeny of the hematopoietic system.* Annu Rev Immunol, 2007. **25**: p. 745-85.
48. Tavian, M. and B. Peault, *Embryonic development of the human hematopoietic system.* Int J Dev Biol, 2005. **49**(2-3): p. 243-50.
49. Epelman, S., K.J. Lavine, and G.J. Randolph, *Origin and functions of tissue macrophages.* Immunity, 2014. **41**(1): p. 21-35.
50. Elinav, E., et al., *Regulation of the antimicrobial response by NLR proteins.* Immunity, 2011. **34**(5): p. 665-79.
51. Kawai, T. and S. Akira, *Toll-like receptors and their crosstalk with other innate receptors in infection and immunity.* Immunity, 2011. **34**(5): p. 637-50.
52. Osorio, F. and C. Reis e Sousa, *Myeloid C-type lectin receptors in pathogen recognition and host defense.* Immunity, 2011. **34**(5): p. 651-64.

53. Lucas, T., et al., *Differential roles of macrophages in diverse phases of skin repair.* J Immunol, 2010. **184**(7): p. 3964-77.
54. Erwig, L.P. and P.M. Henson, *Clearance of apoptotic cells by phagocytes.* Cell Death Differ, 2008. **15**(2): p. 243-50.
55. Woollard, K.J. and F. Geissmann, *Monocytes in atherosclerosis: subsets and functions.* Nat Rev Cardiol, 2010. **7**(2): p. 77-86.
56. Murphy, C.A., et al., *Divergent pro- and antiinflammatory roles for IL-23 and IL-12 in joint autoimmune inflammation.* J Exp Med, 2003. **198**(12): p. 1951-7.
57. Abraham, C. and R. Medzhitov, *Interactions between the host innate immune system and microbes in inflammatory bowel disease.* Gastroenterology, 2011. **140**(6): p. 1729-37.
58. Adams, D.O., *Molecular interactions in macrophage activation.* Immunol Today, 1989. **10**(2): p. 33-5.
59. Krausgruber, T., et al., *IRF5 promotes inflammatory macrophage polarization and TH1-TH17 responses.* Nat Immunol, 2011. **12**(3): p. 231-8.
60. Meraz, M.A., et al., *Targeted disruption of the Stat1 gene in mice reveals unexpected physiologic specificity in the JAK-STAT signaling pathway.* Cell, 1996. **84**(3): p. 431-42.
61. Edwards, J.P., et al., *Biochemical and functional characterization of three activated macrophage populations.* J Leukoc Biol, 2006. **80**(6): p. 1298-307.
62. Jouanguy, E., et al., *IL-12 and IFN-gamma in host defense against mycobacteria and salmonella in mice and men.* Curr Opin Immunol, 1999. **11**(3): p. 346-51.
63. Shaughnessy, L.M. and J.A. Swanson, *The role of the activated macrophage in clearing Listeria monocytogenes infection.* Front Biosci, 2007. **12**: p. 2683-92.
64. Boehm, U., et al., *Two families of GTPases dominate the complex cellular response to IFN-gamma.* J Immunol, 1998. **161**(12): p. 6715-23.
65. Sindrilaru, A., et al., *An unrestrained proinflammatory M1 macrophage population induced by iron impairs wound healing in humans and mice.* J Clin Invest, 2011. **121**(3): p. 985-97.
66. Leuschner, F., et al., *Rapid monocyte kinetics in acute myocardial infarction are sustained by extramedullary monocytopoiesis.* J Exp Med, 2012. **209**(1): p. 123-37.
67. Bellingan, G.J., et al., *Adhesion molecule-dependent mechanisms regulate the rate of macrophage clearance during the resolution of peritoneal inflammation.* J Exp Med, 2002. **196**(11): p. 1515-21.
68. Cao, C., et al., *A specific role of integrin Mac-1 in accelerated macrophage efflux to the lymphatics.* Blood, 2005. **106**(9): p. 3234-41.
69. Janssen, W.J., et al., *Fas determines differential fates of resident and recruited macrophages during resolution of acute lung injury.* Am J Respir Crit Care Med, 2011. **184**(5): p. 547-60.
70. Yona, S., et al., *Fate mapping reveals origins and dynamics of monocytes and tissue macrophages under homeostasis.* Immunity, 2013. **38**(1): p. 79-91.
71. Satoh, T., et al., *The Jmjd3-Irf4 axis regulates M2 macrophage polarization and host responses against helminth infection.* Nat Immunol, 2010. **11**(10): p. 936-44.
72. Ohmori, Y. and T.A. Hamilton, *IL-4-induced STAT6 suppresses IFN-gamma-stimulated STAT1-dependent transcription in mouse macrophages.* J Immunol, 1997. **159**(11): p. 5474-82.
73. Meghari, S., et al., *Persistent Coxiella burnetii infection in mice overexpressing IL-10: an efficient model for chronic Q fever pathogenesis.* PLoS Pathog, 2008. **4**(2): p. e23.
74. Mantovani, A., et al., *The chemokine system in diverse forms of macrophage activation and polarization.* Trends Immunol, 2004. **25**(12): p. 677-86.
75. Watanabe, K., P.J. Jose, and S.M. Rankin, *Eotaxin-2 generation is differentially regulated by lipopolysaccharide and IL-4 in monocytes and macrophages.* J Immunol, 2002. **168**(4): p. 1911-8.
76. Bonecchi, R., et al., *Divergent effects of interleukin-4 and interferon-gamma on macrophage-derived chemokine production: an amplification circuit of polarized T helper 2 responses.* Blood, 1998. **92**(8): p. 2668-71.
77. Katakura, T., et al., *CCL17 and IL-10 as effectors that enable alternatively activated macrophages to inhibit the generation of classically activated macrophages.* J Immunol, 2004. **172**(3): p. 1407-13.
78. Mantovani, A. and M. Locati, *Tumor-associated macrophages as a paradigm of macrophage plasticity, diversity, and polarization: lessons and open questions.* Arterioscler Thromb Vasc Biol, 2013. **33**(7): p. 1478-83.
79. Jenkins, S.J., et al., *Local macrophage proliferation, rather than recruitment from the blood, is a signature of TH2 inflammation.* Science, 2011. **332**(6035): p. 1284-8.
80. Martinez, F.O., et al., *Macrophage activation and polarization.* Front Biosci, 2008. **13**: p. 453-61.

81. Liu, Y., et al., *Glucocorticoids promote nonphlogistic phagocytosis of apoptotic leukocytes.* J Immunol, 1999. **162**(6): p. 3639-46.
82. Sutterwala, F.S., et al., *Reversal of proinflammatory responses by ligating the macrophage Fcgamma receptor type I.* J Exp Med, 1998. **188**(1): p. 217-22.
83. Gustafsson, C., et al., *Gene expression profiling of human decidual macrophages: evidence for immunosuppressive phenotype.* PLoS One, 2008. **3**(4): p. e2078.
84. Pucci, F., et al., *A distinguishing gene signature shared by tumor-infiltrating Tie2-expressing monocytes, blood "resident" monocytes, and embryonic macrophages suggests common functions and developmental relationships.* Blood, 2009. **114**(4): p. 901-14.
85. Ryder, M., et al., *Increased density of tumor-associated macrophages is associated with decreased survival in advanced thyroid cancer.* Endocr Relat Cancer, 2008. **15**(4): p. 1069-74.
86. Zhu, X.D., et al., *High expression of macrophage colony-stimulating factor in peritumoral liver tissue is associated with poor survival after curative resection of hepatocellular carcinoma.* J Clin Oncol, 2008. **26**(16): p. 2707-16.
87. Lin, E.Y., et al., *Colony-stimulating factor 1 promotes progression of mammary tumors to malignancy.* J Exp Med, 2001. **193**(6): p. 727-40.
88. Sapi, E. and B.M. Kacinski, *The role of CSF-1 in normal and neoplastic breast physiology.* Proc Soc Exp Biol Med, 1999. **220**(1): p. 1-8.
89. Qian, B.Z. and J.W. Pollard, *Macrophage diversity enhances tumor progression and metastasis.* Cell, 2010. **141**(1): p. 39-51.
90. Allavena, P., et al., *The inflammatory micro-environment in tumor progression: the role of tumor-associated macrophages.* Crit Rev Oncol Hematol, 2008. **66**(1): p. 1-9.
91. Mantovani, A., A. Sica, and M. Locati, *Macrophage polarization comes of age.* Immunity, 2005. **23**(4): p. 344-6.
92. Schutyser, E., et al., *Identification of biologically active chemokine isoforms from ascitic fluid and elevated levels of CCL18/pulmonary and activation-regulated chemokine in ovarian carcinoma.* J Biol Chem, 2002. **277**(27): p. 24584-93.
93. Curiel, T.J., et al., *Specific recruitment of regulatory T cells in ovarian carcinoma fosters immune privilege and predicts reduced survival.* Nat Med, 2004. **10**(9): p. 942-9.
94. Biswas, S.K., et al., *A distinct and unique transcriptional program expressed by tumor-associated macrophages (defective NF-kappaB and enhanced IRF-3/STAT1 activation).* Blood, 2006. **107**(5): p. 2112-22.
95. Schoppmann, S.F., et al., *Tumor-associated macrophages express lymphatic endothelial growth factors and are related to peritumoral lymphangiogenesis.* Am J Pathol, 2002. **161**(3): p. 947-56.
96. Vignaud, J.M., et al., *The role of platelet-derived growth factor production by tumor-associated macrophages in tumor stroma formation in lung cancer.* Cancer Res, 1994. **54**(20): p. 5455-63.
97. Balkwill, F., *Cancer and the chemokine network.* Nat Rev Cancer, 2004. **4**(7): p. 540-50.
98. Strieter, R.M., et al., *CXC chemokines in angiogenesis of cancer.* Semin Cancer Biol, 2004. **14**(3): p. 195-200.
99. Murdoch, C., A. Giannoudis, and C.E. Lewis, *Mechanisms regulating the recruitment of macrophages into hypoxic areas of tumors and other ischemic tissues.* Blood, 2004. **104**(8): p. 2224-34.
100. Locati, M., et al., *Analysis of the gene expression profile activated by the CC chemokine ligand 5/RANTES and by lipopolysaccharide in human monocytes.* J Immunol, 2002. **168**(7): p. 3557-62.
101. Hagemann, T., et al., *Enhanced invasiveness of breast cancer cell lines upon co-cultivation with macrophages is due to TNF-alpha dependent up-regulation of matrix metalloproteases.* Carcinogenesis, 2004. **25**(8): p. 1543-9.
102. Ohno, S., et al., *The degree of macrophage infiltration into the cancer cell nest is a significant predictor of survival in gastric cancer patients.* Anticancer Res, 2003. **23**(6D): p. 5015-22.
103. Funada, Y., et al., *Prognostic significance of CD8+ T cell and macrophage peritumoral infiltration in colorectal cancer.* Oncol Rep, 2003. **10**(2): p. 309-13.
104. Steidl, C., et al., *Tumor-associated macrophages and survival in classic Hodgkin's lymphoma.* N Engl J Med, 2010. **362**(10): p. 875-85.
105. Chen, J., et al., *CCL18 from tumor-associated macrophages promotes breast cancer metastasis via PITPNM3.* Cancer Cell, 2011. **19**(4): p. 541-55.
106. Tarrant, J.M., et al., *Tetraspanins: molecular organisers of the leukocyte surface.* Trends Immunol, 2003. **24**(11): p. 610-7.
107. Garcia-Espana, A., et al., *Appearance of new tetraspanin genes during vertebrate evolution.* Genomics, 2008. **91**(4): p. 326-34.

108. Charrin, S., et al., *Lateral organization of membrane proteins: tetraspanins spin their web.* Biochem J, 2009. **420**(2): p. 133-54.
109. Hemler, M.E., *Tetraspanin functions and associated microdomains.* Nat Rev Mol Cell Biol, 2005. **6**(10): p. 801-11.
110. Levy, S. and T. Shoham, *The tetraspanin web modulates immune-signalling complexes.* Nat Rev Immunol, 2005. **5**(2): p. 136-48.
111. Yanez-Mo, M., et al., *Tetraspanins in intercellular adhesion of polarized epithelial cells: spatial and functional relationship to integrins and cadherins.* J Cell Sci, 2001. **114**(Pt 3): p. 577-87.
112. Seigneuret, M., et al., *Structure of the tetraspanin main extracellular domain. A partially conserved fold with a structurally variable domain insertion.* J Biol Chem, 2001. **276**(43): p. 40055-64.
113. Berditchevski, F. and E. Odintsova, *Tetraspanins as regulators of protein trafficking.* Traffic, 2007. **8**(2): p. 89-96.
114. Le Naour, F., et al., *Membrane microdomains and proteomics: lessons from tetraspanin microdomains and comparison with lipid rafts.* Proteomics, 2006. **6**(24): p. 6447-54.
115. Kitadokoro, K., et al., *Crystallization and preliminary crystallographic studies on the large extracellular domain of human CD81, a tetraspanin receptor for hepatitis C virus.* Acta Crystallogr D Biol Crystallogr, 2001. **57**(Pt 1): p. 156-8.
116. Min, G., et al., *Structural basis for tetraspanin functions as revealed by the cryo-EM structure of uroplakin complexes at 6-A resolution.* J Cell Biol, 2006. **173**(6): p. 975-83.
117. Berditchevski, F., et al., *Expression of the palmitoylation-deficient CD151 weakens the association of alpha 3 beta 1 integrin with the tetraspanin-enriched microdomains and affects integrin-dependent signaling.* J Biol Chem, 2002. **277**(40): p. 36991-7000.
118. Charrin, S., et al., *Differential stability of tetraspanin/tetraspanin interactions: role of palmitoylation.* FEBS Lett, 2002. **516**(1-3): p. 139-44.
119. Delandre, C., et al., *Mutation of juxtamembrane cysteines in the tetraspanin CD81 affects palmitoylation and alters interaction with other proteins at the cell surface.* Exp Cell Res, 2009. **315**(11): p. 1953-63.
120. Sharma, C., X.H. Yang, and M.E. Hemler, *DHHC2 affects palmitoylation, stability, and functions of tetraspanins CD9 and CD151.* Mol Biol Cell, 2008. **19**(8): p. 3415-25.
121. Stipp, C.S., T.V. Kolesnikova, and M.E. Hemler, *Functional domains in tetraspanin proteins.* Trends Biochem Sci, 2003. **28**(2): p. 106-12.
122. Latysheva, N., et al., *Syntenin-1 is a new component of tetraspanin-enriched microdomains: mechanisms and consequences of the interaction of syntenin-1 with CD63.* Mol Cell Biol, 2006. **26**(20): p. 7707-18.
123. Berditchevski, F., *Complexes of tetraspanins with integrins: more than meets the eye.* J Cell Sci, 2001. **114**(Pt 23): p. 4143-51.
124. Lineberry, N., et al., *The single subunit transmembrane E3 ligase gene related to anergy in lymphocytes (GRAIL) captures and then ubiquitinates transmembrane proteins across the cell membrane.* J Biol Chem, 2008. **283**(42): p. 28497-505.
125. Lazo, P.A., *Functional implications of tetraspanin proteins in cancer biology.* Cancer Sci, 2007. **98**(11): p. 1666-77.
126. Brown, D.A., *Lipid rafts, detergent-resistant membranes, and raft targeting signals.* Physiology (Bethesda), 2006. **21**: p. 430-9.
127. Brown, D.A. and E. London, *Functions of lipid rafts in biological membranes.* Annu Rev Cell Dev Biol, 1998. **14**: p. 111-36.
128. Simons, K. and E. Ikonen, *Functional rafts in cell membranes.* Nature, 1997. **387**(6633): p. 569-72.
129. Cuschieri, J., *Implications of lipid raft disintegration: enhanced anti-inflammatory macrophage phenotype.* Surgery, 2004. **136**(2): p. 169-75.
130. Gaus, K., et al., *Condensation of the plasma membrane at the site of T lymphocyte activation.* J Cell Biol, 2005. **171**(1): p. 121-31.
131. Ha, H., et al., *Membrane rafts play a crucial role in receptor activator of nuclear factor kappaB signaling and osteoclast function.* J Biol Chem, 2003. **278**(20): p. 18573-80.
132. Claas, C., C.S. Stipp, and M.E. Hemler, *Evaluation of prototype transmembrane 4 superfamily protein complexes and their relation to lipid rafts.* J Biol Chem, 2001. **276**(11): p. 7974-84.
133. Cherukuri, A., et al., *B cell signaling is regulated by induced palmitoylation of CD81.* J Biol Chem, 2004. **279**(30): p. 31973-82.
134. Cherukuri, A., et al., *The tetraspanin CD81 is necessary for partitioning of coligated CD19/CD21-B cell antigen receptor complexes into signaling-active lipid rafts.* J Immunol, 2004. **172**(1): p. 370-80.

135. Maecker, H.T., S.C. Todd, and S. Levy, *The tetraspanin superfamily: molecular facilitators.* FASEB J, 1997. **11**(6): p. 428-42.
136. Kazarov, A.R., et al., *An extracellular site on tetraspanin CD151 determines alpha 3 and alpha 6 integrin-dependent cellular morphology.* J Cell Biol, 2002. **158**(7): p. 1299-309.
137. Yang, X.H., et al., *CD151 accelerates breast cancer by regulating alpha 6 integrin function, signaling, and molecular organization.* Cancer Res, 2008. **68**(9): p. 3204-13.
138. Janes, S.M. and F.M. Watt, *New roles for integrins in squamous-cell carcinoma.* Nat Rev Cancer, 2006. **6**(3): p. 175-83.
139. Watt, F.M., *Role of integrins in regulating epidermal adhesion, growth and differentiation.* EMBO J, 2002. **21**(15): p. 3919-26.
140. Hemler, M.E. and R.R. Lobb, *The leukocyte beta 1 integrins.* Curr Opin Hematol, 1995. **2**(1): p. 61-7.
141. Dedhar, S., *Cell-substrate interactions and signaling through ILK.* Curr Opin Cell Biol, 2000. **12**(2): p. 250-6.
142. Sincock, P.M., G. Mayrhofer, and L.K. Ashman, *Localization of the transmembrane 4 superfamily (TM4SF) member PETA-3 (CD151) in normal human tissues: comparison with CD9, CD63, and alpha5beta1 integrin.* J Histochem Cytochem, 1997. **45**(4): p. 515-25.
143. Yauch, R.L., et al., *Direct extracellular contact between integrin alpha(3)beta(1) and TM4SF protein CD151.* J Biol Chem, 2000. **275**(13): p. 9230-8.
144. Yauch, R.L. and M.E. Hemler, *Specific interactions among transmembrane 4 superfamily (TM4SF) proteins and phosphoinositide 4-kinase.* Biochem J, 2000. **351 Pt 3**: p. 629-37.
145. Serru, V., et al., *Selective tetraspan-integrin complexes (CD81/alpha4beta1, CD151/alpha3beta1, CD151/alpha6beta1) under conditions disrupting tetraspan interactions.* Biochem J, 1999. **340 (Pt 1)**: p. 103-11.
146. Takeda, Y., et al., *Deletion of tetraspanin Cd151 results in decreased pathologic angiogenesis in vivo and in vitro.* Blood, 2007. **109**(4): p. 1524-32.
147. Liu, L., et al., *Tetraspanin CD151 promotes cell migration by regulating integrin trafficking.* J Biol Chem, 2007. **282**(43): p. 31631-42.
148. Karamatic Crew, V., et al., *CD151, the first member of the tetraspanin (TM4) superfamily detected on erythrocytes, is essential for the correct assembly of human basement membranes in kidney and skin.* Blood, 2004. **104**(8): p. 2217-23.
149. Lammerding, J., et al., *Tetraspanin CD151 regulates alpha6beta1 integrin adhesion strengthening.* Proc Natl Acad Sci U S A, 2003. **100**(13): p. 7616-21.
150. Nishiuchi, R., et al., *Potentiation of the ligand-binding activity of integrin alpha3beta1 via association with tetraspanin CD151.* Proc Natl Acad Sci U S A, 2005. **102**(6): p. 1939-44.
151. Lagaudriere-Gesbert, C., et al., *Functional analysis of four tetraspans, CD9, CD53, CD81, and CD82, suggests a common role in costimulation, cell adhesion, and migration: only CD9 upregulates HB-EGF activity.* Cell Immunol, 1997. **182**(2): p. 105-12.
152. Trusolino, L. and P.M. Comoglio, *Scatter-factor and semaphorin receptors: cell signalling for invasive growth.* Nat Rev Cancer, 2002. **2**(4): p. 289-300.
153. Sridhar, S.C. and C.K. Miranti, *Tetraspanin KAI1/CD82 suppresses invasion by inhibiting integrin-dependent crosstalk with c-Met receptor and Src kinases.* Oncogene, 2006. **25**(16): p. 2367-78.
154. Todeschini, A.R., et al., *Ganglioside GM2/GM3 complex affixed on silica nanospheres strongly inhibits cell motility through CD82/cMet-mediated pathway.* Proc Natl Acad Sci U S A, 2008. **105**(6): p. 1925-30.
155. Szollosi, J., et al., *Supramolecular complexes of MHC class I, MHC class II, CD20, and tetraspan molecules (CD53, CD81, and CD82) at the surface of a B cell line JY.* J Immunol, 1996. **157**(7): p. 2939-46.
156. Unternaehrer, J.J., et al., *The tetraspanin CD9 mediates lateral association of MHC class II molecules on the dendritic cell surface.* Proc Natl Acad Sci U S A, 2007. **104**(1): p. 234-9.
157. Angelisova, P., I. Hilgert, and V. Horejsi, *Association of four antigens of the tetraspans family (CD37, CD53, TAPA-1, and R2/C33) with MHC class II glycoproteins.* Immunogenetics, 1994. **39**(4): p. 249-56.
158. Imai, T. and O. Yoshie, *C33 antigen and M38 antigen recognized by monoclonal antibodies inhibitory to syncytium formation by human T cell leukemia virus type 1 are both members of the transmembrane 4 superfamily and associate with each other and with CD4 or CD8 in T cells.* J Immunol, 1993. **151**(11): p. 6470-81.
159. Boucheix, C. and E. Rubinstein, *Tetraspanins.* Cell Mol Life Sci, 2001. **58**(9): p. 1189-205.
160. Berditchevski, F., et al., *A novel link between integrins, transmembrane-4 superfamily proteins (CD63 and CD81), and phosphatidylinositol 4-kinase.* J Biol Chem, 1997. **272**(5): p. 2595-8.

161. Barcia, R., et al., *CD53 antigen and epidermal growth factor induce similar changes in the pattern of phorbol ester binding in a B cell lymphoma.* Cell Immunol, 1996. **169**(1): p. 107-12.
162. Bosca, L. and P.A. Lazo, *Induction of nitric oxide release by MRC OX-44 (anti-CD53) through a protein kinase C-dependent pathway in rat macrophages.* J Exp Med, 1994. **179**(4): p. 1119-26.
163. Lazo, P.A., et al., *Ligation of CD53/OX44, a tetraspan antigen, induces homotypic adhesion mediated by specific cell-cell interactions.* Cell Immunol, 1997. **178**(2): p. 132-40.
164. Yunta, M. and P.A. Lazo, *Apoptosis protection and survival signal by the CD53 tetraspanin antigen.* Oncogene, 2003. **22**(8): p. 1219-24.
165. Yunta, M., et al., *Transient activation of the c-Jun N-terminal kinase (JNK) activity by ligation of the tetraspan CD53 antigen in different cell types.* Eur J Biochem, 2002. **269**(3): p. 1012-21.
166. Meyer-Wentrup, F., et al., *Dectin-1 interaction with tetraspanin CD37 inhibits IL-6 production.* J Immunol, 2007. **178**(1): p. 154-62.
167. Levy, S., S.C. Todd, and H.T. Maecker, *CD81 (TAPA-1): a molecule involved in signal transduction and cell adhesion in the immune system.* Annu Rev Immunol, 1998. **16**: p. 89-109.
168. Shoham, T., et al., *The tetraspanin CD81 regulates the expression of CD19 during B cell development in a postendoplasmic reticulum compartment.* J Immunol, 2003. **171**(8): p. 4062-72.
169. Knobeloch, K.P., et al., *Targeted inactivation of the tetraspanin CD37 impairs T-cell-dependent B-cell response under suboptimal costimulatory conditions.* Mol Cell Biol, 2000. **20**(15): p. 5363-9.
170. Miyazaki, T., U. Muller, and K.S. Campbell, *Normal development but differentially altered proliferative responses of lymphocytes in mice lacking CD81.* EMBO J, 1997. **16**(14): p. 4217-25.
171. Tarrant, J.M., et al., *The absence of Tssc6, a member of the tetraspanin superfamily, does not affect lymphoid development but enhances in vitro T-cell proliferative responses.* Mol Cell Biol, 2002. **22**(14): p. 5006-18.
172. van Spriel, A.B., et al., *A regulatory role for CD37 in T cell proliferation.* J Immunol, 2004. **172**(5): p. 2953-61.
173. Wright, M.D., et al., *Characterization of mice lacking the tetraspanin superfamily member CD151.* Mol Cell Biol, 2004. **24**(13): p. 5978-88.
174. Abraham, R.T. and A. Weiss, *Jurkat T cells and development of the T-cell receptor signalling paradigm.* Nat Rev Immunol, 2004. **4**(4): p. 301-8.
175. Hemler, M.E., *Targeting of tetraspanin proteins--potential benefits and strategies.* Nat Rev Drug Discov, 2008. **7**(9): p. 747-58.
176. Nydegger, S., et al., *Mapping of tetraspanin-enriched microdomains that can function as gateways for HIV-1.* J Cell Biol, 2006. **173**(5): p. 795-807.
177. Ruiz-Mateos, E., et al., *CD63 is not required for production of infectious human immunodeficiency virus type 1 in human macrophages.* J Virol, 2008. **82**(10): p. 4751-61.
178. Chen, H., et al., *A critical role for CD63 in HIV replication and infection of macrophages and cell lines.* Virology, 2008. **379**(2): p. 191-6.
179. Grigorov, B., et al., *A role for CD81 on the late steps of HIV-1 replication in a chronically infected T cell line.* Retrovirology, 2009. **6**: p. 28.
180. Sato, K., et al., *Modulation of human immunodeficiency virus type 1 infectivity through incorporation of tetraspanin proteins.* J Virol, 2008. **82**(2): p. 1021-33.
181. Ploss, A., et al., *Human occludin is a hepatitis C virus entry factor required for infection of mouse cells.* Nature, 2009. **457**(7231): p. 882-6.
182. Pileri, P., et al., *Binding of hepatitis C virus to CD81.* Science, 1998. **282**(5390): p. 938-41.
183. Flint, M., et al., *Diverse CD81 proteins support hepatitis C virus infection.* J Virol, 2006. **80**(22): p. 11331-42.
184. Rocha-Perugini, V., et al., *The association of CD81 with tetraspanin-enriched microdomains is not essential for Hepatitis C virus entry.* BMC Microbiol, 2009. **9**: p. 111.
185. Kaji, K., et al., *Infertility of CD9-deficient mouse eggs is reversed by mouse CD9, human CD9, or mouse CD81; polyadenylated mRNA injection developed for molecular analysis of sperm-egg fusion.* Dev Biol, 2002. **247**(2): p. 327-34.
186. Le Naour, F., et al., *Severely reduced female fertility in CD9-deficient mice.* Science, 2000. **287**(5451): p. 319-21.
187. Runge, K.E., et al., *Oocyte CD9 is enriched on the microvillar membrane and required for normal microvillar shape and distribution.* Dev Biol, 2007. **304**(1): p. 317-25.
188. Ziyyat, A., et al., *CD9 controls the formation of clusters that contain tetraspanins and the integrin alpha 6 beta 1, which are involved in human and mouse gamete fusion.* J Cell Sci, 2006. **119**(Pt 3): p. 416-24.
189. Rubinstein, E., et al., *Reduced fertility of female mice lacking CD81.* Dev Biol, 2006. **290**(2): p. 351-8.

190. Higginbottom, A., et al., *Structural requirements for the inhibitory action of the CD9 large extracellular domain in sperm/oocyte binding and fusion.* Biochem Biophys Res Commun, 2003. **311**(1): p. 208-14.
191. Barrena, S., et al., *Discrimination of biclonal B-cell chronic lymphoproliferative neoplasias by tetraspanin antigen expression.* Leukemia, 2005. **19**(9): p. 1708-9.
192. Ono, M., et al., *Motility inhibition and apoptosis are induced by metastasis-suppressing gene product CD82 and its analogue CD9, with concurrent glycosylation.* Cancer Res, 1999. **59**(10): p. 2335-9.
193. Higgins, J.P., et al., *Gene expression patterns in renal cell carcinoma assessed by complementary DNA microarray.* Am J Pathol, 2003. **162**(3): p. 925-32.
194. Si, Z. and P. Hersey, *Expression of the neuroglandular antigen and analogues in melanoma. CD9 expression appears inversely related to metastatic potential of melanoma.* Int J Cancer, 1993. **54**(1): p. 37-43.
195. Houle, C.D., et al., *Loss of expression and altered localization of KAI1 and CD9 protein are associated with epithelial ovarian cancer progression.* Gynecol Oncol, 2002. **86**(1): p. 69-78.
196. Higashiyama, M., et al., *Reduced motility related protein-1 (MRP-1/CD9) gene expression as a factor of poor prognosis in non-small cell lung cancer.* Cancer Res, 1995. **55**(24): p. 6040-4.
197. Kusukawa, J., et al., *Reduced expression of CD9 in oral squamous cell carcinoma: CD9 expression inversely related to high prevalence of lymph node metastasis.* J Oral Pathol Med, 2001. **30**(2): p. 73-9.
198. Uchida, S., et al., *Motility-related protein (MRP-1/CD9) and KAI1/CD82 expression inversely correlate with lymph node metastasis in oesophageal squamous cell carcinoma.* Br J Cancer, 1999. **79**(7-8): p. 1168-73.
199. Sauer, G., et al., *Progression of cervical carcinomas is associated with down-regulation of CD9 but strong local re-expression at sites of transendothelial invasion.* Clin Cancer Res, 2003. **9**(17): p. 6426-31.
200. Hori, H., et al., *CD9 expression in gastric cancer and its significance.* J Surg Res, 2004. **117**(2): p. 208-15.
201. Shi, W., et al., *The tetraspanin CD9 associates with transmembrane TGF-alpha and regulates TGF-alpha-induced EGF receptor activation and cell proliferation.* J Cell Biol, 2000. **148**(3): p. 591-602.
202. Hotta, H., et al., *Molecular cloning and characterization of an antigen associated with early stages of melanoma tumor progression.* Cancer Res, 1988. **48**(11): p. 2955-62.
203. Sauer, G., et al., *Expression of tetraspanin adaptor proteins below defined threshold values is associated with in vitro invasiveness of mammary carcinoma cells.* Oncol Rep, 2003. **10**(2): p. 405-10.
204. Chen, Z., et al., *CD82, and CD63 in thyroid cancer.* Int J Mol Med, 2004. **14**(4): p. 517-27.
205. Berditchevski, F. and E. Odintsova, *Characterization of integrin-tetraspanin adhesion complexes: role of tetraspanins in integrin signaling.* J Cell Biol, 1999. **146**(2): p. 477-92.
206. Penas, P.F., et al., *Tetraspanins are localized at motility-related structures and involved in normal human keratinocyte wound healing migration.* J Invest Dermatol, 2000. **114**(6): p. 1126-35.
207. Yamada, M., et al., *The tetraspanin CD151 regulates cell morphology and intracellular signaling on laminin-511.* FEBS J, 2008. **275**(13): p. 3335-51.
208. Sterk, L.M., et al., *The tetraspan molecule CD151, a novel constituent of hemidesmosomes, associates with the integrin alpha6beta4 and may regulate the spatial organization of hemidesmosomes.* J Cell Biol, 2000. **149**(4): p. 969-82.
209. Hong, I.K., et al., *Homophilic interactions of Tetraspanin CD151 up-regulate motility and matrix metalloproteinase-9 expression of human melanoma cells through adhesion-dependent c-Jun activation signaling pathways.* J Biol Chem, 2006. **281**(34): p. 24279-92.
210. Garcia-Lopez, M.A., et al., *Role of tetraspanins CD9 and CD151 in primary melanocyte motility.* J Invest Dermatol, 2005. **125**(5): p. 1001-9.
211. Zijlstra, A., et al., *The inhibition of tumor cell intravasation and subsequent metastasis via regulation of in vivo tumor cell motility by the tetraspanin CD151.* Cancer Cell, 2008. **13**(3): p. 221-34.
212. Lapointe, J., et al., *Gene expression profiling identifies clinically relevant subtypes of prostate cancer.* Proc Natl Acad Sci U S A, 2004. **101**(3): p. 811-6.
213. Ishibashi, K., et al., *Identification of a new multigene four-transmembrane family (MS4A) related to CD20, HTm4 and beta subunit of the high-affinity IgE receptor.* Gene, 2001. **264**(1): p. 87-93.
214. Aebi, M., H. Hornig, and C. Weissmann, *5' cleavage site in eukaryotic pre-mRNA splicing is determined by the overall 5' splice region, not by the conserved 5' GU.* Cell, 1987. **50**(2): p. 237-46.
215. Xu, H., M.S. Williams, and L.M. Spain, *Patterns of expression, membrane localization, and effects of ectopic expression suggest a function for MS4a4B, a CD20 homolog in Th1 T cells.* Blood, 2006. **107**(6): p. 2400-8.
216. Adra, C.N., et al., *Cloning of the cDNA for a hematopoietic cell-specific protein related to CD20 and the beta subunit of the high-affinity IgE receptor: evidence for a family of proteins with four membrane-spanning regions.* Proc Natl Acad Sci U S A, 1994. **91**(21): p. 10178-82.

217. Hupp, K., et al., *Gene mapping of the three subunits of the high affinity FcR for IgE to mouse chromosomes 1 and 19.* J Immunol, 1989. **143**(11): p. 3787-91.
218. Kuster, H., et al., *The gene and cDNA for the human high affinity immunoglobulin E receptor beta chain and expression of the complete human receptor.* J Biol Chem, 1992. **267**(18): p. 12782-7.
219. Adra, C.N., et al., *Chromosome 11q13 and atopic asthma.* Clin Genet, 1999. **55**(6): p. 431-7.
220. Cookson, W.O., et al., *Linkage between immunoglobulin E responses underlying asthma and rhinitis and chromosome 11q.* Lancet, 1989. **1**(8650): p. 1292-5.
221. Moffatt, M.F. and W.O. Cookson, *Gene identification in asthma and allergy.* Int Arch Allergy Immunol, 1998. **116**(4): p. 247-52.
222. Turner, S., et al., *Prescribing trends in asthma: a longitudinal observational study.* Arch Dis Child, 2009. **94**(1): p. 16-22.
223. Liang, R., L. Wang, and G. Wang, *New insight into genes in association with asthma: literature-based mining and network centrality analysis.* Chin Med J (Engl), 2013. **126**(13): p. 2472-9.
224. Charmley, P., et al., *A primary linkage map of the human chromosome 11q22-23 region.* Genomics, 1990. **6**(2): p. 316-23.
225. Fuzesi, L., et al., *Cytogenetic analysis of 11 renal oncocytomas: further evidence of structural rearrangements of 11q13 as a characteristic chromosomal anomaly.* Cancer Genet Cytogenet, 1998. **107**(1): p. 1-6.
226. Iizuka, M. and T. Sekiya, *[Deletion map of human chromosome 11 in lung cancers].* Nihon Rinsho, 1996. **54**(2): p. 472-7.
227. Iizuka, M., et al., *Allelic losses in human chromosome 11 in lung cancers.* Genes Chromosomes Cancer, 1995. **13**(1): p. 40-6.
228. Gabra, H., et al., *Loss of heterozygosity at 11q22 correlates with low progesterone receptor content in epithelial ovarian cancer.* Clin Cancer Res, 1995. **1**(9): p. 945-53.
229. Schmieder, A., et al., *Synergistic activation by p38MAPK and glucocorticoid signaling mediates induction of M2-like tumor-associated macrophages expressing the novel CD20 homolog MS4A8A.* Int J Cancer, 2011. **129**(1): p. 122-32.
230. Howie, D., et al., *MS4A4B is a GITR-associated membrane adapter, expressed by regulatory T cells, which modulates T cell activation.* J Immunol, 2009. **183**(7): p. 4197-204.
231. Cuajungco, M.P., et al., *Abnormal accumulation of human transmembrane (TMEM)-176A and 176B proteins is associated with cancer pathology.* Acta Histochem, 2012. **114**(7): p. 705-12.
232. Tedder, T.F. and P. Engel, *CD20: a regulator of cell-cycle progression of B lymphocytes.* Immunol Today, 1994. **15**(9): p. 450-4.
233. Bubien, J.K., et al., *Transfection of the CD20 cell surface molecule into ectopic cell types generates a Ca2+ conductance found constitutively in B lymphocytes.* J Cell Biol, 1993. **121**(5): p. 1121-32.
234. Kanzaki, M., et al., *Expression of calcium-permeable cation channel CD20 accelerates progression through the G1 phase in Balb/c 3T3 cells.* J Biol Chem, 1995. **270**(22): p. 13099-104.
235. Ernst, J.A., et al., *Isolation and characterization of the B-cell marker CD20.* Biochemistry, 2005. **44**(46): p. 15150-8.
236. Holder, M.J., et al., *Improved access to CD20 following B cell receptor cross-linking at Burkitt's lymphoma cell surfaces.* Leuk Res, 2004. **28**(11): p. 1197-202.
237. Janas, E., et al., *Rituxan (anti-CD20 antibody)-induced translocation of CD20 into lipid rafts is crucial for calcium influx and apoptosis.* Clin Exp Immunol, 2005. **139**(3): p. 439-46.
238. Anolik, J., et al., *Down-regulation of CD20 on B cells upon CD40 activation.* Eur J Immunol, 2003. **33**(9): p. 2398-409.
239. Petrie, R.J. and J.P. Deans, *Colocalization of the B cell receptor and CD20 followed by activation-dependent dissociation in distinct lipid rafts.* J Immunol, 2002. **169**(6): p. 2886-91.
240. Ghetie, M.A., H. Bright, and E.S. Vitetta, *Homodimers but not monomers of Rituxan (chimeric anti-CD20) induce apoptosis in human B-lymphoma cells and synergize with a chemotherapeutic agent and an immunotoxin.* Blood, 2001. **97**(5): p. 1392-8.
241. von Mehren, M., G.P. Adams, and L.M. Weiner, *Monoclonal antibody therapy for cancer.* Annu Rev Med, 2003. **54**: p. 343-69.
242. McLaughlin, P., et al., *Rituximab chimeric anti-CD20 monoclonal antibody therapy for relapsed indolent lymphoma: half of patients respond to a four-dose treatment program.* J Clin Oncol, 1998. **16**(8): p. 2825-33.
243. Onrust, S.V., H.M. Lamb, and J.A. Balfour, *Rituximab.* Drugs, 1999. **58**(1): p. 79-88; discussion 89-90.
244. Weiner, L.M., *Monoclonal antibody therapy of cancer.* Semin Oncol, 1999. **26**(5 Suppl 14): p. 43-51.

245. Blank, U., et al., *Complete structure and expression in transfected cells of high affinity IgE receptor.* Nature, 1989. **337**(6203): p. 187-9.
246. Kinet, J.P., *The high-affinity IgE receptor (Fc epsilon RI): from physiology to pathology.* Annu Rev Immunol, 1999. **17**: p. 931-72.
247. Dombrowicz, D., et al., *Allergy-associated FcRbeta is a molecular amplifier of IgE- and IgG-mediated in vivo responses.* Immunity, 1998. **8**(4): p. 517-29.
248. Lin, S., et al., *The Fc(epsilon)RIbeta subunit functions as an amplifier of Fc(epsilon)RIgamma-mediated cell activation signals.* Cell, 1996. **85**(7): p. 985-95.
249. Nakajima, T., et al., *Identification of granulocyte subtype-selective receptors and ion channels by using a high-density oligonucleotide probe array.* J Allergy Clin Immunol, 2004. **113**(3): p. 528-35.
250. Donato, J.L., et al., *Human HTm4 is a hematopoietic cell cycle regulator.* J Clin Invest, 2002. **109**(1): p. 51-8.
251. Kutok, J.L., et al., *The cell cycle associated protein, HTm4, is expressed in differentiating cells of the hematopoietic and central nervous system in mice.* J Mol Histol, 2005. **36**(1-2): p. 77-87.
252. Czimmerer, Z., et al., *Identification of novel markers of alternative activation and potential endogenous PPARgamma ligand production mechanisms in human IL-4 stimulated differentiating macrophages.* Immunobiology, 2012. **217**(12): p. 1301-14.
253. Antunez, C., et al., *The membrane-spanning 4-domains, subfamily A (MS4A) gene cluster contains a common variant associated with Alzheimer's disease.* Genome Med, 2011. **3**(5): p. 33.
254. Zekry, D., J.J. Hauw, and G. Gold, *Mixed dementia: epidemiology, diagnosis, and treatment.* J Am Geriatr Soc, 2002. **50**(8): p. 1431-8.
255. Rosenthal, S.L., et al., *Connecting the dots: potential of data integration to identify regulatory SNPs in late-onset Alzheimer's disease GWAS findings.* PLoS One, 2014. **9**(4): p. e95152.
256. Proitsi, P., et al., *Alzheimer's disease susceptibility variants in the MS4A6A gene are associated with altered levels of MS4A6A expression in blood.* Neurobiol Aging, 2014. **35**(2): p. 279-90.
257. Michel, J., et al., *Identification of the novel differentiation marker MS4A8B and its murine homolog MS4A8A in colonic epithelial cells lost during neoplastic transformation in human colon.* Cell Death Dis, 2013. **4**: p. e469.
258. Ye, L., et al., *MS4A8B promotes cell proliferation in prostate cancer.* Prostate, 2014. **74**(9): p. 911-22.
259. Venkataraman, C., G. Schaefer, and U. Schindler, *Cutting edge: Chandra, a novel four-transmembrane domain protein differentially expressed in helper type 1 lymphocytes.* J Immunol, 2000. **165**(2): p. 632-6.
260. Yan, Y., et al., *Anti-MS4a4B treatment abrogates MS4a4B-mediated protection in T cells and ameliorates experimental autoimmune encephalomyelitis.* Apoptosis, 2013. **18**(9): p. 1106-19.
261. Kuek, L.E., *Expression And Function Of A Novel Membrane-Spanning Protein, MS4A8B, In The Airway Epithelium.* American Thoracic Society Journals, 2014.
262. Koslowski, M., et al., *MS4A12 is a colon-selective store-operated calcium channel promoting malignant cell processes.* Cancer Res, 2008. **68**(9): p. 3458-66.
263. Koslowski, M., et al., *Selective activation of tumor growth-promoting Ca2+ channel MS4A12 in colon cancer by caudal type homeobox transcription factor CDX2.* Mol Cancer, 2009. **8**: p. 77.
264. Drickamer, K., *C-type lectin-like domains.* Curr Opin Struct Biol, 1999. **9**(5): p. 585-90.
265. Zelensky, A.N. and J.E. Gready, *The C-type lectin-like domain superfamily.* FEBS J, 2005. **272**(24): p. 6179-217.
266. Sobanov, Y., et al., *A novel cluster of lectin-like receptor genes expressed in monocytic, dendritic and endothelial cells maps close to the NK receptor genes in the human NK gene complex.* Eur J Immunol, 2001. **31**(12): p. 3493-503.
267. Huysamen, C., et al., *CLEC9A is a novel activation C-type lectin-like receptor expressed on BDCA3+ dendritic cells and a subset of monocytes.* J Biol Chem, 2008. **283**(24): p. 16693-701.
268. Kerrigan, A.M. and G.D. Brown, *Syk-coupled C-type lectins in immunity.* Trends Immunol, 2011. **32**(4): p. 151-6.
269. Sancho, D. and C. Reis e Sousa, *Signaling by myeloid C-type lectin receptors in immunity and homeostasis.* Annu Rev Immunol, 2012. **30**: p. 491-529.
270. Brown, G.D., *Dectin-1: a signalling non-TLR pattern-recognition receptor.* Nat Rev Immunol, 2006. **6**(1): p. 33-43.
271. Willment, J.A. and G.D. Brown, *C-type lectin receptors in antifungal immunity.* Trends Microbiol, 2008. **16**(1): p. 27-32.
272. Taylor, P.R., et al., *The beta-glucan receptor, dectin-1, is predominantly expressed on the surface of cells of the monocyte/macrophage and neutrophil lineages.* J Immunol, 2002. **169**(7): p. 3876-82.
273. Willment, J.A., S. Gordon, and G.D. Brown, *Characterization of the human beta -glucan receptor and its alternatively spliced isoforms.* J Biol Chem, 2001. **276**(47): p. 43818-23.

274. Shah, V.B., et al., *Beta-glucan activates microglia without inducing cytokine production in Dectin-1-dependent manner.* J Immunol, 2008. **180**(5): p. 2777-85.
275. Olynych, T.J., D.L. Jakeman, and J.S. Marshall, *Fungal zymosan induces leukotriene production by human mast cells through a dectin-1-dependent mechanism.* J Allergy Clin Immunol, 2006. **118**(4): p. 837-43.
276. Reid, D.M., et al., *Expression of the beta-glucan receptor, Dectin-1, on murine leukocytes in situ correlates with its function in pathogen recognition and reveals potential roles in leukocyte interactions.* J Leukoc Biol, 2004. **76**(1): p. 86-94.
277. Heinsbroek, S.E., et al., *Expression of functionally different dectin-1 isoforms by murine macrophages.* J Immunol, 2006. **176**(9): p. 5513-8.
278. Willment, J.A., et al., *Dectin-1 expression and function are enhanced on alternatively activated and GM-CSF-treated macrophages and are negatively regulated by IL-10, dexamethasone, and lipopolysaccharide.* J Immunol, 2003. **171**(9): p. 4569-73.
279. Ozment-Skelton, T.R., et al., *Leukocyte Dectin-1 expression is differentially regulated in fungal versus polymicrobial sepsis.* Crit Care Med, 2009. **37**(3): p. 1038-45.
280. Ozment-Skelton, T.R., et al., *Prolonged reduction of leukocyte membrane-associated Dectin-1 levels following beta-glucan administration.* J Pharmacol Exp Ther, 2006. **318**(2): p. 540-6.
281. Kato, Y., Y. Adachi, and N. Ohno, *Contribution of N-linked oligosaccharides to the expression and functions of beta-glucan receptor, Dectin-1.* Biol Pharm Bull, 2006. **29**(8): p. 1580-6.
282. Saijo, S., et al., *Dectin-1 is required for host defense against Pneumocystis carinii but not against Candida albicans.* Nat Immunol, 2007. **8**(1): p. 39-46.
283. Taylor, P.R., et al., *Dectin-1 is required for beta-glucan recognition and control of fungal infection.* Nat Immunol, 2007. **8**(1): p. 31-8.
284. Dostert, C. and J. Tschopp, *DEteCTINg fungal pathogens.* Nat Immunol, 2007. **8**(1): p. 17-8.
285. Marshall, A.S., et al., *Identification and characterization of a novel human myeloid inhibitory C-type lectin-like receptor (MICL) that is predominantly expressed on granulocytes and monocytes.* J Biol Chem, 2004. **279**(15): p. 14792-802.
286. Adachi, Y., et al., *Characterization of beta-glucan recognition site on C-type lectin, dectin 1.* Infect Immun, 2004. **72**(7): p. 4159-71.
287. Yokota, K., et al., *Identification of a human homologue of the dendritic cell-associated C-type lectin-1, dectin-1.* Gene, 2001. **272**(1-2): p. 51-60.
288. Xie, J., et al., *Human Dectin-1 isoform E is a cytoplasmic protein and interacts with RanBPM.* Biochem Biophys Res Commun, 2006. **347**(4): p. 1067-73.
289. Rogers, N.C., et al., *Syk-dependent cytokine induction by Dectin-1 reveals a novel pattern recognition pathway for C type lectins.* Immunity, 2005. **22**(4): p. 507-17.
290. Xu, S., et al., *Phospholipase Cgamma2 is critical for Dectin-1-mediated Ca2+ flux and cytokine production in dendritic cells.* J Biol Chem, 2009. **284**(11): p. 7038-46.
291. Klis, F.M., et al., *Dynamics of cell wall structure in Saccharomyces cerevisiae.* FEMS Microbiol Rev, 2002. **26**(3): p. 239-56.
292. McGreal, E.P., et al., *The carbohydrate-recognition domain of Dectin-2 is a C-type lectin with specificity for high mannose.* Glycobiology, 2006. **16**(5): p. 422-30.
293. Ariizumi, K., et al., *Identification of a novel, dendritic cell-associated molecule, dectin-1, by subtractive cDNA cloning.* J Biol Chem, 2000. **275**(26): p. 20157-67.
294. Grunebach, F., et al., *Molecular and functional characterization of human Dectin-1.* Exp Hematol, 2002. **30**(11): p. 1309-15.
295. Brown, G.D. and S. Gordon, *Immune recognition. A new receptor for beta-glucans.* Nature, 2001. **413**(6851): p. 36-7.
296. Adams, E.L., et al., *Differential high-affinity interaction of dectin-1 with natural or synthetic glucans is dependent upon primary structure and is influenced by polymer chain length and side-chain branching.* J Pharmacol Exp Ther, 2008. **325**(1): p. 115-23.
297. Gantner, B.N., R.M. Simmons, and D.M. Underhill, *Dectin-1 mediates macrophage recognition of Candida albicans yeast but not filaments.* EMBO J, 2005. **24**(6): p. 1277-86.
298. Gersuk, G.M., et al., *Dectin-1 and TLRs permit macrophages to distinguish between different Aspergillus fumigatus cellular states.* J Immunol, 2006. **176**(6): p. 3717-24.
299. Nakamura, K., et al., *Toll-like receptor 2 (TLR2) and dectin-1 contribute to the production of IL-12p40 by bone marrow-derived dendritic cells infected with Penicillium marneffei.* Microbes Infect, 2008. **10**(10-11): p. 1223-7.

300. Steele, C., et al., *Alveolar macrophage-mediated killing of Pneumocystis carinii f. sp. muris involves molecular recognition by the Dectin-1 beta-glucan receptor.* J Exp Med, 2003. **198**(11): p. 1677-88.
301. Steele, C., et al., *The beta-glucan receptor dectin-1 recognizes specific morphologies of Aspergillus fumigatus.* PLoS Pathog, 2005. **1**(4): p. e42.
302. Viriyakosol, S., et al., *Innate immunity to the pathogenic fungus Coccidioides posadasii is dependent on Toll-like receptor 2 and Dectin-1.* Infect Immun, 2005. **73**(3): p. 1553-60.
303. Rothfuchs, A.G., et al., *Dectin-1 interaction with Mycobacterium tuberculosis leads to enhanced IL-12p40 production by splenic dendritic cells.* J Immunol, 2007. **179**(6): p. 3463-71.
304. Shin, D.M., et al., *Mycobacterium abscessus activates the macrophage innate immune response via a physical and functional interaction between TLR2 and dectin-1.* Cell Microbiol, 2008. **10**(8): p. 1608-21.
305. Yadav, M. and J.S. Schorey, *The beta-glucan receptor dectin-1 functions together with TLR2 to mediate macrophage activation by mycobacteria.* Blood, 2006. **108**(9): p. 3168-75.
306. Weck, M.M., et al., *hDectin-1 is involved in uptake and cross-presentation of cellular antigens.* Blood, 2008. **111**(8): p. 4264-72.
307. Sancho, D., et al., *Identification of a dendritic cell receptor that couples sensing of necrosis to immunity.* Nature, 2009. **458**(7240): p. 899-903.
308. Franchi, L., et al., *Function of Nod-like receptors in microbial recognition and host defense.* Immunol Rev, 2009. **227**(1): p. 106-28.
309. Isakov, N., *Immunoreceptor tyrosine-based activation motif (ITAM), a unique module linking antigen and Fc receptors to their signaling cascades.* J Leukoc Biol, 1997. **61**(1): p. 6-16.
310. Underhill, D.M. and H.S. Goodridge, *The many faces of ITAMs.* Trends Immunol, 2007. **28**(2): p. 66-73.
311. Barrow, A.D. and J. Trowsdale, *You say ITAM and I say ITIM, let's call the whole thing off: the ambiguity of immunoreceptor signalling.* Eur J Immunol, 2006. **36**(7): p. 1646-53.
312. Fuller, G.L., et al., *The C-type lectin receptors CLEC-2 and Dectin-1, but not DC-SIGN, signal via a novel YXXL-dependent signaling cascade.* J Biol Chem, 2007. **282**(17): p. 12397-409.
313. Gross, O., et al., *Card9 controls a non-TLR signalling pathway for innate anti-fungal immunity.* Nature, 2006. **442**(7103): p. 651-6.
314. LeibundGut-Landmann, S., et al., *Syk- and CARD9-dependent coupling of innate immunity to the induction of T helper cells that produce interleukin 17.* Nat Immunol, 2007. **8**(6): p. 630-8.
315. Colonna, M., *TLR pathways and IFN-regulatory factors: to each its own.* Eur J Immunol, 2007. **37**(2): p. 306-9.
316. Rawlings, D.J., K. Sommer, and M.E. Moreno-Garcia, *The CARMA1 signalosome links the signalling machinery of adaptive and innate immunity in lymphocytes.* Nat Rev Immunol, 2006. **6**(11): p. 799-812.
317. del Fresno, C., et al., *Interferon-beta production via Dectin-1-Syk-IRF5 signaling in dendritic cells is crucial for immunity to C. albicans.* Immunity, 2013. **38**(6): p. 1176-86.
318. Slack, E.C., et al., *Syk-dependent ERK activation regulates IL-2 and IL-10 production by DC stimulated with zymosan.* Eur J Immunol, 2007. **37**(6): p. 1600-12.
319. Geijtenbeek, T.B., Gringhuis SI., *Signalling through C-type lectin receptors: shaping immune responses.* Nat Rev Immunol, 2009. **9**(7): p. 465-79.
320. Fric, J., et al., *Calcineurin/NFAT signalling inhibits myeloid haematopoiesis.* EMBO Mol Med, 2012. **4**(4): p. 269-82.
321. Zenaro, E., M. Donini, and S. Dusi, *Induction of Th1/Th17 immune response by Mycobacterium tuberculosis: role of dectin-1, Mannose Receptor, and DC-SIGN.* J Leukoc Biol, 2009. **86**(6): p. 1393-401.
322. Karumuthil-Melethil, S., et al., *Induction of innate immune response through TLR2 and dectin 1 prevents type 1 diabetes.* J Immunol, 2008. **181**(12): p. 8323-34.
323. Leibundgut-Landmann, S., et al., *Stimulation of dendritic cells via the dectin-1/Syk pathway allows priming of cytotoxic T-cell responses.* Blood, 2008. **112**(13): p. 4971-80.
324. Carter, R.W., et al., *Preferential induction of CD4+ T cell responses through in vivo targeting of antigen to dendritic cell-associated C-type lectin-1.* J Immunol, 2006. **177**(4): p. 2276-84.
325. Goodridge, H.S., et al., *Differential use of CARD9 by dectin-1 in macrophages and dendritic cells.* J Immunol, 2009. **182**(2): p. 1146-54.
326. Rosas, M., et al., *The induction of inflammation by dectin-1 in vivo is dependent on myeloid cell programming and the progression of phagocytosis.* J Immunol, 2008. **181**(5): p. 3549-57.
327. Gantner, B.N., et al., *Collaborative induction of inflammatory responses by dectin-1 and Toll-like receptor 2.* J Exp Med, 2003. **197**(9): p. 1107-17.
328. Dennehy, K.M., et al., *Syk kinase is required for collaborative cytokine production induced through Dectin-1 and Toll-like receptors.* Eur J Immunol, 2008. **38**(2): p. 500-6.

329. Trinchieri, G. and A. Sher, *Cooperation of Toll-like receptor signals in innate immune defence.* Nat Rev Immunol, 2007. **7**(3): p. 179-90.
330. Gerosa, F., et al., *Differential regulation of interleukin 12 and interleukin 23 production in human dendritic cells.* J Exp Med, 2008. **205**(6): p. 1447-61.
331. Valera, I., et al., *Costimulation of dectin-1 and DC-SIGN triggers the arachidonic acid cascade in human monocyte-derived dendritic cells.* J Immunol, 2008. **180**(8): p. 5727-36.
332. Taylor, P.R., et al., *The role of SIGNR1 and the beta-glucan receptor (dectin-1) in the nonopsonic recognition of yeast by specific macrophages.* J Immunol, 2004. **172**(2): p. 1157-62.
333. Mantegazza, A.R., et al., *CD63 tetraspanin slows down cell migration and translocates to the endosomal-lysosomal-MIICs route after extracellular stimuli in human immature dendritic cells.* Blood, 2004. **104**(4): p. 1183-90.
334. van Spriel, A.B., et al., *The tetraspanin protein CD37 regulates IgA responses and anti-fungal immunity.* PLoS Pathog, 2009. **5**(3): p. e1000338.
335. Wu, T.C., et al., *Reprogramming tumor-infiltrating dendritic cells for CD103+ CD8+ mucosal T-cell differentiation and breast cancer rejection.* Cancer Immunol Res, 2014. **2**(5): p. 487-500.
336. Zanoni, I., et al., *Self-tolerance, dendritic cell (DC)-mediated activation and tissue distribution of natural killer (NK) cells.* Immunol Lett, 2007. **110**(1): p. 6-17.
337. Pontiroli, F., et al., *The timing of IFNbeta production affects early innate responses to Listeria monocytogenes and determines the overall outcome of lethal infection.* PLoS One, 2012. **7**(8): p. e43455.
338. Chiba, S., et al., *Recognition of tumor cells by Dectin-1 orchestrates innate immune cells for anti-tumor responses.* Elife, 2014. **3**: p. e04177.
339. Suzuki-Inoue, K., et al., *A novel Syk-dependent mechanism of platelet activation by the C-type lectin receptor CLEC-2.* Blood, 2006. **107**(2): p. 542-9.
340. Kerrigan, A.M. and G.D. Brown, *Syk-coupled C-type lectin receptors that mediate cellular activation via single tyrosine based activation motifs.* Immunol Rev, 2010. **234**(1): p. 335-52.
341. Colonna, M., J. Samaridis, and L. Angman, *Molecular characterization of two novel C-type lectin-like receptors, one of which is selectively expressed in human dendritic cells.* Eur J Immunol, 2000. **30**(2): p. 697-704.
342. Shin, Y. and T. Morita, *Rhodocytin, a functional novel platelet agonist belonging to the heterodimeric C-type lectin family, induces platelet aggregation independently of glycoprotein Ib.* Biochem Biophys Res Commun, 1998. **245**(3): p. 741-5.
343. Bergmeier, W., et al., *Rhodocytin (aggretin) activates platelets lacking alpha(2)beta(1) integrin, glycoprotein VI, and the ligand-binding domain of glycoprotein Ibalpha.* J Biol Chem, 2001. **276**(27): p. 25121-6.
344. Kerrigan, A.M., et al., *CLEC-2 is a phagocytic activation receptor expressed on murine peripheral blood neutrophils.* J Immunol, 2009. **182**(7): p. 4150-7.
345. Mori, J., et al., *G6b-B inhibits constitutive and agonist-induced signaling by glycoprotein VI and CLEC-2.* J Biol Chem, 2008. **283**(51): p. 35419-27.
346. Spalton, J.C., et al., *The novel Syk inhibitor R406 reveals mechanistic differences in the initiation of GPVI and CLEC-2 signaling in platelets.* J Thromb Haemost, 2009. **7**(7): p. 1192-9.
347. Hughes, C.E., et al., *Critical Role for an acidic amino acid region in platelet signaling by the HemITAM (hemi-immunoreceptor tyrosine-based activation motif) containing receptor CLEC-2 (C-type lectin receptor-2).* J Biol Chem, 2013. **288**(7): p. 5127-35.
348. Pollitt, A.Y., et al., *Phosphorylation of CLEC-2 is dependent on lipid rafts, actin polymerization, secondary mediators, and Rac.* Blood, 2010. **115**(14): p. 2938-46.
349. Watson, A.A., et al., *The platelet receptor CLEC-2 is active as a dimer.* Biochemistry, 2009. **48**(46): p. 10988-96.
350. Hughes, C.E., et al., *The N-terminal SH2 domain of Syk is required for (hem)ITAM but not integrin signalling in mouse platelets.* Blood, 2014.
351. Mourao-Sa, D., et al., *CLEC-2 signaling via Syk in myeloid cells can regulate inflammatory responses.* Eur J Immunol, 2011. **41**(10): p. 3040-53.
352. May, F., et al., *CLEC-2 is an essential platelet-activating receptor in hemostasis and thrombosis.* Blood, 2009. **114**(16): p. 3464-72.
353. Ozaki, Y., K. Suzuki-Inoue, and O. Inoue, *Novel interactions in platelet biology: CLEC-2/podoplanin and laminin/GPVI.* J Thromb Haemost, 2009. **7 Suppl 1**: p. 191-4.
354. Suzuki-Inoue, K., et al., *Involvement of the snake toxin receptor CLEC-2, in podoplanin-mediated platelet activation, by cancer cells.* J Biol Chem, 2007. **282**(36): p. 25993-6001.

355. Christou, C.M., et al., *Renal cells activate the platelet receptor CLEC-2 through podoplanin.* Biochem J, 2008. **411**(1): p. 133-40.
356. Wicki, A. and G. Christofori, *The potential role of podoplanin in tumour invasion.* Br J Cancer, 2007. **96**(1): p. 1-5.
357. Chaipan, C., et al., *DC-SIGN and CLEC-2 mediate human immunodeficiency virus type 1 capture by platelets.* J Virol, 2006. **80**(18): p. 8951-60.
358. Caminschi, I., et al., *The dendritic cell subtype-restricted C-type lectin Clec9A is a target for vaccine enhancement.* Blood, 2008. **112**(8): p. 3264-73.
359. Poulin, L.F., et al., *Characterization of human DNGR-1+ BDCA3+ leukocytes as putative equivalents of mouse CD8alpha+ dendritic cells.* J Exp Med, 2010. **207**(6): p. 1261-71.
360. Zhang, J.G., et al., *The dendritic cell receptor Clec9A binds damaged cells via exposed actin filaments.* Immunity, 2012. **36**(4): p. 646-57.
361. Geijtenbeek, T.B., *Actin' as a death signal.* Immunity, 2012. **36**(4): p. 557-9.
362. Ahrens, S., et al., *F-actin is an evolutionarily conserved damage-associated molecular pattern recognized by DNGR-1, a receptor for dead cells.* Immunity, 2012. **36**(4): p. 635-45.
363. Zelenay, S., et al., *The dendritic cell receptor DNGR-1 controls endocytic handling of necrotic cell antigens to favor cross-priming of CTLs in virus-infected mice.* J Clin Invest, 2012. **122**(5): p. 1615-27.
364. Gietz, R.D. and R.A. Woods, *Screening for protein-protein interactions in the yeast two-hybrid system.* Methods Mol Biol, 2002. **185**: p. 471-86.
365. Hershko, A., *The ubiquitin system for protein degradation and some of its roles in the control of the cell-division cycle (Nobel lecture).* Angew Chem Int Ed Engl, 2005. **44**(37): p. 5932-43.
366. Johnson, E.S., et al., *The ubiquitin-like protein Smt3p is activated for conjugation to other proteins by an Aos1p/Uba2p heterodimer.* EMBO J, 1997. **16**(18): p. 5509-19.
367. Schaaf, M.J. and J.A. Cidlowski, *Molecular mechanisms of glucocorticoid action and resistance.* J Steroid Biochem Mol Biol, 2002. **83**(1-5): p. 37-48.
368. Pelaia, G., et al., *Molecular mechanisms of corticosteroid actions in chronic inflammatory airway diseases.* Life Sci, 2003. **72**(14): p. 1549-61.
369. Zhang, Z., et al., *STAT3 acts as a co-activator of glucocorticoid receptor signaling.* J Biol Chem, 1997. **272**(49): p. 30607-10.
370. Wu, Z., N.L. Bucher, and S.R. Farmer, *Induction of peroxisome proliferator-activated receptor gamma during the conversion of 3T3 fibroblasts into adipocytes is mediated by C/EBPbeta, C/EBPdelta, and glucocorticoids.* Mol Cell Biol, 1996. **16**(8): p. 4128-36.
371. Mills, C.D., et al., *M-1/M-2 macrophages and the Th1/Th2 paradigm.* J Immunol, 2000. **164**(12): p. 6166-73.
372. Jemal, A., et al., *Cancer statistics, 2010.* CA Cancer J Clin, 2010. **60**(5): p. 277-300.
373. Panico, L., et al., *Prognostic role of tumor-associated macrophages and angiogenesis in classical Hodgkin lymphoma.* Leuk Lymphoma, 2013. **54**(11): p. 2418-25.
374. Boel, E., et al., *Functional human monoclonal antibodies of all isotypes constructed from phage display library-derived single-chain Fv antibody fragments.* J Immunol Methods, 2000. **239**(1-2): p. 153-66.
375. Deans, J.P., H. Li, and M.J. Polyak, *CD20-mediated apoptosis: signalling through lipid rafts.* Immunology, 2002. **107**(2): p. 176-82.
376. Lucero, H.A. and P.W. Robbins, *Lipid rafts-protein association and the regulation of protein activity.* Arch Biochem Biophys, 2004. **426**(2): p. 208-24.
377. Cuatrecasas, P., *Gangliosides and membrane receptors for cholera toxin.* Biochemistry, 1973. **12**(18): p. 3558-66.
378. Loftsson, T., et al., *Self-association and cyclodextrin solubilization of drugs.* J Pharm Sci, 2002. **91**(11): p. 2307-16.
379. Nishijo, J., S. Moriyama, and S. Shiota, *Interactions of cholesterol with cyclodextrins in aqueous solution.* Chem Pharm Bull (Tokyo), 2003. **51**(11): p. 1253-7.
380. Johnsson, N. and A. Varshavsky, *Split ubiquitin as a sensor of protein interactions in vivo.* Proc Natl Acad Sci U S A, 1994. **91**(22): p. 10340-4.
381. Martinez, F.O., et al., *Transcriptional profiling of the human monocyte-to-macrophage differentiation and polarization: new molecules and patterns of gene expression.* J Immunol, 2006. **177**(10): p. 7303-11.
382. Millington, M., et al., *High-precision FLIM-FRET in fixed and living cells reveals heterogeneity in a simple CFP-YFP fusion protein.* Biophys Chem, 2007. **127**(3): p. 155-64.
383. Hernanz-Falcon, P., et al., *Internalization of Dectin-1 terminates induction of inflammatory responses.* Eur J Immunol, 2009. **39**(2): p. 507-13.

384. Suram, S., et al., *Regulation of cytosolic phospholipase A2 activation and cyclooxygenase 2 expression in macrophages by the beta-glucan receptor.* J Biol Chem, 2006. **281**(9): p. 5506-14.
385. Harada, T. and N. Ohno, *Contribution of dectin-1 and granulocyte macrophage-colony stimulating factor (GM-CSF) to immunomodulating actions of beta-glucan.* Int Immunopharmacol, 2008. **8**(4): p. 556-66.
386. Goodridge, H.S., et al., *Activation of the innate immune receptor Dectin-1 upon formation of a 'phagocytic synapse'.* Nature, 2011. **472**(7344): p. 471-5.
387. Li, B., et al., *Yeast glucan particles activate murine resident macrophages to secrete proinflammatory cytokines via MyD88- and Syk kinase-dependent pathways.* Clin Immunol, 2007. **124**(2): p. 170-81.
388. Gametchu, B., et al., *Plasma membrane-resident glucocorticoid receptors in rodent lymphoma and human leukemia models.* Steroids, 1999. **64**(1-2): p. 107-19.
389. Nathan, C.F. and R.K. Root, *Hydrogen peroxide release from mouse peritoneal macrophages: dependence on sequential activation and triggering.* J Exp Med, 1977. **146**(6): p. 1648-62.
390. Liang, Y., et al., *Structural organization of the human MS4A gene cluster on Chromosome 11q12.* Immunogenetics, 2001. **53**(5): p. 357-68.
391. Tedder, T.F., et al., *The gene that encodes the human CD20 (B1) differentiation antigen is located on chromosome 11 near the t(11;14)(q13;q32) translocation site.* J Immunol, 1989. **142**(7): p. 2555-9.
392. Tedder, T.F., et al., *Cloning of a complementary DNA encoding a new mouse B lymphocyte differentiation antigen, homologous to the human B1 (CD20) antigen, and localization of the gene to chromosome 19.* J Immunol, 1988. **141**(12): p. 4388-94.
393. Stamenkovic, I. and B. Seed, *Analysis of two cDNA clones encoding the B lymphocyte antigen CD20 (B1, Bp35), a type III integral membrane protein.* J Exp Med, 1988. **167**(6): p. 1975-80.
394. Stashenko, P., et al., *Expression of cell surface markers after human B lymphocyte activation.* Proc Natl Acad Sci U S A, 1981. **78**(6): p. 3848-52.
395. Nadler, L.M., et al., *B cell origin of non-T cell acute lymphoblastic leukemia. A model for discrete stages of neoplastic and normal pre-B cell differentiation.* J Clin Invest, 1984. **74**(2): p. 332-40.
396. Riley, J.K. and M.X. Sliwkowski, *CD20: a gene in search of a function.* Semin Oncol, 2000. **27**(6 Suppl 12): p. 17-24.
397. Taylor, R.P. and M.A. Lindorfer, *Immunotherapeutic mechanisms of anti-CD20 monoclonal antibodies.* Curr Opin Immunol, 2008. **20**(4): p. 444-9.
398. Choi, O.H., J.H. Kim, and J.P. Kinet, *Calcium mobilization via sphingosine kinase in signalling by the Fc epsilon RI antigen receptor.* Nature, 1996. **380**(6575): p. 634-6.
399. Maurer, D., et al., *Expression of functional high affinity immunoglobulin E receptors (Fc epsilon RI) on monocytes of atopic individuals.* J Exp Med, 1994. **179**(2): p. 745-50.
400. Majai, G., et al., *PPARgamma-dependent regulation of human macrophages in phagocytosis of apoptotic cells.* Eur J Immunol, 2007. **37**(5): p. 1343-54.
401. Mantovani, A., P. Allavena, and A. Sica, *Tumour-associated macrophages as a prototypic type II polarised phagocyte population: role in tumour progression.* Eur J Cancer, 2004. **40**(11): p. 1660-7.
402. Zhang, Y., et al., *High-infiltration of tumor-associated macrophages predicts unfavorable clinical outcome for node-negative breast cancer.* PLoS One, 2013. **8**(9): p. e76147.
403. Iannacone, M., et al., *Subcapsular sinus macrophages prevent CNS invasion on peripheral infection with a neurotropic virus.* Nature, 2010. **465**(7301): p. 1079-83.
404. Junt, T., et al., *Subcapsular sinus macrophages in lymph nodes clear lymph-borne viruses and present them to antiviral B cells.* Nature, 2007. **450**(7166): p. 110-4.
405. Wynes, M.W. and D.W. Riches, *Induction of macrophage insulin-like growth factor-I expression by the Th2 cytokines IL-4 and IL-13.* J Immunol, 2003. **171**(7): p. 3550-9.
406. Knight, S.C., *Specialized perinodal fat fuels and fashions immunity.* Immunity, 2008. **28**(2): p. 135-8.
407. Charriere, G., et al., *Preadipocyte conversion to macrophage. Evidence of plasticity.* J Biol Chem, 2003. **278**(11): p. 9850-5.
408. Bedford, P.A., et al., *Adipose tissue of human omentum is a major source of dendritic cells, which lose MHC Class II and stimulatory function in Crohn's disease.* J Leukoc Biol, 2006. **80**(3): p. 546-54.
409. Sidler, D., et al., *Colon cancer cells produce immunoregulatory glucocorticoids.* Oncoimmunology, 2012. **1**(4): p. 529-530.
410. Glennie, M.J. and J.G. van de Winkel, *Renaissance of cancer therapeutic antibodies.* Drug Discov Today, 2003. **8**(11): p. 503-10.
411. Van Laethem, F., et al., *Glucocorticoids alter the lipid and protein composition of membrane rafts of a murine T cell hybridoma.* J Immunol, 2003. **170**(6): p. 2932-9.

412. Brown, D.A. and E. London, *Structure and function of sphingolipid- and cholesterol-rich membrane rafts.* J Biol Chem, 2000. **275**(23): p. 17221-4.
413. Awasthi-Kalia, M., P.P. Schnetkamp, and J.P. Deans, *Differential effects of filipin and methyl-beta-cyclodextrin on B cell receptor signaling.* Biochem Biophys Res Commun, 2001. **287**(1): p. 77-82.
414. Zhang, J., A. Pekosz, and R.A. Lamb, *Influenza virus assembly and lipid raft microdomains: a role for the cytoplasmic tails of the spike glycoproteins.* J Virol, 2000. **74**(10): p. 4634-44.
415. Park, S.J., et al., *Oxidative stress induces lipid-raft-mediated activation of Src homology 2 domain-containing protein-tyrosine phosphatase 2 in astrocytes.* Free Radic Biol Med, 2009. **46**(12): p. 1694-702.
416. Persaud-Sawin, D.A., L. Banach, and G.J. Harry, *Raft aggregation with specific receptor recruitment is required for microglial phagocytosis of Abeta42.* Glia, 2009. **57**(3): p. 320-35.
417. Lagaudriere-Gesbert, C., et al., *Signaling through the tetraspanin CD82 triggers its association with the cytoskeleton leading to sustained morphological changes and T cell activation.* Eur J Immunol, 1998. **28**(12): p. 4332-44.
418. Berditchevski, F., G. Bazzoni, and M.E. Hemler, *Specific association of CD63 with the VLA-3 and VLA-6 integrins.* J Biol Chem, 1995. **270**(30): p. 17784-90.
419. Berditchevski, F., M.M. Zutter, and M.E. Hemler, *Characterization of novel complexes on the cell surface between integrins and proteins with 4 transmembrane domains (TM4 proteins).* Mol Biol Cell, 1996. **7**(2): p. 193-207.
420. Tachibana, I., et al., *NAG-2, a novel transmembrane-4 superfamily (TM4SF) protein that complexes with integrins and other TM4SF proteins.* J Biol Chem, 1997. **272**(46): p. 29181-9.
421. Nakamura, K., R. Iwamoto, and E. Mekada, *Membrane-anchored heparin-binding EGF-like growth factor (HB-EGF) and diphtheria toxin receptor-associated protein (DRAP27)/CD9 form a complex with integrin alpha 3 beta 1 at cell-cell contact sites.* J Cell Biol, 1995. **129**(6): p. 1691-705.
422. Yashiro-Ohtani, Y., et al., *Non-CD28 costimulatory molecules present in T cell rafts induce T cell costimulation by enhancing the association of TCR with rafts.* J Immunol, 2000. **164**(3): p. 1251-9.
423. Ferwerda, G., et al., *Dectin-1 synergizes with TLR2 and TLR4 for cytokine production in human primary monocytes and macrophages.* Cell Microbiol, 2008. **10**(10): p. 2058-66.
424. Underhill, D.M., *Collaboration between the innate immune receptors dectin-1, TLRs, and Nods.* Immunol Rev, 2007. **219**: p. 75-87.
425. Ruland, J., *CARD9 signaling in the innate immune response.* Ann N Y Acad Sci, 2008. **1143**: p. 35-44.
426. Reid, D.M., N.A. Gow, and G.D. Brown, *Pattern recognition: recent insights from Dectin-1.* Curr Opin Immunol, 2009. **21**(1): p. 30-7.
427. Underhill, D.M., et al., *Dectin-1 activates Syk tyrosine kinase in a dynamic subset of macrophages for reactive oxygen production.* Blood, 2005. **106**(7): p. 2543-50.